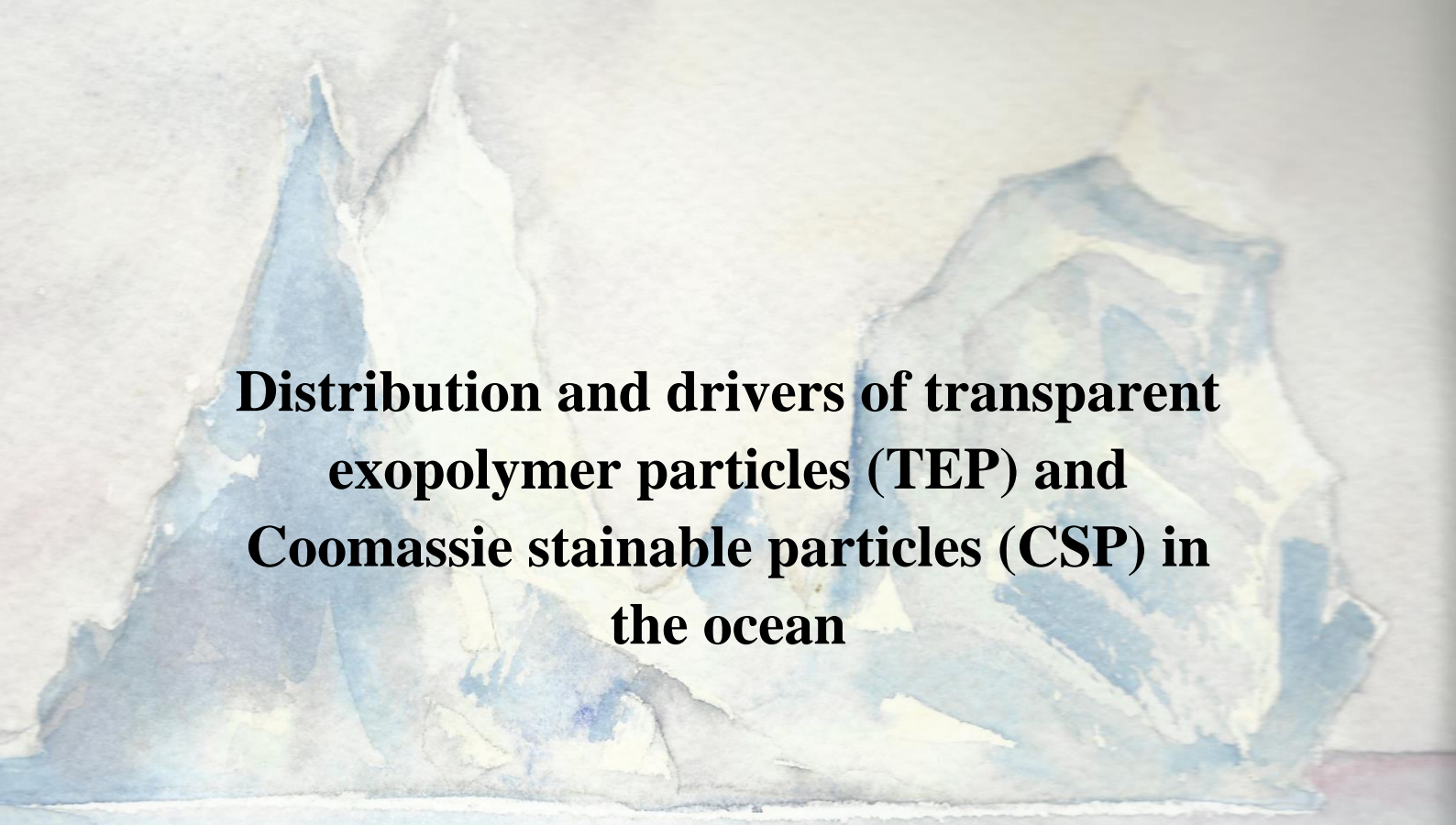


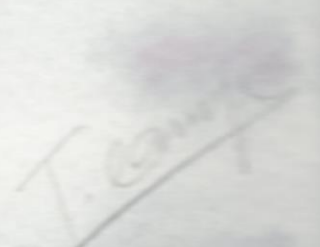
Doctorado en Ciencias del Mar



**Distribution and drivers of transparent  
exopolymer particles (TEP) and  
Coomassie stainable particles (CSP) in  
the ocean**

**Marina Zamanillo Campos**

Barcelona, 2019





UNIVERSITAT POLITÈCNICA  
DE CATALUNYA  
BARCELONATECH

## *Distribution and drivers of transparent exopolymer particles (TEP) and Coomassie stainable particles (CSP) in the ocean*

**Marina Zamanillo Campos**

**ADVERTIMENT** La consulta d'aquesta tesi queda condicionada a l'acceptació de les següents condicions d'ús: La difusió d'aquesta tesi per mitjà del repositori institucional UPCommons (<http://upcommons.upc.edu/tesis>) i el repositori cooperatiu TDX (<http://www.tdx.cat/>) ha estat autoritzada pels titulars dels drets de propietat intel·lectual **únicament per a usos privats** emmarcats en activitats d'investigació i docència. No s'autoritza la seva reproducció amb finalitats de lucre ni la seva difusió i posada a disposició des d'un lloc aliè al servei UPCommons o TDX. No s'autoritza la presentació del seu contingut en una finestra o marc aliè a UPCommons (*framing*). Aquesta reserva de drets afecta tant al resum de presentació de la tesi com als seus continguts. En la utilització o cita de parts de la tesi és obligat indicar el nom de la persona autora.

**ADVERTENCIA** La consulta de esta tesis queda condicionada a la aceptación de las siguientes condiciones de uso: La difusión de esta tesis por medio del repositorio institucional UPCommons (<http://upcommons.upc.edu/tesis>) y el repositorio cooperativo TDR (<http://www.tdx.cat/?locale-attribute=es>) ha sido autorizada por los titulares de los derechos de propiedad intelectual **únicamente para usos privados enmarcados** en actividades de investigación y docencia. No se autoriza su reproducción con finalidades de lucro ni su difusión y puesta a disposición desde un sitio ajeno al servicio UPCommons No se autoriza la presentación de su contenido en una ventana o marco ajeno a UPCommons (*framing*). Esta reserva de derechos afecta tanto al resumen de presentación de la tesis como a sus contenidos. En la utilización o cita de partes de la tesis es obligado indicar el nombre de la persona autora.

**WARNING** On having consulted this thesis you're accepting the following use conditions: Spreading this thesis by the institutional repository UPCommons (<http://upcommons.upc.edu/tesis>) and the cooperative repository TDX (<http://www.tdx.cat/?locale-attribute=en>) has been authorized by the titular of the intellectual property rights **only for private uses** placed in investigation and teaching activities. Reproduction with lucrative aims is not authorized neither its spreading nor availability from a site foreign to the UPCommons service. Introducing its content in a window or frame foreign to the UPCommons service is not authorized (*framing*). These rights affect to the presentation summary of the thesis as well as to its contents. In the using or citation of parts of the thesis it's obliged to indicate the name of the author.



UNIVERSITAT POLITÈCNICA  
DE CATALUNYA  
BARCELONATECH



Institut  
de Ciències  
del Mar



CSIC  
CONSEJO SUPERIOR DE INVESTIGACIONES CIENTÍFICAS

# Distribution and drivers of transparent exopolymer particles (TEP) and Coomassie stainable particles (CSP) in the ocean

Distribución y factores de regulación de partículas exopoliméricas  
transparentes (TEP) y partículas teñibles con Coomassie (CSP) en  
el océano

Marina Zamanillo Campos

Barcelona, septiembre 2019

Tesis doctoral presentada por **Marina Zamanillo Campos** para obtener el  
título de Doctora por la Universidad Politécnica de Cataluña

Programa de Doctorado en Ciencias del Mar

Departamento de Ingeniería Civil y Ambiental

Tesis por compendio de publicaciones

La Doctoranda

Marina Zamanillo Campos

El Director

Rafel Simó Martorell

La Codirectora

Eva Ortega-Retuerta



*“Distribution and main drivers of transparent exopolymer particles (TEP) and Coomassie stainable particles (CSP) in the ocean”*

*“Distribución y factores de regulación de partículas exopoliméricas transparentes (TEP) y partículas teñibles con Coomassie (CSP) en el océano”*

*“Distribució i factors de regulació de partícules exopolimèriques transparents (TEP) i partícules tenyibles amb Coomassie (CSP) a l’oceà”*

The author was supported by a FI-DGR grant (ECO/1639/2013) from the *Agència de Gestió d’Ajuts Universitaris i de Recerca* (AGAUR) (Generalitat de Catalunya) and a FPU grant (FPU13/04630) from the Spanish Ministry of Education and Culture. The research work presented in this thesis was founded by the projects PEGASO (CTM2012–37615) and BIOGAPS (CTM2016–81008–R), supported by the Spanish Ministry of Economy and Competivity (MINECO), and the Antarctic Circumnavigation Expedition (ACE), carried out under the auspices of the Swiss Polar Institute, and supported by funding from the ACE Foundation and Ferring Pharmaceuticals.

The studies were carried out at the Institut de Ciències del Mar de Barcelona (ICM, CSIC; Barcelona, Spain), and at the GEOMAR Helmholtz Centre for Ocean Research Kiel (Kiel, Germany) thanks to three grants the author received: EST15/00512, EST16/00003, Erasmus+.



*A mi familia, amigos/as y todos los que me han acompañado durante este viaje*





*"Todos somos muy ignorantes. Lo que ocurre es que no todos ignoramos las mismas cosas"*

(Albert Einstein)



# CONTENT

<b>Abstract/Resumen/Resum</b>	<b>1</b>
<b>Introduction</b>	<b>5</b>
<b>Aims of the thesis</b>	<b>37</b>
<b>Chapter 1.</b> Main drivers of transparent exopolymer particle distribution across the surface Atlantic Ocean	<b>43</b>
<b>Chapter 2.</b> Distribution of transparent exopolymer particles (TEP) in distinct regions of the Southern Ocean	<b>73</b>
<b>Chapter 3.</b> Seasonal variability of transparent exopolymer particles (TEP) and Coomassie stainable particles (CSP) in the coastal NW Mediterranean Sea	<b>111</b>
<b>Chapter 4.</b> Distribution of transparent exopolymer particles (TEP) and Coomassie stainable particles (CSP) in the Southern Ocean around Antarctica	<b>153</b>
<b>General discussion and future perspectives</b>	<b>175</b>
<b>Conclusions</b>	<b>189</b>
<b>References</b>	<b>193</b>
<b>Acknowledgments/ Agradecimientos</b>	<b>229</b>



# ABSTRACT

Transparent exopolymer particles (TEP) and Coomassie stainable particles (CSP) are operationally defined as organic particles  $> 0.4 \mu\text{m}$  that are stainable with the dyes Alcian Blue (specific for acidic polysaccharides) and Coomassie Brilliant Blue (specific for proteins), respectively. They are ubiquitous in the ocean, where they play important roles in biogeochemical processes such as the carbon cycle and sea-air gas and particle exchanges. However, there is a lack of large-scale studies of TEP and CSP distributions in the ocean, particularly in the open ocean, as well as temporal studies following their dynamics over more than one complete seasonal cycle. In addition, it is not clear yet whether these particles represent independent particle fractions or not and which are their main drivers, with a particular lack of information on CSP. In this thesis, TEP and CSP distributions were characterized, combining the horizontal and vertical scales whenever possible, in distinct regions of the ocean: Atlantic Ocean (October-November 2014), Southern Ocean (January 2015 and January-March 2017) and the NW Mediterranean Sea (October 2015). Besides, a time series study was conducted in two coastal stations in the NW Mediterranean Sea for two complete seasonal cycles (2015-2017). In all cases, a number of physical, chemical and biological variables were determined in parallel in order to explore the main drivers of TEP and CSP distributions. TEP concentrations ranged from below detection limit to  $446 \mu\text{g XG eq L}^{-1}$ , whereas CSP concentrations ranged between 0.3 and  $52.2 \mu\text{g BSA eq L}^{-1}$ . The highest TEP concentrations were found in the edge of the Canary Coastal Upwelling, the Southwestern Atlantic Shelf and some regions of the Southern Ocean, whereas the highest CSP concentrations were found in the Southern Ocean. Phytoplankton biomass, and not heterotrophic prokaryotic biomass or activity, is the best predictor of the concentration of both particle types, yet no single taxonomic group of phytoplankton stand as the universally dominant producer. Other variables that play important roles are the daily solar radiation dose in the mixed layer, surface irradiance, sea ice melt, nutrients and phytoplankton mortality in the case of TEP, and phytoplankton mortality for CSP. Our results suggest that TEP and CSP are independent particles, since they follow different dynamics in the temporal and spatial scales. The estimated contribution of TEP to the particulate organic carbon (POC) pool varies widely among regions and exceeds that of living phytoplankton biomass in some areas (Atlantic Ocean) and seasons (Mediterranean sea during summer).

# RESUMEN

Las partículas exopoliméricas transparentes (TEP) y las partículas teñibles con Coomassie (CSP) se definen operacionalmente como aquellas partículas  $> 0.4 \mu\text{m}$  que se tiñen con las tinciones azul alcían (específico para polisacáridos ácidos) y azul de Coomassie (específico para proteínas), respectivamente. Ambos tipos de partículas están presentes en todo el océano y juegan un papel fundamental en varios procesos biogeoquímicos como el ciclo del carbono y el intercambio de gases y partículas entre el océano y la atmósfera. Sin embargo, existen pocos estudios que describan sus distribuciones en el océano a gran escala, o sus dinámicas temporales a lo largo de más de un ciclo estacional completo. En esta tesis, hemos caracterizado la distribución de TEP y CSP, combinando las escalas horizontal y vertical cuando ha sido posible, en diferentes regiones del océano: El océano Atlántico (octubre-noviembre 2014), el océano Antártico (enero 2015 y enero-marzo 2017), y el Mar Mediterráneo noroccidental (octubre 2015). Además, se llevó a cabo un estudio temporal en dos estaciones costeras del Mar Mediterráneo noroccidental, tomando muestras mensuales durante dos ciclos estacionales completos (2015-2017). En todos los casos se analizaron variables físicas, químicas y biológicas en paralelo a las medidas de TEP y CSP, con el fin de explorar los principales factores de regulación de sus distribuciones. Las concentraciones de TEP oscilaron entre valores bajo del límite de detección y  $446 \mu\text{g XG eq L}^{-1}$ , mientras que las concentraciones de CSP oscilaron entre  $0.3$  y  $52.2 \mu\text{g BSA eq L}^{-1}$ . Las concentraciones más altas de TEP se encontraron en un extremo del afloramiento de la costa canaria, la plataforma continental al suroeste del océano Atlántico y en algunas regiones del océano Antártico, mientras que las concentraciones más elevadas de CSP se observaron en el océano Antártico. La biomasa del fitoplancton, y no la biomasa ni la actividad de los procariontes heterótrofos, es el mejor predictor de la concentración de ambos tipos de partículas. Sin embargo, no se encontró ningún grupo taxonómico concreto de fitoplancton que explicase universalmente su distribución. Otras variables que juegan papeles importantes son la dosis diaria de radiación solar en la capa de mezcla, la irradiancia superficial, los aportes por deshielo marino, la disponibilidad de nutrientes y la mortalidad del fitoplancton en el caso de TEP, y sólo esta última (la mortalidad del fitoplancton) con respecto a CSP. Nuestros resultados sugieren que TEP y CSP son partículas independientes, puesto que siguen dinámicas diferentes tanto en las escalas espacial como temporal. La contribución

estimada de TEP al conjunto total de carbono orgánico particulado (POC) varía ampliamente entre regiones, excediendo la contribución por parte de la biomasa de fitoplancton en algunas áreas (océano Atlántico) y estaciones del año (Mar Mediterráneo durante el verano).

# RESUM

Les partícules exopolimèriques transparents (TEP) i les partícules tenyibles amb Coomassie (CSP) es defineixen operacionalment com aquelles partícules  $> 0.4 \mu\text{m}$  que es tenyeixen amb les tincions blau alcian (específic per polisacàrids àcids) i blau de Coomassie (específic per proteïnes), respectivament. Aquestes partícules son ubíquies a l'oceà i juguen un paper important en processos biogeoquímics com el cicle del carboni i l'intercanvi de gasos i partícules entre el mar i l'atmosfera. No obstant això, hi ha pocs estudis que descriguin les distribucions a gran escala de TEP i CSP a l'oceà, particularment a l'oceà obert, o la seva variació temporal al llarg de més d'un cicle estacional complet. En aquesta tesis hem caracteritzat les distribucions de TEP i CSP, tot combinant les escales horitzontal i vertical quan ha estat possible, en diferents regions de l'oceà: l'oceà Atlàntic (octubre-novembre 2014), l'oceà Antàrtic (gener 2015 i gener-març 2017), i el Mar Mediterrani nord-occidental (octubre 2015). A més, hem dut a terme un estudi temporal en dos estacions costaneres del Mar Mediterrani nord-occidental durant dos cicles estacionals complets (2015-2017). En tots els casos es van mesurar variables físiques, químiques i biològiques en paral·lel, amb la finalitat d'explorar els principals factors de regulació de les distribucions de TEP i CSP. Les concentracions de TEP varen oscil·lar entre per sota del límit de detecció i  $446 \mu\text{g XG eq L}^{-1}$ , mentre que les concentracions de CSP oscil·laren entre 0.3 i  $52.2 \mu\text{g BSA eq L}^{-1}$ . Les concentracions més altes de TEP es van trobar a la vora del aflorament de la costa canària, a la plataforma continental del suroest atlàntic i en algunes regions de l'oceà Antàrtic. La biomassa del fitoplàncton, i no la biomassa ni la activitat dels procariotes heteròtrofs, és el millor predictor de la concentració d'ambdós tipus de partícules. Tanmateix, cap dels grups taxonòmics de fitoplàncton ha resultat ser el productor universalment dominant. Altres variables que juguen papers importants són la dosi de radiació solar diària a la capa de barreja, la irradiància superficial, la fosa del gel marí, la disponibilitat de nutrients i la mortalitat del fitoplàncton en el cas de les TEP, i només aquesta última (la mortalitat del fitoplàncton) per a les CSP. Els nostres resultats suggereixen que TEP i CSP són partícules independents, ja que segueixen dinàmiques diferents en les escales temporal i espacial. La contribució estimada de TEP al conjunt de carboni orgànic particulat (POC) varia àmpliament entre regions, i fins i tot excedeix la de la biomassa de fitoplàncton viu en algunes regions (oceà Atlàntic) i estacions de l'any (Mar Mediterrani durant l'estiu).









Adélie penguins in the Weddell Sea

# INTRODUCTION



## 1. The carbon cycle on Earth and its alteration by anthropogenic activities

Carbon forming either organic or inorganic compounds is found in different reservoirs on Earth: the atmosphere, the ocean, the land, continental waters, sediments of water bodies and geological deposits. The fluxes of these compounds among the reservoirs are commonly termed altogether the global carbon cycle (Fig. 1). The main natural fluxes between land and atmosphere are driven by the primary production and respiration of the land biosphere, while physical air-sea exchange governs fluxes between the atmosphere and the ocean. These fluxes are usually balanced, but even tiny imbalances can affect atmospheric CO<sub>2</sub> concentration over years to centuries. The land biosphere produces organic matter from atmospheric CO<sub>2</sub> through photosynthesis, and respire it back as CO<sub>2</sub>. A fraction of this matter ends up in the inert soil and is either buried forming geological reservoirs, or exported, in the form of dissolved organic carbon (DOC), by rivers or groundwater to the ocean (Schlesinger, 1990). Rivers also export inorganic carbon (DIC) in the form of CaCO<sub>3</sub>, dissolved by weathering. Fluxes of DOC and DIC together through riverine transport comprise 0.8 Pg C yr<sup>-1</sup>. Organic carbon compounds can also be added to the ocean by the activity of marine microbes, the atmospheric transport of organic matter from the continents, and the release of organic matter from the benthic boundary layer (Jurado et al., 2008; Bauer and Bianchi, 2011; Hansell, 2013). Carbon compounds in the ocean can be released again to the atmosphere in the form of CO<sub>2</sub>, or buried in deep-sea sediments, precursors of geological reservoirs such as carbonate rocks or fossil organic carbon (including fossil fuels). These geological deposits can be released to the atmosphere as CO<sub>2</sub> through tectonic processes (Bicke, 1994) (Fig. 1).

Over the last 200 years, the global carbon cycle has been altered significantly by human activities. This has been due to the global utilization of fossil fuels, but also by the production of cement and land-use changes, such as deforestation (Boden et al., 1999; Houghton and Nassikas, 2017) (Fig. 1). These activities have caused the rise of greenhouse gases in the atmosphere, which absorb the infrared radiation emitted from the earth and cause the warming of the lowest layer of the atmosphere (troposphere) (Sabine and Tanhua, 2010). Carbon dioxide (CO<sub>2</sub>) is the largest contributor to climate change due to its large increase in the atmosphere, but other gases such as chlorofluorocarbons, methane and nitrous oxide have higher specific greenhouse effect (Arrhenius, 1896; Mitchell et al., 1995). Some of the expected effects of the increase of

the average global temperature are extreme weather events (Curry and Mauritzen, 2005), spread of tropical diseases, species extinctions (Pounds et al., 2006) and changes in ecosystems (Barnett et al., 2005; Field and Timothy R. Baumgartner, 2006).

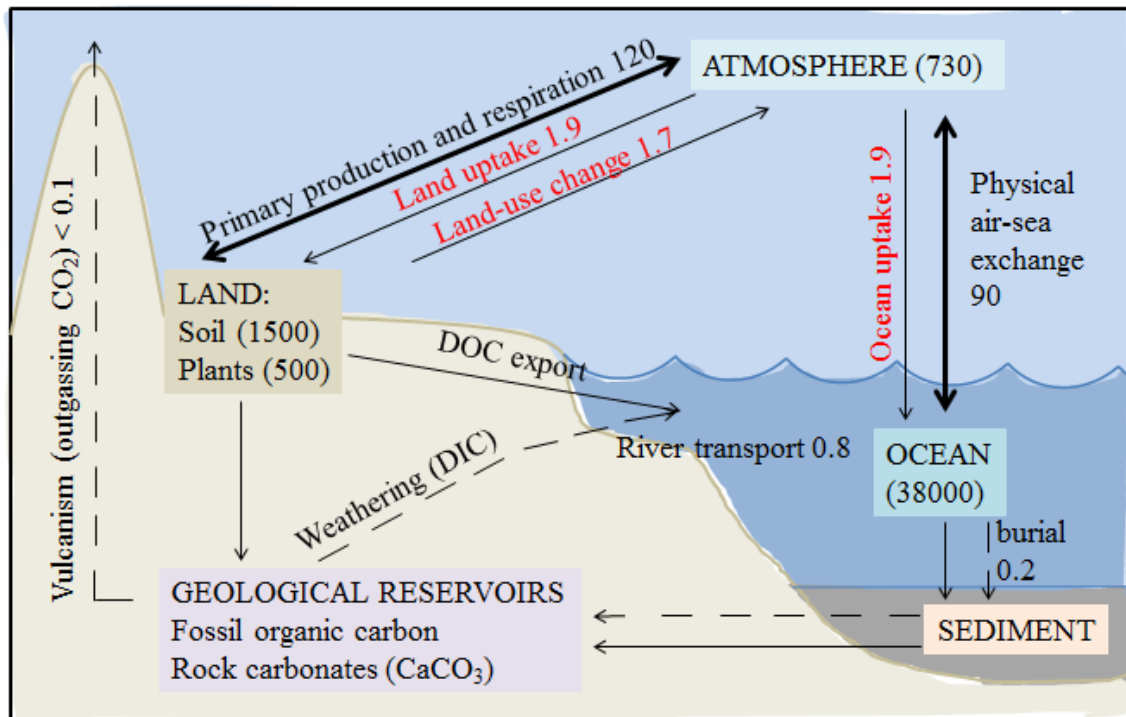


**Figure 1.** The global carbon cycle, main components of the natural cycle (black) and human perturbation (red): storages (Pg C) and fluxes (Pg C/yr) estimated for the 1980s. The thick arrows denote the most important fluxes from the point of view of the contemporary  $\text{CO}_2$  balance of the atmosphere. Dashed lines denote fluxes of carbon as  $\text{CaCO}_3$ . Figure based on Pentice et al. (2001).

In order to minimize the predicted negative consequences of the carbon cycle alteration on mankind, there is a need to develop and implement strategies to reduce  $\text{CO}_2$  emissions and to adapt to these adverse consequences. To take the best decisions in the economic, energy, technology, trade, and security policies, it is necessary to have a good understanding of the global carbon cycle to predict the distribution of carbon compounds under different future  $\text{CO}_2$  emission scenarios. However, there are significant gaps in our knowledge and understanding of the fluxes through the global carbon cycle and the quantification of these fluxes and reservoirs, since there are interactions among physical, chemical and biological processes that hinder their accurate assessment (Honjo et al., 2014). Consequently, this limits our ability to predict the magnitude of changes in the carbon cycle. We require both continuous global

observations and modelling studies to improve our knowledge on the global carbon cycle.

## **2. Carbon in the ocean**

In the ocean, carbon compounds also flux among different reservoirs, driven by physical, chemical and biological processes, within the so-called ocean carbon cycle. Oceanic carbon is mainly connected to atmospheric carbon through the CO<sub>2</sub> exchange (Fig. 1). The ocean is mainly a carbon sink: it has taken up  $118 \pm 18$  Pg of anthropogenic carbon from the atmosphere during the period between the beginning of the industrial revolution and the mid-1990s (Gruber, 2019). This has prevented even higher atmospheric CO<sub>2</sub> concentrations at present (Falkowski et al., 2000; Sabine and Tanhua, 2010). However, the increase of CO<sub>2</sub> in the atmosphere and the associated global warming are having a great impact in the ocean. For example, the CO<sub>2</sub> increase in the atmosphere also causes an increase of dissolved CO<sub>2</sub> in the ocean. This increase is causing ocean acidification, through which the pH of seawater is predicted to decline to 7.8 by the year 2100 (Doney et al., 2009). This will hamper some organisms (pteropods, foraminifera, coccolithophores) to build their CaCO<sub>3</sub> shells, and will dissolve coastal corals (Orr et al., 2005; Doney et al., 2009). On the other hand, global warming is causing sea level rise, increased sea surface temperature and intensified stratification, which also affect mean irradiance levels and nutrient availability in the upper water column of the ocean (Millero, 2007).

### **2.1 Ocean carbon pumps**

Four main processes cause a net flux of inorganic carbon from the atmosphere to the ocean, accounting for the sequestration of CO<sub>2</sub> and therefore contributing to the ocean's buffering capacity for global warming. It must be noticed that sequestration concerns the removal of dissolved inorganic CO<sub>2</sub> from the atmosphere and the surface waters for periods of interest to global warming (i.e. at least a few hundred years) (Legendre and Le Fèvre, 1995). These four processes involved in carbon sequestration are named the ocean carbon pumps, and consist of the “solubility pump”, the “carbonate pump”, the “microbial pump” and the “biological pump” (Sarmiento and Bender, 1994):

-The “solubility pump” consists of the dissolution of CO<sub>2</sub> in the surface water and its posterior transport to its interior driven by the thermohaline circulation. Most of the CO<sub>2</sub> that enters the oceans reacts with seawater, forming carbonic acid, bicarbonate and carbonate (H<sub>2</sub>CO<sub>3</sub>, HCO<sub>3</sub><sup>-</sup> and CO<sub>3</sub><sup>2-</sup>, respectively) (Sabine and Tanhua, 2010) (Fig. 2). In fact, only 1% of the dissolved inorganic carbon (DIC) pool in the ocean is in the form of CO<sub>2</sub>, the molecule required for photosynthesis.



Water mass sinking and hence CO<sub>2</sub> sequestration by physical processes prevail at high latitudes where cold dense water masses are formed, since CO<sub>2</sub> is more soluble in colder than warmer seawater (Broecker and Peng, 1992; Stocker, 1998) (Fig. 3). The carbon removed from the surface to deep waters takes hundreds of years to re-enter the atmosphere.

-The “carbonate pump” consists of the sinking of the biomineral calcium carbonated (CaCO<sub>3</sub>) shells (and to a lesser extent magnesium (MgCO<sub>3</sub>)) formed by phytoplankton and zooplankton species into the interior of the ocean such as coccolithophores and foraminifera. Foraminifera sink up to 2500 m d<sup>-1</sup> (Takahashi and Be, 1984) and coccoliths can be carried in faecal pellets (Honjo, 1980). Half of this carbon is buried in sediments while the other half is dissolved at depth, forming DIC, that will finally return to the atmosphere (Legendre and Le Fèvre, 1995; Falkowski et al., 2000).

-The “biological pump” is the collection of processes that transport organic carbon from the surface euphotic zone to the ocean’s interior, where the material is mineralized and returned to its original dissolved inorganic forms (Hansell et al., 2009; Giering and Humphreys, 2018), being the primary means of removing carbon from the atmosphere and surface ocean on timescales greater than millenia (Honjo et al., 2014). The main pathway of organic carbon formation in the ocean is through photosynthesis by phytoplankton from a fraction of DIC in the euphotic zone, fixing approximately 50 Gt carbon year<sup>-1</sup> (Field et al., 1998; Hugler and Sievert, 2011; De La Rocha and Passow, 2014). The compounds produced by phytoplankton mainly consist of carbohydrates, lipids, proteins and nucleic acids (Giering and Humphreys, 2018), and they can be in the form of particulate (POC) or dissolved (DOC) organic carbon. This organic matter can follow different pathways: the majority of the organic biomass is transformed back to CO<sub>2</sub> by respiration (remineralization) in the surface or consumed by protists and



metazoans, being transferred up the marine food web through predation; 11- 27 % is exported to the dark ocean, below the euphotic zone (Field et al., 1998; Henson et al., 2011), which is called the “biological pump”. This export flux maintains a permanent surface-to-depth CO<sub>2</sub> gradient that is responsible, according to models, of a lower atmospheric CO<sub>2</sub> concentration that would be without ocean biology and the “biological pump” (Volk and Hoffert, 1985; Parekh et al., 2006).

The “biological pump” is driven by three mechanisms: 1) gravitational sinking of POC, mainly formed by phytoplankton, heterotrophic prokaryotes (HP), fecal pellets and gels, 2) downwelling (sinking of higher-density water beneath lower-density water) of POC and DOC 3) active vertical migration of zooplankton (Ducklow et al., 2001; Hansell and Carlson, 2001; Steinberg et al., 2008). The first mechanism is considered the most important pathway, although it is still debatable (Steinberg and Landry, 2017; Stukel et al., 2018; Boyd et al., 2019; Hernández-León et al., 2019). The different methods to determine the efficiency of the “biological pump” through gravitational sinking are reviewed in Bach et al. (2019).

Organic matter in the deep ocean can be remineralized again, although remineralization rates are substantially slower than in surface waters (Ducklow et al., 2001; Ducklow and Doney, 2013). About 0.3 % of the surface production is buried in marine sediments (Dunne et al., 2007), some of which will form rocks or organic rich deposits that will persist for hundreds of millions of years. Ultimately, DIC formed by remineralization of the organic matter in deep water is upwelled and returned to the atmosphere. It is estimated that the “biological pump” transports 5-20 Gt carbon annually from the surface into the ocean interior (below the euphotic zone) (Henson et al., 2011). Depending of the depth reached by organic carbon and where remineralization occurs (remineralization depth), it can take from months to centuries to be returned to the surface for exchange with the atmosphere (Hansell et al., 2009; Kwon et al., 2009). This remineralization depth depends on the balance between particle sinking speeds and their rate of decay (Kwon et al., 2009). It is difficult to predict the response of the pump to ongoing and future changes in the temperature, pH, and oxygen content of the ocean (Henson et al., 2015; Stukel et al., 2015; Siegel et al., 2016).

Part of the organic carbon formed by phytoplankton is used by microbes and transformed in recalcitrant dissolved organic matter. This process is called the

“microbial pump”, since it causes carbon sequestration due to the resistance of this matter to microbial degradation for months to millennia (Jiao et al., 2010; Stone, 2010). The production of refractory DOM is an efficient mechanism of carbon sequestration due to the relatively higher carbon:nitrogen:phosphorus ratio than labile DOM and POC (Hopkinson and Vallino, 2005).

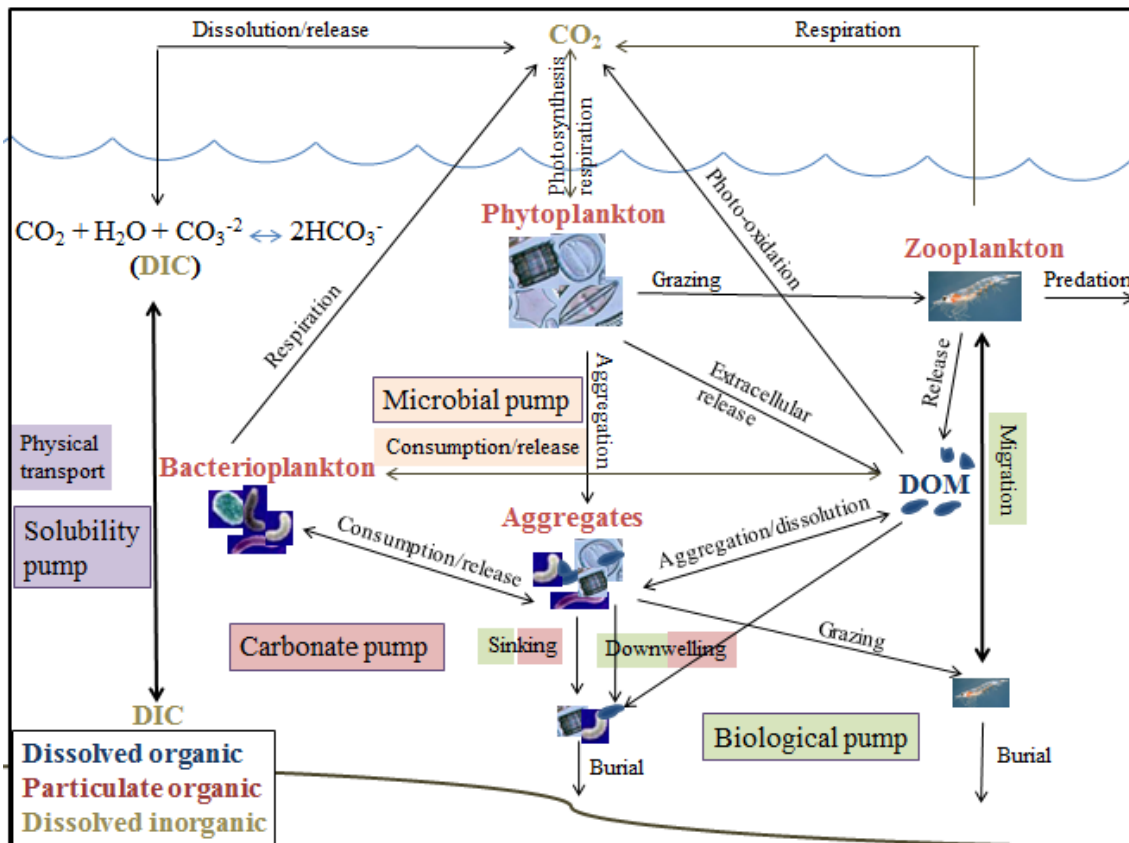


**Figure 2.** Carbon cycling in the ocean and ocean carbon pumps. The main entrance of carbon to the ocean is through  $\text{CO}_2$ , that is dissolved and it can be found in three main forms ( $\text{H}_2\text{CO}_3$ ,  $\text{CO}_3^{2-}$  and  $\text{HCO}_3^-$ ), the sum of which is called dissolved inorganic carbon (DIC). DIC is transported in the ocean by physical and biological processes. Figure done by Marina Z, based on Steinberg and Landry (2017), Pentice et al. (2001), Buchan et al. (2014) and Carlson and Hansell (2015).

## 2.2 Organic carbon in the ocean

The estimated quantity of organic carbon in the ocean is 1000 Pg C (Falkowski et al., 2000). Most of it (662 Pg) exists in the form of dissolved organic carbon (DOC) (Hansell et al., 2009), the same order of magnitude as the total amount of carbon in the atmosphere (750 Pg) (Fasham et al., 2001; Brooks and Thornton, 2018). DOC is operationally defined as the fraction of organic carbon smaller than  $0.7 \mu\text{m}$  (although the size cutoff can vary between  $0.1$  to  $1 \mu\text{m}$ ) (Filella, 2008; Carlson and Hansell,

2015). The organic carbon reservoir in the ocean is complex, containing estimated  $10^{12}$ - $10^{15}$  different organic compounds (Hedges et al., 2002). Thus, the ocean organic carbon pool can be classified depending on properties such as size, chemical composition, lability, physical structure or origin.

-Size: DOM in the ocean can occur as low molecular weight organic matter (LMW-DOM) and high molecular weight organic matter (HMW-DOM, 1-kDa molecular weight cutoff). The rest of organic carbon in the ocean is found in the form of particulate organic carbon (POC), this is, the fraction retained by filters with pore sizes of approximately  $0.7 \mu\text{m}$ . They can reach sizes  $> 10 \text{ cm}$  and tend to sink in the water column. Only a small fraction of the POC pool is formed by living organisms (1-2 Pg C), such as phytoplankton ((Falkowski et al., 2000). The rest occur as non-living components, such as detritus, fecal matter generated by zooplankton and fish, larvacean houses, exuvia, carcasses and plankton hardparts, among others. POC can also occur as organic aggregates that are formed by the adhesion of smaller particles after collision. Organic aggregates are distinguished by size: microscopic aggregates ( $1$  to  $500 \mu\text{m}$ ) and macroscopic aggregates or marine, lake, or river snow ( $> 500 \mu\text{m}$  in diameter), which fall between  $5$  and  $200$  meters per day (Fowler and Knauer, 1986; Alldredge and Silver, 1988; Turner and Millward, 2002). The existence of aggregation and disaggregation processes within the organic matter pool in the ocean makes the division of organic matter into DOC and POC too simplistic. Instead, there is a dynamic continuum of organic matter in different sizes that span the truly dissolved, colloidal, and particulate phases (Verdugo et al., 2004) (Fig. 3).

-Biochemical composition: Three major groups are distinguished; carbohydrates, amino acids and lipids, that together comprise approximately  $80 \%$  of the POC and  $30 \%$  of the DOC fraction, although the percentage varies with depth. Several studies have tried to characterize organic matter by its elemental composition (Aluwihare et al., 2002; Ogawa and Tanoue, 2003; Görs et al., 2007; Shimotori et al., 2016; Cao et al., 2018), but most of it is not chemically characterized (Williams and Druffel, 1987; Hedges et al., 2000; Hansell and Carlson, 2002; Tang et al., 2006).

-Lability: Labile organic matter is the DOM fraction that turns over in time scales of minutes to days. It represents only  $1 \%$  of the global DOC ( $< 0.2 \text{ Pg}$ ) and is present in surface waters mainly. The semilabile DOC turns over in months to years (Cherrier et

al., 1996) and it accumulates in and immediately below the euphotic zone, contributing 3 % of the marine DOC reservoir (50 Gt C) (Carlson et al., 2002; Hansell and Carlson, 2002; Hansell et al., 2009). The refractory DOC is the most abundant fraction (624 Gt C) (Hansell et al., 2009), which turns over in centuries to millennia (Williams and Druffel, 1987), since it does not degrade via the typical microbial and chemical processes that recycle labile and semi-labile DOM. Instead, they can be removed by UV-mediated photolysis at the ocean surface (Mopper et al., 1991), and by transformation to and/or interaction with suspended particles (Druffel et al., 1992)

**-Structure:** Marine gels or hydrogels (Fig. 3) are a distinct group of organic carbon particles due to their structure and behaviour. They are three-dimensional polymer networks embedded in seawater that result from the interaction of organic molecules through physical or chemical connections (Chin et al., 1998; Orellana and Verdugo, 2003; Verdugo et al., 2004; Verdugo, 2012). They are estimated to account for approximately 70 Pg of C in the ocean (Verdugo, 2012). Marine gels can be classified as physical or chemical gels, depending on the type of connections. Physical gels are made up of organic molecules connected physically by low energy ionic forces, hydrophobic linkages, or entanglement, which are continuously being made and broken (Ding et al., 2008). Chemical gels present high-energy covalent bonds and assembly is largely irreversible (Tanaka et al., 1992). Their size can range from ~1 nm to several millimetres (macro gels). In the context of the polymer gel theory, two classes of non-living organic particles have been described based on their stainability, and therefore, their main composition: Transparent exopolymer particles (TEP) and Coomassie stained particles (CSP).

**-Origin:** In pelagic systems, allochthonous organic matter is that whose sources come from external inputs such as the surrounding terrestrial ecosystems, the deep ocean and dust deposition. In contrast, the source of autochthonous organic matter is local primary production (Hunt et al., 2010).

Within the autochthonous organic matter, extracellular exopolymeric substances (EPS) are organic matter compounds of high molecular weight that are excreted by a wide variety of microorganisms (Passow, 2002b; Engel, 2009; Decho and Gutierrez, 2017), such as cyanobacteria (Decho et al., 2005; Han et al., 2014), PH (Grossart et al., 2007; Thavasi and Banat, 2014), and eukaryotic phytoplankton (Mykkestad, 1977, 1995;

Mishra and Jha, 2009; Klein et al., 2011; Raposo et al., 2013). EPS contribute ca. 10-25 % of total oceanic dissolved organic matter (DOM) (Verdugo, 1994; Aluwihare et al., 1997). Some of the functions of EPS are to concentrate nutrients around the organism (Flemming and Wingender, 2001), cell fixation mechanisms (Welch et al., 1999) cell protection (Shimada et al., 1997; Ding et al., 2008) and to solubilise hydrophobic organic chemicals (Decho, 1990). EPS are predominantly composed by polysaccharides (Hoagland et al., 1993), but also contain proteins, lipids, and nucleic acids (Flemming and Wingender, 2001; de Carvalho and Fernandes, 2010; Decho and Gutierrez, 2017). Depending on their source, composition and properties vary; for example, EPS produced by marine PH are sticky, in contrast with those excreted by freshwater/marine eukaryotic phytoplankton and non-marine PH (Kennedy and Sutherland, 1987). The reason is that the former are generally richer in uronic acids that render these macromolecules polyanionic (negatively charged) (De Jong et al., 1979; Kennedy and Sutherland, 1987; Majumdar et al., 1999; Bhaskar and Bhosle, 2005). These sticky macromolecules can form aggregates, such as marine snow (Wotton, 2004). A fraction of EPS are TEP and CSP, classified by their stainability and gel properties. Although TEP and CSP are present as discrete particles, EPS can also be found as cell-surface attached or dissolved molecules (Meng et al., 2013).

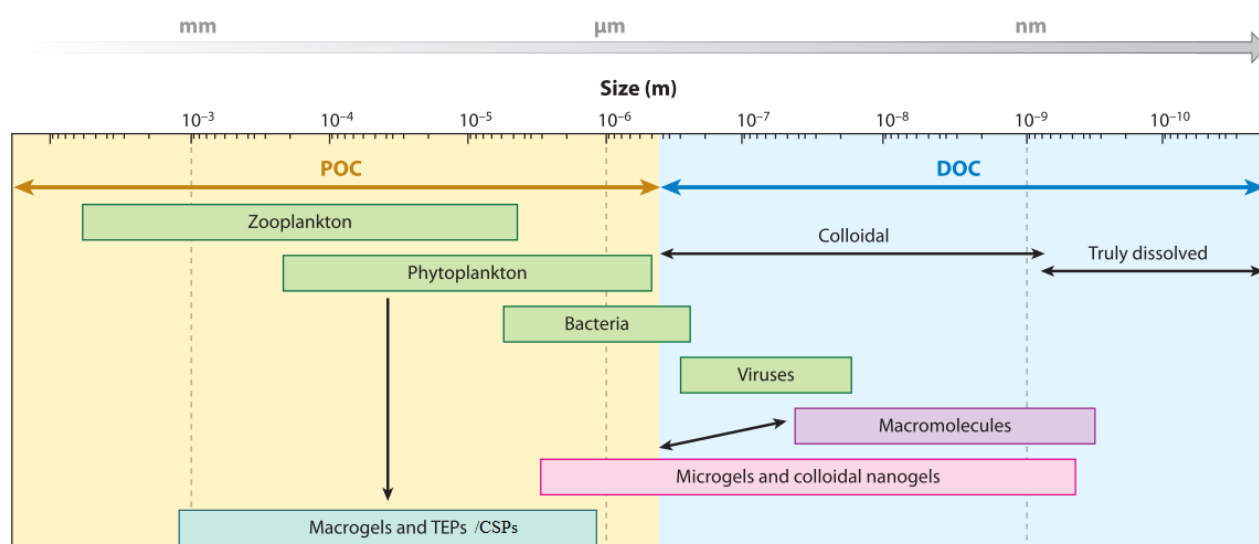


**Figure 3.** Size scale of organic carbon components in seawater. Particulate organic carbon (POC) is considered the material retained in 0.2- $\mu\text{m}$  pore filters, and dissolved organic carbon (DOC) that that percolates through the filter. Figure modified from Verdugo (2012).

### **3. Transparent exopolymer particles (TEP) and Coomassie stainable particles (CSP): Fractions of marine organic matter with an important role in the carbon cycle**

From all the components of organic matter in the ocean, some specific fractions have received interest as they play important roles in biogeochemical processes such as microbial diversity, carbon cycling and carbon exports to the deep ocean and the atmosphere, with further implications in the global carbon cycle. These components are TEP and CSP, and efforts have been made in the latest decades to better understand their role in these processes and to better predict their distribution in the ocean. In the following section, the state of the art about TEP and CSP is described:

#### **Transparent exopolymer particles (TEP)**

##### **-What are TEP? How are they measured? Where are they found?**

Although the presence of gel-like substances suspended in seawater was noticed in the 1970's (Gordon, 1970), transparent exopolymer particles (TEP) were first described by Alldredge et al. (1993) after sample staining with Alcian Blue, a specific dye for carboxylated and sulphated acidic polysaccharides, since it binds ionically with  $-\text{COOH}$  and  $\text{O-SO}_3$  groups (Ramus, 1977; Alldredge et al., 1993; Passow and Alldredge, 1995). TEP are operationally defined as gel particles that are retained on  $0.4 \mu\text{m}$  (sometimes  $0.2 \mu\text{m}$ ; Mari and Robert (2008); Mari et al. (2012); Mari (2008)) polycarbonate filters and stained with the cationic copper phthalocyanine dye Alcian Blue 8GX at pH 2.5 (Fig. 4). Those that occur in sizes between  $0.05$  and  $0.4 \mu\text{m}$  have been classified as colloidal TEP (Villacorte et al., 2009b; Villacorte et al., 2009a), while in the particulate phase they can reach sizes  $> 100 \mu\text{m}$  (Passow, 2002b).

The first method to measure TEP was a microscopic method. It consisted of the filtration of seawater through  $0.4 \mu\text{m}$  Nuclepore filters, which was subsequently stained with Alcian Blue and transferred to a slide to observe and count TEP under a standard light microscopy (Alldredge et al., 1993; Engel et al., 2015). To avoid interference from the filter pores under white light, semitransparent glass slides (CytoClear), that are glazed on one side, can be used (Logan et al., 1994; Engel, 2009; Engel et al., 2015), or TEP can be transferred to transparent glass slides using a freeze-transfer technique

(Hewes and Holm-Hansen, 1983). The advantage of using CytoClear slides is that the particles can be directly viewed on the filter. TEP need to be quantified and sized one by one, manually or automatically, using different microscope magnifications (Fig. 5). TEP concentration is expressed as the number of particles or total surface area covered by TEP per millilitre of water sample. Some disadvantages of the microscopic methods is that stained particles usually do not have strong enough a contrast for subsequent image analysis systems (Passow and Alldredge, 1995), so it is largely time consuming and labour-intensive, which precluded the advance of TEP descriptions in the field. Another disadvantage is that the number of particles in a given water sample may not directly correlate to the mass concentration and quantity of TEP, due to the wide size distribution of TEP. Finally, it is likely that TEP particles harvested for microscopic examination are not all present in a monolayer, so, it is plausible that TEP numbers and the surface area covered by TEP are underestimated (Meng et al., 2013).

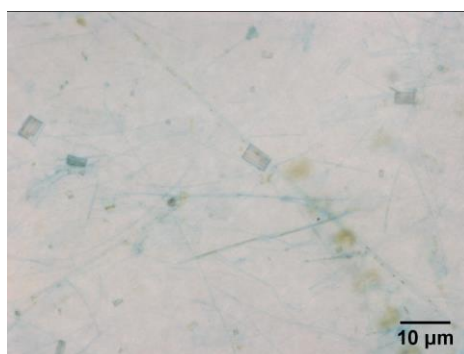


**Figure 4.** Microscopic view of seawater sampled during the ACE cruise on a 0.4  $\mu\text{m}$  membrane filter using a CytoClear slide, and stained with the dye Alcian Blue. TEP appear as blue-stained particles. Phytoplankton cell surfaces are also stained with Alcian Blue. Photo: Marina Z.

In 1995, a spectrophotometric method to measure TEP was developed (Passow and Alldredge, 1995), which was based on the colorimetric determination of the amount of dye complexed with extracellular particles, after being soaked with sulfuric acid to redissolve the dye bound to the particles. This method is a semiquantitative technique, since it uses the relationship between Alcian Blue staining capability with the weight of a polysaccharide (the calibration standard or reference material), and because the staining of TEP is a proxy of TEP acidity, rather than its mass. Many factors influence the measured concentration of TEP, such as the calibration standard (Gum Xanthan or Alginic Acid, Hung et al. (2003a)), the fixation of samples, or the composition (e.g. sulfated or carboxylated) and structure (e.g. linear or branched) of extracellular

polysaccharides. As a consequence, caution must be taken when comparing numerical values of TEP concentrations in natural environments. In addition, pH of the Alcian Blue solution influences the peak of absorbance wavelength (Robinson et al., 2019c). The quantification of TEP relies on calibration against a reference material because the exact TEP chemical composition is unknown and the Alcian Blue staining capacity can be variable for the same weight of Alcian Blue powder. Gum Xanthan (XG) is the most commonly used reference material. The amount of Alcian Blue absorbed to the XG (or another reference material) is directly related to the weight of the XG, so the slope of the linear relationship between the weight of the standard and amount of stain absorbed yields the calibration factor (Engel, 2009). Alcian Blue does not stain cell interiors or colony matrices. The TEP concentration is finally expressed as micrograms of Gum Xanthan equivalent (XG eq.) per liter of water. Lately, some problems have been found doing the calibration (Kuznetsova et al., 2005; Kahl et al., 2008; Harlay et al., 2009; Vardi et al., 2012; Discart et al., 2014), and Bittar et al. (2018) found to be related with the currently available XG powder, that no longer exhibits the same solubility properties as the used in the original method. Consequently, they provided a new protocol for the calibration, using the new, commercially available XG powder (Bittar et al., 2018). There are also some challenges related with the spectrophotometric method. The staining capacity of Alcian Blue is related to its concentration (Passow and Alldredge, 1995) and it undergoes self-coagulation over time, causing a significant reduction of dye concentration. For this reason, the dye solution must be filtered before use and it must be calibrated with high frequency. It has been proposed to express TEP level relative to a referenced TEP concentration, but it would make the quantitative interpretation of the results difficult and uncertain (Villacorte et al., 2009b).

The choice between the microscopic or the spectrophotometric method depends on the purpose of the study. The advantage of the microscopic method is that allows the observation and quantification of individual TEP particles, as well as their size distribution and total area.

The FlowCAM method has been developed recently by Cisternas-Novoa et al. (2015). It consists of the addition of Alcian Blue to aqueous samples and the later visualization of in-situ particles with the FlowCAM flow-imaging microscope. The method allows to measure parameters as shape, size and transparency of the particles and their total



concentration. It measures TEP (defined as  $> 0.4 \mu\text{m}$ ), but also acidic polysaccharides ( $< 0.04 \mu\text{m}$ ), without distinguishing if they are free or attached to cells. In the case of seawater samples, a previous dialysis step to desalt marine samples is required for quantitative applications. Otherwise, salts present in seawater interfere with the direct staining of marine samples (Passow and Alldredge, 1995; Hayat, 2000), and only a qualitative study is possible.

Another method is the centrifugation method (Arruda Fatibello et al., 2004), only usable for freshwater samples. It consists of the filtration of water through  $70 \mu\text{m}$  to remove large particles such as zooplankton and phytoplankton and subsequent tangential filtration through  $0.45 \mu\text{m}$  to concentrate TEP. Alcian Blue is added into harvested TEP sample, and the insoluble pigments produced after the reaction between acidic group of polysaccharides and Alcian Blue are separated by centrifugation. Finally, the excess of Alcian Blue remaining in the sample is measured at  $602 \text{ nm}$  and the difference between total Alcian Blue added to the sample and that left after centrifugation represents the quantity of TEP in the samples. The units are micrograms of XG  $\text{eq mL}^{-1}$ . A drawback of this method is that TEP larger than  $70 \mu\text{m}$  are removed, even though the size range of TEP typically is  $2\text{-}200 \mu\text{m}$  (Berman and Passow, 2007). Finally, the method cannot distinguish TEP from other dissolved acid polysaccharides in terms of their sizes (Meng et al., 2013).

A general disadvantage of all these methods is that Alcian Blue can form insoluble pigments with dissolved substrates in aqueous solution or to be adsorbed by many inert substances other than TEP present in water samples (Horobin, 1988). As a consequence, this leads to a remarkable uncertainty in the determination of TEP by the Alcian Blue - based staining methods. The combination of Alcian Blue with other analyses, such as LC-OCD (liquid chromatography-organic carbon detection), could be useful for a better interpretation of TEP results (Meng et al., 2013). Another drawback is that depending on the presence and the number of acidic groups  $-\text{COOH}$  and  $\text{O-SO}_3$  “available” to bind with Alcian Blue, the staining efficiency of TEP varies. Consequently, the staining is a proxy of an inherent TEP property (its acidity), rather than its mass, and therefore the technique provides only a semiquantitative assessment of TEP concentration (Bittar et al., 2018).

TEP are ubiquitous in aquatic systems, including freshwater and seawater. TEP abundance is usually in the order of  $10^6$  particles  $L^{-1}$ , although during phytoplankton blooms, higher abundances have been reported (in the order of  $10^8$  particles  $L^{-1}$  or  $1000 \mu\text{g XG eq } L^{-1}$ ). TEP concentrations are generally higher in the euphotic zone and surface mixed layer than below it, in coastal areas compared to the open ocean, and in vernal seasons than out of them (Passow, 2002b).

### **-What are the sources of TEP? How are they formed?**

The main sources of TEP are microorganisms, due to algal exudation, bacterial mucus and the gelatinous envelopes that surround phytoplankton (Hong et al., 1997; Berman-Frank et al., 2007). Until nowadays, the phytoplankton groups that have been found to produce TEP are cyanobacteria (Grossart et al., 1998; Mazuecos, 2015; Deng et al., 2016), diatoms (Passow and Alldredge, 1994; Mari and Kiorboe, 1996; Passow, 2002a), dinoflagellates (Passow and Alldredge, 1994), Prymnesiophyceae (Riebesell et al., 1995; Engel, 2004; Leblanc et al., 2009) and Cryptomonads (Kozłowski and Vernet, 1995; Passow et al., 1995a). They are thought to be the primary source of TEP due to the general positive relationship between TEP and Chl *a* concentration on a global scale (Passow, 2002a; Kodama et al., 2014). In addition, heterotrophic prokaryotes (Biddanda, 1986; van Loosdrecht et al., 1989; Stoderegger and Herndl, 1998; Passow, 2002a; Cho et al., 2004; Radic et al., 2006; Ortega-Retuerta et al., 2010; Ortega-Retuerta et al., 2019), seagrass (Iuculano et al., 2017b), macroalgae (Ramaiah et al., 2001; Thornton, 2004), zooplankton (Prieto et al., 2001) and benthic suspension feeders (Heinonen et al., 2007) are also able to produce TEP.

There are two pathways for the formation of TEP (Fig. 5): In the direct pathway (Fig. 6A), TEP (0.4  $\mu\text{m}$ -300  $\mu\text{m}$ ) are directly released by organisms to the aquatic environment, for example via sloughing and lysis of senescent colonies (Hong et al., 1997; Beauvais et al., 2003; Berman-Frank et al., 2007). In the indirect pathway (Fig. 6), the organisms release TEP precursors in the form of dissolved polymers, particularly certain classes of dissolved polysaccharides, that self-assemble abiotically forming TEP by coagulation, gelation or annealing (Passow and Alldredge, 1994; Logan et al., 1995; Passow, 2000, 2002b; Thuy et al., 2015). The abiotic processes promoting TEP assembly include Brownian motion, laminar shear and water turbulence (Passow, 2000; Burd and Jackson, 2009). TEP self-assembly process has been described as an

alternative pathway to form particulate organic carbon from DOM, hence a DOM sink that is alternative to DOM consumption by microorganisms (Engel et al., 2004b).

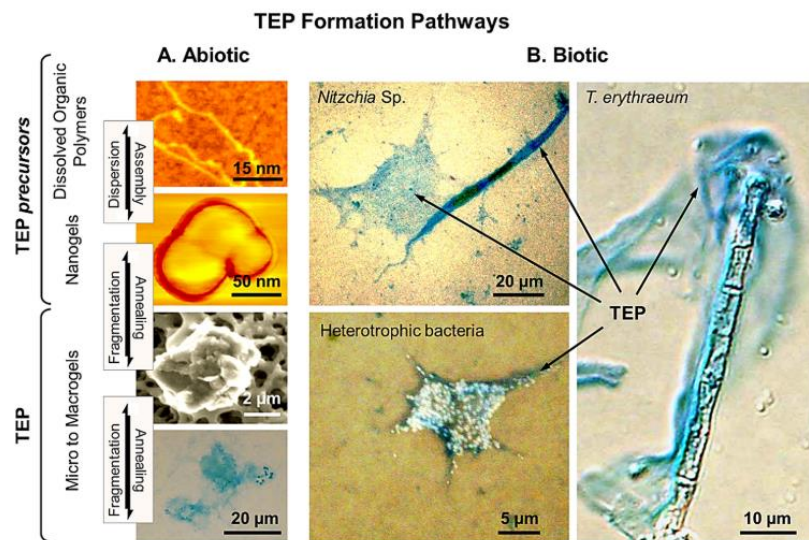


**Figure 5.** TEP formation pathways; A. Abiotic and B. Biotic. Figure from Bar-Zeev et al. (2015).

### -What are the composition and properties of TEP?

TEP are mainly composed of acidic polysaccharides, enriched in deoxysugars and covalently bound sulfate (Mopper et al., 1995). However, their exact chemical composition is not known, and can be highly variable depending on the species that release them and the prevailing growth conditions (Mopper et al., 1995; Mykkestad, 1995; Zhou et al., 1998; Aluwihare and Repeta, 1999; Passow, 2002b). It is known that TEP present similar composition to EPS, containing polysaccharides, proteins, lipids and amino acids (Passow, 2002b). They present gel properties, like high flexibility, high stickiness (defined as the probability that two particles remain attached after collision) (Engel, 2000; Engel, 2004) and their volume to mass ratios depend on environmental factors, like pH, temperature, pressure and ion density (reviewed in Passow (2002b)). Their stickiness is due to their highly content of active polysaccharides that tend to form strongly metal ion bridges and hydrogen bonds (Mopper et al., 1991; Passow, 2002b). Their stickiness is about 2 to 4 orders of magnitude higher than those of phytoplankton or mineral particles (Passow, 2002b; Engel et al., 2004b; Mari and Dam, 2004), and consequently, they trigger aggregation of various organic and mineral solid particles from natural or anthropogenic origin (Passow and De La Rocha, 2006; Long et al., 2015; Mari et al., 2017; Zhao et al., 2017). They are deformable particles and appear in

various forms, e.g., amorphous blobs, strings, films, sheets, clumps or clouds. TEP often have a density significantly lower than seawater (Azetsu-Scott and Passow, 2004).

### **-What are the sinks of TEP?**

TEP can be captured and ingested by protists and small zooplankton (Decho and Moriarty, 1990; Shimeta, 1993; Tranvik et al., 1993; Dilling et al., 1998; Passow and Alldredge, 1999; Ling and Alldredge, 2003), but also larval stages of metazoans (Bochdansky and Herndl, 1992) and fish (Grossart et al., 1998), when TEP form marine snow. PH can also utilize TEP, although it depends heavily on their chemical composition, since not all the components of TEP are labile (Zhou et al., 1998; Aluwihare and Repeta, 1999; Passow et al., 2001; Simon et al., 2002; Taylor and Cunliffe, 2017). TEP are also colonized by PH (Alldredge et al., 1993; Schuster and Herndl, 1995; Mari and Kiorboe, 1996), which can release exopolymeric enzymes (mainly fucosidase,  $\beta$ -glucosidase and esterase) that converts high-molecular-weight organic matter into smaller substrates (Weiss et al., 1991; Bar-Zeev and Rahav, 2015), that can be transported into the cells (Arnosti, 2011).

Aggregates containing TEP can also be fragmented by organisms such as euphausiids (Dilling and Alldredge, 2000), or under UVB radiation (Orellana and Verdugo, 2003; Ortega-Retuerta et al., 2009a).

Another loss process of TEP is sedimentation and burial in sediments; TEP can associate with other particles and sink into the deep ocean (Passow et al., 2001; Engel, 2004), where they will be respired, converted back to CO<sub>2</sub>, or buried in the sediments. TEP favour aggregate-formation by two mechanisms; they increase bulk particle volume concentration and hence collision rates between particles, and they raise the bulk stickiness of particles (Engel, 2004). However, since TEP by themselves are low dense, the proportion of TEP with respect to other particles in aggregates will determine their sinking rates (Mari et al., 2017).

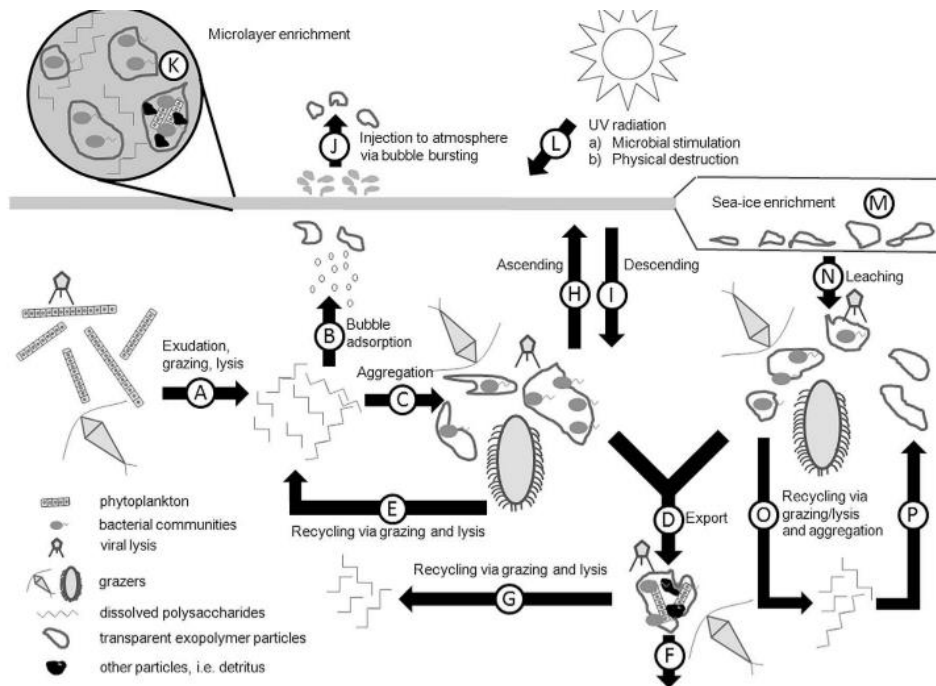


**Figure 6.** Conceptual model of TEP cycling in the ocean. TEP are released through exudation, grazing and lysis (A). TEP can form aggregates with other components (C) or be recycled via grazing (zooplankton consume TEP, potentially releasing TEP precursors) and lysis (E, P, O). TEP that forms aggregates can sink in the deep ocean (D, F). TEP can also ascend in the column water, by itself due to the low density (H), or through bubble adsorption (B). TEP can also be formed in the SML (K), grow, and sink back into the water column (I). The sinking versus ascending velocities of TEP ((H) and (I)) are affected by the relative proportions of POC, TEP, and interstitial water within aggregates and by the density of the surrounding water. TEP in the SML can also be released to the atmosphere via bubble bursting (J). In the SML, UV radiation can stimulate TEP production by microorganisms as a protection mechanism, but it can also produce photolysis (L). Ice is a source of TEP in the ocean (M). Figure from Wurl et al. (2011a).

TEP present in the surface microlayer (SML) can be released to the atmosphere by bubble bursting (Aller et al., 2005; Kuznetsova et al., 2005; Leck and Bigg, 2005; Bigg and Leck, 2008; Russell et al., 2010; Orellana et al., 2011; O'Dowd et al., 2015; Rastelli et al., 2017). The SML is operationally defined as the top 50-10  $\mu\text{m}$  of the ocean surface (Wurl et al., 2009; Cunliffe and Wurl, 2014) and it is usually enriched in TEP (Wurl et al., 2016). TEP can ascend in the column water due to their low density when they are not ballasted by detritus or other organic matter, at rates of 0.1-1  $\text{m d}^{-1}$  (Passow, 2002a). The ascension is greatly enhanced by bubble-associated scavenging (Zhou et al., 1998; Azetsu-Scott and Passow, 2004; Robinson et al., 2019a; Robinson et al., 2019c), which can be formed by wind, density gradients, respiration of marine organisms and the release of trapped bubbles from within melting ice (Norris et al., 2011). TEP can also be produced directly at the microlayer (Wurl et al., 2011a). It is not known to what extent

transferred TEP remain in the atmosphere or return back to the SML, which is likely dependent on atmospheric features (Fig. 6).

### **-What influences the sources and sinks of TEP?**

There are many factors that influence TEP production. Regarding production by phytoplankton, different species generate different amounts of TEP. For example, it was observed with batch cultures that Chl *a*-related TEP production by *Emiliana huxleyi* (coccolithophorid) was smaller than that produced by *Phaeocystis antarctica* (prymnesiophyte) (Hong et al., 1997; Passow, 2002a). However, it has been observed that TEP production by the same species can also vary widely depending on a number of variables. One of the variables is the physiological state, since the release of TEP is usually different depending of the growth phase of the cycle, and varies among species (Passow, 2002a). For example, *Phaeocystis antarctica* generate TEP during growth, stationary phase and senescence (Hong et al., 1997), whereas other species (i.e. colonial cyanobacteria) only release TEP during senescence, despite the fact that a cell surface mucus coat can be formed during growth (Grossart and Simon, 1997; Grossart et al., 1998). Along this same line, it has been observed that nutrient depletion usually favours TEP production due to dissolved inorganic carbon overconsumption, although its effect can vary depending on the major inorganic nutrient that is first depleted (nitrogen or phosphorus): In concrete, P over N limitation enhances TEP production by microbes (Chen; Corzo et al., 2000; Staats et al., 2000; Engel et al., 2002a; Passow, 2002a; Underwood et al., 2004; Mari et al., 2005; Beauvais et al., 2006; Radic et al., 2006; Berman-Frank et al., 2007; Schartau et al., 2007; Pedrotti et al., 2010). However, large TEP production also occur under nutrient-replete conditions (Claquin et al., 2008). Temperature can also modulate TEP production by phytoplankton, although it is species-specific (Claquin et al., 2008). For example, in *Thalassiosira pseudonana*, TEP production increases with temperature until a maximum TEP release rate at ~25 °C and then decreases. However, in *Emiliana huxleyi*, no relationship was found between temperature and TEP production (Claquin et al., 2008). CO<sub>2</sub> concentrations also affect TEP production by phytoplankton; a positive relationship was observed on most occasions by Engel (2002) and Pedrotti et al. (2012). Viral infection is promotor of TEP production by several phytoplankton taxa, such as *Emiliana huxleyi* (Vardi et al., 2012; Nissimov et al., 2018), *Phaeocystis globosa* (Grossart et al., 1998; Brussaard et al.,

2005; Mari et al., 2005) and *Micromonas pusilla* (Lønborg et al., 2013). Interactions between microbes also influence TEP production (Guerrini et al., 1998). For example, under in vitro conditions, the attachment of specific bacterial strains to *Thalassiosira weissflogii* is necessary for TEP production (Grossart et al., 2006; Gärdes et al., 2011). PH influence TEP production by *Emiliana huxleyi* (Van Oostende et al., 2013) and by *Prochlorococcus* (Cruz and Neuer, 2019), and they can also increase the stickiness of phytoplankton-derived EPS (Grossart et al., 2006; Rochelle-Newall et al., 2010; Cruz and Neuer, 2019)

However, it must be noted that under nutrient limitation, the influence of PH on TEP production may also differ. In fact, the presence of associated PH may have a role in algal TEP production except under stressing conditions such as nitrogen limitation (Pannard et al., 2015) or nutrient imbalances (Gärdes et al., 2012).

Oxidative stress caused by ultraviolet radiation (UVR), high photosynthetic active radiation (PAR) and hydrogen peroxide (H<sub>2</sub>O<sub>2</sub>) stress can also induce TEP production by *Synechococcus* (Callieri et al., 2019). High solar radiation has also been observed to favour TEP release due to *Prochlorococcus* cell decay (Iuculano et al., 2017c). Turbulence can increase TEP due to the enhancement of autotrophic production (Pedrotti et al., 2010).

The formation of TEP by heterotrophic prokaryotes and other organisms such as macroalgae also varies between species, growth conditions and activity (Schuster and Herndl, 1995; Grossart, 1999; Stoderegger and Herndl, 1999; Ramaiah et al., 2001). For example, the production of polysaccharide by PH is increased under P limitation (Mohamed et al., 1998) .

The formation of TEP through abiotic assembly and the dissolution/fragmentation of TEP also depend on a number of variables. For example, light can favour the abiotic self-assembly of dissolved precursors into TEP (Shammi et al., 2017), but it can also cause TEP photolysis (UVB radiation specifically) (Ortega-Retuerta et al., 2009a) and inhibit the self-assembly of TEP precursors (Orellana and Verdugo, 2003). PH may also facilitate self-assembly, e.g., through the release of amphiphilic exopolymers that induce microgel formation (Ding et al., 2008). Turbulence has been shown to favour TEP assembly due to the enhancement of encounter rates of TEP-precursors

(Stoderegger and Herndl, 1999; Burns et al., 2019). Dust deposition has also been suggested to trigger the abiotic formation of TEP, leading to the formation of organic-mineral aggregates (Louis et al., 2017).

The sink of TEP through degradation by organisms can be influenced by the nutrient availability, since nutrient limitation has been observed to impede prokaryotic consumption of TEP (Bar-Zeev and Rahav, 2015). It also depends on the chemical composition of TEP as long as it influences their lability.

Regarding the release of TEP to the air into small droplets of sea spray (Andreae, 2009) (Zhou et al., 1998; Leck and Bigg, 2005), it is affected by wind friction, bubble bursting and breaking waves (Andreae, 2009), which are the main factors that affect sea spray production.

### **-Why are TEP important?**

TEP play important roles in ecosystem properties and biogeochemical processes such as microbial diversity, carbon cycling and carbon exports to the deep ocean and the atmosphere, with implications in the global carbon cycle.

On the one hand, TEP play an important role in the biological carbon pump, which eventually affects the long-term ocean-atmosphere CO<sub>2</sub> exchanges. The influence of TEP in the biological pump is due to two reasons. TEP comprise by themselves around 5-10 % of the planktonic primary production (Mari et al., 2017), which can sink into the deep ocean through the biological carbon pump. In addition, TEP promote the formation of larger aggregates of organic matter such as marine snow and the vertical export of carbon from surface to deep waters (Passow et al., 2001; Passow, 2002b; Verdugo et al., 2004), thereby enhancing the biological carbon pump. Thanks to the sinking of the carbon fixed in the upper ocean favoured by TEP, this carbon can stay in the deep oceans for hundreds to millions of years before returning to the atmosphere, constituting a powerful way of carbon sequestration. Consequently, there is a need to better predict the role of TEP in the biological carbon pump.

TEP present in the SML, where they are usually enriched (Azetsu-Scott and Passow, 2004; Aller et al., 2005; Kuznetsova et al., 2005; Wurl and Holmes, 2008; Cunliffe et al., 2009; Wurl et al., 2009; Wurl et al., 2011b; Gao et al., 2012; Karavoltzos et al.,



2015; Wurl et al., 2016), also affect air-sea gas exchange. Some studies, reviewed in Cunliffe et al. (2013), show the influence of surface active components of the SML (including biogenic polysaccharides, TEP among them) on air-sea gas exchange, either acting as a physicochemical barrier or modifying sea surface hydrodynamics, which in turn results in a suppression of air-water gas exchange, such as CO<sub>2</sub> (Calleja et al., 2009; Jenkinson et al., 2018).

TEP also seem to affect the chemistry and physics of the Earth's atmosphere, influencing cloud formation and climate. Consequently, marine organic matter in the surface ocean should be included in aerosol climate models (Orellana et al., 2011; Brooks and Thornton, 2018). The reason is that TEP present in the SML can be released to the atmosphere and form aerosols (solid or liquid particles suspended in the air) (Aller et al., 2005; Kuznetsova et al., 2005; Bigg and Leck, 2008; Russell et al., 2010; Orellana et al., 2011; Leck et al., 2013; Wilson et al., 2015; Rastelli et al., 2017). Aerosols influence the radiation balance of the earth since they scatter and absorb solar radiation, either directly or acting as cloud condensation nuclei (CCN) and ice-nucleating particles (INPs) (Slingo, 1990; O'Dowd et al., 1999; Wilson et al., 2015). CCN are aerosol particles that have the potential to nucleate liquid droplets, forming clouds (Andreae and Rosenfeld, 2008). It must be taken into account that although TEP are operationally defined as particles with sizes > 0.4 µm, smaller TEP can also act as CCN and INP, and they are more abundant. Aerosols with a largest contribution to the CCN and INPs pools are those with a size range of 0.05-1 µm (Simó, 2011), due to their highest abundance, although larger particles are more efficient as CCN.

TEP also provide surfaces for microbial colonization (PH, algae and picocyanobacteria that remain attached) (Passow and Alldredge, 1994; Mari and Kiorboe, 1996; Worm and Søndergaard, 1998; Passow, 2002b; Azam and Malfatti, 2007; Berman and Parparova, 2010; Zäncker et al., 2019), serving as “hot spots” of intense microbial and chemical activity within the water mass, and playing an active role in the development of aquatic biofilms (Berman and Hølenberg, 2005; Bar-Zeev et al., 2012; Meng et al., 2013; Bar-Zeev et al., 2015). The process of attachment of PH to aggregates is not yet clear, but it is suggested that PH join passively to aggregates (Mari and Kiorboe, 1996), or that PH could actively colonize them (Kiorboe and Thygesen, 2001). In addition, bacterial community composition associated with TEP is different from that of free-

living PH in the surrounding water, and attached PH express high cell-specific enzymatic activities (Lemarchand et al., 2006). Since predation by zooplankton of PH is dependent on the size of prey, TEP concentration could affect the proportion of free vs attached PH, and consequently the availability of PH to zooplankton (Burd and Jackson, 2009; Deng et al., 2015). It has been demonstrated the reduction of prey availability for micro-grazers under high TEP concentrations due to the increase of food size spectra, whereas it may become available for large-particle grazers (Mari and Rassoulzadegan, 2004).

TEP aggregates, with their associated flora and fauna, can also serve as “food packages” for protists, microzooplankton and even larval fish (Grossart et al., 1998). TEP also affect food web dynamics in benthic and pelagic ecosystems. For example, suspension feeders produce TEP, that, in turn, favour particle deposition and delivery of POM to the benthos, strengthening the degree of benthic-pelagic coupling (Heinonen et al., 2007). TEP have also been found in hydrothermal plumes, where they could support populations of attached PH and serve as a potential food source to zooplankton (Shackelford and Cowen, 2006).

TEP are able to absorb trace elements and nutrients such as thorium (Th) (Guo et al., 2002; Quigley et al., 2002; Azetsu-Scott and Niven, 2005; Santschi et al., 2006). Recently, it has also been detected that TEP could be a key factor affecting the fate and toxicity of nanoplastics on marine diatoms, since they promote the aggregation of nanoplastics (González-Fernández et al., 2019), and their particle size may affect their toxicity (Paul-Pont et al., 2018).

### **Coomassie stainable particles (CSP)**

#### **-What are CSP? How are they measured? Where are they found?**

Coomassie stainable particles (CSP) were first described and measured by Long and Azam (1996) off the Scripps Pier (Southern California) and in the Arabian Sea. CSP are defined as gel particles retained on 0.4 µm polycarbonate filters that are stained with a solution of Coomassie Brilliant Blue G (CCB) at pH 7.4 (Long and Azam, 1996) (Fig. 7). This dye is amino acid-specific (Bradford, 1976), and therefore, CSP are protein-containing particles. The average concentration of CSP in the ocean according to

published studies is  $721 \pm 2622 \text{ mm}^2 \text{ L}^{-1}$ , and in terms of particle abundance,  $47 \times 10^6 \pm 61 \times 10^6 \text{ particles L}^{-1}$  (reviewed in Thornton (2018)).

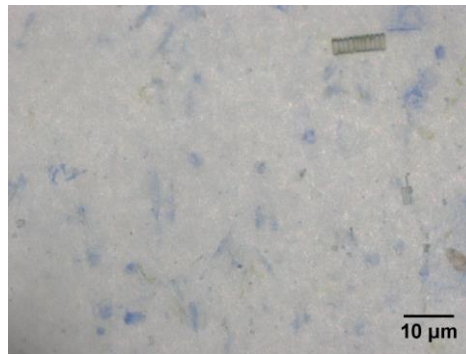


**Figure 7.** Microscopic view of seawater sampled during the ACE cruise on a  $0.4 \mu\text{m}$  membrane filter using a CytoClear slide, and stained with the dye Coomassie brilliant blue. CSP appear as blue-stained particles. Photo: Marina Z.

The microscopic method was the first developed to measure CSP in water (Fig. 7), and only recently a new colorimetric method was developed, which consists of the extraction of a dye complexed to protein-containing particles with isopropanol. It is a semiquantitative technique, where several factors influence the measured concentration, such as the calibration standard (bovine serum albumin), or the composition of proteins. As a consequence, caution must be taken when comparing values of CSP concentrations in natural environments. The FlowCAM method developed by Cisternas-Novoa et al. (2015) also allows to measure CSP, as described for TEP in the previous section, but adding CBB instead of Alcian Blue to the water sample.

#### **-Which are the sources of CSP?**

Studies on the sources of CSP have only been conducted with cultures of diatoms (Bhaskar et al., 2005; Grossart et al., 2006; Galgani and Engel, 2013; Thornton, 2014; Thornton and Chen, 2017) and cyanobacteria (Endres et al., 2013; Cisternas-Novoa et al., 2015; Thornton and Chen, 2017), but it is likely that other phytoplankton groups, heterotrophic protists and PH are also sources. In fact, PH have already been thought to produce CSP (Radic et al., 2006). It has been suggested (Cisternas-Novoa et al., 2015), but not demonstrated explicitly, that CSP can also be formed through abiotic self-assembly from precursors with divalent cations.

**-What are the composition and properties of CSP?**

CSP are protein-enriched particles, but the exact composition of these proteins is not known, and CSP can also embed other classes of organics. Since it is assumed that CSP are largely derived from phytoplankton, the composition of CSP likely reflects the composition of phytoplankton proteins, since 65% in weight of phytoplankton cells are proteins (Hedges et al., 2002). Assuming that CSP has a C:N ratio similar to that of average plankton protein (3.8:1, Hedges et al. (2002)), then the nitrogen content of CSP is five to seven times greater than in TEP (Thornton, 2018). Efforts have been done in the last years to elucidate if TEP and CSP are totally different or overlapping components, since the stains, both blue and thus indistinguishable, cannot be combined in a single sample. These previous studies seem to indicate that TEP and CSP are different populations of exopolymer particles (Cisternas-Novoa et al., 2015; Thornton and Chen, 2017), as in situ measurements indicate that TEP and CSP present different distributions and dynamics (Cisternas-Novoa et al., 2015; Thornton et al., 2016). Physical properties of CSP, such as density or stickiness, remain unknown.

**-What are the sinks of CSP?**

Since microbial colonization of CSP has been observed (Long and Azam, 1996), it is thought, but not demonstrated, that CSP can be degraded by prokaryotes (Endres et al., 2013; Cisternas-Novoa, 2015; Engel et al., 2015). It is also plausible that heterotrophic protists and mixotrophic phytoplankton may affect the breakdown of CSP. CSP have also been found enriched in the sea surface microlayer (Wurl et al., 2011b; Engel and Galgani, 2016; Galgani et al., 2016; Thornton et al., 2016; Zancker et al., 2017; Sun et al., 2018), thus it is likely that they are released to the atmosphere. Indeed, protein particles have been observed in sea spray aerosols (Kuznetsova et al., 2005; Aller et al., 2017; Dall'Osto et al., 2017).

**-What influences the sources and sinks of CSP?**

Very few studies have looked at drivers of CSP production and degradation. Physical disruption of the cells, through mechanisms such as sloppy feeding by grazers (Møller et al., 2003; Møller, 2007) and viral lysis (Bratbak et al., 1993; Gobler et al., 1997; Mojica et al., 2016), would be expected to play a significant role in CSP production.

However, Thornton and Chen (2017) showed that, in contrast with TEP, CSP dynamics did not correlate to indicators of phytoplankton stress and cell death.

### **-Why are CSP important?**

The little information available on CSP in the ocean points to their importance in marine processes. It has been observed that CSP are usually enriched in the surface microlayer in a greater extent than TEP (Engel and Galgani, 2016; Galgani et al., 2016; Thornton et al., 2016), so they could have an impact on air-sea gas exchanges.

In addition, CSP and protein compounds have been observed in sea spray aerosols (Kuznetsova et al., 2005; Aller et al., 2017; Dall'Osto et al., 2017), so it is plausible that CSP can be released to the atmosphere through bubble bursting, forming aerosols that affect the Earth's radiative budget (Brooks and Thornton, 2018).

CSP are also appropriate habitats for HP colonization, and the associated HP community composition is different from that of free-living HP in the surrounding water (Lemarchand et al., 2006). It has been suggested that they could be a source of carbon and nitrogen for bacterioplankton (Ding et al., 2008).

In contrast, it is believed that CSP do not enhance particle aggregation in the biological carbon pump context (Prieto et al., 2002; Cisternas-Novoa et al., 2015), although more studies are needed to confirm or reject this hypothesis.

**Table 1.** Summary of some characteristics of TEP and CSP.

	TEP	CSP
First discover	Allredge et al. (1993)	Long and Azam (1996)
Composition	Acidic polysaccharides	Proteins
Size	>0.4 $\mu\text{m}$	>0.4 $\mu\text{m}$
Used stain	Alcian Blue	Coomassie Brilliant Blue
Processes affected		
- <i>Air-sea exchanges</i>	√	√
- <i>Carbon export</i>	√	?
- <i>Microbial diversity</i>	√	√
- <i>Trace elements and nutrients</i>	√	?
- <i>Nanoplastics fate</i>	√	?

#### 4. Expanding the knowledge of TEP and CSP distributions across the ocean

There is a need to gather in situ measurements of these particle types, in order to better understand and predict the different processes affected by the presence of these substances. However, due to the limitations of the quantification protocols, in situ measurements of TEP and CSP in the ocean are scarce, especially for CSP (Fig. 8). The development of the spectrophotometric methods has allowed processing a large number of samples in shorter times. Consequently, the number of measurements is gradually increasing.

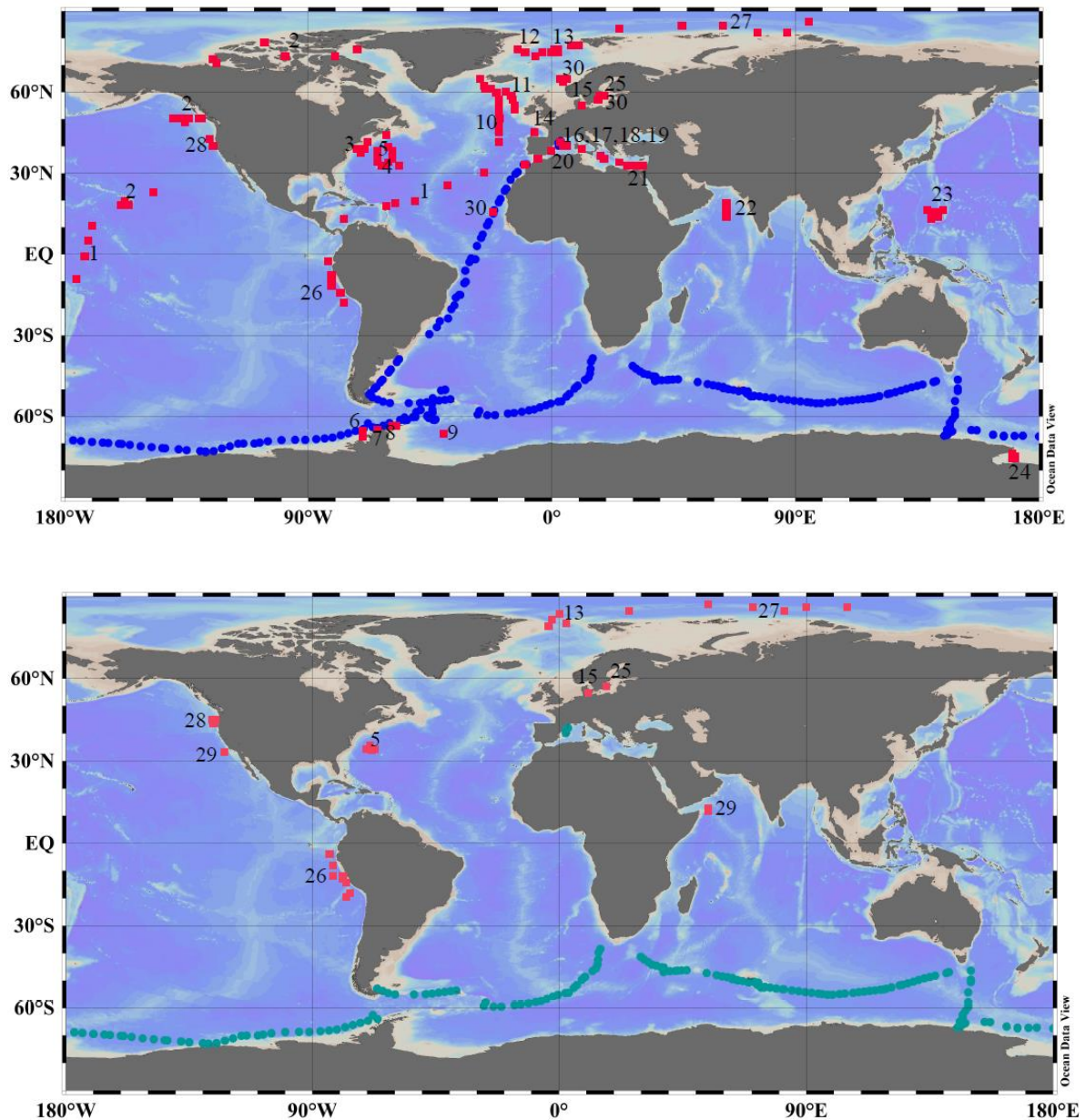


**Figure 8.** Map showing TEP (upper panel) and CSP (bottom panel) measurements available in the literature (red symbols) and performed in this thesis (blue symbols): 1. Iuculano et al. (2017c); 2. Wurl et al. (2011a); 3. Aller et al. (2017); 4. Jennings et al. (2017); 5. Cisternas-Novoa et al. (2015); 6. Passow et al. (1995b); 7. Corzo et al. (2005); 8. Ortega-Retuerta et al. (2009b); 9. Marchant et al. (1996); 10. Engel (2004); 11. Leblanc et al. (2009); 12. Engel et al. (2017); 13. Busch et al. (2017)\*; 14. Harlay et al. (2009); 15. Dreshchinskii and Engel (2017)\*; 16. Ortega-Retuerta et al. (2010); 17. Ortega-Retuerta et al. (2017); 18. Ortega-Retuerta et al. (2018); 19. Ortega-Retuerta et al. (2019); 20. Iuculano et al. (2017a); 21. Bar-Zeev et al. (2011); 22. Ramaiah et al. (2000); 23. Kodama et al. (2014); 24. Hong et al. (1997); 25. Cisternas-Novoa et al. (2019); 26. Engel and Galgani (2016)\*; 27. Galgani et al. (2016)\*; 28. Thornton et al. (2016)\*; 29. Long and Azam (1996)\*; 30. Robinson et al. (2019b). \*microscopic method.







Gerlache Strait (Antarctica)

## **Aims of the Thesis**



The present thesis project was conceived to provide a better knowledge of TEP and CSP distribution in the ocean, in a temporal and spatial scale, as well as to improve the knowledge on the main drivers of these particles across different ocean basins. Some of the study sites visited did not have any previous measurements of TEP and CSP (Fig. 8). The main questions were:

- 1) What is the distribution and main drivers of TEP in the Atlantic Ocean? (addressed in chapter 1)
- 2) How are TEP distributed across contrasting regions of the Antarctic Peninsula region (Southern Ocean), and what are the main factors explaining area-specific TEP distributions? (addressed in chapter 2)
- 3) Do TEP and CSP present similar or different seasonal variabilities in the coastal NW Mediterranean Sea? Are their horizontal (coast-to-offshore) and vertical (surface to bottom) distributions connected? (addressed in chapter 3).
- 4) What are the concentrations and distribution patterns of TEP and CSP around the Southern Ocean? (addressed in chapter 4).

In order to answer these questions, we carried out four different cruises across the Atlantic Ocean (October-November 2014), the Southern Ocean (January 2015 and January-March 2017) and the NW Mediterranean Sea (October 2015). We also carried out a time series study in two coastal stations in the NW Mediterranean Sea for two complete seasonal cycles (2015-2017). During these studies, TEP, CSP and a broad suite of physical, chemical and biological variables were measured in parallel.

The specific objectives of the different chapters of the thesis are the following:

### **Chapter 1. Main drivers of transparent exopolymer particle distribution across the surface Atlantic Ocean**

This chapter describes the horizontal distribution of TEP across a north-south transect in the Atlantic Ocean, from 20 October to 21 November 2014, in parallel with other physical and biological variables. The study region included several biogeographical provinces, both in the open ocean and the Southwestern Atlantic Shelf (SWAS). The aims of this chapter were:

- To find the main drivers of TEP distribution across contrasting environmental conditions.

- To study the contribution of TEP to the total particulate organic carbon (POC) pool and compare it with the contribution of phytoplankton and heterotrophic prokaryote biomasses to this pool.

## **Chapter 2. Distribution of transparent exopolymer particles (TEP) in distinct regions of the Southern Ocean**

This chapter studies the distribution of TEP along with other physical, chemical and biological variables, in both the horizontal and vertical (within the euphotic layer) scales, in distinct regions of the Southern Ocean, in the austral summer (January) of 2015. In addition, the short-term (diel) variability of TEP along with other biological variables was also described. Experimental incubations were conducted to compare TEP production under a natural microbial community or leaving only prokaryotes. The objectives of this chapter were:

- To identify the main biological and abiotic variables that drove TEP distribution across contrasting environmental conditions, both in the horizontal and vertical scale.
- To examine TEP variability along short-term diel cycles and to study if they were related to variation of other biological variables.
- 

## **Chapter 3. Seasonal variability of transparent exopolymer particles (TEP) and Coomassie stainable particles (CSP) in the coastal NW Mediterranean Sea**

This chapter describes the temporal dynamics of TEP and CSP over two complete seasonal cycles, from June 2015 to October 2017, in two coastal sites of the NW Mediterranean Sea (Blanes Bay Microbial Observatory and l'Estartit Oceanographic Station). In one of the sites, the seasonal variation of the vertical distribution was also studied. In addition, a transect between the Catalan Coast and the north of Mallorca Island was carried out. The objectives of this chapter were:

- To elucidate whether TEP and CSP follow similar patterns, at the surface and across the vertical profile, over the annual cycle (temporal scale).
- To elucidate whether TEP and CSP follow similar patterns in a coast-offshore transect (spatial scale).

- To identify the main biological and abiotic variables that drive TEP and CSP dynamics over seasons.

#### **Chapter 4. Distribution of TEP and CSP across the Southern Ocean**

This chapter studies the distribution of TEP and CSP together with other physical, chemical and biological variables, in both the horizontal and vertical (within the euphotic layer) scales, in the Southern Ocean, along a circular transit around Antarctica, in the austral summer (January-March) of 2017. The aims of this chapter were:

- To elucidate whether TEP and CSP present similar patterns across the horizontal and vertical scales.
- To identify the main planktonic drivers of TEP and CSP distributions.



# Chapter 1

Atlantic Ocean on board the RV *Hespérides*

## **Main drivers of transparent exopolymer particle distribution across the surface Atlantic Ocean**

*Marina Zamanillo, Eva Ortega–Retuerta, Sdena Nunes, Pablo Rodríguez–Ros, Manuel Dall’Osto, Marta Estrada, Maria Montserrat Sala, Rafel Simó, 2019. Biogeosciences, 16, 733-749*





## Abstract

Transparent exopolymer particles (TEP) are a class of gel particles, produced mainly by microorganisms, which play important roles in biogeochemical processes such as carbon cycling and export. TEP (a) are colonized by carbon-consuming microbes; (b) mediate aggregation and sinking of organic matter and organisms, thereby contributing to the biological carbon pump; and (c) accumulate in the surface microlayer (SML) and affect air–sea gas exchange. The first step to evaluate the global influence of TEP in these processes is the prediction of TEP occurrence in the ocean. Yet, little is known about the physical and biological variables that drive their abundance, particularly in the open ocean. Here we describe the horizontal TEP distribution, along with physical and biological variables, in surface waters along a north–south transect in the Atlantic Ocean during October–November 2014. Two main regions were separated due to remarkable differences; the open Atlantic Ocean (OAO,  $n = 30$ ), and the Southwestern Atlantic Shelf (SWAS,  $n = 10$ ). TEP concentration in the entire transect ranged 18.3–446.8  $\mu\text{g XG eq L}^{-1}$  and averaged  $117.1 \pm 119.8 \mu\text{g XG eq L}^{-1}$ , with the maximum concentrations in the SWAS and in a station located at the edge of the Canary Coastal Upwelling (CU), and the highest TEP to chlorophyll *a* (TEP:Chl *a*) ratios in the OAO ( $183 \pm 56$ ) and CU (1760). TEP were significantly and positively related to Chl *a* and phytoplankton biomass, expressed in terms of C, along the entire transect. In the OAO, TEP were positively related to some phytoplankton groups, mainly *Synechococcus*. They were negatively related to the previous 24 h averaged solar irradiance, suggesting that sunlight, particularly UV radiation, is more a sink than a source for TEP. Multiple regression analyses showed the combined positive effect of phytoplankton and heterotrophic prokaryotes (HPs) on TEP distribution in the OAO. In the SWAS, TEP were positively related to high nucleic acid–containing prokaryotic cells and total phytoplankton biomass, but not to any particular phytoplankton group. Estimated TEP–carbon constituted an important portion of the particulate organic carbon pool in the entire transect (28 %–110 %), generally higher than the phytoplankton and HP carbon shares, which highlights the importance of TEP in the cycling of organic matter in the ocean.



## 1.1 Introduction

Transparent exopolymer particles (TEP) are defined as a class of nonliving organic particles in aqueous media, mainly consisting of acidic polysaccharides, which are stainable with Alcian Blue (Alldredge et al., 1993). They are formed from dissolved precursors that self-assemble to form TEP (operationally defined as particles  $> 0.4 \mu\text{m}$ ) (Passow and Alldredge, 1994; Chin et al., 1998; Thuy et al., 2015). TEP are stabilized by covalent links or ionic strength (Cisternas-Novoa et al., 2015) and, therefore, the formation and fragmentation of TEP from/to dissolved precursor material spans the dissolved-to-particulate continuum of organic matter in the sea. Due to their stickiness, TEP favor the formation of large aggregates of organic matter and organisms (typically named marine snow), enhancing particle ballast and sinking and thereby contributing to the biological carbon pump (Logan et al., 1995; Kumar et al., 1998; Passow et al., 2001; Burd and Jackson, 2009). The presence of TEP also affects the microbial food-web, as they can be used as a food source for zooplankton (Decho and Moriarty, 1990; Dilling et al., 1998; Ling and Alldredge, 2003) Decho and Moriarty, 1990; Dilling et al., 1998; Ling and Alldredge, 2003) and heterotrophic prokaryotes (HPs) (Passow, 2002a) through microbial colonization of aggregates (Alldredge et al., 1986; Grossart et al., 2006; Azam and Malfatti, 2007). On their way to aggregation, and due to their low density, TEP and TEP-rich microaggregates formed near the surface may ascend and accumulate in the sea surface microlayer (SML) (Engel and Galgani, 2016), a process that is largely enhanced by bubble-associated scavenging (Azetsu-Scott and Passow, 2004; Wurl et al., 2009; Wurl et al., 2011b). This accumulation in the SML, also contributed by local TEP production (Wurl et al., 2011b), can suppress the air-sea exchange of  $\text{CO}_2$  and other trace gases by acting as a physicochemical barrier or modifying sea surface hydrodynamics at low wind speeds (Calleja et al., 2008; Cunliffe et al., 2013; Wurl et al., 2016). Sea surface TEP can also be released to the atmosphere by bubble bursting (Zhou et al., 1998; Aller et al., 2005; Kuznetsova et al., 2005), contributing to organic aerosol and possibly acting as cloud condensation nuclei and ice-nucleating particles (Orellana et al., 2011; Leck et al., 2013; Wilson et al., 2015). All in all, TEP play important roles in microbial diversity, carbon cycling and carbon exports to both the deep ocean and the atmosphere.

TEP distribution in marine systems depends on the complex balance between the sources and the sinks (Alldredge et al., 1998; Passow, 2002b). TEP sinks include some of the abovementioned processes (sinking of aggregates to the deep ocean, release to the atmosphere and consumption by organisms), and also photolysis by UV radiation (Ortega-Retuerta et al., 2009b). Regarding the sources, TEP are produced by organisms, mainly microorganisms, during metabolic and decomposition processes (Hong et al., 1997; Berman-Frank et al., 2007). Phytoplankton are major TEP producers in the ocean, although HPs are also able to produce TEP (Biddanda, 1986; Stoderegger and Herndl, 1998; Passow, 2002a; Ortega-Retuerta et al., 2010). Some phytoplankton groups that have been shown to produce TEP include cyanobacteria (Grossart et al., 1998; Mazuecos, 2015; Deng et al., 2016); diatoms (Passow and Alldredge, 1994; Mari and Kiorboe, 1996; Passow, 2002a); dinoflagellates (Passow and Alldredge, 1994); Prymnesiophyceae, including coccolithophores (Riebesell et al., 1995; Engel, 2004; Leblanc et al., 2009); and Cryptomonads (Kozłowski and Vernet, 1995; Passow et al., 1995a). Other organisms such as *Posidonia oceanica* (Iuculano et al., 2017b), zooplankton (Passow and Alldredge, 1999; Prieto et al., 2001) and benthic suspension feeders (Heinonen et al., 2007) have also been identified as TEP producers.

TEP sources and sinks in the ocean depend not only on the taxonomic composition of TEP producers, but they are also influenced by other variables such as the organism's physiological state (Passow, 2002a), temperature (Nicolaus et al., 1999; Claquin et al., 2008), light (Trabelsi et al., 2008; Ortega-Retuerta et al., 2009a; Iuculano et al., 2017c), carbon dioxide concentration (Engel, 2002), nutrient availability (Guerrini et al., 1998; Radic et al., 2006), turbulence (Passow, 2000, 2002a), microbe–microbe interactions (Gärdes et al., 2011), or viral infection (Shibata et al., 1997; Vardi et al., 2012). For example, limitation by nutrients often increases TEP production, due to dissolved inorganic carbon overconsumption (Corzo et al., 2000; Engel et al., 2002a; Schartau et al., 2007), and also impedes prokaryotic consumption of TEP (Bar-Zeev and Rahav, 2015). High solar radiation can stimulate TEP production by *Prochlorococcus* during cell decay (Iuculano et al., 2017c), but also can limit TEP formation inhibiting the aggregation of the precursor polymers (Orellana and Verdugo, 2003). HP have been found to stimulate TEP production by diatoms, suggesting that HP–diatom interaction is required for TEP formation (Guerrini et al., 1998; Gärdes et al., 2011). HP may also facilitate the self–assembly of dissolved TEP precursors (Sugimoto et al., 2007), e.g.,

through the release of amphiphilic exopolymers that induce microgel formation (Ding et al., 2008).

The aforementioned importance of TEP in carbon fluxes in the pelagic ocean can be further stressed by considering the following rough numbers: if the percentage of extracellular carbon release during planktonic primary production is generally constrained within 10–20 % (Nagata, 2000; Mari et al., 2017), but can reach > 50 % (López-Sandoval et al., 2011), and half of the extracellular release is in the form of reactive polysaccharides (Biddanda and Benner, 1997), then the production rate of TEP precursors may represent 5–10 %, but can reach > 25% of planktonic primary production, without considering production by heterotrophs. This calls for the need to quantify their occurrence across the oceans, elucidate their main distribution drivers, and determine their contribution to the organic carbon reservoir. To date, large-scale studies of TEP distributions in the ocean are scarce, particularly in the open ocean. In this study, we describe the horizontal distribution of TEP (> 0.4  $\mu\text{m}$ ) in surface waters across a north–south transect in the Atlantic Ocean, including several biogeographical provinces in the open ocean as well as the highly productive Southwestern Atlantic Shelf (SWAS). Our aims were (a) to identify the main biological and abiotic drivers of TEP distribution across contrasting environmental conditions, and (b) to quantify the TEP contribution to the total particulate organic carbon (POC) pool and compare it with those of phytoplankton and heterotrophic prokaryote biomasses.

## **1.2 Material and methods**

### **2.1 Study sites and sampling**

Sampling was conducted during the TransPEGASO cruise aboard the Spanish RV *Hespérides*, from 20 October to 21 November 2014. A total of 41 stations were sampled within a transit across the Atlantic Ocean from Cartagena (SE Spain) to Punta Arenas (S Chile, Fig. 1.1). During the cruise, the ship crossed six biogeographical provinces (Longhurst, 1998): the Northeastern Subtropical Gyre, the Canary Current Coastal, the North Atlantic Tropical Gyre, the Western Tropical Atlantic, the South Tropical Gyre

and the SWAS. Seawater was collected from 4 m depth using the ship's underway pump (BKMKC-10.11, Tecnum, Manresa, Spain) and screened through a 150  $\mu\text{m}$  Nylon mesh to remove large particles. Temperature and salinity were measured continuously using a SBE21 Sea Cat Thermosalinograph. Solar irradiance was also measured continuously using a LI-COR Biospherical PAR Sensor. The rest of the variables were collected twice a day (09:00:00 and 16:00:00 local time) with the ship moving at approximately 10 knots.

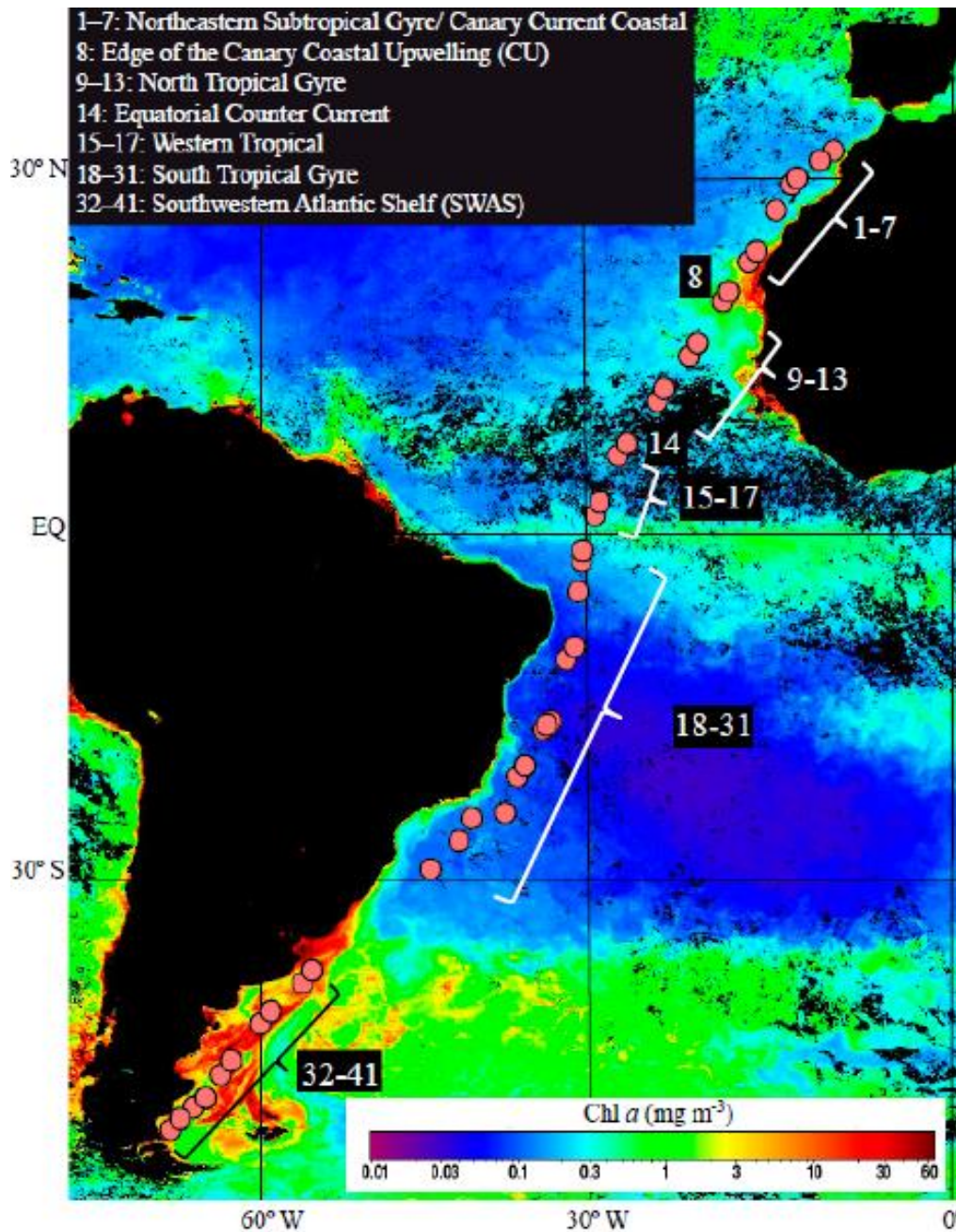


**Figure 1.1.** Hydrographic stations (filled circles) of the TransPEGASO cruise, sampled during October–November 2014 in the Atlantic Ocean. Chl *a* concentration (background color;  $\text{mg m}^{-3}$ ) values during November 2014 were taken from a NASA MODIS Aqua 9-km product composite.

## 1.2.2 Chemical and biological analysis

### 1.2.2.1 Particulate organic matter (TEP and POC)

TEP concentrations were determined by spectrophotometry following Passow and Alldredge (1995). Duplicate samples (100–500 mL each) were filtered through 25 mm diameter 0.4  $\mu\text{m}$  pore size polycarbonate filters (DHI) using a constant low filtration pressure ( $\sim 150$  mmHg). The samples were immediately stained with 500  $\mu\text{L}$  of Alcian Blue solution (0.02 %, pH 2.5) for 5 s and rinsed with Milli-Q water. The filters were stored frozen until further processing in the laboratory (within 8 months). Duplicate blanks (empty filters stained as stated earlier) were prepared twice a day to correct the interference of stained particles in TEP estimates. Both the sample and blank filters were soaked in 5 mL of 80 % sulfuric acid for 3 h. The filters were shaken intermittently during this period. The samples were then measured spectrophotometrically at 787 nm (Varian Cary 100 Bio). The absorbance values of filter blanks did not change substantially between batches of samples, suggesting stability in the staining capacity of the Alcian Blue solution throughout the cruise. The Alcian Blue dye solution was calibrated just before the cruise using a standard solution of xanthan gum (XG) passed through a tissue grinder and subsequently filtered through two sets of filters (four points in triplicate): preweighted filters to determine the actual concentration of the XG solution, and filters that were subsequently stained, frozen and analyzed in the spectrophotometer. The detection limit was set to 0.034 absorbance units and the mean range between duplicates was 18.7 %. We estimated the TEP carbon content (TEP-C) using the conversion factor of  $0.51 \mu\text{g TEP-C L}^{-1}$  ( $\mu\text{g XG eq L}^{-1}$ ) (Engel and Passow, 2001).

POC was measured by filtering 1000 mL of seawater on precombusted (4 h, 450  $^{\circ}\text{C}$ ) GF/F glass fibre filters (Whatman). The filters were stored frozen ( $-20$   $^{\circ}\text{C}$ ) until processed. Prior to analysis, the filters were dried at 60  $^{\circ}\text{C}$  for 24 h in an atmosphere of HCl fumes to remove carbonates. Then filters were dried again and analyzed by high-temperature (900  $^{\circ}\text{C}$ ) combustion in an elemental analyzer (Perkin-Elmer 2400 CHN). No POC replicates were run, but replication in a previous study yielded a coefficient of variation of around 5 %.

### 1.2.2.2 Chlorophyll *a* (Chl *a*)

Samples for fluorometric Chl *a* analyses were filtered (250 mL) on glass fibre filters (Whatman GF/F, 25 mm diameter) and stored at -20 °C until further processing in the ship's laboratory. Pigments were extracted with 90 % acetone at 4 °C in the dark for 24 hours. Fluorescence of extracts was measured according to the procedure described in Yentsch and Menzel (1963), with a calibrated Turner Designs fluorometer. No "phaeophytin" correction was applied.

### 1.2.2.3 Inorganic nutrients

Samples for dissolved inorganic nutrients (nitrate, phosphate and silicate) were stored in 10 mL sterile polypropylene bottles at -20 °C until analysis. The samples were further processed in the laboratory using standard segmented flow analyses with colorimetric detection (Hansen and Grasshoff, 1983), using a Skalar Autoanalyzer.

### 1.2.2.4 Microscopic phytoplankton identification

We quantified phytoplankton groups by microscopy. Water was fixed with hexamine-buffered formaldehyde solution (4 % final formalin concentration) in a glass bottle, immediately after collection, and then was allowed to settle for 48 h in a 100 cm<sup>3</sup> composite chamber. An inverted microscope (Utermöhl, 1958) was used to enumerate the smaller phytoplankton cells (< 20 µm, 312× magnification) and the larger phytoplankton cells (> 20 µm, 125× magnification). Micro-phytoplankton was identified to the species level when possible, and finally classified into four groups: diatoms, dinoflagellates, coccolithophores and other microplankton cells referred to from now on as "other microalgae". Cell C content was calculated using conversion equations of Menden-Deuer and Lessard (2000),  $\log \text{ pg C cell}^{-1} = \log a$  (95 % confidence intervals) +  $b$  (95 % confidence intervals)  $\times \log \text{ volume (V; } \mu\text{m}^3)$ : one for diatoms ( $\log \text{ pg C cell}^{-1} = \log -0.541 (0.099) + 0.811 (0.028) \times \log V$ ) and one for the other algae groups ( $\log \text{ pg C cell}^{-1} = \log -0.665 (0.132) + 0.939 (0.041) \times \log V$ ). Total carbon biomass was calculated from cell C content and cell abundance. Uncertainty sources for micro-phytoplankton biomass estimates are the conversion factors,



biovolume estimates, and proper identification based on morphological characteristics, harder for naked cells and those at the lower size edge (5–10  $\mu\text{m}$ ) (Kozłowski et al., 2011; Cassar et al., 2015).

#### 1.2.2.5 Picoplankton abundance

To enumerate picoplankton cells, samples (4.5 mL) were fixed with 1 % paraformaldehyde plus 0.05 % glutaraldehyde (final concentrations), for 15 min. at room temperature, deep frozen in liquid nitrogen and stored frozen at  $-80\text{ }^{\circ}\text{C}$ . Samples were then analyzed 6 months after the cruise end, using a FACS Calibur (Becton and Dickinson) flow cytometer equipped with a 15 mW argon-ion laser emitting at 488 nm. Before analysis, samples were thawed and we added 10  $\mu\text{L}$  per 600  $\mu\text{L}$  sample of a  $10^5\text{ mL}^{-1}$  solution of yellow–green 0.92  $\mu\text{m}$  Polysciences latex beads as an internal standard. Samples were then run at high speed (approx.  $75\text{ }\mu\text{L min}^{-1}$ ) for 4 min. with Milli–Q water as a sheath fluid. Three groups of phytoplankton (*Prochlorococcus*, *Synechococcus* and picoeukaryotic algae) were distinguished and enumerated on the basis of the differences in their autofluorescence properties and scattering characteristics (Olson et al., 1993; Zubkov et al., 1998). Abundances were converted to biomass ( $\mu\text{g L}^{-1}$ ) using average C-to-cell conversion factors gathered in Simó et al. (2009):  $51 \pm 18\text{ fg C cell}^{-1}$  for *Prochlorococcus*,  $175 \pm 73\text{ fg C cell}^{-1}$  for *Synechococcus* and  $1319 \pm 813\text{ fg C cell}^{-1}$  for picoeukaryotes.

#### 1.2.2.6 Heterotrophic prokaryotic abundance (HPA)

Heterotrophic prokaryotic abundance (HPA) was determined by flow cytometry using the same fixing protocol and instrument as for picoplankton. Before analyses, samples were thawed, stained with SYBRGreen I (Molecular Probes) at a final concentration of 10  $\mu\text{M}$  and left in the dark for about 15 min. Samples were run at a low flow rate (approximately  $15\text{ }\mu\text{L min}^{-1}$ ) for 2 min with Milli–Q water as a sheath fluid. We added 10  $\mu\text{L}$  per sample of a  $10^5\text{ mL}^{-1}$  solution of yellow–green 0.92  $\mu\text{m}$  Polysciences latex beads as an internal standard. Heterotrophic prokaryotes were detected by their signature in a plot of side scatter versus FL1 (green fluorescence). HP were enumerated separately as high–nucleic–acid–containing (HNA) and low–nucleic–acid–containing

(LNA) cells, and the prokaryote counts presented are the sum of these two types. Data were gated and counted in the SSC vs FL1 plot using the BD CellQuest<sup>TM</sup> software. HPA was expressed in cells mL<sup>-1</sup>. Only one replicate was analyzed since standard errors of duplicates are usually very low (around 1.5 % at Pernice et al. (2015)). HPA was converted into a carbon unit (HP-C) using the conversion factor of 12 fg C cell<sup>-1</sup>. Ducklow (2000) summarized the carbon contents of free-living marine bacteria reported in the literature for a number of oceanic regions, bays and estuaries. The average  $\pm$  standard deviation for open-ocean regions was  $12.3 \pm 2.5$  fg C cell<sup>-1</sup>. A factor of 12 fg C cell<sup>-1</sup> is equivalent to use the empirical equation proposed by Norland (1993),  $\text{fg C cell}^{-1} = 0.12 (\mu\text{m}^3 \text{ cell volume})^{0.72}$ , for an average bacterial biovolume of  $0.04 \mu\text{m}^3$ .

### 1.2.3 Statistical analyses

We used R software packages lmodel2 and ggplot2 (RStudio Team, 2016) to test for covariations and to explore the potential controlling variables of TEP distribution across the Atlantic Ocean. We performed pairwise Spearman correlation analyses between TEP and POC concentrations. We performed bivariate and multiple regression analyses (ordinary least squares, OLS) between TEP concentrations and several physical, chemical and biological variables. Data were log transformed to fulfil the requirements of parametric tests. Ranged major axis (RMA) regression would have been more suitable since there were errors in both our dependent and independent variables. However, we decided to perform OLS regressions for a better comparison of slopes between our study and those available in the literature. The nonparametric Wilcoxon–Mann–Whitney test was carried out to compare variables, like TEP and POC, among regions. Two main regions were analyzed separately due to remarkable differences in nutrient, Chl *a* and TEP concentration: the open Atlantic Ocean (OAO,  $n = 30$ ), with exclusion of the single sample from the edge of the Canary Coastal Upwelling (CU), which had a much higher TEP concentration; and the SWAS ( $n = 10$ ).

## 1.3 Results

### 1.3.1 TEP distribution across the surface Atlantic Ocean

TEP concentrations ranged from 18.3 to 446.8  $\mu\text{g XG eq L}^{-1}$  along the entire Atlantic Ocean transect. Across OAO, CU included, nitrate and phosphate concentrations were low and relatively homogeneous (nitrate:  $0.47 \pm 0.51 \mu\text{mol L}^{-1}$ ; phosphate:  $0.11 \pm 0.06 \mu\text{mol L}^{-1}$ ). Silicate ranged between 0.20 and  $1.42 \mu\text{mol L}^{-1}$ , and presented the minimum concentrations in the CU station and surroundings, and the maximum concentration at station 14. The temperatures ranged from 20.7 to 29.6 °C ( $25.6 \pm 23.8$  °C), with maximum values in the Equatorial Counter Current ( $\sim 0\text{--}20^\circ \text{N}$ , 29.1–29.6 °C), and minimum values around the CU and in the southernmost stations of the OAO (22.6–23.6 °C). The salinity ranged between 34.8 and 37.4, with the minimum values in the Equatorial Counter Current and the maximum values around  $10\text{--}30^\circ \text{S}$ . The Chl *a* concentration was low and quite homogeneous ( $0.36 \pm 0.22 \text{ mg m}^{-3}$ ), even at the CU ( $0.25 \text{ mg m}^{-3}$ ).

In the Northeastern Subtropical Gyre and the Canary Current Coastal (stations 1 to 7, Fig. 1.1) Chl *a* concentration ranged from 0.24 to  $0.37 \text{ mg m}^{-3}$ . The phytoplankton biomass was generally dominated by *Prochlorococcus*, with an average of  $1.68 \times 10^5 \pm 0.81 \times 10^5 \text{ cells mL}^{-1}$ , which corresponded to a biomass of  $8.58 \pm 4.16 \mu\text{g C L}^{-1}$ . TEP concentration in this region ranged from 54.2 to  $131.7 \mu\text{g XG eq L}^{-1}$  (average  $73.9 \pm 27.3 \mu\text{g XG eq L}^{-1}$ ). In the station 8 we sampled the edge of the CU. The decrease in silicate ( $0.26 \mu\text{mol L}^{-1}$ ) was accompanied by a relative increase in diatoms (9.4-fold increase) and dinoflagellates (1.3-fold increase) with respect to surrounding stations (Fig. 1.2b,e). *Prochlorococcus* abundance decreased to  $9 \times 10^3 \text{ cell mL}^{-1}$  and a biomass of  $0.46 \mu\text{g C L}^{-1}$ . In this station, TEP concentrations were the highest found along the whole transect ( $446.7 \mu\text{g XG eq L}^{-1}$ ) but the Chl *a* concentration ( $0.25 \text{ mg m}^{-3}$ ) was lower than in the neighbouring region. Consequently the TEP:Chl *a* ratio was the highest of the whole transect (1760.4). Moving south, the North Tropical Gyre (stations 9 to 13) showed an increase in silicate concentration, from 0.20 to  $0.79 \mu\text{mol L}^{-1}$ . The Chl *a* concentration ranged from 0.41 to  $0.57 \text{ mg m}^{-3}$  (Fig. 1.2c). In the northernmost part of this region (stations 9 to 11), phytoplankton biomass was dominated by

*Synechococcus*, with an average of  $7.7 \times 10^4 \pm 0.8 \times 10^4$  cells mL<sup>-1</sup>, which corresponded to a biomass of  $13.5 \pm 1.4$  µg C L<sup>-1</sup>. By contrast, the southernmost stations (12 and 13) were dominated by *Prochlorococcus*, with an average of  $2.6 \times 10^5 \pm 0.5 \times 10^5$  cells mL<sup>-1</sup>, that corresponded to a biomass of  $13.2 \pm 2.7$  µg C L<sup>-1</sup> (Fig. 1.2e). TEP concentrations were similar to those in the Northeastern Subtropical Gyre and the Canary Current Coastal, ranging between 78.1 and 123.9 µg XG eq L<sup>-1</sup>. Station 14, with a relatively high temperature (29.0 °C) and low salinity (35.2) was probably the most influenced by the Equatorial Counter Current. In this station, the silicate concentration (1.41 µmol L<sup>-1</sup>) was the maximum observed in the whole transect, and there was an increase in dinoflagellates and “other microalgae”, and a decrease in *Prochlorococcus*. The Chl *a* concentration (0.48 mg m<sup>-3</sup>) was similar to the surrounding stations and TEP were 49.4 µg XG eq L<sup>-1</sup>. Moving further south, in the Western Tropical and the South Tropical Gyre (stations 15 to 31) Chl *a* ranged from 0.20 to 0.41 mg m<sup>-3</sup> and the silicate concentration decreased (0.42–1.39 µmol L<sup>-1</sup>). TEP presented the lowest average values of the whole transect, ranging from 25.5 to 80.4 µg XG eq L<sup>-1</sup>. Overall in the OAO (excluding CU), TEP ranged from 18.3 to 131.7 µg XG eq L<sup>-1</sup> (average  $59.9 \pm 27.4$  µg XG eq L<sup>-1</sup>) and the TEP:Chl *a* ratio ranged between 81 and 360 (average  $183 \pm 56$ ; Table 1.1).

The southernmost part of the cruise transect corresponded to the SWAS (stations 32 to 41). In this region, temperature (7.6–13.9 °C) and salinity (32.6–33.6) were lower on average than those found in the OAO (Table 1.1). The SWAS could be further divided into two regions according to different inorganic nutrient (nitrate and phosphate) concentrations ( $p < 0.05$ ) and phytoplankton composition. The northern SWAS (stations 32 to 36) presented lower nitrate (0.16 to 4.15 µmol L<sup>-1</sup>) and phosphate (0.31 to 0.62 µmol L<sup>-1</sup>) concentrations than the southern SWAS (stations 37 to 41; nitrate: 2.16 to 8.92 µmol L<sup>-1</sup>, phosphate: 0.51 to 0.89 µmol L<sup>-1</sup>). Silicate was more homogeneous throughout (0.31 to 1.27 µmol L<sup>-1</sup>). Chl *a* concentration across the entire SWAS (1.07–3.75 mg m<sup>-3</sup>) was significantly higher than in the OAO, with no major differences between the northern and the southern parts. In most of the northern SWAS, phytoplankton biomass was dominated by “other microalgae”, with an average of  $10.2 \times 10^5 \pm 6.1 \times 10^5$  cells L<sup>-1</sup>, which corresponded to a biomass of  $43.7 \pm 25.8$  µg C L<sup>-1</sup>. In station 35, an increase in diatoms (58121 cells L<sup>-1</sup> and a biomass of 145.2 µg C L<sup>-1</sup>) and dinoflagellates (44896 cells L<sup>-1</sup> and a biomass of 3.3 µg C L<sup>-1</sup>) was observed,

coinciding with a decrease in silicate ( $0.32 \mu\text{mol L}^{-1}$ ). Here in northern SWAS, TEP ranged from 98.6 to 427.2  $\mu\text{g XG eq L}^{-1}$ , with the maxima in stations 34 and 35 (Fig. 2f). In the southern SWAS (stations 37 to 41), phytoplankton biomass was dominated by picoeukaryotes, with an average of  $6.34 \times 10^4 \pm 1.93 \times 10^4 \text{ cells mL}^{-1}$ , which corresponded to a biomass of  $83.6 \pm 25.5 \mu\text{g C L}^{-1}$ . TEP concentration ranged 168.6–395.7  $\mu\text{g XG eq L}^{-1}$ . Overall in the SWAS, TEP ranged from 98.6 to 427.2  $\mu\text{g XG eq L}^{-1}$  (average  $255.7 \pm 130.4 \mu\text{g XG eq L}^{-1}$ ) and the TEP:Chl *a* ratio ranged from 31 to 165 (average  $97 \pm 42$ ) (Table 1.1).

**Table 1.1.** Mean, standard deviation and range of temperature ( $^{\circ}\text{C}$ ), salinity, 24 h-accumulated solar irradiance ( $\text{W m}^{-2}$ ), nitrate ( $\mu\text{mol L}^{-1}$ ), silicate ( $\mu\text{mol L}^{-1}$ ), phosphate ( $\mu\text{mol L}^{-1}$ ), Chl *a* ( $\text{mg m}^{-3}$ ), POC ( $\mu\text{mol L}^{-1}$ ), HPA ( $\times 10^5 \text{ cells mL}^{-1}$ ), TEP ( $\mu\text{g XG eq L}^{-1}$ ) and TEP:Chl *a* in the OAO, the edge of the Canary Coastal Upwelling (CU) and the SW Atlantic Shelf.

	OAO		CU		SW Atlantic Shelf	
	Mean $\pm$ SD (ranges)	n	Value (n = 1)	Mean $\pm$ SD (ranges)	n	
Temperature ( $^{\circ}\text{C}$ )	$26.0 \pm 2.1$ (22.6–29.6)	30	23.6	$10.7 \pm 2.2$ (7.6–13.9)	9	
Salinity	$36.4 \pm 0.6$ (34.8–37.4)	30	36.1	$33.2 \pm 0.3$ (32.6–33.6)	9	
Solar irradiance 24 h ( $\text{W m}^{-2}$ )	$265 \pm 73$ (144–362)	26	–	$369 \pm 52$ (264–425)	10	
Nitrate ( $\mu\text{mol L}^{-1}$ )	$0.49 \pm 0.53$ (0.09–0.77)	30	0.13	$4.08 \pm 3.08$ (0.16–8.9)	10	
Silicate ( $\mu\text{mol L}^{-1}$ )	$0.74 \pm 0.27$ (0.20–1.41)	30	0.26	$0.63 \pm 0.35$ (0.31–1.27)	10	
Phosphate ( $\mu\text{mol L}^{-1}$ )	$0.11 \pm 0.06$ (0.05–0.18)	30	0.16	$0.57 \pm 0.21$ (0.31–0.89)	10	
Chl <i>a</i> ( $\text{mg m}^{-3}$ )	$0.32 \pm 0.10$ (0.20–0.57)	29	0.25	$2.73 \pm 0.87$ (1.07–3.75)	10	
POC ( $\mu\text{mol L}^{-1}$ )	$4.2 \pm 1.9$ (1.7–7.1)	12	–	$16.6 \pm 15.8$ (6.8–44.3)	5	
HPA ( $\times 10^5 \text{ cells mL}^{-1}$ )	$7.83 \pm 2.16$ (4.34–14.90)	30	14.56	$29.04 \pm 5.39$ (13.00–70.20)	10	
TEP ( $\mu\text{g XG eq L}^{-1}$ )	$59.8 \pm 27.4$ (18.3–131.7)	30	446.8	$255.7 \pm 130.4$ (98.6–427.2)	10	
TEP:Chl <i>a</i>	$183.1 \pm 55.8$ (81.2–359.7)	29	1760.4	$97.2 \pm 42.1$ (30.8–164.9)	10	

### 1.3.2 TEP contribution to POC

TEP and POC covaried significantly and positively across the entire TransPEGASO transect (Spearman *rs* analysis,  $r = 0.91$ ,  $p < 0.01$ ,  $n = 17$ ). The contribution of TEP–C to the POC pool (TEP–C%POC) ranged between 34 and 103 % in the OAO (average  $66 \pm 19$  %), and between 28 and 110 % in the SWAS (average  $73 \pm 36$  %). POC was not analyzed in the CU (Fig. 3). To better explore the importance of TEP–C with respect to

other major quantifiable POC pools, we estimated phytoplankton biomass (phyto-C) and HP biomass (HP-C) throughout the whole cruise (Fig. 1.2). It is worth mentioning that POC also includes other fractions of nonliving non-TEP organic carbon (e.g., cell fragments and Coomassie stainable particles), but phytoplankton and heterotrophic prokaryotes are generally considered the most abundant in open sea water (Ortega-Retuerta et al., 2009b; Yamada et al., 2015). TEP-C contributed the most to the POC pool in the OAO, where it represented twice the share of phyto-C and HP-C. In the SWAS, conversely, TEP-C was not significantly different than phyto-C, and was 3 times higher than HP-C (Fig. 1.3).

### 1.3.3 Relationship to other variables

TEP were significantly and positively related to Chl *a* along the entire transect ( $R^2 = 0.61$ ,  $p < 0.001$ ,  $n = 39$ , table 1.3). The regression equation for log converted TEP vs Chl *a* was  $\log \text{TEP} = 2.09 (\pm 0.04) + 0.66 (\pm 0.08) \times \log \text{Chl } a$ . Considering the two study regions separately, only in the OAO was the relationship significant, with a higher slope than in the entire transect ( $\log \text{TEP} = 2.31 (\pm 0.10) + 1.13 (\pm 0.20) \times \log \text{Chl } a$ ;  $R^2 = 0.56$ ,  $p < 0.001$ ,  $n = 29$ ).

Across the whole transect, TEP presented a significant ( $p < 0.05$ ) positive relationship with total phytoplankton biomass (Table 1.3) and with some phytoplankton biomass groups: *Synechococcus* ( $R^2 = 0.30$ ), picoeukaryotes ( $R^2 = 0.49$ ), diatoms ( $R^2 = 0.19$ ) and “other microalgae” ( $R^2 = 0.27$ ), and with HPA ( $R^2 = 0.60$ ). TEP were negatively related to silicate ( $R^2 = 0.19$ ) and coccolithophores ( $R^2 = 0.15$ ). Some differences arose from examining the two regions separately. Within the OAO, TEP presented a significant ( $p < 0.001$ ) positive relationship with Chl *a* ( $R^2 = 0.56$ ), total phytoplankton biomass ( $R^2 = 0.47$ ) and some phytoplankton groups (*Synechococcus*, picoeukaryotes, diatoms, dinoflagellates and “other microalgae”, Table 1.3), but not with HPA. TEP showed a significant ( $p < 0.001$ ) negative relationship with the previous 24 h averaged solar irradiance ( $R^2 = 0.43$ , Fig. 1.4). Multiple regression analyses showed the combined positive effect of Chl *a* and HPA on TEP distribution in the OAO (Table 1.4). By contrast, within the SWAS, TEP only presented a significant ( $p < 0.05$ ) positive

relationship with total phytoplankton biomass ( $R^2 = 0.62$ ) and HNA ( $R^2 = 0.46$ , Table 1.3).

## 1.4 Discussion

### 1.4.1 TEP across the surface Atlantic Ocean

We present the first distribution of surface (4 m) TEP concentration along a latitudinal gradient in the Atlantic Ocean, covering both open sea and shelf waters. It is worth mentioning that vertical variability within the top surface meters ( $< 4$  m) has sometimes been observed (Wurl et al., 2009), but 4 m is usually considered “surface ocean” in studies where samples are collected with either an oceanographic rosette or an underway pumping system. The existing information about TEP distribution in surface waters of the open oceans is compiled in Table 1.2. The TEP concentrations we measured across the OAO (CU included) generally fall within the range reported in other studies from the open ocean (Table 1.2). However, our levels are higher than those observed in the Mediterranean Sea (Ortega-Retuerta et al., 2010; Ortega-Retuerta et al., 2017), Pacific Ocean (Ramaiah et al., 2005; Kodama et al., 2014; Iuculano et al., 2017c) and one study in the Northwestern Atlantic Ocean (Cisternas-Novoa et al., 2015), and lower than that reported in the Eastern Mediterranean Sea (Bar-Zeev et al., 2011). We believe that one of the reasons for the higher values found in our study compared with these previous studies is the depth. Mean TEP values in some of them (Ortega-Retuerta et al., 2010; Kodama et al., 2014; Cisternas-Novoa et al., 2015; Ortega-Retuerta et al., 2017) correspond to the above mixed layer depth or from 0 to 100 or 200 m. As TEP tend to accumulate in the surface and our values correspond only to the surface (4 m), this could explain the higher values obtained in our dataset. Another reason seems to be the different Chl *a* concentrations, as the main TEP producer is phytoplankton. Chl *a* concentration in the OAO ( $0.4 \pm 0.2$  mg m<sup>-3</sup> (0.2–0.6 mg m<sup>-3</sup>)) was generally higher than in the other studies referred in the Table 1.2. For example, in Iuculano et al. (2017c) Chl *a* ranged 0.05–0.31 mg m<sup>-3</sup>, and in (Kodama et al., 2014) it averaged  $0.05 \pm 0.01$  mg m<sup>-3</sup>. We also cannot discard either that differences in TEP chemical composition could cause differences in staining capacity.

We found maximum TEP concentrations in the regions with high nutrient supply, namely in the station located in the CU and within the SWAS. Ours are the first TEP concentrations ever measured in the SWAS (Table 1.1), and only three more studies have reported TEP concentrations in coastal or shelf waters of the Atlantic Ocean (Harlay et al., 2009; Harlay et al., 2010; Jennings et al., 2017). The SWAS is a high-nutrient region due to the arrival of cold nutrient-rich Subantarctic water with the Malvinas Current. This current collides near 40 °S with the southward-flowing Brazil Current (Gordon, 1989; Piola and Gordon, 1989; Peterson and Stramma, 1991; Palma et al., 2008). The nutrient-rich water in the region is responsible for the proliferation of phytoplankton and HP, which could partly explain the high TEP concentrations in this region. It is also known that large freshwater discharges occur in the shelf (Piola, 2005). These discharges could bring allochthonous HP directly to the shelf or bring DOM loads, which would stimulate autochthonous microbes. Besides, DOM inputs associated with freshwater discharges could also contain TEP and their precursors. Although no previous information on TEP distribution exists for this area, previous studies in similarly productive areas or during phytoplankton blooms already observed high TEP concentrations (Long and Azam, 1996; Harlay et al., 2009; Klein et al., 2011). The TEP levels we measured at the SWAS are generally within the range of those reported for coastal areas (Passow and Alldredge, 1995; Passow et al., 1995a; Riebesell et al., 1995; Kiorboe et al., 1996; Hong et al., 1997; Jähmlich et al., 1998; Wild, 2000; Ramaiah et al., 2001; Engel et al., 2002b; García et al., 2002; Radic et al., 2005; Scoullos et al., 2006; Sugimoto et al., 2007; Harlay et al., 2009; Wurl et al., 2009; Harlay et al., 2010; Fukao et al., 2011; Klein et al., 2011; Sun et al., 2012; Van Oostende et al., 2012; Dreshchinskii and Engel, 2017; Jennings et al., 2017). Only two studies, in the western Baltic Sea and the Dona Paula Bay (Arabian Sea), reported TEP levels higher than ours (Engel, 2000; Bhaskar and Bhosle, 2006).



**Table 1.2.** Review of open-ocean surface TEP concentrations (mean and ranges;  $\mu\text{g XG eq L}^{-1}$ ), Chl *a* (mean and ranges;  $\text{mg m}^{-3}$ ) and TEP:Chl *a* ratio (mean  $\pm$  SE and/or range) available in the literature. bdl: below detection limit.

Geographic area	Conditions	Sampling date	Depth (m)	TEP mean (range) ( $\mu\text{g XG eq. L}^{-1}$ )	Chl <i>a</i> mean (range) ( $\text{mg m}^{-3}$ )	TEP:Chl <i>a</i> mean (range)	Reference
Fram Strait (Arctic Ocean)	Bloom and non bloom	Summer 2009–2012 and 2014 (time series) and summer 2014 (transect)	5–150	$75 \pm 78$ (5–517)	0–4.2	$45 \pm 3$ – $107 \pm 10$	Engel et al. (2017)
Arctic Ocean	Sea ice covered	Autumn and Spring 2009–2010	Above mixed layer depth	125–1750 <sup>a</sup>	0.1–7.8 <sup>b</sup>	–	Wurl et al. (2011a)
Eastern tropical and Eastern subarctic, North Pacific Ocean	Eutrophic and oligotrophic	Summer 2009	Above mixed layer depth	78–970 <sup>a</sup>	0.3–1.7 <sup>b</sup>	–	Wurl et al. (2011)
Western subarctic and North Pacific Ocean	Non bloom	Summer 2001	5	40–60	0.2–1.9	–	Ramaiah et al. (2005)
Northeast Atlantic Ocean	Different bloom stages	Summer 1996	0–70	10 <sup>c</sup> –124	0.1–1.1 <sup>c,d</sup>	49–104	Engel (2004)
		Autumn 1996	0–50	$28.5 \pm 10.2$	0.07–0.6	61	
Northeast Atlantic Ocean	Late stages bloom	Spring 2005	0–10	20–420 <sup>c</sup>	0.1–3 <sup>c,e</sup>	–	Leblanc et al. (2009)
Western tropical North Pacific Ocean	Non bloom Oligotrophic	Spring 2013	Surface mixed layer ( $36 \pm 12$ )	$43 \pm 7$ (18–67 <sup>c</sup> )	$0.05 \pm 0.01$	$832 \pm 314$	Kodama et al. (2014)
Western North Atlantic Ocean	Oligotrophic	Spring 2014	1	161–460	0.1–1 <sup>c</sup>	–	Jennings, et al. (2017)
Western North Atlantic Ocean and Sargasso Sea	Eutrophic and oligotrophic	Spring 2014	2–5	100–200 <sup>c</sup>	0.1–2.2	–	Aller (2017)
Sargasso Sea	Oligotrophic	Spring, summer, autumn 2012 and spring 2013	0–100	$21 \pm 2$ – $57 \pm 3$	0.05–1 <sup>c</sup>	–	Cisternas–Novoa et al. (2015)
Mediterranean Sea	Non bloom	Spring 2007	Upper mixed	29 (19–53)	bdl–1.8 <sup>f</sup>	484 (178–1293)	Ortega–Retuerta et al.

			layer				(2010)
Western Mediterranean Sea	Oligotrophic	Spring 2012	0–200	16–25 <sup>c,g,h</sup>	0.1–0.7 <sup>c,h</sup>	–	Ortega–Retuerta et al. (2017)
Eastern Mediterranean Sea	Oligotrophic	Winter–Autumn 2008 Summer 2009	5	345 ± 143.2 (116–420)	0.04 ± 0.01 (0.04–0.07)	–	Bar–Zeev et al. (2011)
Gulf of Aqaba (Eilat, Israel)	Oligotrophic	Spring 2008	5	110–228 <sup>c</sup>	0.3–1.3 <sup>i</sup>	–	Bar–Zeev et al. (2009)
Tropical Atlantic Ocean	Oligotrophic	Spring–Summer 2011	3	8.18 ± 4.56	0.05–0.31	78.6 ± 9.3	Iuculano et al. (2017b)
Pacific Ocean	Oligotrophic	Spring–Summer 2011	3	24.45 ± 2.3		357 ± 127	Iuculano et al. (2017b)
Global Subtropical Atlantic, Indian and Pacific Oceans	Non bloom	Winter 2010– Summer 2011	0–200	14.0 (0.4–173.6)	0–3 <sup>c</sup>	–	Mazuecos (2015)
North Indian Ocean -Arabian Sea -Bay of Bengal	Eutrophic	-August 1996 -September 1996	0–1000	-60 <sup>j,k</sup> (< 5–102 <sup>j</sup> ) -7–13 <sup>c,j</sup>	–	–	Kumar et al. (1998), Ramaiah et al. (2000)
OAO OAO (CU excluded) CU	Oligotrophic	Autumn 2014	4	72 ± 74 (18–446) 60 ± 27(18–132) 446	0.4 ± 0.2 (0.2–0.6) 0.3 ± 0.1 (0.2–0.6) 0.25	236 ± 293 (81–1760) 183 ± 56 (81–360) 1760	This study
Ross Sea	Bloom	Spring 1994	Surface	308 (0–2800)	3.6 (0.3–8.8)	85	Hong et al. (1997)

<sup>a</sup> TEP concentrations were given in  $\mu\text{mol C L}^{-1}$ . For transformation into XG units, the Engel and Passow (2001) conversion factor of  $0.51 \mu\text{g TEP-C L}^{-1}$  per  $\mu\text{g XG eq L}^{-1}$  was applied. <sup>b</sup> 1–8 m. <sup>c</sup> extracted from graphs. <sup>d</sup> 5 m. <sup>e</sup> TChl *a*. <sup>f</sup> 0–200 m. <sup>g</sup> Depth-averaged TEP. <sup>h</sup> stations 6–9. <sup>i</sup> DCM (30–40 m). <sup>j</sup> TEP concentrations were given in milligram equivalent of alginic acid  $\text{L}^{-1}$  and absorbance was measured at 745 nm instead of 787 nm. <sup>k</sup> 0–50 m.

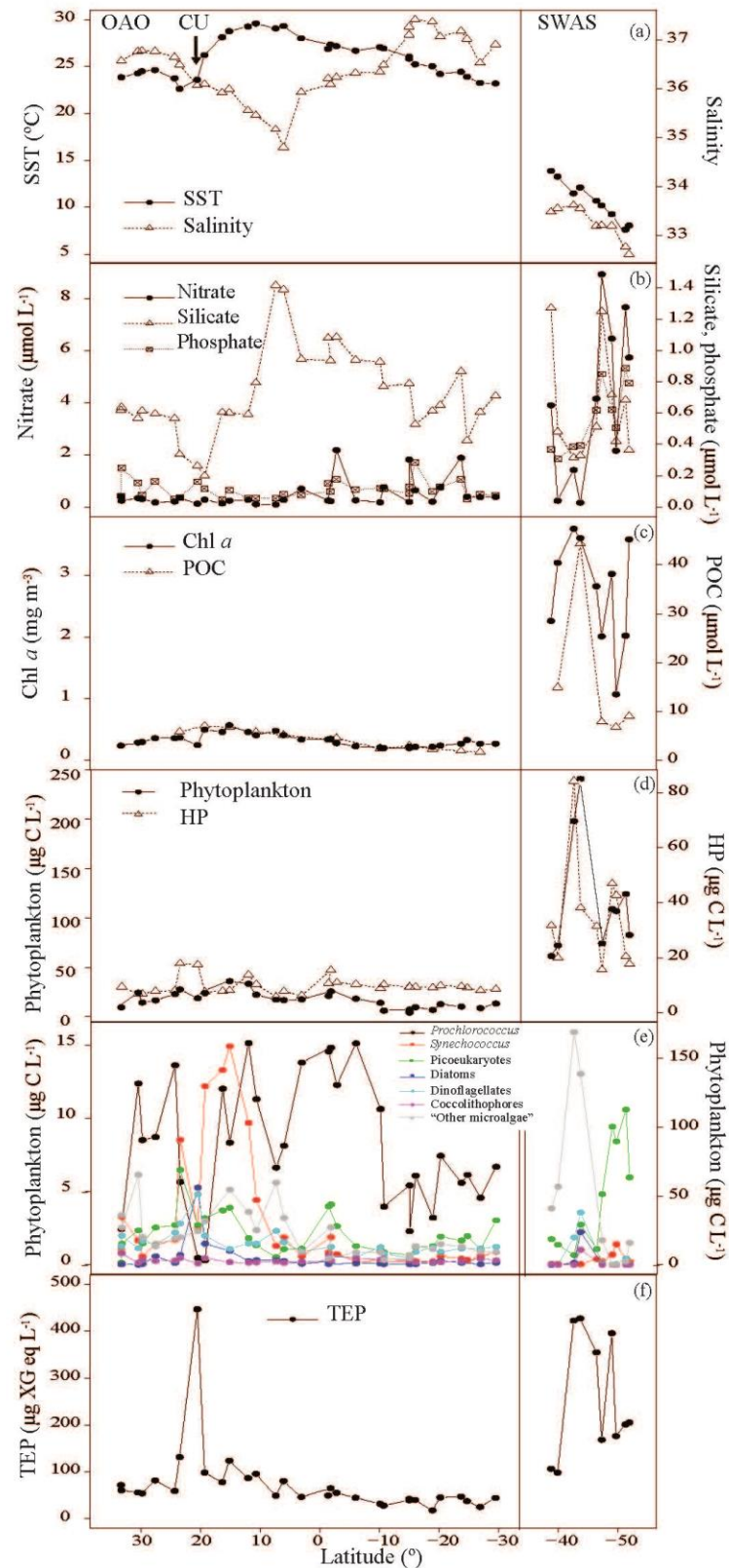


**Figure 1.2:** Variations of sea surface temperature (SST, °C) and salinity (panel (a)), nitrate, silicate and phosphate ( $\mu\text{mol L}^{-1}$ ) (panel (b)), Chl *a* ( $\text{mg m}^{-3}$ ) and POC ( $\mu\text{mol L}^{-1}$ ) (panel (c)), biomass of phytoplankton and HP ( $\mu\text{g CL}^{-1}$ ) (panel (d)), biomass of *Prochlorococcus*, *Synechococcus*, picoeukaryotes, diatoms, dinoflagellates, coccolithophores and "other microalgae" ( $\mu\text{g CL}^{-1}$ ) (panel (e): For OAO use left axis, for SWAS use right axis) and TEP ( $\mu\text{g XG eq L}^{-1}$ ) (panel (f)) in the TransPEGASO cruise.

### 1.4.2 TEP as an important contributor to ocean surface POC

The significant positive correlation between TEP and POC observed in our study highlighted the importance of TEP-determining POC horizontal variations in the surface Atlantic Ocean, suggesting a high contribution of TEP to this pool. A few values of TEP-C%POC were unrealistically higher than 100 %, a feature that has also been observed in other studies (Engel and Passow, 2001; Bar-Zeev et al., 2011; Yamada et al., 2015). This suggests the inaccuracy of the use of standard TEP-to-carbon conversion factors (CFs,  $0.51 \mu\text{g TEP-C L}^{-1}$  ( $\mu\text{g Xeq. L}^{-1}$ ) in our case). Therefore there is a need to define specific CFs for diverse regions or environmental conditions. Nonetheless, an alternative explanation for the apparent oversizing of the relative TEP-C pool may be strictly methodological: TEP are determined on filters of  $0.4 \mu\text{m}$  pore size, whereas POC is measured on glass fibre filters with nominal pore size of  $0.7 \mu\text{m}$ . It is plausible, thus, that some of the smaller TEP particles are not taken into account in the POC measurement.

All in all, our results clearly show that TEP-C constituted an important portion of the POC pool in the Atlantic Ocean (from 28 to 110 %). This contribution is comparable to that reported in the eastern Mediterranean Sea (Bar-Zeev et al., 2011; Parinos et al., 2017), lower than in the western Arctic (Yamada et al., 2015), but higher than in the Northeast Atlantic Ocean (Harlay et al., 2009; Harlay et al., 2010). Both in the OAO and SWAS, TEP comprised the largest share of the POC pool, with phyto-C being equal or the second most important contributor to POC (Fig. 1.3). Phyto-C surpassed TEP-C in only one station in the WAS. The contribution of phyto-C and HP-C to the POC pool should be considered with caution, as the glass fibre filters (nominal pore size  $0.7 \mu\text{m}$ ) used to analyze POC could have not retained all the small phytoplankton organisms and prokaryotes (Gasol and Morán, 1999), causing underestimation of the actual POC pool. Furthermore, conversion factors carry quite an uncertainty, as pointed out in the Methods section.

A previous study in a eutrophic system reported TEP-C as the dominant POC contributor (Yamada et al., 2015), whereas others found that phyto-C represented the largest share to POC compared to TEP-C and HP-C (Bhaskar and Bhosle, 2006;

Ortega-Retuerta et al., 2009b; de Vicente et al., 2010). With our results taken all together, we hypothesize that in oligotrophic conditions TEP–C is the predominant POC fraction, because nutrient limitation favors TEP production by phytoplankton and limits TEP consumption by bacteria. Conversely, in eutrophic conditions, the predominant POC fraction depends on many variables like the community composition, the bloom stage and sources of TEP other than phytoplankton.

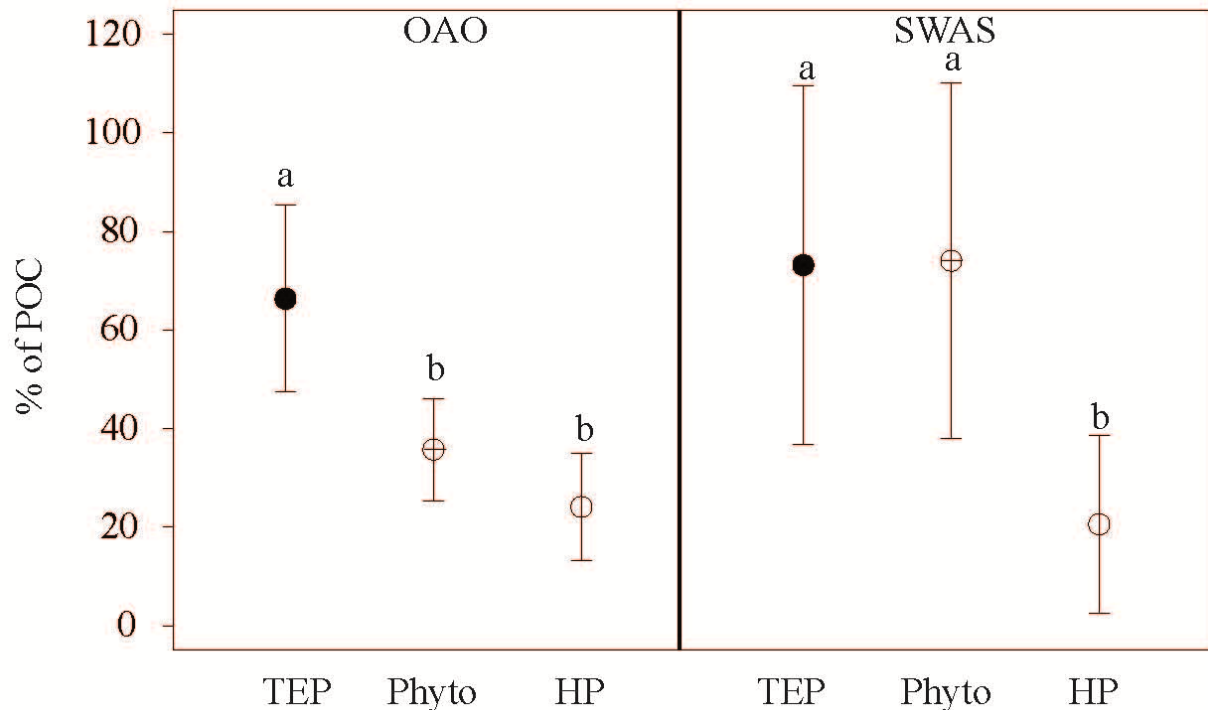


**Figure 1.3:** Average and standard deviation of the contribution of TEP, phytoplankton and HP to the POC pool (%) in the OAO and the SWAS.

### 1.4.3 Main drivers of TEP distribution in the surface ocean

In order to better understand and even predict the occurrence of TEP in the surface ocean, it is important to describe their distribution together with those of their main putative sources (phytoplankton and heterotrophic prokaryotes), sinks and environmental modulators, across large-scale gradients. However, most of the previous studies of TEP in the Atlantic Ocean were restricted to local areas, and, to our knowledge, only one included a complete description of these variables together in a long transect (Mazuecos, 2015).

Our dataset suggests that phytoplankton is the main driver of TEP distribution in the surface Atlantic Ocean at the horizontal scale, since significant positive relationships were observed between TEP and both Chl *a* and phytoplankton biomass (Table 1.3). It is worth noting that Chl *a* was a good estimator of phytoplankton biomass when the entire cruise was considered, as these variables were tightly related ( $R^2 = 0.79$ ,  $p$  value  $< 0.001$ ,  $n = 36$ ). The slope of the log converted TEP–Chl *a* relationship for the whole study ( $\beta = 0.66 \pm 0.08$ , Table 1.3) was within the upper range amongst published data (Fig. 1.5), and the slope in the OAO ( $\beta = 1.13 \pm 0.20$ ) was the highest reported so far (Table 1.3, Fig. 1.5). In the SWAS, the TEP–Chl *a* relationship was not significant ( $p$  value  $> 0.05$ ), yet it was for TEP–phytoplankton biomass (see below).

TEP:Chl *a* ratios were significantly ( $p < 0.001$ ) higher in the OAO (both including or excluding the CU) than in the SWAS (Table 1.1), with the maximum value in the station located in the CU. TEP:Chl *a* values in the OAO (CU included) were comparable to those observed in other oligotrophic areas (Riebesell et al., 1995; García et al., 2002; Prieto et al., 2006; Harlay et al., 2009; Ortega-Retuerta et al., 2010; Kodama et al., 2014; Iuculano et al., 2017c; Parinos et al., 2017) (Table 1.2), while the values in the SWAS were comparable to those reported in eutrophic waters (Hong et al., 1997; Ramaiah et al., 2001; Engel et al., 2002b; Corzo et al., 2005; Ortega-Retuerta et al., 2009b). The higher TEP:Chl *a* ratios in oligotrophic waters (Prieto et al., 2006) are related to nutrient scarcity, which is suggested to enhance TEP production by phytoplankton and prokaryotes (Myklestad, 1977; Guerrini et al., 1998; Mari et al., 2005; Beauvais et al., 2006). The highest TEP:Chl *a* ratio of the entire transect observed in the station located in the CU was probably associated with the high relative abundance of diatoms and dinoflagellates. These groups are known to be strong TEP producers (Passow and Alldredge, 1994), and besides, previous studies have shown that TEP production rates reach maxima at late stages of the growth cycle, once nutrients have been exhausted (Corzo et al., 2000; Pedrotti et al., 2010; Borchard and Engel, 2015). In the CU, the relatively low Chl *a* level along with low silicate concentrations suggests that the upwelling–triggered bloom maximum had already passed, which resulted in a high TEP:Chl *a* ratio. Although POC was not measured in the CU, high TEP:Chl *a* suggests a high proportion of TEP with respect to other organic particles. In the SWAS, the lower TEP:Chl *a* ratios could be related with a lower rate of TEP production under relatively replete nutrient conditions. Extending our comparison to the

literature, the TEP:Chl *a* ratio is generally higher in oligotrophic regions (Prieto et al., 2006; Ortega-Retuerta et al., 2010; Kodama et al., 2014; Iuculano et al., 2017c) than in eutrophic regions (Hong et al., 1997; Engel et al., 2002b; Corzo et al., 2005; Ortega-Retuerta et al., 2009b; Klein et al., 2011; Engel et al., 2017).

In the OAO, the phytoplankton groups that showed a significant ( $p < 0.05$ ) positive relationship to TEP and hence were candidates to be considered as the main producers of TEP or their precursors were *Synechococcus*, picoeukaryotes, diatoms, dinoflagellates and “other microalgae” (Table 1.3). All the abovementioned groups have been reported to produce TEP (see references in the introduction). Conversely, coccolithophores and *Prochlorococcus* did not present a significant relationship with TEP. It has been shown in cultures that coccolithophores do not produce high amounts of TEP (Passow, 2002a), and a previous study showed temporal disconnections between coccolithophores and TEP maxima (Ortega-Retuerta et al., 2018). However, in a previous study in the Atlantic Ocean, Leblanc et al. (2009) found an association of TEP with coccolithophores.

The oligotrophic ocean covers a big portion of the global ocean and it is mostly dominated by picophytoplankton (Agawin et al., 2000), chiefly *Prochlorococcus* and *Synechococcus* (Partensky et al., 1999). (Iuculano et al., 2017c) reported relatively high rates of TEP production by *Prochlorococcus* in culture, and Mazuecos (2015) found a significant and positive relationship of TEP with *Prochlorococcus* abundance in the low-latitude oceans. The absence of significant covariation between TEP and the abundant *Prochlorococcus* in our study suggests that these picophytoplankters are not the main TEP producers, or their production is strongly modulated by environmental conditions. It is remarkable that, amongst the phytoplankton groups of the present study, *Synechococcus* biomass presented the highest correlation ( $R^2 = 0.72$ ) with TEP concentration in the OAO. Deng et al. (2016) demonstrated TEP production by marine *Synechococcus* in a laboratory study, but only Mazuecos (2015) had previously found a significant and positive relationship ( $R^2 = 0.26$ – $0.36$ ) between these two variables in the ocean, particularly in the Atlantic, North Pacific and Indian oceans. This author actually found that *Synechococcus* was the phytoplankton group with the highest relationship with TEP concentration. Our study supports the importance of *Synechococcus* as a TEP source in the oligotrophic ocean.

**Table 1.3.** Regression equations and statistics describing the relationship between TEP and different variables throughout the TransPEGASO cruise (note all variables were  $\log_{10}$ -transformed). B= biomass.

Dep. Var.	Ind. Var.	Open Atlantic Ocean (CU excluded)					SW Atlantic Shelf					All			
		R <sup>2</sup>	<i>p</i>	intercept	slope	n	R <sup>2</sup>	<i>p</i>	intercept	slope	n	R <sup>2</sup>	<i>p</i>	intercept	slope
TEP	SST	0.07	0.16			29	0.06	0.51			9	<b>0.48</b>	<b>&lt; 0.001</b>	<b>3.80</b>	<b>-1.43</b>
	Salinity	<b>0.26</b>	<b>&lt; 0.05</b>	<b>21.78</b>	<b>-12.84</b>	<b>29</b>	0.002	0.90			9	<b>0.57</b>	<b>&lt; 0.001</b>	<b>25.13</b>	<b>-14.97</b>
	Solar irradiance 24 h	<b>0.43</b>	<b>&lt; 0.001</b>	<b>5.67</b>	<b>-1.04</b>	<b>30</b>	0.08	0.40			10	0.02	0.33		
	Nitrate	0.06	0.21			30	0.002	0.91			10	<b>0.13</b>	<b>0.02</b>	<b>1.97</b>	<b>0.23</b>
	Phosphate	0.04	0.29			30	0.02	0.69			10	<b>0.37</b>	<b>&lt; 0.001</b>	<b>2.39</b>	<b>0.58</b>
	Silicate	0.07	0.15			30	0.24	0.15			10	<b>0.19</b>	<b>&lt; 0.005</b>	<b>1.75</b>	<b>-0.80</b>
	Chl <i>a</i>	<b>0.56</b>	<b>&lt; 0.001</b>	<b>2.31</b>	<b>1.13</b>	<b>29</b>	0.16	0.24			10	<b>0.61</b>	<b>&lt; 0.001</b>	<b>2.09</b>	<b>0.66</b>
	HPA	0.04	0.31			29	0.36	0.06			10	<b>0.60</b>	<b>&lt; 0.001</b>	<b>-4.28</b>	<b>1.03</b>
	HNA	0.01	0.57			29	<b>0.46</b>	<b>0.03</b>	<b>-0.44</b>	<b>0.46</b>	<b>10</b>	<b>0.51</b>	<b>&lt; 0.001</b>	<b>-2.31</b>	<b>0.75</b>
	LNA	0.02	0.43			29	0.02	0.71			10	<b>0.17</b>	<b>&lt; 0.05</b>	<b>-1.96</b>	<b>0.68</b>
	<i>Prochlorococcus</i> B	0.002	0.80			30	-	-				-	-		
	<i>Synechococcus</i> B	<b>0.72</b>	<b>&lt; 0.001</b>	<b>1.72</b>	<b>0.28</b>	<b>30</b>	0.005	0.84			10	<b>0.30</b>	<b>&lt; 0.001</b>	<b>1.87</b>	<b>0.34</b>
	Picoeukaryotes B	<b>0.15</b>	<b>&lt; 0.05</b>	<b>1.68</b>	<b>0.23</b>	<b>30</b>	0.005	0.84			10	<b>0.49</b>	<b>&lt; 0.001</b>	<b>1.71</b>	<b>0.37</b>
	Diatoms B	<b>0.37</b>	<b>&lt; 0.001</b>	<b>1.96</b>	<b>0.26</b>	<b>27</b>	0.40	0.07	2.43	0.14	9	<b>0.23</b>	<b>&lt; 0.05</b>	<b>2.10</b>	<b>0.24</b>
	Dinoflagellates B	<b>0.20</b>	<b>&lt; 0.05</b>	<b>1.70</b>	<b>0.42</b>	<b>27</b>	0.30	0.13			9	0.09	0.07		
	Coccolithophores B	0.005	0.73			27	0.002	0.90			9	<b>0.14</b>	<b>&lt; 0.05</b>	<b>1.75</b>	<b>-0.20</b>
	“Other microalgae” B	<b>0.38</b>	<b>&lt; 0.001</b>	<b>1.66</b>	<b>0.37</b>	<b>27</b>	0.0002	0.97			9	<b>0.27</b>	<b>&lt; 0.001</b>	<b>1.79</b>	<b>0.27</b>
Phytoplankton B	<b>0.53</b>	<b>&lt; 0.001</b>	<b>1.01</b>	<b>0.61</b>	<b>26</b>	<b>0.73</b>	<b>&lt; 0.05</b>	<b>0.24</b>	<b>1.03</b>	<b>9</b>	<b>0.69</b>	<b>&lt; 0.001</b>	<b>0.97</b>	<b>0.65</b>	

R<sup>2</sup> explained variance, *n* sample size, *p* level of significance



In the SWAS, unlike in the OAO, the significant relationship between TEP and the total phytoplankton biomass ( $R^2 = 0.62$ ) was not accompanied by any relationship to any phytoplankton group (Table 1.3). This could be due to the high variability of the phytoplankton composition in the SWAS stations. Since many phytoplankton taxa are capable of TEP production, it is difficult to discern one group playing the main role. Moreover, as mentioned before, in these shelf waters TEP formation could have been further modulated by aggregation of colloids carried by freshwater discharges.

Regarding the influence of abiotic factors in TEP distribution, we found a negative relationship ( $R^2 = 0.43$ ) between TEP concentration and the 24 h averaged solar irradiance in the OAO (Fig. 1.4). The OAO stations were exposed to high solar radiation due to water transparency and their location in tropical and subtropical regions. Ultraviolet (UV) radiation causes TEP loss by photolysis (Ortega-Retuerta et al., 2009a) and inhibits TEP formation from precursors (Orellana and Verdugo, 2003). However, it has also been proved that solar radiation harms picophytoplanktonic cells through photobiological stress, inducing TEP production (Agustí and Llabrés, 2007; Iuculano et al., 2017c). Our results suggest that the roles of UV radiation in breaking up TEP and/or limiting their formation from precursors overcome UV stress-induced TEP production.

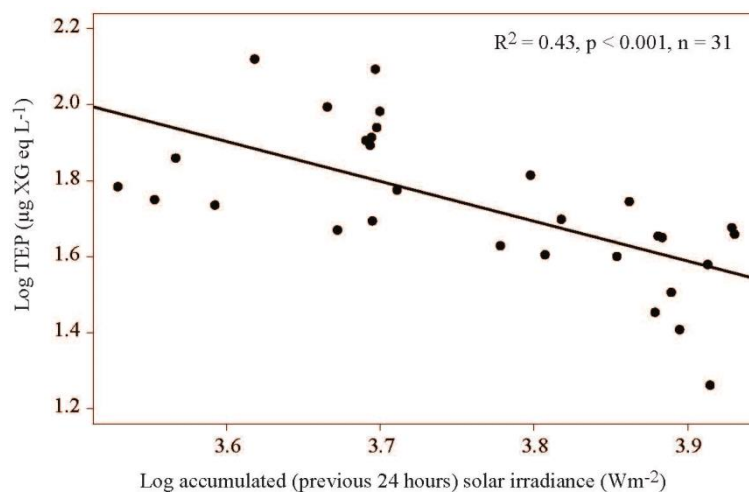


**Figure 1.4:** Relationship between the 24 hour–accumulated (previous to sampling) solar irradiance ( $\text{W m}^{-2}$ ) and TEP ( $\mu\text{g XG eq. L}^{-1}$ ) in the OAO (CU sample excluded). The linear regression line is plotted and the equation indicated.

The role of HPs as potential drivers of TEP distribution is not straightforward, since their net effect on TEP accumulation depends on local conditions. Across the entire transect, TEP concentration was significantly ( $p < 0.001$ ) and positively related to HPA (Table 1.3). However, the relationship was not significant considering the regions separately, and only in the SWAS were TEP significantly ( $p < 0.05$ ) and positively related to HNA, considered to be a proxy of the more active cells (Servais et al., 1999; Lebaron et al., 2001). This relationship in the SWAS could indicate that HPs used TEP as a significant carbon source or that both HPs and TEP were controlled by the same drivers, such as the presence of dissolved polysaccharides, which are substrates for HP as well as TEP precursors (Mari and Kiorboe, 1996). In the OAO, despite the lack of a paired relationship between TEP and HPA, multiple regression analyses showed that both phytoplankton and HPs contributed significantly to explain TEP concentration variance (Table 1.4).

In summary, our study describes for the first time the horizontal distribution of TEP across a north–south transect in the Atlantic Ocean. TEP constituted a large portion of the POC pool, larger than phytoplankton at most stations and always larger than heterotrophic prokaryotic biomass. This supports the important role of TEP in the carbon cycle. The drivers of TEP distribution were primarily phytoplankton and, to a lesser extent, heterotrophic prokaryotes among sources, with *Synechococcus* playing an outstanding role in the oligotrophic ocean. In the oligotrophic ocean, solar irradiance was a major identifiable sink. We call for the need to carry out more extensive studies in the ocean, across both space and time, in order to better predict the occurrence of TEP and incorporate diagnostic relationships in model projections. These diagnostic studies must be combined with further process studies if we are to relate TEP concentrations to important biogeochemical processes such as microbial colonization of particles, organic matter export to the deep ocean, gas exchange at the air–water interface and organic aerosol formation.

**Table 1.4.** Results of multiple regression analyses between TEP and combined variables, all log<sub>10</sub>-transformed.

Dep. Var.	Ind.Var.	OAO (CU excluded)				SWAS				All			
		Partial coefficient	Partial <i>p</i>	R <sup>2</sup>	<i>p</i>	Partial coefficient	Partial <i>p</i>	R <sup>2</sup>	<i>p</i>	Partial coefficient	Partial <i>p</i>	R <sup>2</sup>	<i>p</i>
TEP	Phyto B HPA	0.64	< 0.001	0.60	< 0.001	0.82	< 0.05	0.66	< 0.05	0.52	< 0.001	0.73	< 0.001
		0.21	0.58			0.38	0.13	0.74		0.34	0.08		
	Phyto B HNA	0.67	< 0.001	0.59	< 0.001	0.91	0.05	0.74	0.65	<b>0.55</b>	<b>&lt; 0.001</b>	<b>0.75</b>	<b>&lt; 0.001</b>
		0.09	0.59			0.08	0.70			<b>0.28</b>	<b>&lt; 0.05</b>		
	Chl <i>a</i> HPA	<b>1.26</b>	<b>&lt; 0.001</b>	<b>0.67</b>	<b>&lt; 0.001</b>	0.48	0.26	0.33	0.10	<b>0.39</b>	<b>&lt; 0.005</b>	<b>0.66</b>	<b>&lt; 0.001</b>
		<b>0.56</b>	<b>&lt; 0.05</b>			0.59	0.08			<b>0.54</b>	<b>&lt; 0.01</b>		
	Chl <i>a</i> HNA	1.28	< 0.001	0.60	< 0.001	0.30	0.48	0.36	0.08	<b>0.47</b>	<b>&lt; 0.001</b>	<b>0.67</b>	<b>&lt; 0.001</b>
		0.20	0.20			0.42	0.06			<b>0.37</b>	<b>&lt; 0.01</b>		

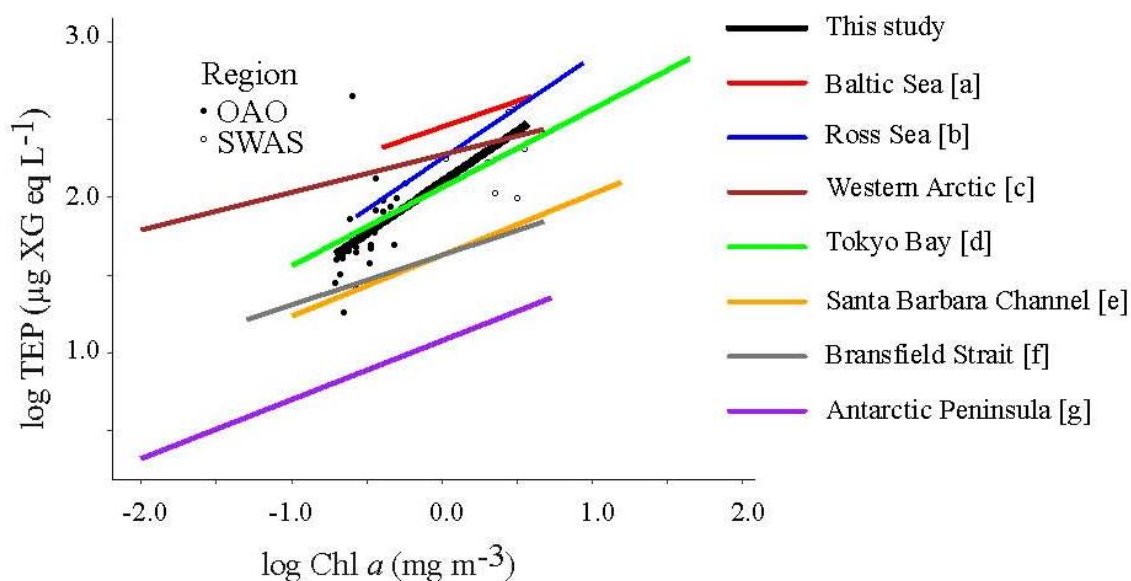
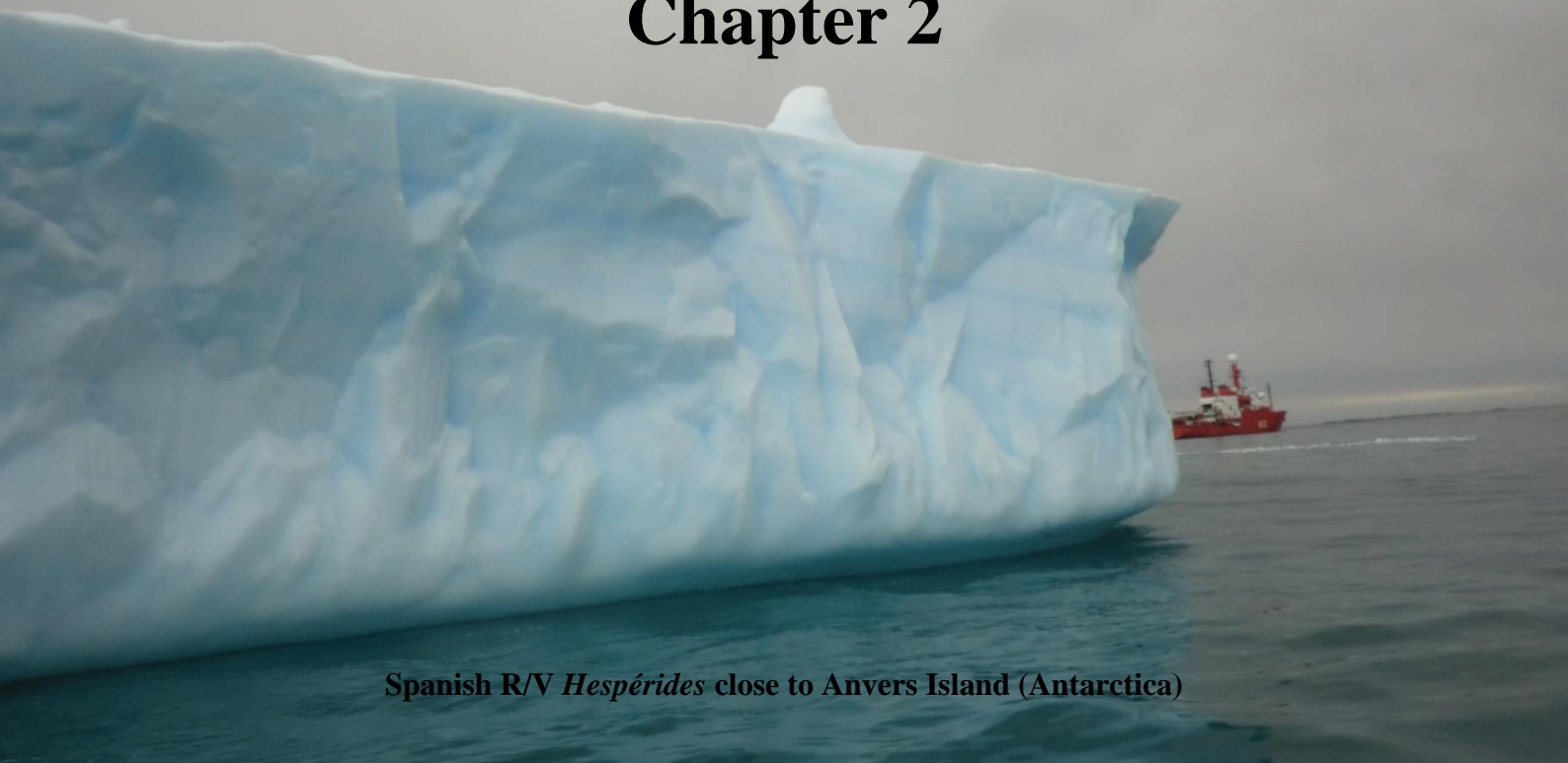


**Figure 1.5:** Relationship between TEP and Chl *a* concentration from the TransPEGASO cruise, with the linear regression line (regression equation in the text). Two regions are distinguished: open Atlantic Ocean (OAO, CU included, filled circles) and SW Atlantic Shelf (SWAS, empty circles). Regression lines from the literature are also shown for comparison.  $\alpha$  and  $\beta$  indicate the y intercept and slope, respectively;  $\log \text{TEP} (\mu\text{g XGeq. L}^{-1}) = \alpha + \beta \times \log \text{Chl } a (\text{mg m}^{-3})$ ; [a]  $\alpha = 2.45$  and  $\beta = 0.33$ , (Engel, 1998 in Passow, 2002a); [b]  $\alpha = 2.25$  and  $\beta = 0.65$ , (Hong et al., 1997); [c]  $\alpha = 2.27$  and  $\beta = 0.24$ , (Yamada et al., 2015); [d]  $\alpha = 2.06$  and  $\beta = 0.50$ , (Ramaiah and Furuya, 2002); [e]  $\alpha = 1.63$  and  $\beta = 0.39$ , (Passow and Alldredge, 1995); [f]  $\alpha = 1.63$  and  $\beta = 0.32$ , (Corzo et al., 2005); [g]  $\alpha = 1.08$  and  $\beta = 0.38$ , (Ortega-Retuerta et al., 2009b).

## 1.5 Acknowledgements

This research was funded by the Spanish Ministry of Economy and Competitiveness through projects PEGASO (CTM2012–37615) and BIOGAPS (CTM2016–81008–R) to R.S. M.Z. was supported by a FPU predoctoral fellowship from the Spanish Ministry of Education and Culture. E.O–R. was supported by a Marie Curie Actions Intra–European Fellowship (H2020–MSCA–IF–2015–703991). The authors thank Pep Gasol and Carolina Antequera for assistance with flow cytometry; Maximino Delgado for microscopic phytoplankton counts; Rocío Zamanillo and Rafael Campos for assistance with R software; and the scientists, the Marine Technology Unit (UTM–CSIC) and crew on board the RV *Hespérides* for help during the cruise.

## Chapter 2



Spanish R/V *Hespérides* close to Anvers Island (Antarctica)

### **Distribution of transparent exopolymer particles (TEP) in distinct regions of the Southern Ocean**

*Marina Zamanillo, Eva Ortega-Retuerta, Sdena Nunes, Marta Estrada, María Montserrat Sala, Sarah-Jeanne Royer, Daffne C. López-Sandoval, Mikhail Emelianov, Dolors Vaqué, Cèlia Marrasé, Rafel Simó, 2019.*

*Science of the Total Environment, 691, 736-748*





**Abstract**

Transparent exopolymer particles (TEP) are an abundant class of suspended organic particles, mainly formed by polysaccharides, which play important roles in biogeochemical and ecological processes in the ocean. In this study we investigated horizontal and vertical TEP distributions (within the euphotic layer, including the upper surface) and their short-term variability along with a suite of environmental and biological variables in four distinct regions of the Southern Ocean. TEP concentrations in the surface (4 m) averaged  $102.3 \pm 40.4 \mu\text{g XG eq L}^{-1}$  and typically decreased with depth. Chlorophyll *a* (Chl *a*) concentration was a better predictor of TEP variability across the horizontal ( $R^2 = 0.66$ ,  $p < 0.001$ ) and vertical ( $R^2 = 0.74$ ,  $p < 0.001$ ) scales than prokaryotic heterotrophic abundance and production. Incubation experiments further confirmed the main role of phytoplankton as TEP producers. The highest surface TEP concentrations were found north of the South Orkney Islands ( $144.4 \pm 21.7 \mu\text{g XG eq L}^{-1}$ ), where the phytoplankton was dominated by cryptophytes and haptophytes; however, the highest TEP:Chl *a* ratios were found south of these islands ( $153.4 \pm 29.8 \mu\text{g XG eq } (\mu\text{g Chl } a)^{-1}$ ), compared to a mean of  $79.3 \pm 54.9 \mu\text{g XG eq } (\mu\text{g Chl } a)^{-1}$  in the whole cruise, in association with haptophyte dominance, proximity of sea ice and high exposure to solar radiation. TEP were generally enriched in the upper surface (10 cm) respect to 4 m, despite a lack of biomass enrichment, suggesting either upward transport by positive buoyancy or bubble scavenging, or higher production at the upper surface by light stress or aggregation. TEP concentrations did not present any significant cyclic diel pattern. Altogether, our results suggest that photobiological stress, sea ice melt and turbulence add to phytoplankton productivity in driving TEP distribution across the Antarctic Peninsula area and Atlantic sector of the Southern Ocean.





## 2.1 Introduction

Transparent exopolymer particles (TEP) are gel-like organic particles stainable with Alcian Blue, a specific dye for acidic polysaccharides (Alldredge et al., 1993), that have deserved attention due to their influence in biogeochemical and ecological processes (Passow, 2002b). TEP are partly formed by the abiotic self-assembly from dissolved precursors (Chin et al., 1998; Orellana and Verdugo, 2003), thus connecting the dissolved to particulate organic matter continuum (Engel et al., 2004b). In addition, TEP affect the biological carbon pump, not only because TEP by themselves may comprise a mean of 5-10 % of primary production synthates (Mari et al., 2017) that can sink into the deep ocean, but also because they promote particle aggregation (Engel et al., 2004b), thus favoring the sinking of marine snow to the deep ocean (Burd and Jackson, 2009). TEP also influence air-sea gas exchanges like that of carbon dioxide (CO<sub>2</sub>) (Wurl et al., 2016; Jenkinson et al., 2018), since they tend to accumulate at the surface microlayer (SML, the uppermost water layer, Cunliffe et al. (2013)), either after ascending through the water column (Azetsu-Scott and Passow, 2004) or upon direct production in this layer (Wurl et al., 2011b).

Phytoplankton are believed to be the main source of TEP and their precursors (Alldredge et al., 1993; Passow, 2002b; Van Oostende et al., 2012; Engel et al., 2015), being diatoms (Passow et al., 1994; Mari and Burd, 1998; Passow et al., 2001; Passow, 2002a) and haptophytes, like *Phaeocystis* (Hong et al., 1997), the groups that seem to release larger amounts. Prokaryotic heterotrophs (Stoderegger and Herndl, 1999; Ortega-Retuerta et al., 2010) and other organisms, such as suspension feeders (Heinonen et al., 2007), zooplankton (Prieto et al., 2001) and seagrass (Iuculano et al., 2017b), can also produce TEP.

Sinks of TEP comprise photolysis by UV radiation (Ortega-Retuerta et al., 2009a), sinking to the deep ocean, entrance to the atmosphere (Kuznetsova et al., 2005), and degradation and consumption by microorganisms (Ling and Alldredge, 2003). Many variables influence either sources, sinks or both, hindering the prediction of TEP distribution in the ocean. For example, high solar radiation has a dual effect; it stimulates TEP release by microbes (Iuculano et al., 2017c) but also causes TEP photolysis (Ortega-Retuerta et al., 2009a) or affect positively (Shammi et al., 2017) or negatively (Orellana and Verdugo, 2003) the abiotic self-assembly of dissolved

exopolymers into TEP. Other variables such as temperature (Nicolaus et al., 1999; Claquin et al., 2008), CO<sub>2</sub> concentration (Engel, 2002), nutrient availability (Mari et al., 2005) and viral infections (Nissimov et al., 2018) can also influence TEP cycling. Moreover, the TEP production per phytoplankton biomass increases along the bloom stages (Pedrotti et al., 2010), thus adding complexity to the TEP dynamics.

The Southern Ocean (SO) is characterized by the presence of the Antarctic Circumpolar Current, which connects the waters of the Pacific, Indian and Atlantic Oceans, and by having strong upwellings that enrich surface waters with macronutrients (Sarmiento et al., 2004). Productivity is generally limited by the lack of iron in combination with deep surface mixing and low light and temperature (Moore et al., 2013; Hoppe et al., 2017), although some regions are locally supplied with iron, particularly in the vicinity of islands (Morris and Sanders, 2011).

The study of TEP distributions in the SO is of particular importance in light of these ocean's peculiarities. The SO is considered the largest region for anthropogenic CO<sub>2</sub> sequestration in the world (Frölicher et al., 2015), especially around the island systems (Pollard et al., 2009), through higher CO<sub>2</sub> solubility in cold waters and a relatively high particulate organic carbon (POC) surface export flux in comparison to lower latitudes (Boyd and Trull, 2007; Marinov et al., 2008). Indeed, C export fluxes have been reported to attain 30-50 % of net primary production (Buesseler, 2001). Since TEP may account for an important fraction of POC mass (Engel, 2004; Zamanillo et al., 2019c) and export flux (Passow, 2002b; Wurl et al., 2011a), their study in the SO is important to better predict the magnitude of the biological carbon pump and the future dynamics of atmospheric CO<sub>2</sub>.

In this study we describe the horizontal and vertical (within the euphotic layer) distributions, and short-term (diel) variability of TEP, along with relevant physical, chemical and biological variables, in four distinct regions of the SO. The four regions were characterized by distinct phytoplankton communities, bloom stages and environmental and ecological properties. Our objectives were: (a) to identify the main drivers of TEP distribution across contrasting environmental conditions, both horizontally and vertically, and (b) to examine the short-term temporal variability of TEP and biological variables, over diel cycles. Data co-variation analyses and

experimental incubations were conducted to ascertain the role of microorganisms (phytoplankton vs. heterotrophic prokaryotes) in TEP production.

## 2.2 Material and methods

### 2.2.1 Study site and sampling

Sampling was performed during the PEGASO cruise, on board the Spanish R/V *Hespérides*, conducted from 7<sup>th</sup> January to 3<sup>rd</sup> February, in the austral summer of 2015. A total of 70 stations were sampled within the Southern Ocean (Fig. S2.1). Four regions were occupied for several days, following a Lagrangian approach; the north of the South Orkney Islands (NSO), the southeast of the South Orkney Islands (SSO), the northwest of South Georgia (NSG) and the west of Anvers Island (WA). NSO, NSG and WA were selected due to their relatively high chlorophyll *a* (Chl *a*) concentrations, different nutrient conditions and relatively slow currents with the absence of stable direction (Nunes et al., 2019). SSO was selected for its vicinity to the sea ice edge. In order to track the studied water bodies, WOCE (World Ocean Circulation Experiment) standard drifters provided with Iridium communication system were used in the NSO, NSG and WA regions; in SSO, two icebergs were used as natural Lagrangian drifters.

During the transit between the regions, seawater was collected from 4 m depth using the ship's underway pump (BKMKC-10.11. Tecnum, Manresa, Spain), approximately at 9:00 and 15:00 local time (UTC-3). During the Lagrangian occupation of the main stations, CTD casts were carried out using a SBE 911 Plus probe attached to a rosette of 24 12-L PVC Niskin bottles, at least once a day, generally at 9:00 and 15:00 local time (UTC-3). The underway sampling was used when conditions were too rough for CTD launch (a total of 3 times). A 36-h cycle was also sampled in each region, with CTD casts every 4 h, generally from 9:30 to 17:00 (solar times) the day after. NASA Solar Calculator (<https://www.esrl.noaa.gov/gmd/grad/solcalc/>, accessed on 15 December 2017) was used to perform solar time calculations (Nunes et al., 2019). The position of the main hydrographic fronts was determined as described in Nunes et al. (2019).

TEP, major nutrients, POC, prokaryotic heterotrophic abundance (PHA) and production (PHP), primary production (PP), phytoplankton recount and identification by microscopy and flow cytometry, extracellular enzyme activities and virus concentrations

were analysed in surface samples. At 7 stations (three in NSO, two in SSO, one in NSG and one in WA), Chl *a*, phytoplankton pigment analyses and PHA were carried out for 6 different depths, generally from 4 to 120-150 m, while TEP were analysed for 4 depths, from 4 m to the second deepest depth. In some of these stations, phytoplankton identification and recount by microscopy and flow cytometry were done from 2 to 4 depths, including the depth of maximum fluorescence. Mixed layer depth (MLD) estimation was done from CTD profiles following Monterey and Levitus (1997).

A total of 14 samples (one in the transit between regions, seven in NSO, four in SSO, one in NSG and one in WA) were collected from the upper surface (10 cm) using a zodiac boat, away and upstream from the ship to avoid contamination. Sampling was carried out with a device of our own design, consisting of a 50 mL glass syringe connected to a PTFE tube 1.5 m long, whose other end was fixed onto a floating item so that the inlet of the tube remained at a depth of 10 cm regardless of the motion of the sea surface. All material was prewashed with HCl (10 %) and Milli-Q water. Typical collected volume was 400 mL; usually, sampling took place around 10:00 local time (UTC-3) during standard stations and at 11:00 and 17:00 local time during intensive day-night cycles. TEP, Chl *a*, PHA, PHP and extracellular enzyme activities were analysed at the upper surface. In order to compare these measurements with those at the nominal surface (4 m depth of the nearest CTD casts), we calculated an enrichment factor ( $EF_{us}$ ), defined as:

$$EF_{us} = \frac{[X]_{\text{upper surface}}}{[X]_{\text{surface}}}$$

where  $[X]$  is the concentration of a given variable, in the upper surface and surface respectively.  $EF_{us} > 1$  indicates enrichment of a component in the upper surface and  $EF_{us} < 1$  indicates depletion. It is worth mentioning that the time difference between the upper surface sampling and the nearest surface sampling was 1-3 h. When the upper surface sampling occurred exactly between two CTD casts, the average of the two was used.

### 2.2.2 Physical measurements

Surface temperature and salinity were obtained continuously with the SBE21 Sea Cat Thermosalinograph, while vertical profiles were recorded down to 400 m with a CTD

SBE911 plus. Average diffuse attenuation coefficient in the euphotic zone for PAR broadband (400-700 nm;  $K_d$  (PAR)), from both CTD and PRR-800 vertical profiles of downwelling spectral irradiance ( $E_d$ ), were determined as the slope of the linear regression between logarithmic irradiances and depth. Prior to analysis, the data were carefully examined for irregularities (Mueller et al., 2003). Near-surface noise caused by smooth waves and ripples was eliminated from  $E_d$  (PAR) profiles. The obtained  $R^2$  of regression analyses were always above 0.98 at all evaluated casts. The depth of the euphotic layer was then calculated as  $4.605/K_d$  (PAR), being the depth at which  $K_d$  (PAR) is reduced to 1 % of its value just below the surface. Solar radiation dose was calculated in every station using the following formula:

$$\text{Solar radiation dose} = \frac{I}{K_d(\text{PAR}) \times \text{MLD}} \times (1 - e^{(-K_d(\text{PAR}) \times \text{MLD})})$$

where,  $I$  is the average surface intensity radiation ( $\text{W m}^{-2}$ ) in the 24 h previous to sampling,  $K_d$  (PAR) is the average diffuse attenuation coefficient in the euphotic zone for PAR broadband ( $\text{m}^{-1}$ ), and MLD is the mixed layer depth (m).

## 2.2.3 Chemical and biological analyses

### 2.2.3.1 Particulate organic matter (TEP and POC)

TEP were analysed by spectrophotometry following the method proposed by Passow and Alldredge (1995). Samples were filtered under low constant filtration pressure (~150 mmHg) in duplicate (200-550 mL) using 25 mm diameter polycarbonate filters (DHI) with a pore size of 0.4  $\mu\text{m}$ . All sampling material was pre-washed with HCl (10 %) and Milli-Q water. Filters were immediately stained with 500  $\mu\text{L}$  of Alcian Blue solution (0.02 %, pH 2.5) for 5 s, and then rinsed with Milli-Q water. Two empty filters (blanks) were taken at every station and stained in the same way. All filters remained frozen until further processing some months later at the home laboratory. There, filters were soaked in 80 % sulfuric acid (5 mL) for 3 h and shaken intermittently. Absorbance of the acid solutions was then measured at 787 nm with a Varian Cary 100 Bio spectrophotometer. The absorbance of filter blanks, taken in duplicate for every batch of samples, was subtracted from the absorbance of samples. Calibration of the Alcian Blue solution was conducted immediately after the cruise using xanthan gum (XG) solution as a standard. The detection limit was set to 0.045 absorbance units, and the mean range

between duplicates was 25.5 %. TEP carbon content (TEP-C) was estimated using the conversion factor of 0.51  $\mu\text{g}$  TEP-C per  $\mu\text{g}$  XG eq (Engel and Passow, 2001).

For POC analysis, we filtered water samples (1000 mL) through pre-combusted (4 h, 450 °C) GF/F glass fiber filters (Whatman) that remained frozen (-20 °C) until further processing. Filters were dried, acidified to remove carbonates and analyzed with an elemental analyser (Perkin-Elmer 2400 CHN).

### **2.2.3.2 Chl *a***

For Chl *a* analyses, 250 mL of sea water were filtered through 25 mm diameter glass filters (Whatman GF/F). Filters were stored frozen (-20 °C) until further processing in the home laboratory. Ninety % acetone was used to extract pigments at 4 °C in the dark for 24 h. The procedure of Yentsch and Menzel (1963) was followed to measure fluorescence of extracts, with a calibrated Turner Designs fluorometer.

### **2.2.3.3 Inorganic nutrients**

To analyse dissolved inorganic nutrients (nitrate, phosphate and silicate), unfiltered water samples were stored frozen (-20 °C) in 10 mL sterile polypropylene bottles and further processed in the home laboratory using a Skalar Autoanalyser and the standard segmented flow analyses with colorimetric detection elemental analyser (Hansen and Grasshoff, 1983).

### **2.2.3.4 HPLC pigment analysis and CHEMTAX**

As described in Nunes et al. (2019), HPLC was used to determine pigment composition, following Latasa (2014). Thirty-two pigments were identified at 474 and 664 nm. Version 1.95 of the CHEMTAX chemical taxonomy software was used to derive the contribution of microalgal groups to the total Chl *a* biomass ( $\text{ng Chl } a \text{ L}^{-1}$ ), from pigment data (Mackey et al., 1996). Seven pigmentary classes were quantified: chlorophytes, cryptophytes, diatoms, dinoflagellates, haptophytes, prasinophytes and pelagophytes. Pigments were also used as indicators of phytoplankton photoacclimation. Diadinoxanthin (Ddx) is the main light-protecting pigment in diatoms, dinoflagellates, haptophytes and pelagophytes. The Ddx:LHC ratio, between Ddx and the sum of the main light-harvesting carotenoids (LHC: fucoxanthin, 19'-butanoyloxyfucoxanthin, 19'-hexanoyloxyfucoxanthin and peridinin) was measured,

since it varies with the exposure of phytoplankton to underwater solar radiation (Higgins et al., 2011; Nunes et al., 2019).

### **2.2.3.5 Picophytoplankton abundance and biomass**

Abundance of picoplankton was determined by flow cytometry in a FACS Calibur instrument (Becton and Dickinson), as described in Zamanillo et al. (2019c). *Prochlorococcus* and *Synechococcus* were undetectable in all samples. Biomass of picoeukaryotic algae was measured using the average C:cell conversion factor from Simó et al. (2009):  $1319 \pm 813 \text{ fg C cell}^{-1}$ .

### **2.2.3.6 Microphytoplankton identification and biomass**

We identified and quantified phytoplankton groups by microscopy, using the inverted microscope method (Utermöhl, 1958) as described in Nunes et al. (2019). We measured the biomass of phytoplankton groups using conversion equations of Menden-Deuer and Lessard (2000), as explained in Zamanillo et al. (2019c). The total biomass of phytoplankton (Phyto B) was obtained as the sum of all the phytoplankton groups.

### **2.2.3.7 Primary production (PP)**

Phytoplankton primary production rates at four depths within the water column were determined by using  $20 \mu\text{Ci}$  of  $\text{NaH}^{14}\text{CO}_3$  (Steeman-Nielsen, 1952) in a series of 2-3 h-long, on-deck incubations in flowing surface seawater and under simulated in situ light levels. During the 36-h cycles, water was collected directly from the Niskin bottles in 72 mL acid-washed polystyrene bottles at different sampling times (8:30, 16:30, 4:00 and 12:00 local time (UTC-3)). PP rates were estimated from radioisotope incorporation into particles retained on a  $0.2 \mu\text{m}$  PC filter, after acid removal of inorganic  $^{14}\text{C}$  and subtraction of the incorporation in dark controls. Daily rates were estimated by taking into account the daylight period.

### **2.2.3.8 Prokaryotic heterotrophic abundance (PHA) and production (PHP)**

Prokaryotic heterotrophic abundance (PHA) was determined by flow cytometry following standard methods, after fixation with 1 % paraformaldehyde plus 0.05 % glutaraldehyde (Gasol and del Giorgio, 2000). PHP was estimated following the Kirchman et al. (1985) method after the centrifugation method described in Smith and



Azam (1992). Final leucine concentration was 40 nM. The incubations were carried out in the dark at in situ temperature in a water bath during 3-4 h.

#### **2.2.3.9 Viral abundance (VA)**

Viral abundance was quantified using flow cytometry (Brussaard, 2004). We discriminated three viral subpopulations with different green fluorescence properties (Brussaard et al., 2010) and classified them as “phage viruses” (PV), “large viruses” (LV) and “total viruses” (TV).

#### **2.2.3.10 Extracellular enzyme activities**

We determined the activity of the extracellular enzymes  $\beta$ -glucosidase, esterase and fucosidase following the method detailed in Sala et al. (2016).

#### **2.2.3.11 Maximum quantum efficiency of photosystem II photochemistry ( $F_v:F_m$ )**

Maximum quantum efficiency of photosystem II photochemistry ( $F_v:F_m$ ) was measured using a Fast Repetition Rate fluorometer (FRRf; FASTracka, Chelsea Technologies, Surrey, UK) on continuous seawater pumped from ca. 4 m deep, as described in Royer et al. (2015).

#### **2.2.4 TEP production by microbes during experimental incubations**

To examine TEP production by microbes (phytoplankton and heterotrophic prokaryotes), we conducted two incubation experiments using surface water (4 m) from the NSO (Experiment NSO) and the NSG (Experiment NSG). Seawater was prefiltered through 200  $\mu\text{m}$  to exclude the presence of mesozooplankton. Each experiment consisted of two treatments: 1) unfiltered seawater (total (T) treatment), 2) seawater filtered through 0.8  $\mu\text{m}$  pore-size Nucleopore filters to exclude most phytoplankton and heterotrophic flagellates, leaving mainly prokaryotes (prokaryotic (P) treatment). Both treatments were set up in triplicates in 25 L teflonated containers under in situ irradiance and temperature conditions. Treatments were incubated for 8 and 13 days for the experiments NSO and NSG, respectively. Experiment NSO was sampled at initial time ( $t_0$ ) and after 3 ( $t_1$ ) and 8 ( $t_2$ ) days, and the experiment NSG was sampled at initial time ( $t_0$ ) and after 2 ( $t_1$ ) and 13 ( $t_2$ ) days. The variables analysed were TEP, PHP and Chl *a*, and we calculated TEP production rate per growth rate ( $\Delta\text{TEP}$ :  $\Delta\text{Chl } a$ ).

### 2.2.5 Statistical analyses

The packages *lmodel2* and *ggplot2* of R software were used to test for covariations and to study the potential control of variables on TEP distribution in this study. Bivariate analyses (ordinary least squares, OLS) between TEP concentrations and different chemical, physical and biological variables were used to determine their main predictors. Although ranged major axis (RMA) regression would have been more suitable, due to the presence of errors in our dependent and independent variables, we performed OLS regressions to better compare the slopes between our study and others present in the literature. We used pairwise Spearman correlation analyses to compare different variables in the upper surface (10 cm) and in the surface (4 m). The data were log-transformed to fulfil the requirements of parametric tests. Non-parametric ANOVA followed by post-hoc tests (Tukey) were carried out to compare variables among the four regions. Principal component analysis (PCA) (*devtools* and *ggbiplot* packages in R) was applied to all samples after centering and scaling variables. One PCA was done with a total number of 21 physical, chemical and biological variables, TEP included, while the other one was done replacing TEP and Chl *a* by the TEP:Chl *a* ratio, which is indicative of how prone the plankton community was to net TEP production. The map in Fig. S2.1 was produced using the Ocean Data View software (version 4) (Schlitzer and 2017). The rest of plots were drawn using R programming software (version 3.5.1).

## 2.3 Results

### 2.3.1 General characterization of sea surface waters

The four study regions (NSO, SSO, NSG and WA, Fig. S2.1) presented distinct physical, chemical and biological properties, summarized in Table 21. Surface temperatures in the whole transect ranged from -0.9 to 5.1 °C and salinity varied over a narrow range (33.1-34.2). Surface nitrate concentrations ranged from 14.6 to 32.5  $\mu\text{mol L}^{-1}$  and covaried with those of phosphate (1.0-2.5  $\mu\text{mol L}^{-1}$ ). Silicate concentrations were significantly lower in the NSG region ( $2.0 \pm 0.4 \mu\text{mol L}^{-1}$ ) than in the other three regions ( $48.1 \pm 4.2 \mu\text{mol L}^{-1}$ ). Within the whole transect, surface Chl *a* concentrations ranged between 0.28 and 8.95  $\mu\text{g L}^{-1}$  and averaged  $2.36 \pm 1.92 \mu\text{g L}^{-1}$ , with a coefficient of variation of 81 %. PHA ranged from 1.60 to  $8.44 \times 10^5 \text{ cells mL}^{-1}$ , while PHP ranged

between  $0.09$  and  $2.65 \text{ mg C m}^{-3} \text{ d}^{-1}$ . POC ranged from  $3.85$  to  $25.63 \text{ } \mu\text{mol L}^{-1}$  and was higher in NSG and WA ( $11.37$ - $25.63 \text{ } \mu\text{mol L}^{-1}$ ). Primary production was highest in the NSG, averaging  $111.6 \pm 85.4 \text{ mg C m}^{-3} \text{ d}^{-1}$ , while in the other three regions it averaged  $16.2 \pm 15.8 \text{ mg C m}^{-3} \text{ d}^{-1}$ , being lower in the SSO ( $3.7 \pm 0.8 \text{ mg C m}^{-3} \text{ d}^{-1}$ ). Solar radiation dose and Ddx:LHC ratio were higher in the NSO and SSO regions, whereas  $F_v:F_m$  was lower in these regions.

The NSO was located within a meander of the Southern Boundary of the Antarctic Circumpolar Current (Fig. S2.1) and two months before sampling, this region was covered by  $> 25 \%$  of sea ice (<https://seaice.uni-bremen.de/start/>). The average values of the surface temperature were  $0.59 \pm 0.15 \text{ }^\circ\text{C}$  (Fig. S2.2). The Chl *a* concentration averaged  $1.87 \pm 0.23 \text{ } \mu\text{g L}^{-1}$  (Fig. 2.1), and phytoplankton was dominated by cryptophytes, haptophytes and diatoms (Fig. S2.2). The main planktonic cells identified by microscopy at the surface of this region included the diatoms *Corethron pennatum*, *Fragilariopsis* spp. and *Thalassiosira* spp., unidentified autotrophic cryptophytes and nanoflagellates, and heterotrophic (like *Gyrodinium* spp.) and autotrophic dinoflagellates (Nunes et al., 2019).

The SSO was placed north of the Weddell Front (Fig. S2.1). During the sampling month, the ice cover was  $> 25 \%$  in the region (<https://seaice.uni-bremen.de/start/>) (Nunes et al., 2019). The month before, the ice cover was  $> 50 \%$ ; therefore, we sampled waters of the receding ice edge. The surface temperature was the lowest among the four regions ( $-0.75 \pm 0.11 \text{ }^\circ\text{C}$ ). Surface Chl *a* averaged  $0.32 \pm 0.06 \text{ } \mu\text{g L}^{-1}$ , i.e., significantly ( $p < 0.05$ ) lower than in the other regions (Fig. 2.1). Phytoplankton was dominated by haptophytes, followed by cryptophytes, chlorophytes and diatoms (Fig. S2.2). The main planktonic cells identified by microscopy were the same as in the NSO but with a higher proportion of *Fragilariopsis* spp., a characteristic diatom marker of sea ice influence. The SSO presented the highest Ddx:LHC ratio ( $0.58 \pm 0.09$ ; Fig. 2.1) and the lowest  $F_v:F_m$  ratio ( $0.16 \pm 0.05$ ), consistently indicating exposure to higher solar radiation intensities in a shallower mixed layer (Table 2.1).

The NSG was located right south of the Polar Front, north of the subAntarctic South Georgia Islands (Fig. S2.1). Sea surface temperature was the highest among regions ( $4.77 \pm 0.45 \text{ }^\circ\text{C}$ ), and the MLD was deepest. The relatively low silicate concentrations found in this region coincided with the dominance of well-silicified diatoms in the

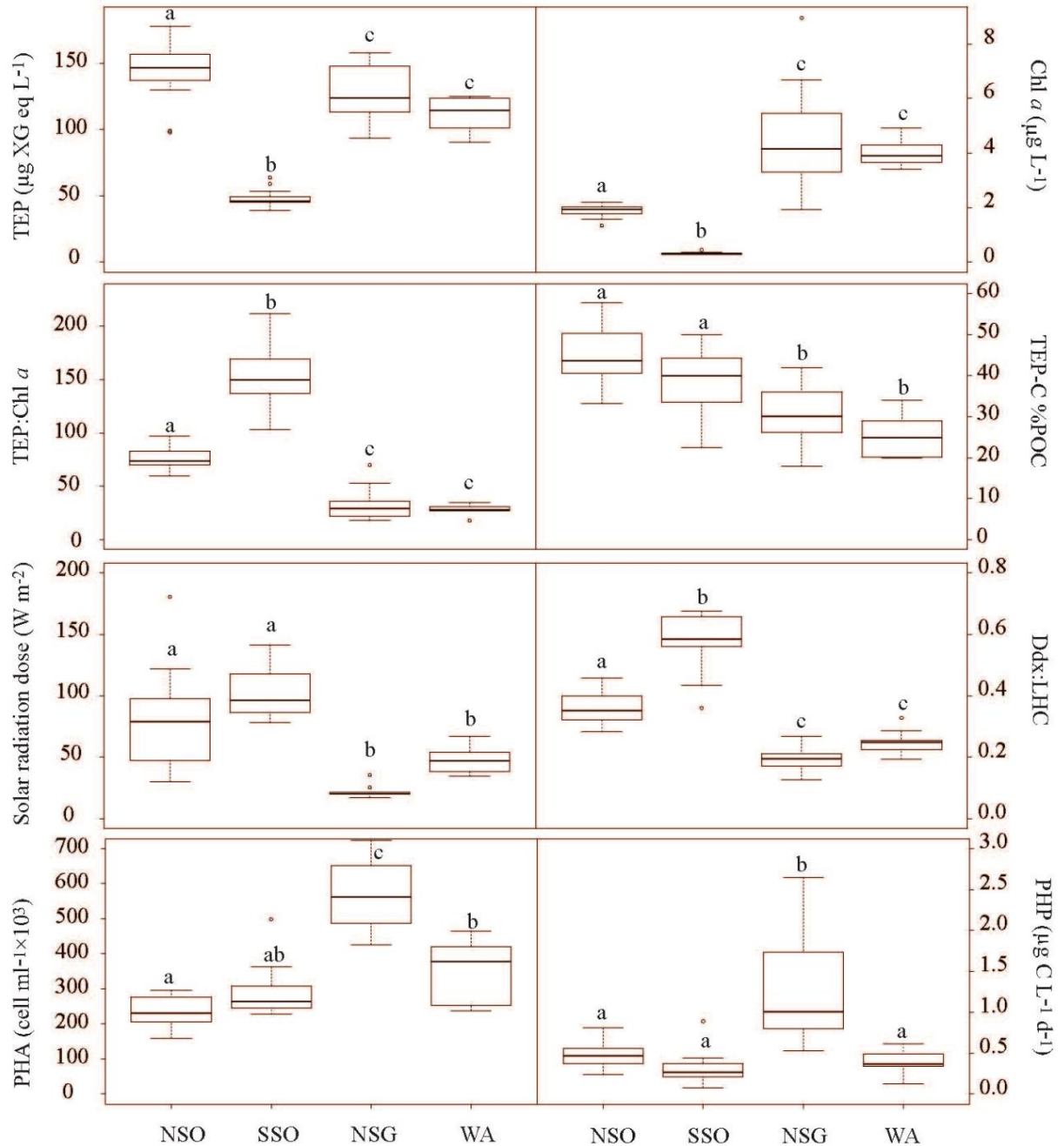


**Figure 2.1:** Boxplots of transparent exopolymer particles (TEP), chlorophyll *a* (Chl *a*), TEP:Chl *a*, contribution of TEP-C to the POC (particulate organic carbon) pool (TEP-C%POC), solar radiation dose, Ddx:LHC ratio (Ddx: Diadinoxanthin, LHC: sum of the main light-harvesting carotenoids), prokaryotic heterotrophic abundance (PHA) and prokaryotic heterotrophic production (PHP) in the surface of the four visited regions :North of the South Orkney Islands (NSO), South of the South Orkney Islands (SSO), Northwest of South Georgia Island (NSG), West of Anvers Island (WA). The horizontal lines of the boxes represent 25%, 50% (median) and 75% percentiles (from bottom to top). Whiskers represent minimum and maximum values.

phytoplankton community (like *Eucampia Antarctica*, *Thalassiosira* and *Porosira* spp. and *Odontella weissflogii*; Fig. S2.2) and a smaller proportion of haptophytes and pelagophytes. Surface Chl *a* concentration averaged  $4.59 \pm 1.97 \mu\text{g L}^{-1}$  (Fig. 2.1). The phytoplankton community was complemented by haptophytes and pelagophytes. Total viral abundances (TVA), PHP, PHA and  $F_v:F_m$  were significantly higher ( $p < 0.05$ ) in this region than in the others, whereas the solar radiation dose and Ddx:LHC were the lowest.

The WA region was placed at the southernmost limit of the Antarctic Circumpolar Current (Southern Boundary) (Fig. S2.1). The average surface temperature was  $1.46 \pm 0.09 \text{ }^\circ\text{C}$ . Chl *a* concentration was slightly lower than in the NSG, with an average of  $4.05 \pm 0.48 \mu\text{g L}^{-1}$  (Fig. 2.1). The phytoplankton community was dominated by cryptophytes, haptophytes and diatoms (Fig. S2.2).

### **2.3.2 TEP concentrations, TEP:Chl *a*, TEP:Phyto B and TEP:PP ratios and contribution of TEP to POC in the sea surface of the study regions**

Surface TEP concentrations in the entire study regions and transects ranged from 39.2 to  $177.6 \mu\text{g XG eq L}^{-1}$  and averaged  $102.3 \pm 40.4 \mu\text{g XG eq L}^{-1}$ , with a coefficient of variation of 39 %. Mean TEP concentrations were significantly different among regions ( $p < 0.05$ ; Table 2.1). NSO presented the maximum TEP concentrations ( $144.4 \pm 21.7 \mu\text{g XG eq L}^{-1}$ ) and SSO presented the lowest ones ( $48.1 \pm 6.5 \mu\text{g XG eq L}^{-1}$ ), while NSG and WA presented similar TEP concentrations ( $125.5 \pm 21.1$  and  $111.6 \pm 13.0 \mu\text{g XG eq L}^{-1}$ , respectively; Fig. 2.1).

The TEP:Chl *a* ratios were also significantly different among regions ( $p < 0.05$ ; Fig. 2.1). SSO presented the highest TEP:Chl *a* values ( $153.4 \pm 29.8$ ), while NSG and WA presented the lowest ratios ( $32.3 \pm 15.0$  and  $28.2 \pm 4.8$ , respectively; Fig. 2.1). The ratio in NSO was  $76.7 \pm 10.6$ . In the case of TEP:Phyto B and TEP:PP ratios, the SSO presented the highest values and the NSG the lowest ones (Table 2.1).

TEP and POC were significantly and positively correlated across the entire transect ( $R^2 = 0.70$ ,  $p < 0.001$ ,  $n = 68$ ; Table 2.2). The contribution of TEP-C to the POC pool (TEP-C%POC) ranged between 17.9 and 97.3 % (average  $38.8 \pm 12.3$  %). TEP-C%POC in the NSO and the SSO were similar ( $44.7 \pm 6.7$  and  $38.5 \pm 8.7$  %, respectively) and higher than in NSG ( $30.6 \pm 6.2$  %) and WA ( $25.2 \pm 5.3$  %; Fig. 2.1).

**Table 2.1.** Mean  $\pm$  standard deviation of several variables and dominant phytoplankton groups in the sea surface (4 m depth) of the four study regions. MLD: mixed layer depth. Phyto B: Phytoplankton biomass. PP: Primary production. POC: Particulate organic carbon. PHA and PHP: Prokaryote heterotrophic abundance and production, respectively. TVA and LVA: Total and large viral abundance, respectively.  $F_v:F_m$ : Maximum quantum efficiency of photosystem II photochemistry. Ddx:LHC: Ddx, diadinoxanthin; LHC, sum of the main light-harvesting carotenoids. TEP: Transparent exopolymer particles. See Fig. 2.1 for abbreviations of regions.

	NSO (n= 16)	SSO (n= 15)	NSG (n= 14)	WA (n= 9)
Date (d/m/y)	10-15/01/2015	16-20/01/2015	23-25/01/2015	02-03/02/2015
Temperature ( $^{\circ}\text{C}$ )	$0.59 \pm 0.15^a$	$-0.75 \pm 0.11^b$	$4.77 \pm 0.45^c$	$1.46 \pm 0.09^d$
Salinity	$33.83 \pm 0.08^a$	$33.15 \pm 0.05^b$	$33.74 \pm 0.02^c$	$33.41 \pm 0.03^d$
MLD (m)	$28.9 \pm 11.8^a$	$15.8 \pm 5.4^b$	$49.3 \pm 11.8^c$	$22.9 \pm 5.6^{ab}$
Ice cover (%)	$0^e$	$> 25$	0	0
Solar radiation dose ( $\text{W m}^{-2}$ )	$80.3 \pm 40.4^a$	$101.7 \pm 20.3^a$	$22.4 \pm 5.4^b$	$47.0 \pm 10.6^b$
Nitrate ( $\mu\text{mol L}^{-1}$ )	$27.3 \pm 1.9^a$	$27.5 \pm 3.2^a$	$17.2 \pm 1.6^b$	$18.7 \pm 0.9^b$
Phosphate ( $\mu\text{mol L}^{-1}$ )	$2.0 \pm 0.2^{aa}$	$2.1 \pm 0.3^{ab}$	$1.3 \pm 0.2^c$	$1.8 \pm 0.2^{aa}$
Silicate ( $\mu\text{mol L}^{-1}$ )	$47.9 \pm 4.1^a$	$47.3 \pm 4.7^a$	$2.0 \pm 0.4^b$	$49.7 \pm 3.7^a$
Chl <i>a</i> ( $\mu\text{g L}^{-1}$ )	$1.87 \pm 0.23^a$	$0.32 \pm 0.06^b$	$4.59 \pm 1.97^c$	$4.05 \pm 0.48^c$
Phyto B ( $\mu\text{g C L}^{-1}$ )	$95.7 \pm 21.0^a$	$22.3 \pm 4.4^b$	$222.1 \pm 53.1^c$	$94.4 \pm 37.5^a$
PP ( $\text{mg C m}^{-3} \text{d}^{-1}$ )	$13.0 \pm 4.0^a$	$3.7 \pm 0.8^a$	$111.6 \pm 85.4^b$	$34.6 \pm 15.7^a$
POC ( $\mu\text{mol L}^{-1}$ )	$13.8 \pm 2.6^a$	$5.5 \pm 1.2^b$	$18.0 \pm 4.4^c$	$19.3 \pm 3.5^c$
PHA ( $\text{cells mL}^{-1} \times 10^5$ )	$2.34 \pm 0.46^a$	$2.89 \pm 0.70^{ab}$	$5.68 \pm 0.98^c$	$3.43 \pm 0.95^b$
PHP ( $\mu\text{g C L}^{-1} \text{d}^{-1}$ )	$0.50 \pm 0.16^a$	$0.32 \pm 0.19^a$	$1.23 \pm 0.66^b$	$0.40 \pm 0.14^a$
TVA ( $\text{virus mL}^{-1} \times 10^5$ )	$44.8 \pm 21.8^a$	$32.3 \pm 17.1^a$	$211.2 \pm 99.8^b$	$137.1 \pm 42.5^c$
LVA ( $\text{virus mL}^{-1} \times 10^5$ )	$2.8 \pm 0.9^a$	$2.5 \pm 2.3^a$	$25.3 \pm 19.5^b$	$8.9 \pm 5.1^a$
Dominant phytoplankton groups	Cryptophytes > haptophytes > diatoms	Haptophytes > cryptophytes ~ chlorophytes ~ diatoms	Diatoms	Cryptophytes >>haptophytes > diatoms
$F_v:F_m$	$0.18 \pm 0.06^a$	$0.16 \pm 0.05^a$	$0.29 \pm 0.05^b$	$0.21 \pm 0.06^a$
Ddx:LHC	$0.36 \pm 0.06^a$	$0.58 \pm 0.09^b$	$0.19 \pm 0.04^c$	$0.25 \pm 0.04^c$
TEP ( $\mu\text{g XG eq L}^{-1}$ )	$144.4 \pm 21.7^a$	$48.1 \pm 6.5^b$	$125.5 \pm 21.1^c$	$111.6 \pm 13.0^c$
TEP:Chl <i>a</i> ( $\mu\text{g XG eq } \mu\text{g}^{-1}$ )	$76.7 \pm 10.6^a$	$153.4 \pm 29.8^b$	$32.3 \pm 15.0^c$	$28.2 \pm 4.8^c$
TEP:Phyto B	$1.56 \pm 0.35^a$	$2.24 \pm 0.54^b$	$0.61 \pm 0.18^c$	$1.26 \pm 0.36^a$
TEP:PP	$12.5 \pm 3.1^{a,b}$	$14.0 \pm 5.7^a$	$1.8 \pm 1.3^c$	$4.6 \pm 4.1^{b,c}$
TEP:POC ( $\mu\text{g XG } \mu\text{g C}^{-1}$ )	$0.9 \pm 0.1^a$	$0.8 \pm 0.2^a$	$0.6 \pm 0.1^b$	$0.5 \pm 0.1^b$

<sup>a, b, c, d</sup> significantly different ( $p < 0.05$ ) groups using non-parametric ANOVA followed by post-hoc tests (Tukey). <sup>e</sup> ice cover was  $> 25$  % two months before our study

**Table 2.2.** Regression equations and statistics describing the relationship between transparent exopolymer particles (TEP) (dependent variable) and several independent variables across surface samples in the entire PEGASO cruise (note all variables were  $\log_{10}$ -transformed). Regressions with  $p < 0.05$  are highlighted in bold. PVA: phage viral abundance. See Table 2.1 for abbreviations.

Dep. var.	Independent var.	R <sup>2</sup>	p	Intercept	Slope	n
TEP	Temperature <sup>a</sup>	<b>0.27</b>	<b>&lt; 0.001</b>	<b>-78.1</b>	<b>32.8</b>	66
	Salinity	<b>0.25</b>	<b>&lt; 0.001</b>	<b>-33.74</b>	<b>23.38</b>	66
	Wind speed	<b>0.08</b>	<b>&lt; 0.05</b>	<b>2.13</b>	<b>-0.19</b>	67
	Nitrate	<b>0.10</b>	<b>&lt; 0.05</b>	<b>2.84</b>	<b>-0.63</b>	69
	Phosphate	<b>0.14</b>	<b>&lt; 0.05</b>	<b>2.18</b>	<b>-0.77</b>	69
	Silicate	<b>0.06</b>	<b>&lt; 0.05</b>	<b>2.08</b>	<b>-0.08</b>	69
	Solar radiation dose	<b>0.24</b>	<b>&lt; 0.001</b>	<b>2.65</b>	<b>-0.38</b>	46
	Chl <i>a</i>	<b>0.66</b>	<b>&lt; 0.001</b>	<b>1.90</b>	<b>0.35</b>	65
	Phyto B	<b>0.66</b>	<b>&lt; 0.001</b>	<b>1.17</b>	<b>0.43</b>	67
	PP	<b>0.43</b>	<b>&lt; 0.05</b>	<b>1.67</b>	<b>0.25</b>	19
	PHA	0.01	> 0.05			71
	PHP	<b>0.18</b>	<b>&lt; 0.001</b>	<b>2.07</b>	<b>0.25</b>	68
	TVA	<b>0.16</b>	<b>&lt; 0.001</b>	<b>0.45</b>	<b>0.22</b>	71
	LVA	<b>0.08</b>	<b>&lt; 0.05</b>	<b>1.27</b>	<b>0.12</b>	71
	PVA	<b>0.18</b>	<b>&lt; 0.001</b>	<b>0.41</b>	<b>0.23</b>	71
	POC <sup>b</sup>	<b>0.70</b>	<b>&lt; 0.001</b>	<b>-1.00</b>	<b>1.03</b>	68
	PHA:Chl <i>a</i>	<b>0.71</b>	<b>&lt; 0.001</b>	<b>4.07</b>	<b>-0.39</b>	64
	F <sub>v</sub> :F <sub>m</sub>	0.04	> 0.05			71
	Ddx:LHC	<b>0.18</b>	<b>&lt; 0.001</b>	<b>1.74</b>	<b>-0.42</b>	68
	Prasinophytes <sup>c</sup>	<b>0.68</b>	<b>&lt; 0.001</b>	<b>1.86</b>	<b>0.14</b>	37
	Chlorophytes <sup>c</sup>	<b>0.17</b>	<b>&lt; 0.05</b>	<b>1.72</b>	<b>0.23</b>	38
	Dinoflagellates <sup>c</sup>	<b>0.67</b>	<b>&lt; 0.001</b>	<b>1.57</b>	<b>0.32</b>	38
	Cryptophytes <sup>c</sup>	<b>0.47</b>	<b>&lt; 0.001</b>	<b>1.65</b>	<b>0.18</b>	38
Diatoms <sup>c</sup>	<b>0.67</b>	<b>&lt; 0.001</b>	<b>1.62</b>	<b>0.18</b>	38	
Pelagophytes <sup>c</sup>	<b>0.58</b>	<b>&lt; 0.001</b>	<b>1.83</b>	<b>0.15</b>	38	
Haptophytes <sup>c</sup>	<b>0.52</b>	<b>&lt; 0.001</b>	<b>0.78</b>	<b>0.51</b>	38	

R<sup>2</sup>: explained variance; p: level of significance; n: sample size

<sup>a</sup> Kelvin degrees, <sup>b</sup> POC as dependent variable, <sup>c</sup> ng Chl *a* L<sup>-1</sup>

### 2.3.3 TEP in relation with other variables at the sea surface

TEP were significantly and positively related to Chl *a* across the entire study area ( $R^2=0.66$ ,  $p<0.001$ ,  $n=65$ ; Table 2.2) and phytoplankton biomass ( $R^2=0.66$ ,  $p<0.001$ ,  $n=67$ ; Table 2.2). The regression equation for log converted TEP vs Chl *a* was  $\log \text{TEP} = 1.90 (\pm 0.02) + 0.35 (\pm 0.03) \times \log \text{Chl } a$ .

TEP also presented significant positive relationships with temperature, salinity ( $p<0.001$ ) and all the phytoplankton groups ( $p<0.05$ ; Table 2.2), with explained variances higher than 60 % for prasinophytes, dinoflagellates and diatoms. By contrast, TEP were negatively related to the solar radiation dose, PHA:Chl *a*, Ddx:LHC, nutrients and wind speed at the sampling time (1-h average; Table 2.2). TEP did not present any significant relationship with PHA, although it was weakly but significantly related to PHP (Table 2.2).

PCA(a) and PCA(b) were performed to visualize the differences between regions and the subset of variables that better explained TEP and TEP:Chl *a* patterns (Fig. 2.2). At PCA(a) principal components 1 and 2 explained 57.1 % and 16.5 % of the variability, respectively. SSO and NSG occupied the extremes of the PC1 gradient, characterized by high solar radiation dose and Ddx:LHC ratio on one side (SSO) and higher TEP concentrations and phytoplankton abundance, and lower macronutrient availability on the other (NSG). WA and NSO showed intermediate values of PC1, but their position in relationship with PC2, indicating an association with high cryptophytes and low wind speed values, was opposite to that of SSO and NSG. At PCA(b), where TEP and Chl *a* were replaced by TEP:Chl *a*, the regions were separated along PC1 and 2 similarly to PCA(a). The major loadings to component 1 positively related to Ddx:LHC, TEP:Chl *a* and solar radiation dose, and negatively related to diatoms, temperature and POC. The major loadings to component 2 included cryptophytes, chlorophytes and, negatively, wind speed,  $F_v:F_m$  and TVA.



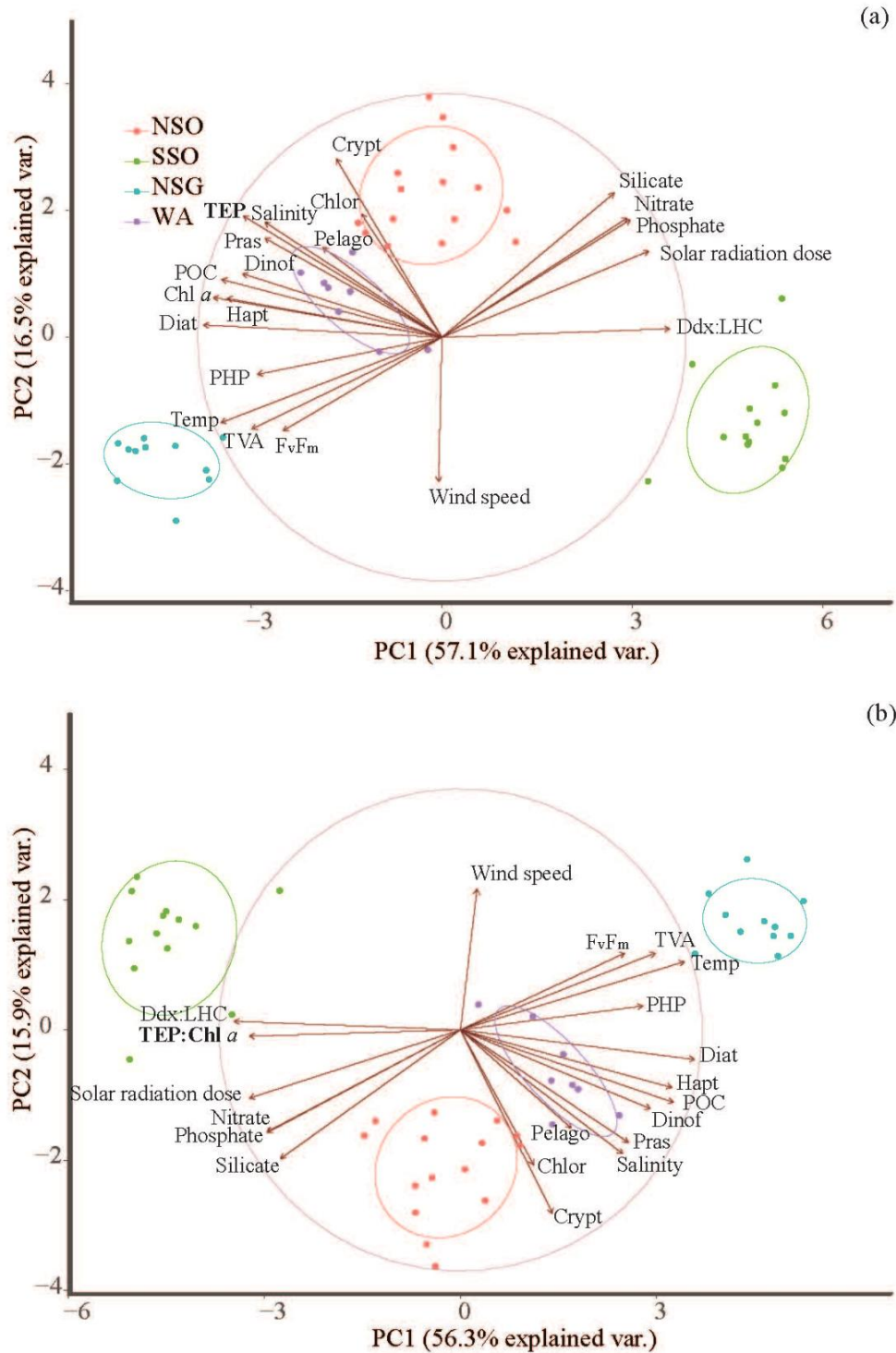
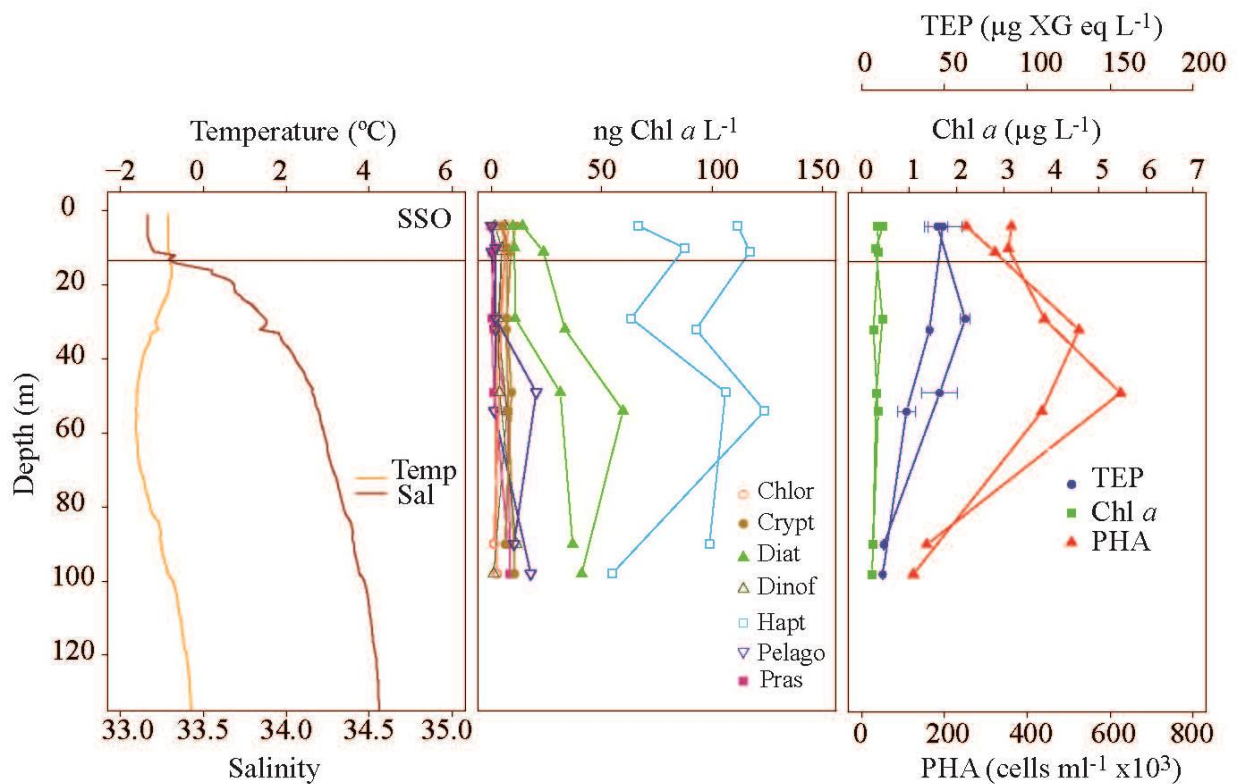
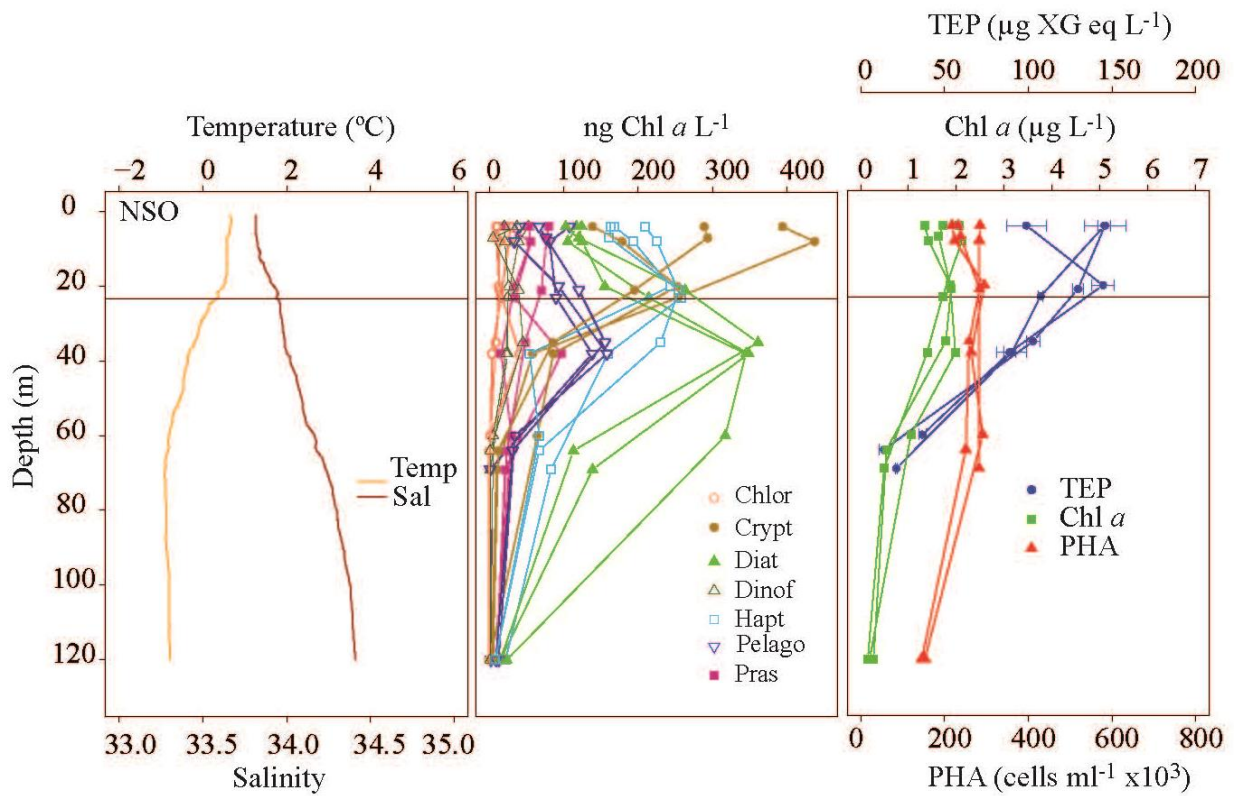


**Figure 2.2:** Principal component analyses (PCA) of surface (4 m) samples. The % of the overall explained variance is given on each principal component axis. The plot (b) is the same as (a) plot after replacing transparent exopolymer particles (TEP) and chlorophyll *a* (Chl *a*) by TEP:Chl *a*. Note that the opposite direction of axes in PCA(a) and (b) is only due to calculations Chlorophytes (Chlor), cryptophytes (Crypt), diatoms (Diat), dinoflagellates (Dinof), haptophytes (Hapt), prasinophytes (Pras), pelagophytes (Pelago), Ddx:LHC (see Fig. 2.1 for abbreviations), Maximum quantum efficiency of photosystem II photochemistry (FvFm), temperature (Temp), total viral abundance (TVA), prokaryotic heterotrophic production (PHP) and particulate organic carbon (POC).

### 2.3.4. TEP vertical distribution and relationship with other variables

TEP concentrations were generally higher within the upper mixed layer (average  $119.2 \pm 39.0 \mu\text{g XG eq L}^{-1}$ ) than below it (average  $53.1 \pm 45.2 \mu\text{g XG eq L}^{-1}$ ), and decreased with depth in 4 out of 7 stations. In the other three stations, TEP maxima were found at the deep Chl *a* maximum (DCM) or close to it (Fig. 2.3). The vertical distribution of Chl *a* differed among regions, but Chl *a* concentration was generally higher in the upper 50 m of the water column. TEP vertical distributions were significantly related to those of Chl *a* considering profiles of all regions ( $R^2 = 0.74$ ,  $p < 0.001$ ,  $n = 26$ ). The equation obtained for the TEP-Chl *a* vertical relationship is  $\log_{10}(\text{TEP}) = 1.78 (\pm 0.04) + 0.67 (\pm 0.08) \times \log_{10}(\text{Chl } a)$ . By contrast, the relationship between TEP and PHA was weak ( $R^2 = 0.18$ ,  $n = 24$ ,  $p < 0.05$ ). The Ddx:LHC ratio decreased strongly below 20-40 m depth in all regions. TEP:Chl *a* ratios increased towards the surface in the NSO and SSO, while in the other regions were constant or with the opposite pattern (Fig. S2.3). TEP:Phyto B ratios, when available, generally followed a similar pattern than TEP:Chl *a* ratios in the profiles (data not shown).

In NSO and WA, TEP vertical distribution was highly coupled with haptophytes and cryptophytes (Fig. 2.3). In the NSO diatoms were higher below TEP maximum. In the SSO, TEP maxima were found above or coincident with the Chl *a* peaks and always above PHA maxima, and the most important phytoplankton groups (haptophytes and diatoms) increased their concentration deeper in the water column (Fig. 2.3). In NSG, the vertical TEP profile was similar to that of diatoms, which dominated the phytoplankton assemblage at all depths (Fig. 2.3).



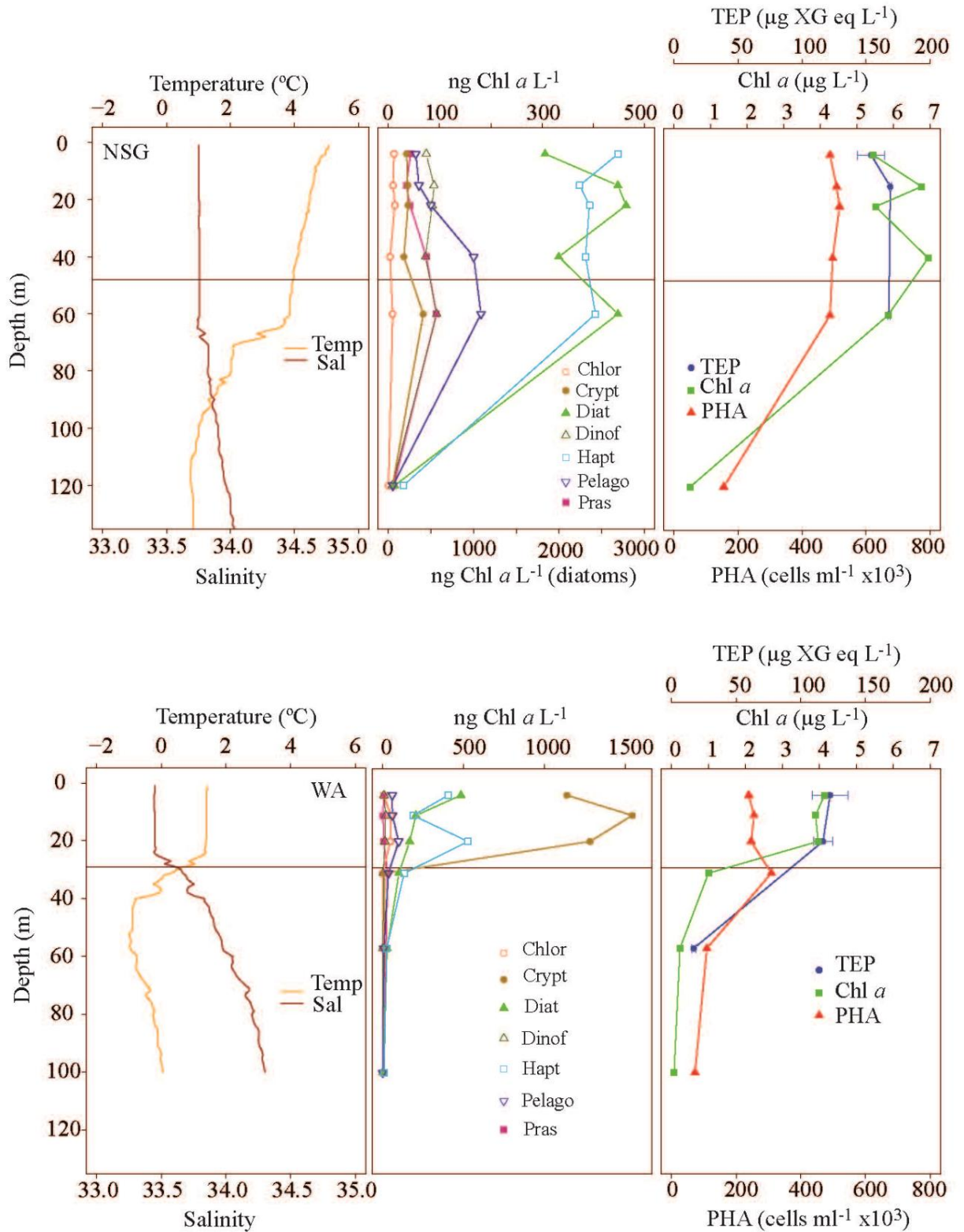


**Figure 2.3:** Vertical profiles of temperature (Temp), salinity (Sal), concentration of the different phytoplankton groups derived from CHEMTAX (see Fig. 2.2 for abbreviations), transparent exopolymer particles (TEP), chlorophyll *a* (Chl *a*) and prokaryotic heterotrophic abundance (PHA) in every region (see Fig. 2.1 for abbreviations of regions).

### 2.3.5. Organic matter accumulation in the upper surface (10 cm)

Among all the parameters measured in the upper surface, TEP concentration ( $r= 0.71$ ,  $n= 14$ ), Chl *a* concentration ( $r= 0.70$ ,  $n= 13$ ), PHA ( $r= 0.71$ ,  $n= 13$ ), fucosidase ( $r=0.56$ ,  $n= 14$ ) and esterase activity ( $r= 0.82$ ,  $n= 12$ ) were significantly correlated (Spearman) with the measurements of the same variables at 4 m depth ( $p< 0.05$ ).

At most stations, TEP and the activity of the enzymes  $\beta$ -glucosidase, esterase and fucosidase were enriched in the upper surface (10 cm; Fig. 2.4) relative to 4 m. TEP- $EF_{us}$  averaged  $1.19 \pm 0.19$ , and the  $EF_{us}$  average for the enzymatic activities were  $2.75 \pm 3.24$  ( $\beta$ -glucosidase),  $4.75 \pm 1.19$  (esterase) and  $31.40 \pm 100.78$  (fucosidase). TEP- $EF_{us}$  was positively related to the 1 h-average wind speed at the time of the upper surface sampling ( $R^2= 0.58$ ,  $p< 0.005$ ,  $n= 14$ ) ( $\log_{10}$  transformed), which varied among 0.5 and  $8.6 \text{ m s}^{-1}$ , with an average of  $5.4 \pm 2.5 \text{ m s}^{-1}$ .

By contrast, Chl *a*, PHA and PHP were not usually enriched in the upper surface. Their enrichment factors averaged  $0.97 \pm 0.37$  (Chl *a*),  $1.00 \pm 0.27$  (PHA) and  $0.77 \pm 0.47$  (PHP) (Fig. 2.4, 2.7). TEP- $EF_{us}$  and Chl *a*- $EF_{us}$  were not significantly related ( $p> 0.05$ ), but TEP:Chl *a* ratios were generally higher at the upper surface than at the surface (average TEP:Chl *a*- $EF_{us}$   $1.37 \pm 0.44$ ).

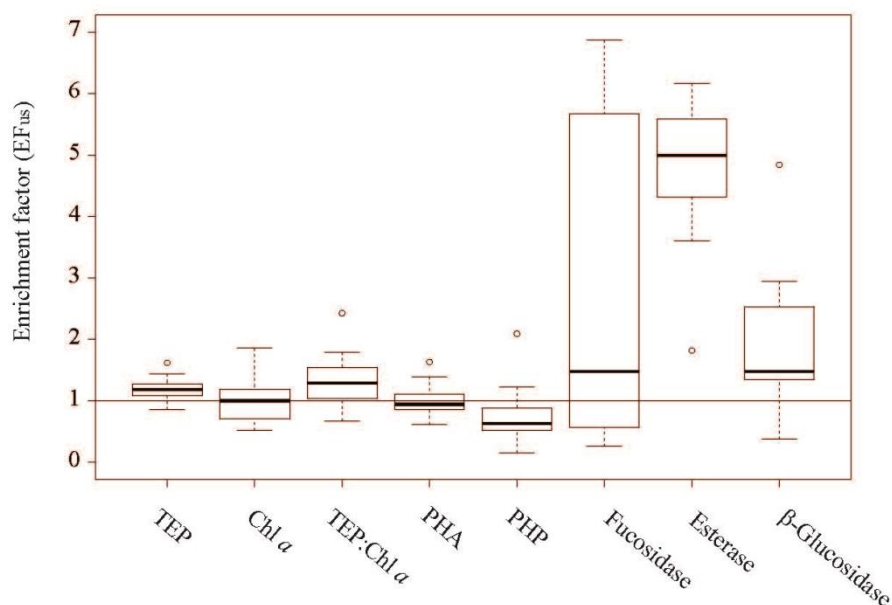


**Figure 2.4:** Boxplots of  $EF_{us}$  of transparent exopolymer particles (TEP), chlorophyll *a* (Chl *a*), TEP:Chl *a*, prokaryotic heterotrophic abundance (PHA), prokaryotic heterotrophic production (PHP), and fucosidase, esterase and  $\beta$ -glucosidase activities across the study regions ( $n= 14$ ). See Fig. S2.4 for the definition of  $EF_{us}$ .

### 2.3.6 TEP variations in the 36-h cycles

We did not detect recurrent diel patterns of Chl *a*, PHP or TEP in the diel cycle studies (Fig. S2.5). TEP showed a relative amplitude (max-min/mean) of 0.31, 0.20, 0.29 and 0.31 in NSO, SSO, NSG and WA, respectively. Chl *a* relative amplitude (0.33, 0.07, 0.95 and 0.37, respectively) was highest in NSG. Looking at covariations (Spearman) of TEP with other biological variables in diel cycles, TEP were only significantly ( $p < 0.05$ ) coupled with Chl *a* ( $r = 0.81$ ,  $n = 8$ ) in NSG.

### 2.3.7 TEP production by microbes during experimental incubations

In the two incubation experiments (conducted in NSO and NSG), and in both treatments (T and P), all measured variables (TEP, Chl *a* and PHP) increased over time, except PHP in experiment NSG (Fig. 2.5). In the T treatments, the increases were steeper (higher daily increase rates), and TEP evolved in parallel with Chl *a* concentration. The TEP production rate per growth rate was 78 in the experiment NSO and 18 in the experiment NSG. These values were very similar to the TEP:Chl *a* ratio average of the regions where the water was collected from ( $76.7 \pm 10.6$  in the NSO and  $32.5 \pm 14.5$  in the NSG).

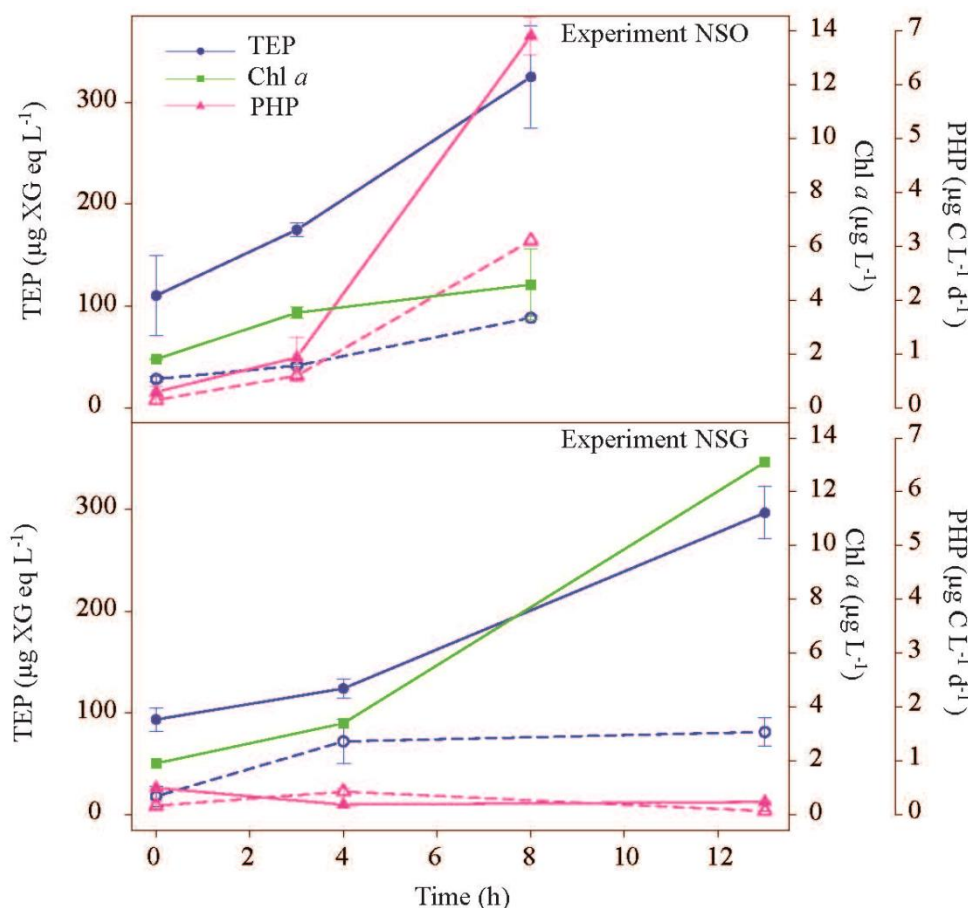


**Figure 2.5:** Incubation experiments at NSO (top) and NSG (bottom). Transparent exopolymer particles (TEP) concentration (blue circle), prokaryotic heterotrophic production (PHP) (pink triangle) and chlorophyll *a* (Chl *a*) (green square) are plotted over time (h). Filled symbols and continuous lines: unfiltered water (treatment T). Empty symbols and dashed lines: water filtered through 0.8  $\mu\text{m}$ , hence, only with prokaryotes (treatment P).

## 2.4 Discussion

### 2.4.1 TEP concentrations in the Southern Ocean

In the present study, we advance the existing knowledge on TEP variability across environmental conditions in the Southern Ocean, with a combination of surface observations, vertical profiles, short-term variability and changes associated with microbial growth during laboratory incubations. The few previous studies describing TEP distributions in the Southern Ocean were located around the Antarctic Peninsula (Passow et al., 1995b; Corzo et al., 2005; Ortega-Retuerta et al., 2009b), the Drake Passage (Corzo et al., 2005) and the Ross Sea (Hong et al., 1997). Our study was carried out in four distinct regions of the peninsular area, and the PCA analyses (Fig. 2.2) confirmed a clear separation of these regions.

Our surface TEP concentrations are in the upper range of published values from around the Antarctic Peninsula (Corzo et al., 2005; Ortega-Retuerta et al., 2009b; Table S2.1). In contrast, the TEP:Chl *a* ratios in our study are not substantially higher than those reported in previous works. It is worth mentioning that Ortega-Retuerta et al. (2009b) found remarkably lower TEP and TEP:Chl *a* ratios in the western Weddell Sea area compared with our SSO data (northern Weddell Sea), although the two sampling sites are geographically close. Difference in the sampling periods can account for this variability, since the previous study was conducted later in the season, when TEP may have been consumed or degraded. The values reported by Hong et al. (1997) in the Ross Sea were higher than our observations in NSO and SSO, probably because they found a bloom of colonial *Phaeocystis antarctica* with higher Chl *a* concentrations and the characteristic presence of mucilage flocs. Regarding vertical TEP distribution, the general pattern of higher TEP concentrations in the upper mixed layer has already been reported in previous studies in the SO (Hong et al., 1997; Corzo et al., 2005; Ortega-Retuerta et al., 2009b) and potential causes for this pattern will be discussed below.

#### **2.4.2 TEP distribution and its main drivers in the Southern Ocean**

Phytoplankton appears to be the main driver of TEP distribution in this study at both the horizontal and vertical scales, as suggested by the positive relationships between TEP and Chl *a* and phytoplankton biomass. However, it is worth mentioning that the coefficient of variation of surface Chl *a* concentration along the entire cruise track (81 %) was much higher than that of TEP (39 %). This suggested that TEP concentrations were relatively more stable than those of their main sources: total phytoplankton biomass expressed as Chl *a* concentration and biomass of the different phytoplankton groups. Considering surface (4 m) samples only, the slope of the log-converted TEP-Chl *a* relationship for the entire study ( $\beta = 0.35 (\pm 0.03)$ ; Table 2.2, Fig. 2.6) was very similar to that obtained in the Antarctic Peninsula area (Corzo et al., 2005; Ortega-Retuerta et al., 2009b) but lower than those observed in the Ross Sea (Hong et al., 1997), driven by the aforementioned bloom of the TEP-producing *Phaeocystis*, and in the Gerlache Strait (Corzo et al., 2005). Concerning surface waters, TEP presented significant positive relationships with all the phytoplankton groups. At the vertical scale, the positive relationship between TEP and Chl *a* corroborates findings of previous studies in the area (Corzo et al., 2005; Ortega-Retuerta et al., 2009b) and suggests that phytoplankton abundance, generally higher in the upper mixed layer, is the main cause



for the general higher TEP concentrations found in this layer too. Our work presents for the first time the vertical TEP distribution along with the phytoplankton group distributions in the SO, showing that haptophytes and cryptophytes were closely associated with TEP vertical distribution in the NSO and WA regions, while diatoms did in the NSG region.

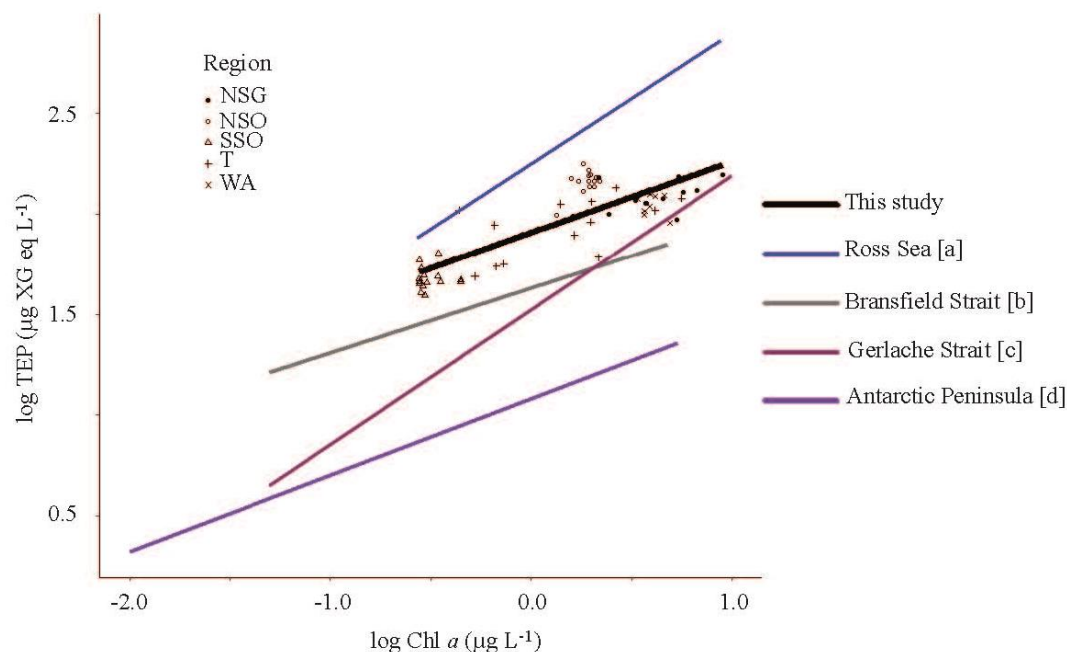


**Figure 2.6:** Log-log relationship between transparent exopolymer particles (TEP) and chlorophyll *a* (Chl *a*) concentration from the PEGASO cruise, with the linear regression line (regression equation in the text). Four regions are distinguished: NSO (empty circles), SSO (empty triangles), NSG (filled circles), WA (crosses) (see Fig. 2.1 for abbreviations of regions), T: transect (plus). Regression lines from the literature in the Southern Ocean are also shown for comparison.  $\alpha$  and  $\beta$  indicate the intercept and the slope, respectively;  $\log \text{TEP} (\mu\text{g XG eq L}^{-1}) = \alpha + \beta \times \log \text{Chl } a (\mu\text{g L}^{-1})$ ; [a]  $\alpha = 2.25$  and  $\beta = 0.65$ , (Hong et al., 1997); [b]  $\alpha = 1.63$  and  $\beta = 0.32$ , (Corzo et al., 2005); [c]  $\alpha = 1.52$  and  $\beta = 0.67$ , (Corzo et al., 2005); [d]  $\alpha = 1.08$  and  $\beta = 0.38$ , (Ortega-Retuerta et al., 2009b).

The fact that TEP:Chl *a* and TEP:Phyto B ratios were different across regions and depths, further supports the role of drivers other than phytoplankton biomass on TEP distribution. On this line, phytoplankton light stress appeared to control TEP distributions in our study area. The SSO presented the highest solar radiation doses and Ddx:LHC ratios, and the lowest  $F_v:F_m$  values, which indicates stronger sunlight exposure and the need for active photoacclimation (Bergmann et al., 2002; Kaiblinger et al., 2007). The NSO also presented relatively high Ddx:LHC ratios and solar radiation doses (Table 2.1). In these regions, TEP:Chl *a* ratios were the highest, which could be

related to a decrease of Chl *a* per cell due to photoadaptation (Kiefer et al., 1976) but also to a stimulation of TEP production, as previously suggested by Iuculano et al. (2017c) and Agustí and Llabrés (2007). The fact that TEP:Phyto B and TEP:PP ratios were also higher in these regions than in the NSG and WA is in line with this second explanation. In the PCA(b) analysis (Fig. 2.2), we could clearly determine that high TEP:Chl *a* ratios corresponded to regions with higher macronutrient availability, solar radiation dose and Ddx:LHC ratio, highlighting the role of light stress in driving TEP:Chl *a* ratios.

The occurrence of sea ice cover and sea ice melting also seemed to influence TEP concentration in the SSO region. It is known that microorganisms living in sea ice release organic substances (Assmy et al., 2013; Vancoppenolle et al., 2013), including TEP, as a survival strategy (Ewert and Deming, 2013). In fact, TEP concentrations measured in sea ice samples during our cruise were  $> 600 \mu\text{g XG eq L}^{-1}$ , i.e., way above concentrations in sea water, although it must be noticed that the selection of ice chunks was based on their colour, picking the brownish as indicative of colonisation by algae (Dall'Osto et al., 2017). The lower salinity at the surface and the larger proportion of *Fragilariopsis* spp. were indicative of sea ice melt influence in SSO (Cefarelli et al., 2011). Consequently, the highest TEP:Phyto B ratios in surface waters of SSO may have partially resulted from an enhancement of TEP release due to sea ice melt. This result agrees with previous studies suggesting sea ice melt being a source of TEP into seawater (Assmy et al., 2013; Galgani et al., 2016), although this role should be studied more in detail if we are to predict TEP concentrations in polar regions.

Nutrient depletion and the phase stage of the phytoplankton blooms could have also influenced TEP distribution too, but we cannot assess this hypothesis with the data at hand. NSG was the only case that presented macronutrient-deplete conditions (silicate restriction; Nunes et al., 2019). The other regions probably were iron-limited, but this micronutrient was not monitored. Regarding the phase stage of the phytoplankton blooms, since in NSO the sea ice retreat occurred earlier in the season, we hypothesize that NSO hosted an advanced phase of the SSO bloom, favoring TEP production (Corzo et al., 2000). Therefore, the bloom phase as sea ice recedes, the influence of sea ice melt, and the aforementioned high insolation in shallow mixed layer, all possibly contributed to TEP distribution.

Regarding the vertical distribution, the increase of Ddx:LHC above 20-40 m in all cases, indicative of protection against light stress, suggests that light stress could have also triggered TEP production near surface of some regions (Iuculano et al., 2017c). NSO and SSO, the regions with the strongest solar radiation doses, presented a general increase of TEP:Chl *a* ratio towards the surface (Fig. S2.1), and also of TEP:Phyto B ratio in the single profile from SSO. However, caution must be taken due to the limited data available of TEP:Phyto B ratios across the profiles.

Heterotrophic prokaryotes did not contribute significantly to explain TEP variations across the horizontal or vertical scales, given the weak relationship between TEP and PHA and PHP (Table 2.2). Other studies have also found a lack or a negative relationship between TEP and PHA or PHP (Passow and Alldredge, 1994; Bhaskar and Bhosle, 2006; Zamanillo et al., 2019c). In contrast, some works, including two in the Southern Ocean, have found a positive relationship between these variables (Passow et al., 2001; Hung et al., 2003b; Santschi et al., 2003; Corzo et al., 2005; Ortega-Retuerta et al., 2009b; Ortega-Retuerta et al., 2010; Zamanillo et al., 2019c).

Viral abundances did not significantly contribute to explain TEP variations neither in the horizontal nor in the vertical scale (Table 2.2), although some studies have found a link between TEP production and the viral infection of different phytoplankton taxa, such as *Emiliana huxleyi* (Nissimov et al., 2018), *Phaeocystis globosa* (Grossart et al., 1998; Stoderegger and Herndl, 1999; Passow, 2002b; Brussaard et al., 2005; Mari et al., 2005) and *Micromonas pusilla* (Lønborg et al., 2013). This result suggests the predominance of other factors driving TEP distribution in this study.

Few studies have measured and compared the distribution of TEP and other organic matter compounds within the first few meters of the ocean surface (Wurl et al., 2011a; Bélanger et al., 2013; Taylor et al., 2014; Thornton et al., 2016). The significant positive correlations we found for most of the measured parameters (TEP, Chl *a*, PHA, esterase and fucosidase activities) at 10 cm vs 4 m, indicates that the horizontal variability of these parameters at the surface (4 m) is mirrored at the upper surface (10 cm). TEP were generally enriched in the upper surface. The TEP-EF<sub>us</sub> average ( $1.19 \pm 0.19$ ) was lower than that found in the SML with respect to underlying water in most previous studies (Wurl and Holmes, 2008; Cunliffe et al., 2009; Wurl et al., 2009; Wurl et al., 2011b; Engel and Galgani, 2016; Galgani et al., 2016). This is somehow expected owing to the

distinct properties of the SML, which forms by the accumulation of surface-active compounds (Wurl et al., 2017). However, despite the modest TEP enrichment at 10 cm, TEP could be responsible for the enhancement of the activities of the ectoenzymes  $\beta$ -glucosidase, fucosidase and esterase (Fig. 2.4), which are secreted by heterotrophic prokaryotes to hydrolyze polysaccharides such as TEP into smaller, bio-available macromolecules (Bar-Zeev and Rahav, 2015).

The enrichment of TEP in the upper surface was not associated with higher abundances of microorganisms or higher prokaryotic heterotrophic activity (Fig. S2.4). Chl *a* and PHA were not generally enriched in the upper surface. Therefore, reasons for the TEP enrichment could be the following; (1) the increase of per-cell TEP production in the upper surface due to high solar radiation (Ortega-Retuerta et al., 2009a; Iuculano et al., 2017c); (2) an allochthonous source of TEP and/or their precursors at 10 cm, namely sea ice melt waters of lower density; (3) ascending TEP from underlying waters, embedded in low density particles or captured and transported by air bubbles (Zhou et al., 1998); and (4) an increase of TEP self-assembly of dissolved precursors in the upper surface due to higher turbulence (Passow, 2000; Beauvais et al., 2006). The last two mechanisms are the most plausible since we found a positive relationship between TEP- $EF_{us}$  and wind speed ( $R^2 = 0.58$ ) (Fig. S2.4). Winds stronger than about  $5 \text{ m s}^{-1}$  cause the entrainment of bubbles down from breaking waves (Andreas and Monahan, 2000; Deane and Stokes, 2002), and when these bubbles rise they can bring TEP or their precursors towards the surface, among other items such as prokaryotic cells (Mayol et al., 2017), where aggregation is favoured by enhanced turbulence. A recent study (Robinson et al., 2019c) has shown that deliberate bubbling of seawater (mimicking the effect of wind in the field) increases TEP concentrations in the SML, and although they did not observe an increase of TEP concentration at 1 m, it is plausible that an increase at 10 cm was also occurring, which is in line with our observations.

### **2.4.3 TEP variations in the 36-h cycle**

We did not find a cyclic diel pattern of any of the measured variables (TEP, Chl *a* and PHP) similarly to the outcome of the only published study on short-term TEP variation (Ortega-Retuerta et al., 2017). This result illustrates the influence of many processes in driving TEP distribution.

#### 2.4.4 TEP production by microbes in incubation experiments

The results of the incubation experiments supported the idea that phytoplankton are the main TEP producer in the study area (Fig. 2.5). In treatments with only prokaryotes, TEP were formed at low rates by abiotic self-assembly and/or the action of heterotrophic prokaryotes and archaea. In unfiltered treatments, TEP increased much faster and nearly parallel to the Chl *a* increase. Net TEP production rates per net phytoplankton growth rate varied between experiments and were very similar to the average of TEP:Chl *a* ratios of the respective regions, confirming our observations that phytoplankton were the main TEP producers in the study area. Interestingly, TEP production rate per phytoplankton growth rate was higher in the NSO experiment than in the NSG experiment, despite the higher biomass and dominance of diatoms in the latter. This contradicts the common view that diatoms are highly specific TEP producers (Passow, 2002a), and supports the aforementioned discussed idea that environmental conditions, associated physiological stress and the phytoplankton bloom stage influence TEP production by phytoplankton beyond biomass, primary productivity and taxonomical composition.

### 2.5 Conclusions

Our study expands the existing knowledge on TEP distribution in the Southern Ocean and for the first time provides information on TEP variability in the first meters of the ocean surface and with high temporal resolution. Phytoplankton abundance was the main predictor of TEP distribution in both the horizontal and vertical scales, and the outcome of experimental incubations further supported this observation in situ. Photoacclimation and sea ice melt played complementary but important roles driving differences in TEP distribution across regions. Phytoplankton composition was also an important driver, especially along the vertical scale, but diatoms were not the main producers. TEP were generally enriched at centimetres under the surface, likely due to scavenging by bubbles and turbulence-derived aggregation, contrasting with the null enrichment of microorganism abundances. We highlight the need to carry out more field studies in the area, extending to temporal dynamics along the entire ice-receding and ice-free season, to better predict TEP concentration in the Southern Ocean and

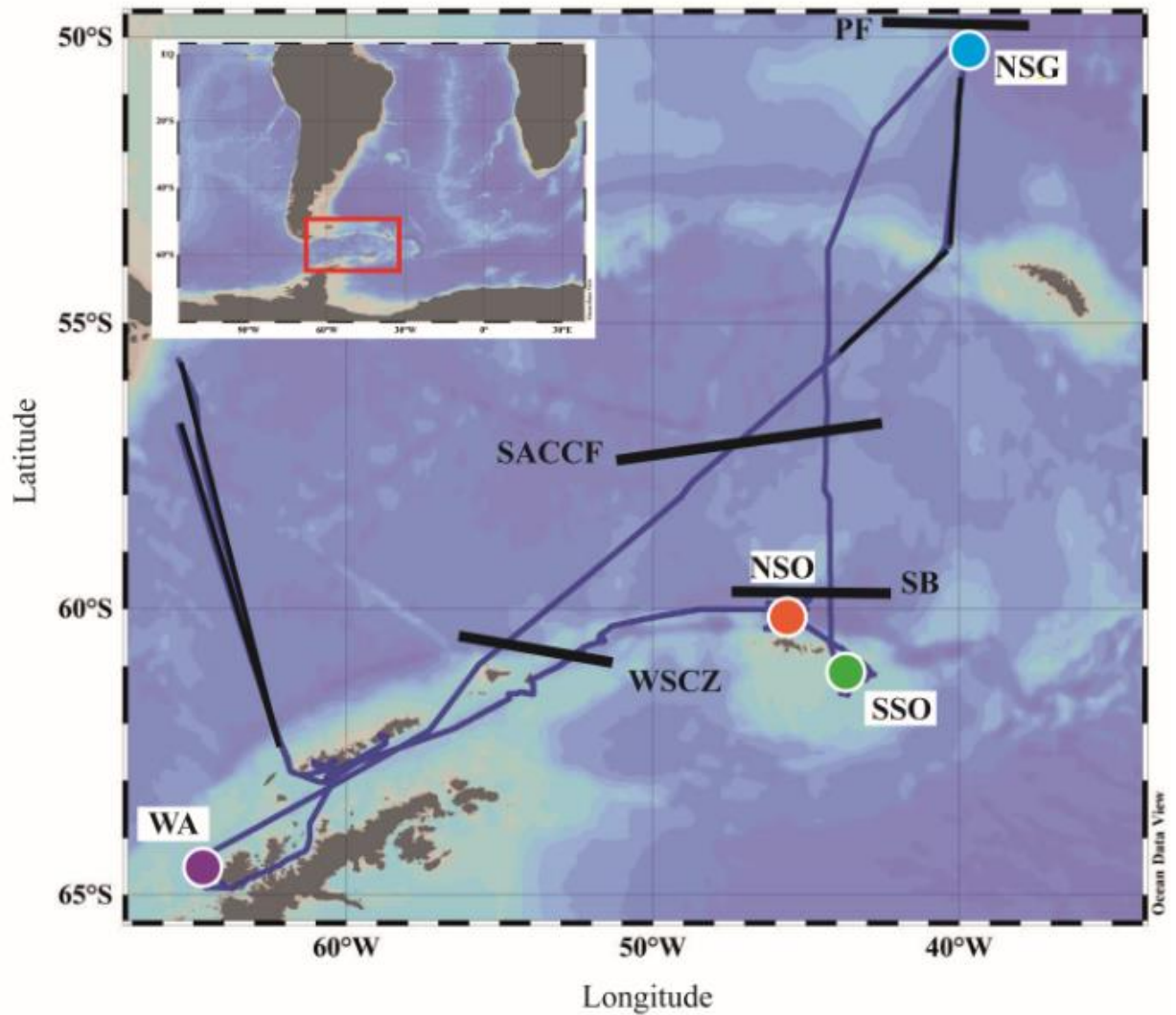
quantitatively evaluate their effects in biogeochemical processes such as the biological carbon pump and organic aerosol formation.

## **2.6 Acknowledgements**

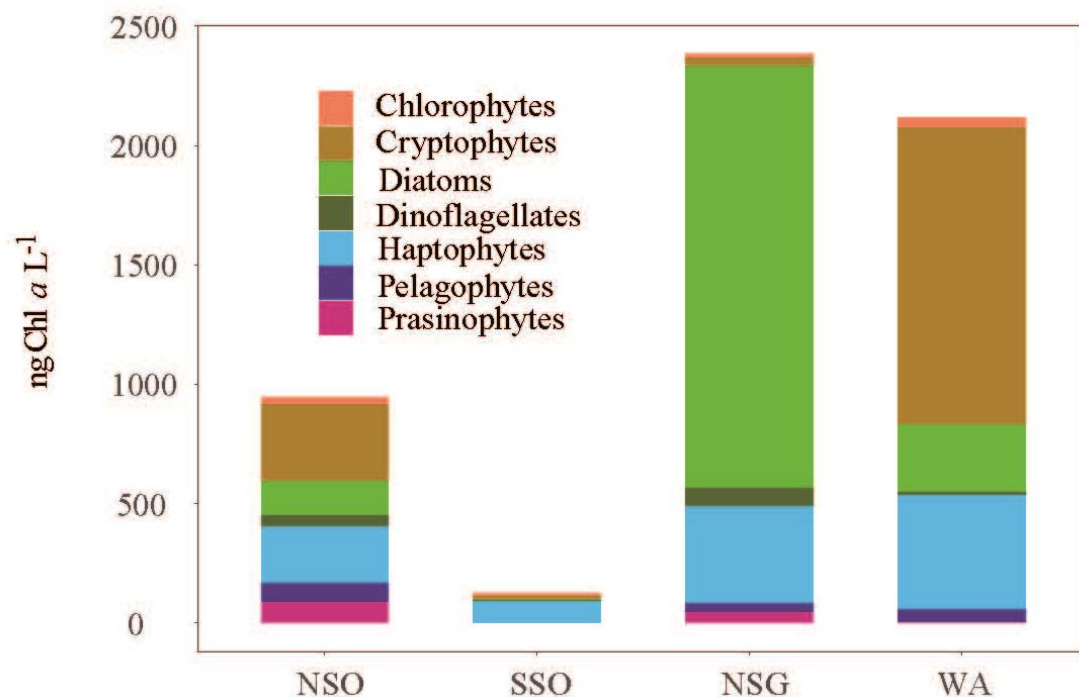
This research was supported by the Spanish Ministry of Economy and Competitiveness through projects PEGASO (CTM2012–37615) and BIOGAPS (CTM2016–81008–R) to RS. MZ was supported by a FPU predoctoral fellowship (FPU13/04630) from the Spanish Ministry of Education and Culture. Gonzalo Luis Pérez, Maximino Delgado, Alicia Duró, Encarna Borrull, Carolina Antequera, Clara Cardelús and Pablo Rodríguez-Ros are greatly acknowledged for providing data and technical support. The authors also want to thank the captain, officers and crew of RV *Hespérides*, engineers of the Marine Technology Unit and researchers for their support and help during the cruise.

## 2.7 Supplementary material

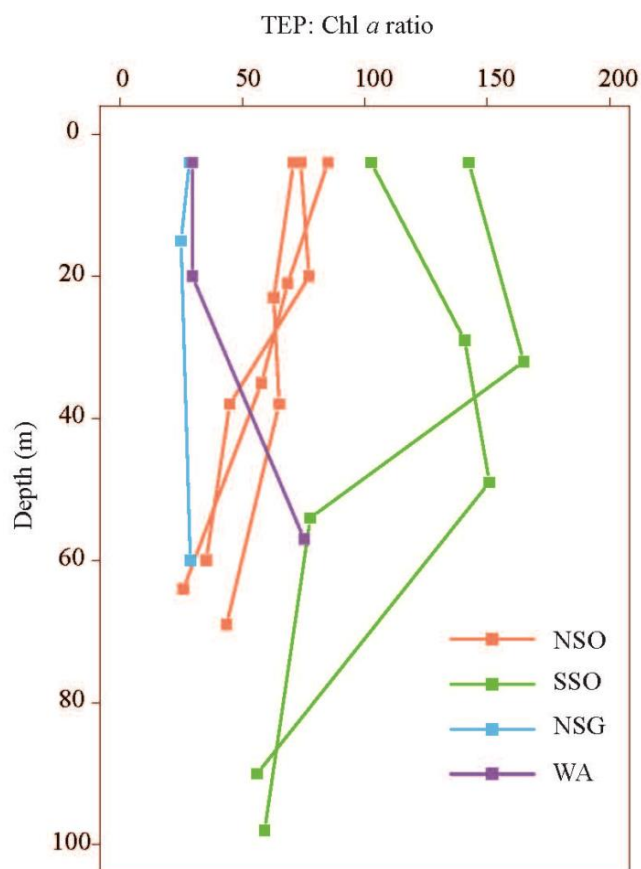
### 2.7.1 Supplementary Figures



**Supplementary Figure S2.1.** Study area. Ship trajectory (blue line) and the four case studies with Lagrangian occupation (circles, see Fig. 1 for abbreviations of regions). Main hydrographic fronts (black lines) along the cruise: Antarctic Polar Front (PF), Southern Antarctic Circumpolar Current Front (SACCF), Southern Boundary of the Antarctic Circumpolar Current (SB), and Weddell Scotia Confluence Zone (WSCF). Figure produced with the Ocean Data View software.

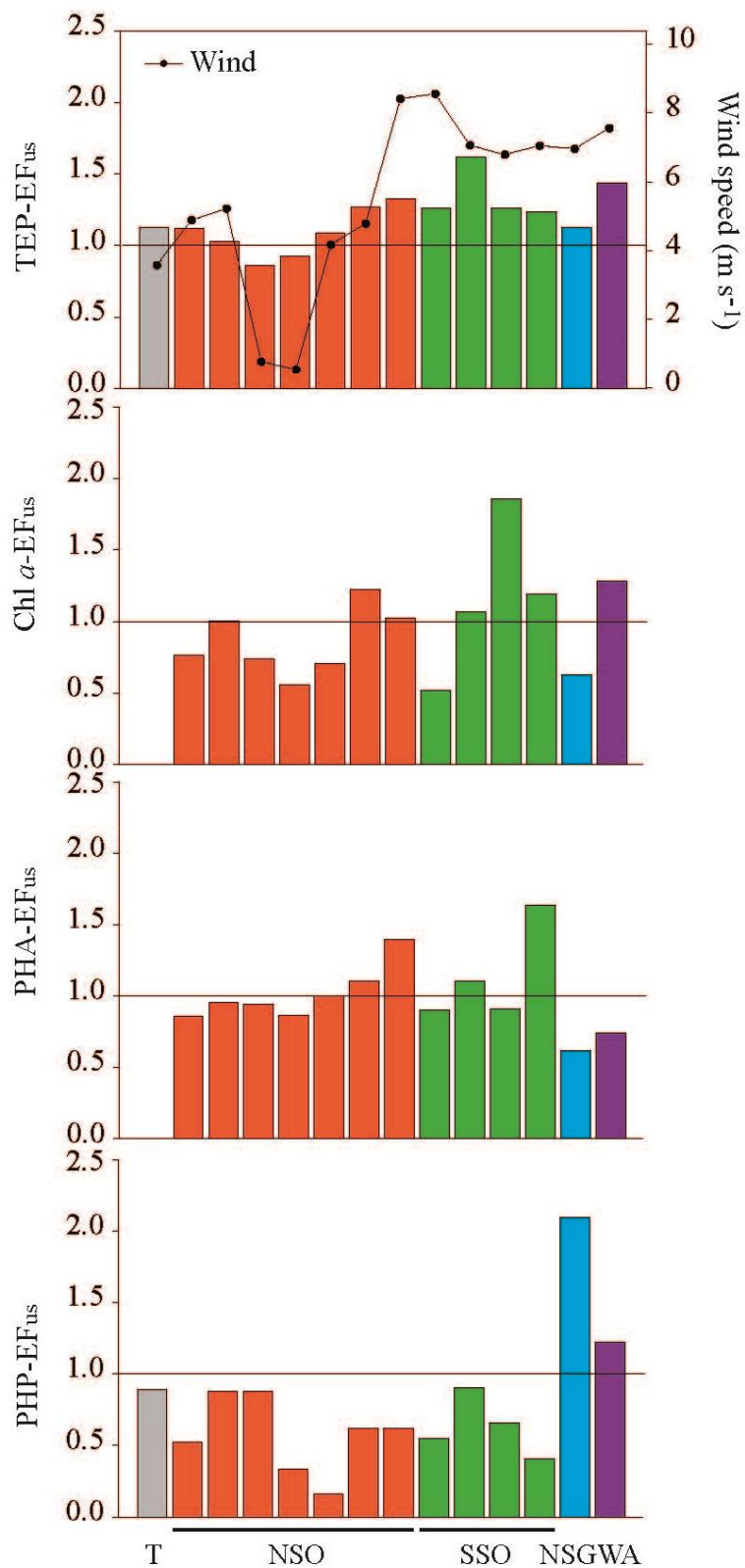


**Supplementary Figure S2.2:** Average concentration of each phytoplankton group in the sea surface of the four visited regions derived from CHEMTAX (contribution to the total Chl *a*, ng Chl *a* L<sup>-1</sup>) (see Fig. 1 for abbreviations of regions).

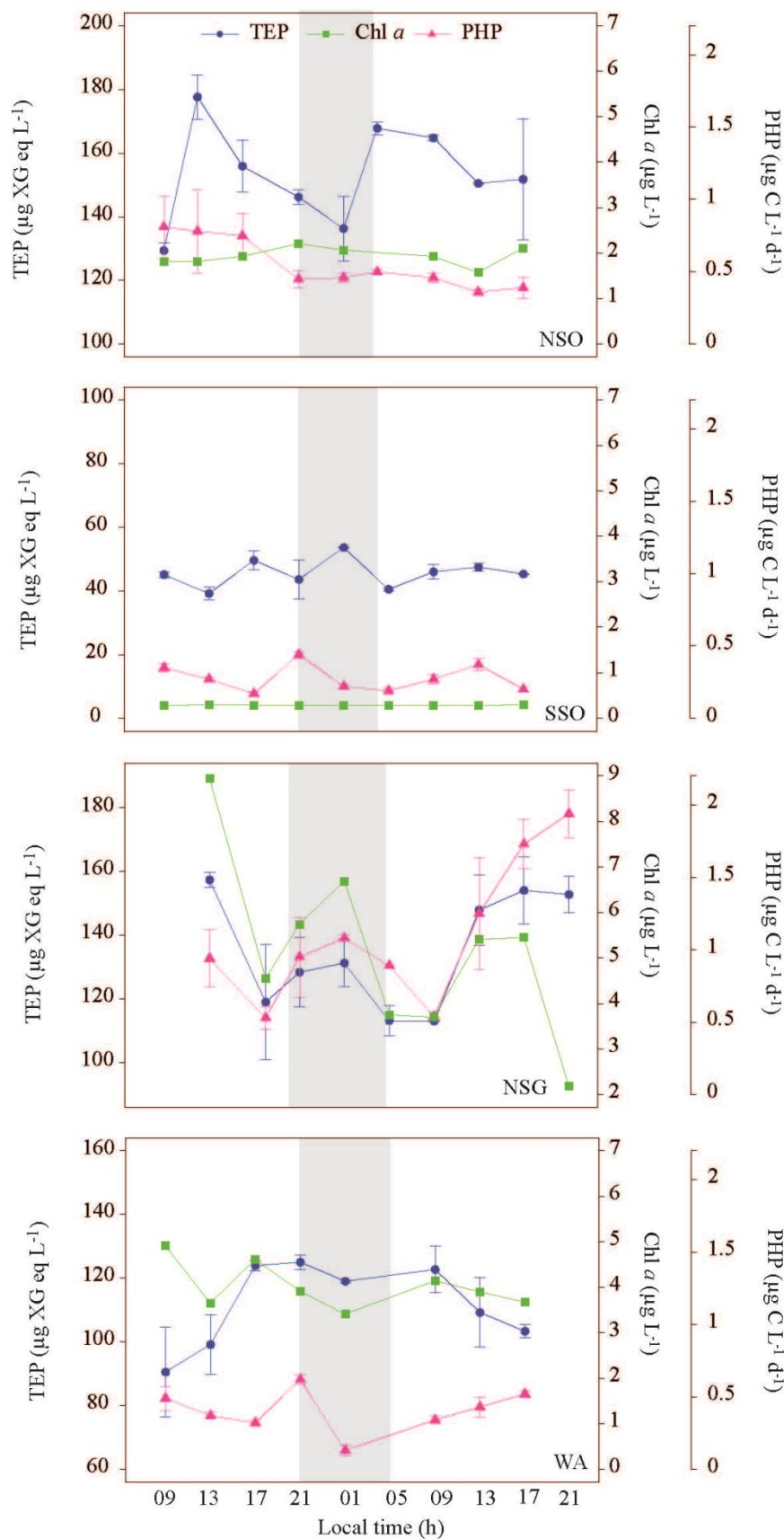


**Supplementary Figure S2.3:** Vertical profiles of TEP:Chl *a* ratio (transparent exopolymer particles (TEP), chlorophyll *a* (Chl *a*)) in every study region (see Fig. 1 for abbreviations of regions).





**Supplementary Figure S2.4:** Enrichment factor between the upper surface (10 cm) and the surface (4 m) ( $EF_{us} = [X]_{\text{upper surface}} / [X]_{\text{surface}}$ ) for transparent exopolymer particles (TEP), chlorophyll *a* (Chl *a*), prokaryotic heterotrophic abundance (PHA) and prokaryotic heterotrophic production (PHP) (bars) in the different regions (see Fig. 1 for abbreviations of regions). Horizontal line denotes  $EF_{us} = 1$ . Wind speed is indicated by filled circles. T: transect.



**Supplementary Figure S2.5:** Transparent exopolymer particles (TEP) concentration (blue circle), prokaryotic heterotrophic production (PHP) (pink triangle) and chlorophyll *a* (Chl *a*) (green square) in the 36-h cycles (local time, UTC-3) in every visited region (see Fig. 1 for abbreviations of regions). Grey shaded areas indicate night by enclosing the period when global solar radiation was  $< 10 \text{ W m}^{-2}$ .

## 2.7.2 Supplementary Table.

**Supplementary Table S2.1.** Compilation of published transparent exopolymer particles (TEP) concentrations (mean  $\pm$  SE and ranges;  $\mu\text{g XG eq L}^{-1}$ ), chlorophyll *a* (Chl *a*) concentrations (mean  $\pm$  SE and ranges;  $\mu\text{g L}^{-1}$ ) and TEP:Chl *a* ratios (mean  $\pm$  SE and ranges;  $\mu\text{g XG eq } (\mu\text{g Chl } a)^{-1}$ ) in the Southern Ocean. Bdl: below detection limit.

Location	Comments	TEP	Chl <i>a</i>	TEP:Chl <i>a</i>	Reference
Anvers Island	Summer (November 1994-February 1995) 2- 6 m, coastal samples Two blooms observed (Cryptomonads and diatoms)	15 - >500	-	-	Passow et al. (1995)
Kita-no-seto Strait	Mid-January 1994 15 m	<b>26 <math>\pm</math> 6-41<math>\pm</math>4</b> particles mL <sup>-1</sup>	-	-	Marchant et al. (1996)
Ross Sea	Summer (November, December 1994) 0-150 m, <i>Phaeocystis</i> and diatoms bloom	Surface 308 (0-2800)	3.61 (0.27-8.81) (surface)	89.1 (surface)	Hong et al. (1997)
Bransfield Strait	Summer (13 December 1990- 3	56.77 $\pm$ 54.50 (bdl-345.9)	0.98 $\pm$ 0.83 (0.05-4.81)	51.0	Corzo et al. (2005)
Gerlache Strait	January 2000)	38 (0-283)	1.16	32.7	
Drake Passage	0-100 m	35 (0-157)	1.17	29.9	
Antarctic Peninsula (all the study)	Summer (February 2005), 0-200 m	15.4 $\pm$ 10.0 (bdl-48.9)	0.01-5.36	40.9 $\pm$ 157.8 (bdl-1492)	Ortega-Retuerta et al. (2009b)
Bellingshausen Sea		14.3 $\pm$ 9.5 (bdl-33.8)		84.2 $\pm$ 257.5 (bdl-1492)	
Weddell Sea		16.3 $\pm$ 12.5 (bdl-48.9)		9.8 $\pm$ 7.4 (1.2-28.4)	
Bransfield and Gerlache Strait		15.8 $\pm$ 8.9 (bdl-35.8)		15.0 $\pm$ 20.4 (3.0-18.0)	
Southern Ocean (all transect)	Summer (7 January-3 February 2015) 4 m	102.3 $\pm$ 40.4 (39.2- 177.6)	2.36 $\pm$ 1.92 (0.28-8.95)	79.3 $\pm$ 54.9 (10.9-239.0)	This study
South Orkney Islands (NSO)		144.4 $\pm$ 21.7 (97.8-177.6)	1.87 $\pm$ 0.23 (1.58-2.21)	76.7 $\pm$ 10.6 (60.4-97.5)	
southeast of the South Orkney Islands (SSO)		48.1 $\pm$ 6.5 (39.2-63.8)	0.32 $\pm$ 0.06 (0.28-0.45)	153.4 $\pm$ 29.8 (102.5-211.6)	
northwest of South Georgia (NSG)		125.5 $\pm$ 21.1 (93.6-157.4)	4.59 $\pm$ 1.97 (1.92-8.95)	32.3 $\pm$ 15.0 (17.6-70.0)	
west of Anvers Island (WA)		111.6 $\pm$ 13.0 (90.5-125.0)	4.05 $\pm$ 0.48 (3.41-4.91)	28.2 $\pm$ 4.8 (18.4-34.9)	



## Chapter 3

Coastal NW Mediterranean Sea

### **Seasonal variability of transparent exopolymer particles (TEP) and Coomassie stainable particles (CSP) in the coastal NW Mediterranean Sea**

*Marina Zamanilo, Eva Ortega-Retuerta, Carolina Cisternas-Novoa, Cèlia Marrasé, Carles Pelejero, Josep Maria Gasol, Anja Engel, Rafel Simó*





**Abstract**

Transparent exopolymer particles (TEP) and Coomassie stainable particles (CSP) are gel-like particles, ubiquitous in the ocean, that affect important biogeochemical processes such as the ocean carbon cycle mediated by planktonic food webs. However, whether they are distinctly stainable fractions of the same particles or independent substances is still unclear. To elucidate this, we describe the surface temporal dynamics of both TEP and CSP particles over two complete seasonal cycles at two coastal sites in the Northwestern Mediterranean Sea, the Blanes Bay Microbial Observatory (BBMO) and the L'Estartit Oceanographic Station (EOS), as well as their spatial distribution along a coast-to-offshore transect nearby. Biological, chemical and physical variables were measured and analyzed in parallel. The dynamics of TEP and CSP were uncoupled at both coastal sites and the transect, suggesting they are different types of particles. Surface TEP concentrations averaged  $36.7 \pm 21.5 \mu\text{g XG eq L}^{-1}$  at BBMO and  $36.6 \pm 28.3 \mu\text{g XG eq L}^{-1}$  at EOS, showing similar seasonal dynamics between the two sites, with higher concentrations in summer. In contrast, CSP seasonality was different between the two stations, though showing highest concentrations from late winter to early summer in both cases. Surface CSP concentrations averaged  $11.9 \pm 6.1 \mu\text{g BSA eq L}^{-1}$  at BBMO and  $13.0 \pm 5.9 \mu\text{g BSA eq L}^{-1}$  at EOS. Vertical TEP distributions, only recorded at EOS, were quite uniform, except in summer that they were higher at depths shallower than 20 m. Conversely, highest CSP concentrations were detected at the surface in spring. Phytoplankton were the main drivers of TEP and CSP distributions, although other factors such as nutrient limitation, saturating irradiance and the proportion of TEP and solid particles in aggregates also seemed to play important roles driving TEP distribution across the temporal scale.

### 3.1 Introduction

Gel-like exopolymer particles, such as transparent exopolymer particles (TEP) and Coomassie stainable particles (CSP), have gained interest for their roles in ocean biogeochemistry. TEP are a relevant player in the carbon cycle since they constitute an estimated mean of 5-10 % of primary production in the ocean (Mari et al., 2017) and favour the aggregation and sinking of suspended particles (Engel et al., 2004a; Burd and Jackson, 2009). In addition, due to their low density (Azetsu-Scott and Passow, 2004), TEP can ascend through the upper water column, accumulate in the sea surface microlayer (SML) and influence air-sea gas exchanges (Calleja et al., 2009; Wurl et al., 2016; Jenkinson et al., 2018). They can also be released to the atmosphere, contributing to organic aerosols (Aller et al., 2005) and impacting the Earth's radiative budget (Brooks and Thornton, 2018). Unlike TEP, CSP do not seem to significantly impact aggregation processes (Prieto et al., 2002; Cisternas-Novoa et al., 2015), although more studies should be done to address this issue. CSP also accumulate in the SML (Wurl et al., 2011b; Engel and Galgani, 2016; Zancker et al., 2017; Sun et al., 2018) and have been observed in sea spray aerosols (Kuznetsova et al., 2005; Aller et al., 2017).

TEP and CSP are transparent gel particles mostly formed by acidic polysaccharides and proteins, respectively. These particle types are defined by their capability to be stained with specific dyes: Alcian Blue in the case of TEP (Alldredge et al., 1993; Passow and Alldredge, 1995), and Coomassie brilliant blue for CSP (Long and Azam, 1996; Engel, 2009). CSP are thought to present five to seven times greater nitrogen content than TEP (Engel and Passow, 2001; Mari et al., 2001). TEP have been largely studied in the ocean (reviewed by Passow (2002b), Bar-Zeev et al. (2015) and Mari et al. (2017)). Conversely, CSP have been scantily described since a spectrometric method, which is less time consuming and labor intensive than the classical microscopic quantification, has been developed only recently (Cisternas-Novoa et al., 2014). There is growing evidence that both particle types are ubiquitous in the ocean and are present in similar concentrations, but they likely represent independent particle fractions with distinct properties and distribution (Cisternas-Novoa et al., 2015; Thornton et al., 2016; Thornton and Chen, 2017); this latter issue requires confirmation.

Phytoplankton are the main source of TEP and presumably also of CSP in the ocean (Passow, 2002b; Thornton and Chen, 2017), although heterotrophic prokaryotes (HP)



can also produce them (Stoderegger and Herndl, 1999; Radic et al., 2006). Diatoms and cyanobacteria have been shown to produce both CSP and TEP. Although CSP production by other phytoplankton groups have not been tested yet (reviewed in Thornton (2018)), it is known that dissolved organic nitrogen (DON), including proteins, are released by phytoplankton into the surrounding medium (Hu and Smith Jr., 1998; Suratman et al., 2008). TEP can also form abiotically from precursors through ionic bonding (Alldredge et al., 1993; Thornton, 2004); so do presumably CSP (Cisternas-Novoa et al., 2015), but this has not yet been directly tested. Zooplankton (Ling and Alldredge, 2003) and HP (Passow, 2002a; Grossart et al., 2006; Azam and Malfatti, 2007) can use TEP as a food source; this is probably the case for CSP too Endres et al. (2013); (Cisternas-Novoa et al., 2015; Engel et al., 2015), and indeed CSP have also been found colonized by HP. Environmental and biological variables other than taxon composition impact the production of TEP in the ocean: phytoplankton physiological state (Passow, 2002a), temperature (Claquin et al., 2008), light intensity (Trabelsi et al., 2008) and nutrient availability (Radic et al., 2006). TEP loss is affected by UV-induced photolysis (Ortega-Retuerta et al., 2009a). Owing to the lack of similar studies with CSP (Thornton and Chen, 2017), it is not yet known which and how biological and environmental factors affect CSP production.

The Mediterranean Sea is a temperate, oligotrophic sea, characterized by the enhancement of water stratification in late spring and summer due to solar radiation increase, which leads to low nutrient concentrations in surface waters (Sala et al., 2002; Duarte et al., 2004; Lucea et al., 2005), and by vertical mixing in fall through winter. Chlorophyll *a* (Chl *a*) concentration is usually highest in late winter or early spring months, triggered by the onset of thermal stratification after winter mixing, coinciding with nutrient availability and high light (Buchan et al., 2014; Gasol et al., 2016). However, the exact conditions that prompt the onset of the bloom in the Mediterranean Sea and other regions is still debatable (Smetacek and Cloern, 2008; Behrenfeld, 2010; Taylor and Ferrari, 2011). Minimum Chl *a* values are found at the end of the summer period, due to the strong stratification.

Previous studies of the temporal dynamics of TEP in the Mediterranean Sea, other than those conducted in eutrophic coastal areas or zones heavily influenced by the presence of seagrass meadows (Radic et al., 2005; Scoullou et al., 2006; Iuculano et al., 2017b), showed maximum TEP concentrations in summer, both at coastal and offshore sites

(Beauvais et al., 2003; Ortega-Retuerta et al., 2018), with a temporal disconnection between TEP and Chl *a* (Ortega-Retuerta et al., 2018).

Temporal dynamics of CSP in the Mediterranean Sea have not been studied before. A previous study on temporal CSP dynamics took place in a temperate coastal system in the Baltic Sea and showed that CSP, measured in both the SML and the subsurface water (SSW), increased in summer, and CSP abundance was generally similar to that of TEP (Dreshchinskii and Engel, 2017). Another study in the Sargasso Sea showed that both particle types presented different temporal and vertical distributions (Cisternas-Novoa et al., 2015). TEP were higher in the shallowest sample (usually 50 m), while CSP were maximum between 70 and 100 m, coinciding with the Chl *a* fluorescence maximum. In addition, Cisternas-Novoa et al. (2015) observed, in a mesocosm, nutrient-induced phytoplankton bloom, that TEP and CSP were temporally uncoupled, being CSP better related to Chl *a* than TEP, and showing their maximum coinciding with the Chl *a* peak.

In this study, for the first time we describe the temporal dynamics of TEP and CSP simultaneously over two complete seasonal cycles at two coastal sites of the Northwestern (NW) Mediterranean Sea. In one of them we also examined seasonal variations in TEP and CSP vertical distributions. Physical, chemical and biological variables were measured and analyzed in parallel. In addition, TEP and CSP were also analysed at two depths in a nearby coast-to-offshore transect in the NW Mediterranean Sea. The objectives of the study were to elucidate whether or not these two pools of organic particles follow similar trends along the year and also over the horizontal and vertical scales. Based on previous works, we hypothesize that CSP distributions and temporal dynamics would be closely related to those of phytoplankton biomass, while TEP distribution and dynamics would be rather related to the combination of phytoplankton biomass, solar radiation and nutrient limitation.

## 3.2 Material and methods

### 3.2.1 Study sites and sampling

Samples were collected in different locations within the Catalan Sea (NW Mediterranean): (1) the Blanes Bay Microbial Observatory (BBMO, <http://www.icm.csic.es/bio/projects/icmicrobis/bbmo/>) (41.40° N, 2.48° E), (2) the L'Estartit Oceanographic Station (EOS), 70 km north (42.05° N, 3.25° E), and (3) a transect between the Catalan Coast and north of Mallorca Island, on board the RV “García del Cid” (cruise Mifasol II) (Fig. 3.1). The BBMO is located around 800 m offshore, in an open bay with shallow waters (sandy bottom at 20 m depth), where most terrestrial inputs arrive as runoff from the surrounding coastal area (details in Guadayol et al. (2009) and Gasol et al. (2012)). The EOS is located 3.2 km off the main coast and 2 km off the Medes Islands, within a ~92 m water depth (Fig. 3.1), and it is characterized by its proximity to an area catalogued as a “Specially Protected Area of Mediterranean Importance (SPAMI)” zone.

The BBMO and EOS samplings were performed once per month (plus the June solstice in BBMO), from June solstice 2015 to October 2017, except during adverse weather conditions. At BBMO, water samples were taken with an acid-cleaned bucket from the surface (0.5 m) and kept in 20-L acid-cleaned polycarbonate carboys, after water pre-filtration through acid-cleaned 200- $\mu$ m mesh net to remove large planktonic organisms. Carboys were preserved under dim light, covering with black plastic bags to avoid photo-degradation. Further processing of samples was done within 1.5 h in the home laboratory. At EOS, four depths (0.5, 20, 50 and 80 m) were sampled using 5 L Niskin bottles, and then filtered through acid-cleaned 200- $\mu$ m nylon mesh. Water for TEP and CSP analyses were collected in 1 L acid-cleaned polycarbonate bottles, while those for the rest of variables were kept in 8 L acid-cleaned polyethylene carboys, all of them covered with black plastic bags. Polycarbonate bottles were transported in a fridge with pack ice. Sample processing was done in the home laboratory within 4 h.

The coast-to-offshore transect was conducted during the Mifasol II cruise, from 22<sup>nd</sup> to 24<sup>th</sup> October 2015, including stations on the shelf (M1), slope (M2-4) and basin (M5-7), until 145 km from the shore. Seawater was collected at 2 depths (surface (5 m) and DCM (when present)) using a rosette on CTD casts (12 Niskin bottles with external spring, 12 L each).

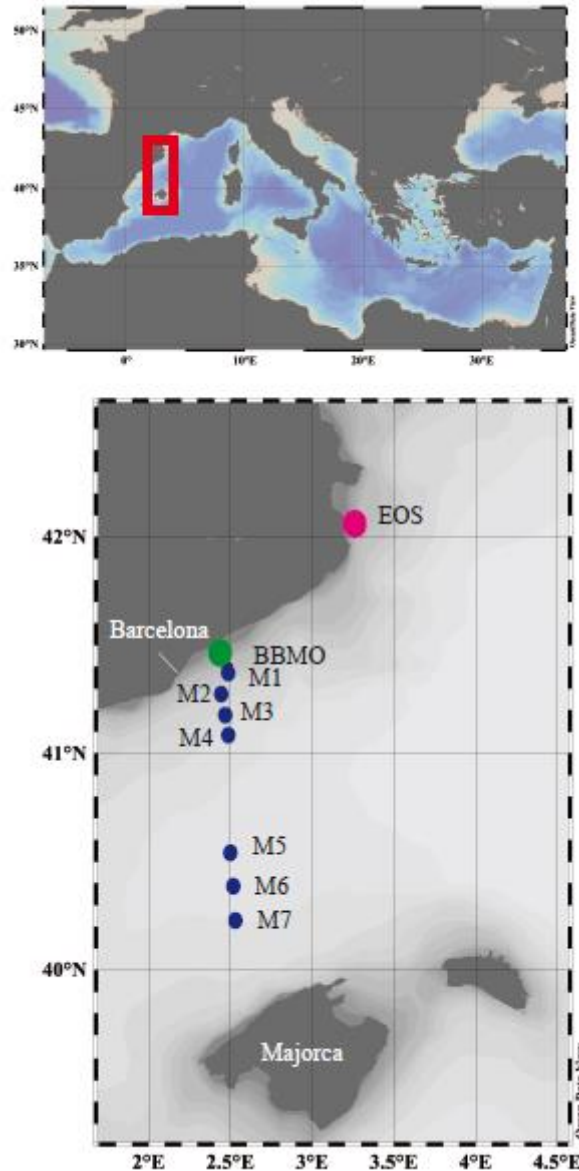


**Figure 3.1:** Map of the study area. The Blanes Bay Microbial Observatory (BBMO, green circle), L’Estretit Oceanographic Station (EOS, pink circle) and the transect between the Catalan Coast and north of Mallorca Island (M1-M7, blue circles).

### 3.2.2 Physical variables

A calibrated SAIVA/S SD204 sensor was used to measure vertical profiles of temperature and salinity with 0.5 and 1 m resolution in BBMO and EOS, respectively. In August 2016 in BBMO and from May to June 2016 at EOS, the sensor was inoperative. We calculated the mixed layer depth (MLD) as the depth where temperature changed more than 0.15 °C with respect to a reference depth of 1 m. At BBMO, we calculated a stratification index that we defined as the temperature

difference between the surface and near the sea bottom (20 m). Water transparency (in meters) was measured with a Secchi disk in the BBMO and with white-faced Niskin bottles (used as analogous of a Secchi disk) in the EOS. The light extinction coefficient ( $K_d$ ;  $\text{m}^{-1}$ ) was calculated as  $1.7/\text{water transparency}$  (Kirk, 1994). Total irradiance was recorded hourly by a pyranometer at Malgrat de Mar station (approximately 40 km southwest of BBMO) and Sant Pere Pescador station (approximately 7 km southwest of EOS) (Catalan Meteorological Service, SMC). We measured the average solar radiation of the 24 h previous to the sampling, and calculated the daily-averaged solar radiation dose, defined as:

$$\text{Solar radiation dose} = \frac{I}{K_d \times \text{MLD}} \times (1 - e^{(-K_d \times \text{MLD})})$$

where,  $I$  is the average surface irradiance ( $\text{W m}^{-2}$ ) in the 24 h previous to sampling,  $K_d$  is the light extinction coefficient ( $\text{m}^{-1}$ ), and MLD is the mixed layer depth (m).

During the MIFASOL II cruise, the hydrological and optical variables were measured with a Sea-Bird Conductivity-Temperature-Depth (CTD) profiler, a WET Labs C-Star transmissometer and a SeaPoint optical backscatter sensor coupled to the rosette.

### 3.2.3 Chemical and biological variables

#### 3.2.3.1 Particulate organic matter (TEP, CSP, POC and PON)

Transparent exopolymer particles (TEP) were analysed following the spectrophotometric method proposed by Passow and Alldredge (1995). Filtration of samples (150-500 mL) was done in duplicate under low constant pressure ( $\sim 150$  mm Hg) onto 25 mm diameter  $0.4 \mu\text{m}$  pore size Polycarbonate filters (DHI). Immediately, filters were stained with Alcian Blue solution (500  $\mu\text{L}$ , 0.02 %, pH 2.5) for 5 s, and rinsed with Milli-Q water. All sampling material was pre-washed with HCl (10 %) and Milli-Q water, and the first millilitres of sample were discarded. All filters remained frozen until further processing. Filters were soaked in 5 mL of 80 % sulfuric acid for 3 h, shaking them intermittently, and absorbance of the solution was measured with the spectrophotometer at 787 nm (Varian Cary 100 Bio). The absorption of every batch of Alcian Blue was calibrated using a Xanthan Gum (XG) solution that was homogenized with a tissue grinder and measured by weight difference. A total of 7 calibrations of different Alcian Blue solutions were carried out during the temporal series, and

detection limits ranged from 0.0210 to 0.0480 absorbance units. Duplicate blanks (empty filters stained with Alcian Blue) were also prepared with every batch of filtered samples. We conducted TEP analyses in formalin-fixed (1% final concentration) samples, which were preserved at 4 °C until filtration (within 4 months at most). We decided to conduct TEP analyses on fixed samples, since formalin does not interfere with the measurement (Passow and Alldredge, 1995; Ortega-Retuerta et al., 2018), in order to optimize the number of samples processed every time a new calibration curve was constructed (one every four months). The conversion factor of 0.51  $\mu\text{g TEP-C } \mu\text{g XG eq}^{-1}$  (Engel and Passow, 2001) was used to estimate TEP carbon content (TEP-C).

CSP concentration was determined by spectrophotometry following (Cisternas-Novoa et al., 2014). Duplicate samples (200-350 mL) were filtered onto 25 mm diameter 0.4  $\mu\text{m}$  pore size Polycarbonate filters (Whatman and DHI) using a constant low filtration pressure (~150 mmHg). The samples were immediately stained with 1 mL of Coomassie Brilliant Blue (CBB-G 250) solution (0.04 %, pH 7.4) for 30 s, prepared always with the same filtered 0.2  $\mu\text{m}$  seawater from Medes, 80 m depth, and rinsed with Milli-Q water three times. The filters were stored frozen in 15mL- polypropylene tubes until further processing in the laboratory (within 4 months). Duplicate blanks (empty filters stained as stated earlier) were prepared with every batch of filtered samples. Both the sample and blank filters were soaked in 4 mL of extraction solution (3 % SDS in 50 % isopropyl alcohol) and the tubes were incubated in a water bath for 2 h at 37 °C. The filters were shaken every 30 minutes during this period. We avoided sonication since it was previously observed that DHI filters did not resist sonication. We tested previously that the water bath and shaking were enough to remove the stain from the filters. We measured the absorbance after extraction in the water bath for 2 h, and then we sonicated the same filters for 2 h and measured the absorbance again. More than 90 % of absorbance was recuperated without sonication in our samples. The samples were then measured spectrophotometrically at 615nm (Varian Cary 100 Bio and Shimadzu UV-Vis spectrophotometer UV120). Concentrations of CSP are reported relative to a bovine serum albumin standard and expressed in micrograms of bovine serum albumin equivalents per liter ( $\mu\text{g BSA eq L}^{-1}$ ) after Cisternas-Novoa et al. (2014). A total of 3 calibrations of different CBB solutions were carried out during the temporal series, and detection limits ranged from 0.0440 to 0.0609 absorbance units.

At BBMO in four months (November 2016 and April, August and October 2017), TEP and CSP were also measured following the microscopy method (Engel et al., 2015). Duplicate samples of 50 mL were filtered onto 25 mm diameter 0.4  $\mu\text{m}$  pore size Polycarbonate filters (DHI), stained, and the excess dye was removed. Blanks were prepared as empty filters stained. The filters were placed on the white side of a semi-transparent glass slide (CytoClear, Poretics Corp., Livermore, US) and stored frozen ( $-20\text{ }^{\circ}\text{C}$ ) until microscopic analysis. Following Engel (2009), abundance, area and size–frequency distribution of TEP and CSP in the size range 1–760  $\mu\text{m}$  were determined using a light microscope (Olympus Bx61) connected to a camera (Olympus DP72). Filters were screened at 200 $\times$  magnification. Thirty pictures were taken randomly from each filter along two perpendicular cross sections (15 pictures each; resolution 1360 $\times$ 1024 pixel, 8 bit color depth). WCIF ImageJ image analysis software (version 1.44, public domain, developed at the US National Institutes of Health, courtesy of Wayne Rasband, National Institute of Mental Health, Bethesda, Maryland) was used to semi-automatically analyse particle numbers and area. TEP-C content was calculated following Mari (1999). We compared TEP-C estimates with those from the spectrophotometry method.

For particulate organic carbon (POC) and nitrogen (PON) analyses, seawater (1000 mL) was filtered through combusted (4 h, 450  $^{\circ}\text{C}$ ) GF/F glass fibre filters (Whatman) and filters were frozen at  $-20\text{ }^{\circ}\text{C}$  until processed. Prior to analysis, the filters were thawed in an HCl-saturated atmosphere for 24 h to remove inorganic compounds. Then the filters were dried and analysed with an elemental analyser (Perkin-Elmer 2400 CHN).

### **3.2.3.2 Chlorophyll *a* (Chl *a*)**

Chl *a* measurements started filtering 150 mL (BBMO) or 100 mL (EOS) of seawater on GF/F filters (Whatman, 25 mm diameter) and storing filters at  $-20\text{ }^{\circ}\text{C}$  until further processing. The pigment was extracted in acetone (90 % v:v) at 4  $^{\circ}\text{C}$  in the dark for 24 hours. Fluorescence was measured with a calibrated Turner Designs fluorometer, following Yentsch and Menzel (1963).

### **3.2.3.3 Inorganic nutrients**

Dissolved inorganic nutrients (nitrate, phosphate and silicate) were measured with standard segmented flow analysis with colorimetric detection (Hansen and Grasshoff,

1983), using a SEAL Auto Analyzer AA3 HR (BBMO) or Bran + Luebe autoanalyser (EOS).

#### **3.2.3.4 Phytoplankton identification and biomass**

Phytoplankton were identified and counted with an inverted microscope. Seawater was fixed with hexamine-buffered formaldehyde solution (4 % final concentration) and 100 mL were allowed to settle in Utermöhl chambers at 4 °C until analysis (Guadayol et al., 2009). Phytoplankton was identified to the species level when possible, and finally classified into four groups: diatoms, dinoflagellates, coccolithophores and other microplankton cells classified as “other microalgae”. We used conversion equations to calculate the cell C content (Menden-Deuer and Lessard, 2000). For diatoms we used  $\log \text{ pg C cell}^{-1} = \log -0.541 (0.099) + 0.811 (0.028) \times \log V$ , and for the other algae groups,  $\log \text{ pg C cell}^{-1} = \log -0.665 (0.132) + 0.939 (0.041) \times \log V$ , where V is cell volume in  $\mu\text{m}^3$  and the values inside parentheses are the 95 % confidence intervals.

#### **3.2.3.5 Picophytoplankton and prokaryotic heterotrophic (PH) abundance**

Enumeration of picophytoplankton and heterotrophic prokaryotes (PH) was done by flow cytometry after fixation with 1% paraformaldehyde plus 0.05% glutaraldehyde (final concentrations), following standard methods (Gasol and del Giorgio, 2000). The carbon content of PH was estimated empirically from the bead-standardized side scatter of the relevant populations following Calvo-Díaz and Morán (2006). Size was converted to C content following Norland (1993). The estimated average value of PH biomass per cell was  $19 \pm 0.5 \text{ fg C}$ .

### **3.2. 4 Statistical analyses**

Tukey Test was used to check for statistical differences of the different environmental variables among seasons. The seasons were separated by the winter/summer solstices and the spring/fall equinoxes. We used the nonparametric Wilcoxon-Mann-Whitney to test for statistical differences of the different variables among regions (BBMO and EOS). We performed pairwise Spearman correlation analyses to test for covariations between environmental and biological variables in the BBMO, EOS and Mifasol II dataset and also to test for covariations of these variables between BBMO and EOS. Bivariate analyses (ordinary least squares, OLS) between TEP and CSP concentrations and several biological, chemical and physical variables were performed in EOS profiles. We log transformed data to fulfil the requirements of parametric tests. Principal



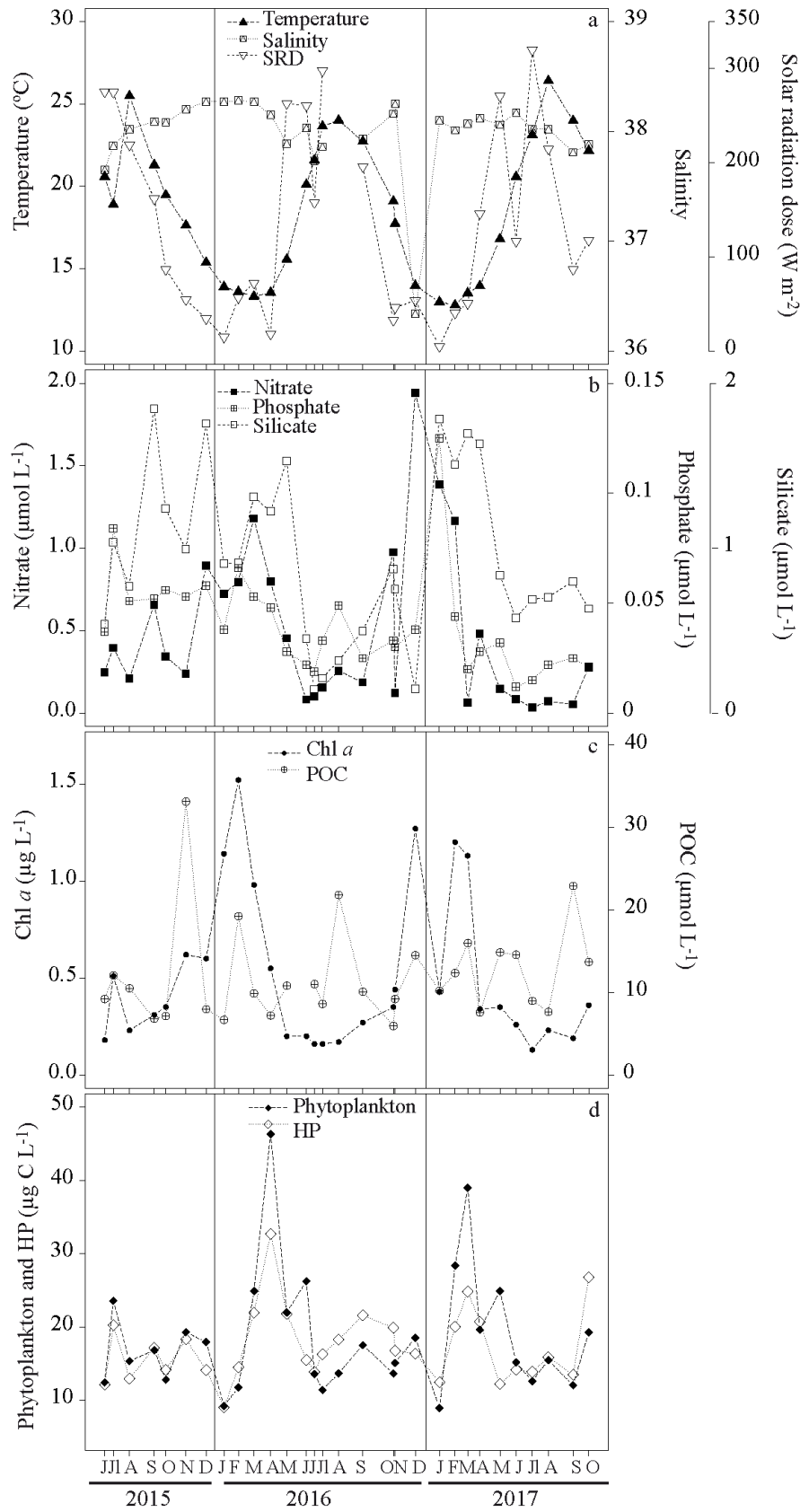
component analysis (*devtools* and *ggbiplot* packages in R) was applied to all samples of BBMO and EOS dataset after centering and scaling a total number of 20 and 19 physical, chemical and biological variables, respectively. At EOS, we calculated depth integrated values for the water column (0-92 m) by linear interpolation of values obtained at 4 sampling depths in the range 0-92 m. Depth averaged values were measured dividing depth integrated values by depth (92 m). Statistical tests, calculations and illustration were performed with Microsoft Office Excel 2010, Ocean Data View software (version 4) (Schlitzer and 2017) and R programming software (version 3.5.1).

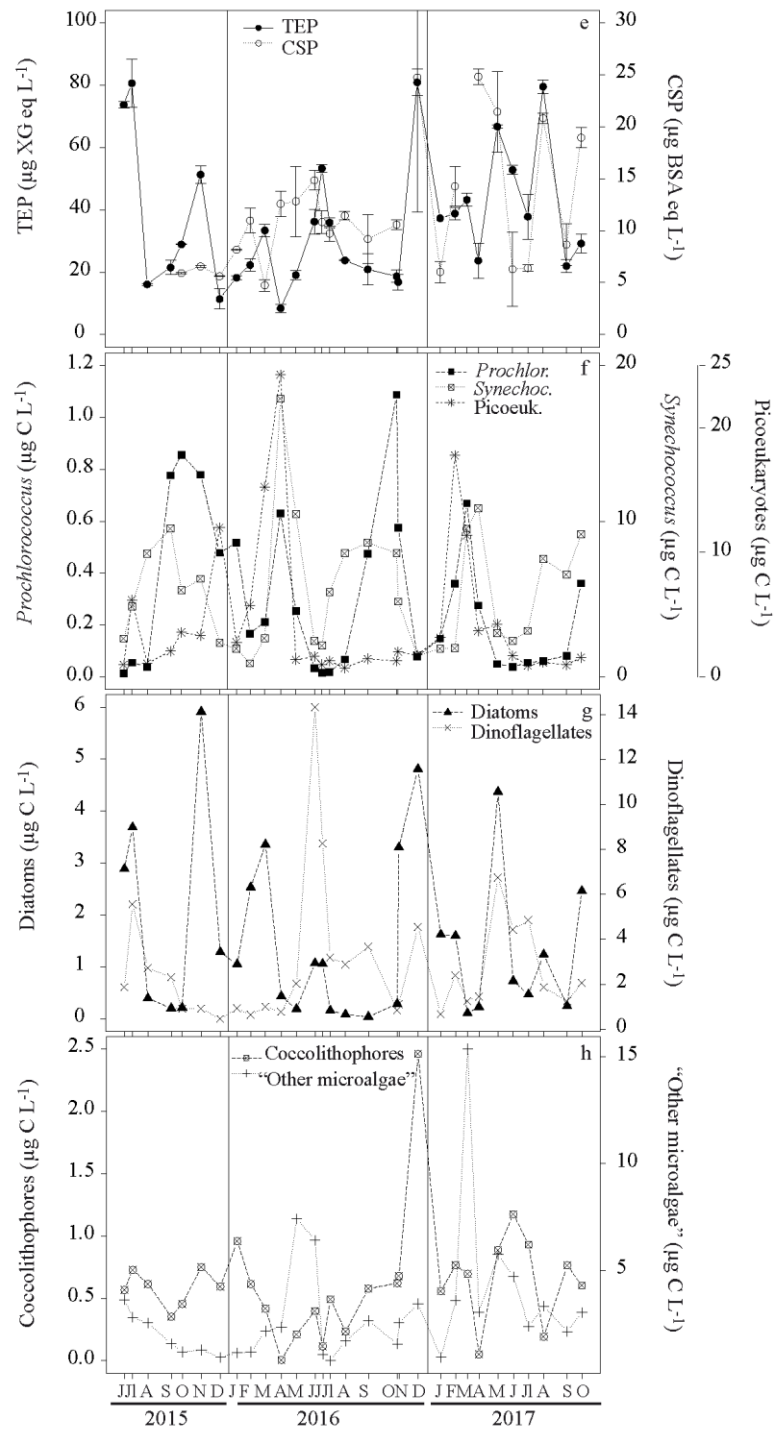
### 3.3 Results

#### 3.3.1 Variation of the main physical and chemical variables over the time series

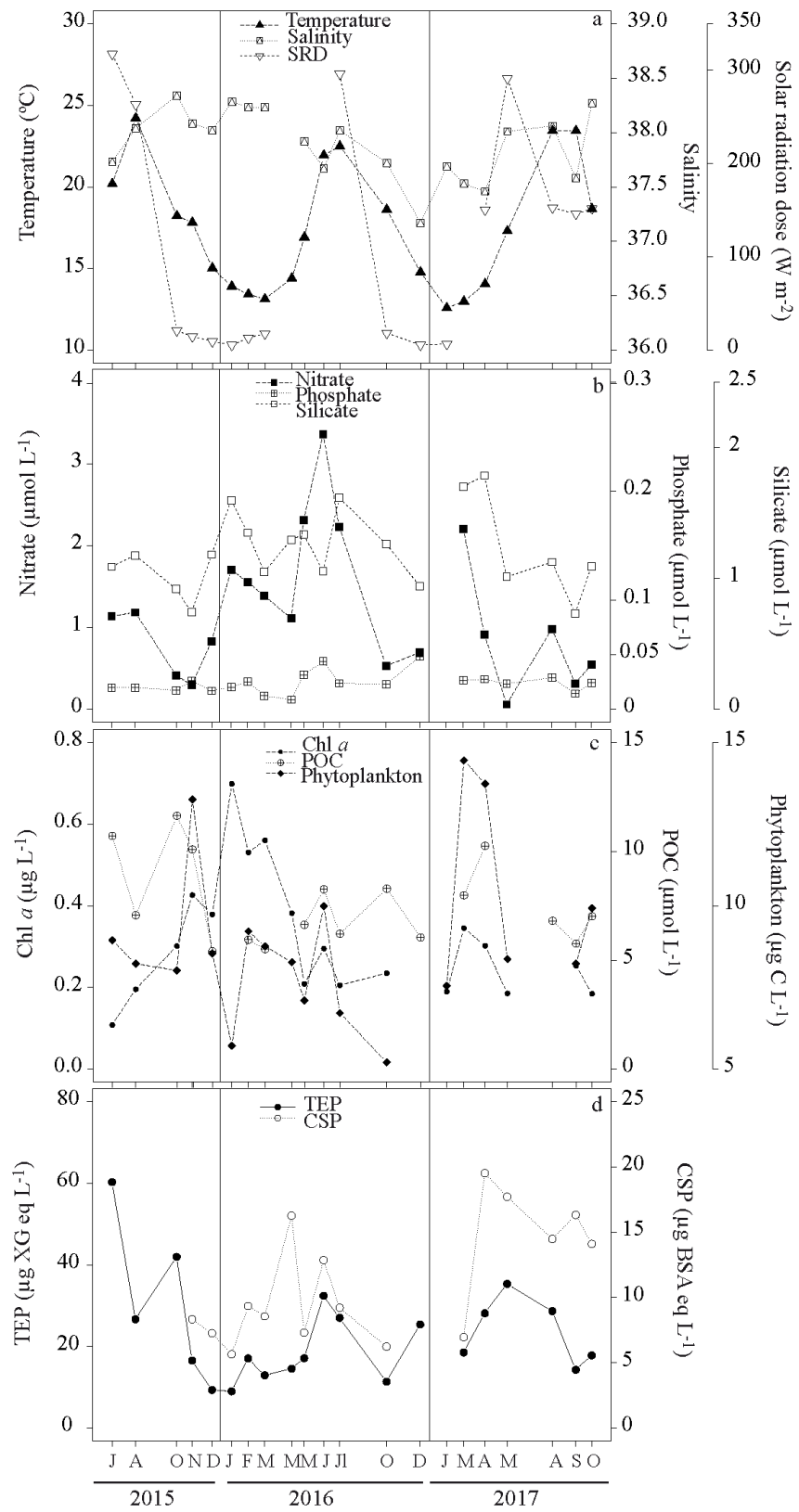
BBMO and EOS are two sites relatively unaffected by human impacts and river discharges (Guadayol et al., 2009; Ros and Gili, 2015), where oceanographic variables present a seasonal cycle typical for a temperate coastal system. Sea surface temperature (SST) was similar in BBMO and EOS, following a marked seasonal cycle due to the differences in the number of light hours through the year (maximum in June and July and minimum in December and January). SST changed from an average of  $13.4 \pm 0.4$  °C (BBMO) and  $13.2 \pm 0.5$  °C (EOS) in winter to  $22.9 \pm 2.2$  °C (BBMO) and  $22.6 \pm 1.4$  °C (EOS) in summer (Figs. 3.2 and 3.3). In summer, high surface temperatures caused the presence of a shallower stratified layer (average MLD of  $6.5 \pm 5.7$  m in BBMO and  $4.6 \pm 4.7$  m in EOS) (Table 3.1). Water transparency ranged from 5 to 20 m in BBMO and 5 to 24 m in EOS, with the highest values in summer at both stations. Dissolved nitrate and silicate concentrations in the surface were lowest in summer in both BBMO and EOS (Table 3.1). However, surface phosphate concentrations (average  $0.04 \pm 0.02$   $\mu\text{mol L}^{-1}$  in BBMO and  $0.04 \pm 0.06$   $\mu\text{mol L}^{-1}$  in EOS) did not exhibit marked seasonal variations but were low throughout the year in both stations (Table 3.1). Looking at the vertical distribution of dissolved inorganic nutrients in EOS, these usually increased with depth in summer, while they were more homogeneously distributed in the other seasons, though with variations (Fig. S3.1 and Table 3.1).

Figure 2





**Figure 3.2:** Values of a) temperature, salinity and one-day averaged solar radiation dose (SRD), b) nitrate, phosphate and silicate c) particulate organic carbon (POC) and chlorophyll *a* (Chl *a*), d) phytoplankton and heterotrophic prokaryotic (PH) biomasses, e) transparent exopolymer particles (TEP) and Coomassie stainable particles (CSP) concentrations, f) *Prochlorococcus*, *Synechococcus* and picoeukaryotes biomasses, g) diatoms and dinoflagellates biomasses, h) coccolithophores and “other microalgae” biomasses, over the study in BBMO. Time scale is in Julian days, starting on 1 June 2015. Every tick indicates the sampling month.



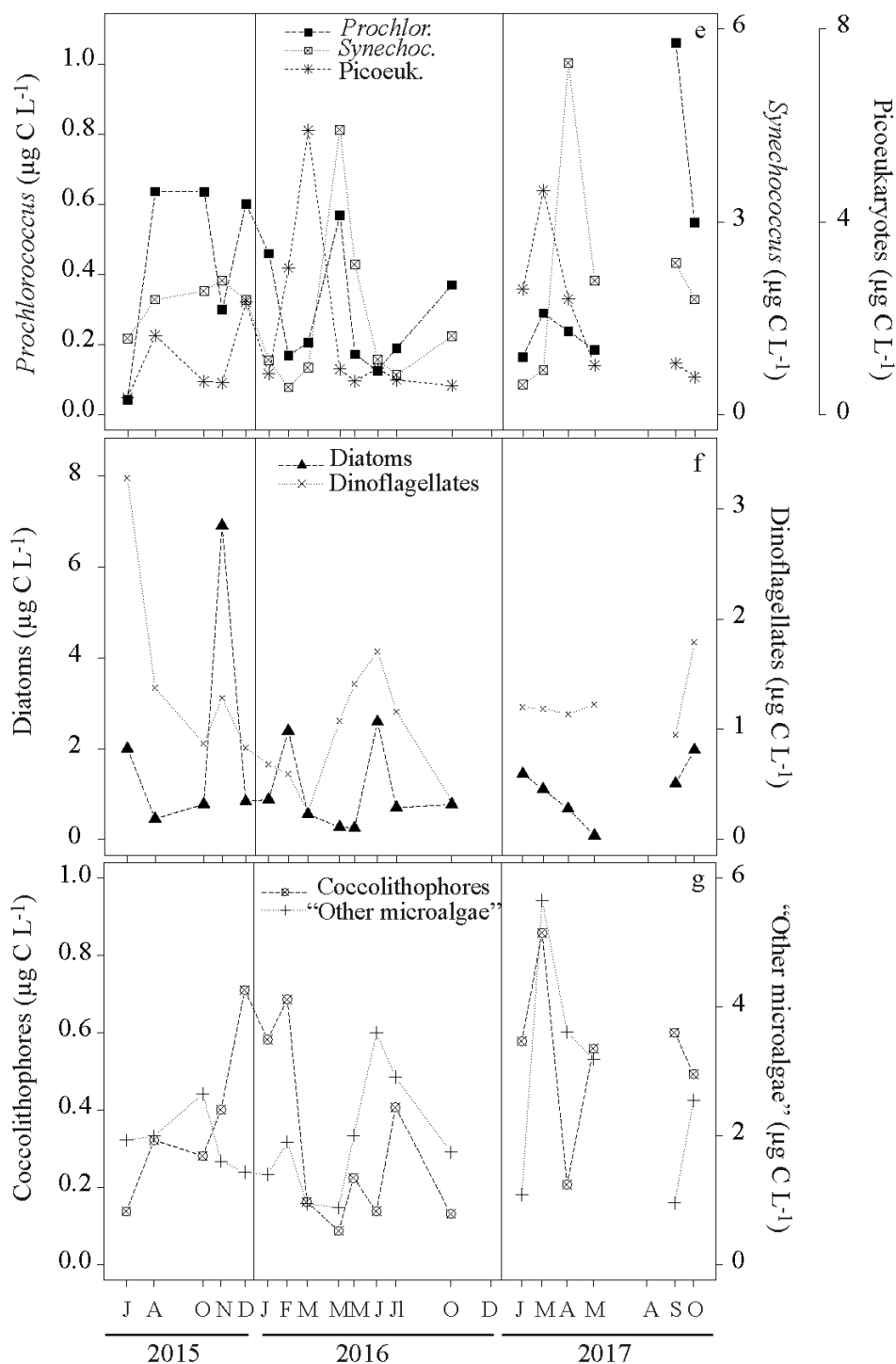


**Figure 3.3:** Values of a) temperature, salinity and one-day averaged solar radiation dose (SRD) in the surface (0.5 m) and b) nitrate, phosphate and silicate, c) particulate organic carbon (POC), chlorophyll *a* (Chl *a*) and phytoplankton biomass, d) transparent exopolymer particles (TEP) and Coomassie stainable particles (CSP) concentrations, e) *Prochlorococcus*, *Synechococcus* and picoeukaryotes biomasses, f) diatoms and dinoflagellates biomasses, g) coccolithophores and "other microalgae" biomasses, depth-averaged over the study in EOS. Time scale is in Julian days, starting on 1 June 2015. Every tick indicates the sampling month.

**Table 3.1.** Averages and standard deviation (SD) of the main physical and biological variables in each season at the surface of the BBMO (0.5 m) and EOS (0.5 m) time series, between June 2015 and November 2017. MLD: mixed layer depth, Chl *a*: chlorophyll *a*, POC: particulate organic carbon, PON: particulate organic nitrogen, PHA: prokaryotic heterotrophic abundance, TEP: transparent exopolymer particles, CSP: Coomassie stainable particles, C: phytoplankton biomass.

Variable	BBMO				EOS			
	Winter	Spring	Summer	Fall	Winter	Spring	Summer	Fall
	Average ( $\pm$ SD)	Average ( $\pm$ SD)	Average ( $\pm$ SD)	Average ( $\pm$ SD)	Average ( $\pm$ SD)	Average ( $\pm$ SD)	Average ( $\pm$ SD)	Average ( $\pm$ SD)
Temperature ( $^{\circ}$ C)	13.4 $\pm$ 0.4a	16.8 $\pm$ 3.0a,c	22.9 $\pm$ 2.2b	17.9 $\pm$ 2.7b,c	13.2 $\pm$ 0.5a	15.7 $\pm$ 1.7b,a	22.6 $\pm$ 1.4c	17.2 $\pm$ 1.8b
Salinity	38.2 $\pm$ 0.1a	38.1 $\pm$ 0.1a	37.9 $\pm$ 0.1a	37.9 $\pm$ 0.7a	38.0 $\pm$ 0.4a	37.8 $\pm$ 0.3a	37.8 $\pm$ 0.2a	37.9 $\pm$ 0.4a
Stratification Index ( $^{\circ}$ C)	0.04 $\pm$ 0.06a	1.24 $\pm$ 1.35a	2.01 $\pm$ 1.73a	0.49 $\pm$ 1.63a	-	-	-	-
Water transparency (m)	11.0 $\pm$ 4.0a	16.5 $\pm$ 3.1b	17.5 $\pm$ 3.0a,b	15.3 $\pm$ 3.5a,b	11.2 $\pm$ 2.9a	12.8 $\pm$ 3.6a	17.7 $\pm$ 3.5a	14.2 $\pm$ 6.7a
MLD (m)	10.0 $\pm$ 3.2	8.6 $\pm$ 6.8	6.5 $\pm$ 5.7	13.9 $\pm$ 5.4	76.8 $\pm$ 31.9	6.0 $\pm$ 5.7	4.6 $\pm$ 4.7	52.2 $\pm$ 38.8
Averaged-24h solar radiation dose ( $Wm^{-2}$ )	40.2 $\pm$ 25.7a	179.3 $\pm$ 102.9b	220.4 $\pm$ 72.b	61.1 $\pm$ 30.8a	10.8 $\pm$ 5.7a	221.0 $\pm$ 99.5b	235.2 $\pm$ 80.6b	36.9 $\pm$ 56.6a
Nitrate ( $\mu$ mol L $^{-1}$ )	0.89 $\pm$ 0.47a	0.34 $\pm$ 0.29a,b	0.22 $\pm$ 0.18b	0.68 $\pm$ 0.65a,b	1.67 $\pm$ 0.20a	0.77 $\pm$ 0.58a	0.27 $\pm$ 0.41a	1.36 $\pm$ 1.23a
Phosphate ( $\mu$ mol L $^{-1}$ )	0.06 $\pm$ 0.04a	0.03 $\pm$ 0.01a	0.04 $\pm$ 0.02a	0.04 $\pm$ 0.01a	0.02 $\pm$ 0.01a	0.03 $\pm$ 0.02a	0.03 $\pm$ 0.01a	0.08 $\pm$ 0.10a
Nitrate:P	15.7 $\pm$ 8.5a	10.9 $\pm$ 6.4a	5.3 $\pm$ 2.9a	17.7 $\pm$ 17.2a	81.5 $\pm$ 27.7a	42.5 $\pm$ 41.2a,b	8.3 $\pm$ 8.7b	37.0 $\pm$ 54.0a,b
Silicate ( $\mu$ mol L $^{-1}$ )	1.35 $\pm$ 0.38a	1.04 $\pm$ 0.50a,b	0.69 $\pm$ 0.47b	0.91 $\pm$ 0.50a,b	1.53 $\pm$ 0.33a	1.29 $\pm$ 0.42a,b	0.48 $\pm$ 0.17b	1.03 $\pm$ 0.80a,b
Chl <i>a</i> ( $\mu$ g L $^{-1}$ )	1.07 $\pm$ 0.36a	0.32 $\pm$ 0.13b,c	0.23 $\pm$ 0.11b	0.57 $\pm$ 0.33c	0.50 $\pm$ 0.20a	0.27 $\pm$ 0.12a,b	0.14 $\pm$ 0.03b	0.33 $\pm$ 0.19a,b
POC ( $\mu$ mol L $^{-1}$ )	12.4 $\pm$ 4.5a	11.0 $\pm$ 3.7a	11.8 $\pm$ 5.4a	13.1 $\pm$ 9.4a	8.8 $\pm$ 2.1a	10.8 $\pm$ 3.4a	10.2 $\pm$ 4.8a	9.7 $\pm$ 5.1a
PON ( $\mu$ mol L $^{-1}$ )	1.7 $\pm$ 0.7a	1.6 $\pm$ 0.6a	1.7 $\pm$ 1.0a	2.0 $\pm$ 1.6a	1.0 $\pm$ 0.3a	1.3 $\pm$ 0.6a	1.1 $\pm$ 0.6a	2.3 $\pm$ 3.0a

PHA ( $\times 10^5$ cells mL <sup>-1</sup> )	9.04 ± 3.09a	10.21 ± 4.04a	8.35 ± 1.64a	9.69 ± 2.51a	-	-	-	-
TEP ( $\mu\text{g XG eq L}^{-1}$ )	32.2 ± 9.9a	34.5 ± 22.0a	42.3 ± 25.2a	33.9 ± 24.5a	25.8 ± 20.2a	29.2 ± 8.7a	57.2 ± 38.3a	28.2 ± 23.6a
CSP ( $\mu\text{g BSA eq L}^{-1}$ )	8.8 ± 3.8a	15.5 ± 6.7a	11.0 ± 4.6a	12.1 ± 8.0a	11.0 ± 6.6ab	19.8 ± 2.5a	12.8 ± 4.3a,b	9.3 ± 4.6b
TEP:Chl <i>a</i>	37.0 ± 26.3a	125.8 ± 76.9a,b	202.4 ± 123.1b	60.2 ± 24.8a	48.8 ± 39.9a	136.2 ± 98.2a,b	443.9 ± 314.4b	94.7 ± 86.1a
CSP:Chl <i>a</i>	9.0 ± 3.8a	53.2 ± 23.5b	59.0 ± 18.0b	23.2 ± 16.4a	20.5 ± 13.7a	87.8 ± 51.5a	86.2 ± 25.8a	42.9 ± 47.0a
TEP:C	1.98 ± 1.13a	1.64 ± 1.22a	2.88 ± 1.64a	1.99 ± 1.25a	1.58 ± 0.56a	2.52 ± 0.87a,b	4.95 ± 2.62b	2.03 ± 1.42a,b
CSP:C	0.64 ± 0.30a	0.66 ± 0.36a	0.80 ± 0.28a	0.70 ± 0.41a	0.80 ± 0.43a	1.79 ± 0.64a	1.25 ± 0.60a	0.77 ± 0.08a
TEP:POC	2.8 ± 0.9a	2.8 ± 1.4a	4.3 ± 3.0a	2.8 ± 1.5a	3.6 ± 1.5a	2.7 ± 0.5a	5.5 ± 2.2a	3.1 ± 2.0a
CSP:POC	0.8 ± 0.4a	1.6 ± 1.0a	1.0 ± 0.8a	1.1 ± 0.6a	1.4 ± 0.4a	2.0 ± 0.7a	1.8 ± 0.9a	1.1 ± 0.5a
C: Chl <i>a</i>	20.0 ± 10.5a	85.3 ± 29.7b	69.4 ± 14.1b	34.2 ± 11.8a	31.2 ± 28.5a	50.5 ± 21.3a	83.8 ± 27.6a	51.2 ± 48.9a
POC:Chl <i>a</i>	154 ± 73a	452 ± 231a,b	712 ± 427b	300 ± 184a	204 ± 49a	565 ± 297a,b	992 ± 413b	429 ± 253a,b

### 3.3.2 Variation of TEP, CSP, POC and PON over the time series

The ranges and averages of surface TEP concentrations were similar at both coastal stations, and they followed similar seasonal dynamics ( $r= 0.58$ ,  $p< 0.05$ ,  $n= 20$ , Table 3.2). At BBMO, surface TEP concentrations ranged from 8.4 to 80.9  $\mu\text{g XG eq L}^{-1}$  (average  $36.7 \pm 21.5 \mu\text{g XG eq L}^{-1}$ ) (Fig. 3.2), while in the EOS they ranged from 5.8 to 126.7  $\mu\text{g XG eq L}^{-1}$ , with an average of  $36.6 \pm 28.3 \mu\text{g XG eq L}^{-1}$  (Fig. 3.3). At surface, the coefficient of variation of TEP was 58 % in BBMO and 77 % in EOS. Although in none of the two stations TEP followed a significant seasonal pattern throughout the study (autocorrelation test,  $p> 0.05$ ), the highest TEP concentrations were recurrently observed in early summer (Figs. 3.2 and 3.3). When vertical profiles were measured (only in EOS), TEP typically decreased with depth (Fig. 3.4) but differences were found among seasons (Fig. S3.1). In the entire sampled water column in EOS, depth-averaged TEP values were  $31.6 \pm 15.3 \mu\text{g XG eq L}^{-1}$  in summer,  $20.4 \pm 11.9 \mu\text{g XG eq L}^{-1}$  in fall,  $19.0 \pm 5.5 \mu\text{g XG eq L}^{-1}$  in winter and  $23.8 \pm 9.7 \mu\text{g XG eq L}^{-1}$  in spring (Table 3.3).

In summer, TEP peaks were found at the surface or at 20 m, coinciding with shallow mixed layers, while they were usually homogeneously distributed during the rest of the year, despite the presence of a mixed layer in certain months (April, May, September and October 2017). Conversely, in December 2016, although the water column was mixed, a TEP peak at the surface was observed (Fig. S3.1).

Regarding TEP size distribution, determined by image analysis in the surface of EOS in 4 months, one per season (November 2016 and April, August and October 2017), it followed an exponential distribution, with the smallest particles, ranging 0-1.25  $\mu\text{m}$ , being the most abundant in 3 of the 4 samples. In April 2017, particles ranging 2.50-3.54  $\mu\text{m}$  were the most abundant, followed by the smallest ones (Fig. S3.3).



**Table 3.2.** Spearman correlations of environmental and biological variables between BBMO and surface EOS during the 2015-2017 period. ns: no significant. TEP: transparent exopolymer particles. CSP: Coomassie stainable particles. Chl *a*: chlorophyll *a*. B: biomass. POC: particulate organic carbon.

Variable	r	p	n
TEP	0.58	<0.05	20
CSP		ns	17
Temperature (°C)	0.97	<0.001	21
Salinity		ns	21
Water transparency (m)		ns	21
Solar radiation dose (Wm <sup>-2</sup> )	0.93	<0.001	17
Nitrate (µmol L <sup>-1</sup> )	0.56	<0.05	20
Phosphate (µmol L <sup>-1</sup> )		ns	20
Silicate (µmol L <sup>-1</sup> )	0.65	<0.05	20
Chl <i>a</i> (µg L <sup>-1</sup> )	0.72	<0.001	19
<i>Prochlorococcus</i> (µg C L <sup>-1</sup> )	0.64	<0.05	19
<i>Synechococcus</i> (µg C L <sup>-1</sup> )	0.58	<0.05	19
Picoeukaryotes (µg C L <sup>-1</sup> )	0.87	<0.001	19
Dinoflagellates (µg C L <sup>-1</sup> )	0.67	<0.001	19
Diatoms (µg C L <sup>-1</sup> )		ns	19
Coccolithophores (µg C L <sup>-1</sup> )	0.56	<0.05	19
“Other microalgae” (µg C L <sup>-1</sup> )		ns	19
Phytoplankton B (C) (µg C L <sup>-1</sup> )	0.61	<0.05	19
POC (µmol L <sup>-1</sup> )		ns	19

r: Spearman's correlation coefficient; p: level of significance; n: sample size

**Table 3.3.** Depth-averages and standard deviation (SD) of the main physical and biological variables in each season at EOS time series, between June 2015 and November 2017. POC: particulate organic carbon, TEP: transparent exopolymer particles, CSP: Coomassie stainable particles.

Variable	EOS			
	Winter	Spring	Summer	Fall
	Average (± SD)	Average (± SD)	Average (± SD)	Average (± SD)
Nitrate (µmol L <sup>-1</sup> )	1.71 ± 0.35a	1.10 ± 0.93a	1.54 ± 1.09a	0.55 ± 0.19a
Phosphate (µmol L <sup>-1</sup> )	0.03 ± 0.01a	0.02 ± 0.01a	0.03 ± 0.01a	0.03 ± 0.01a
Silicate (µmol L <sup>-1</sup> )	1.32 ± 0.29a	1.36 ± 0.32a	1.13 ± 0.28a	1.02 ± 0.19a
Chl <i>a</i> (µg L <sup>-1</sup> )	0.37 ± 0.20a	0.27 ± 0.09a,b	0.21 ± 0.07b	0.31 ± 0.10a,b
POC (µmol L <sup>-1</sup> )	6.9 ± 1.3a	8.4 ± 2.6a	7.5 ± 1.8a	8.1 ± 2.4a
TEP (µg XG eq L <sup>-1</sup> )	19.0 ± 5.5a	23.8 ± 9.7a	31.6 ± 15.3a	20.4 ± 11.9a
CSP (µg BSA eq L <sup>-1</sup> )	7.6 ± 1.6a	15.2 ± 5.4a	10.6 ± 6.5a	9.0 ± 3.5a

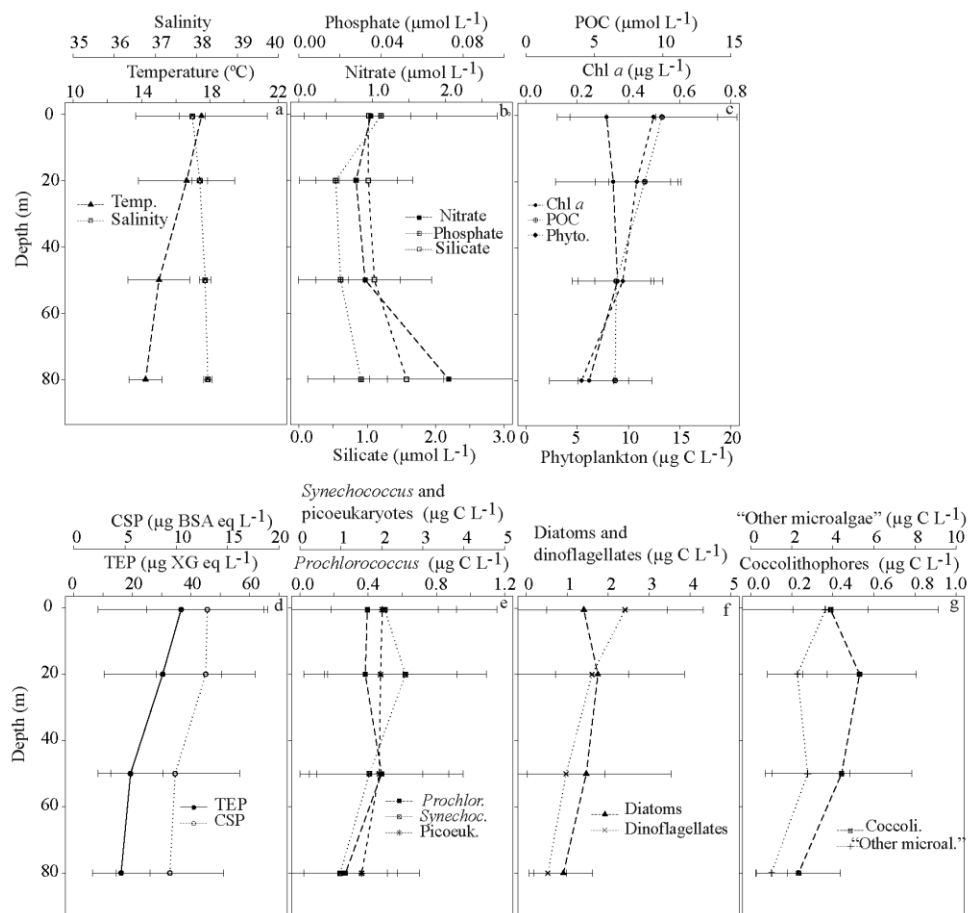


**Figure 3.4:** Average values along the whole temporal series in the vertical profile at EOS of a) temperature and salinity, b) nitrate, phosphate and silicate, c) particulate organic carbon (POC), chlorophyll *a* (Chl *a*) and carbon biomass (C) d) transparent exopolymer particles (TEP) and Coomassie stainable particles (CSP) concentration, e) *Prochlorococcus*, *Synechococcus* and picoeukaryotes biomasses, f) diatoms and dinoflagellates biomasses, g) coccolithophores and “other microalgae” biomasses. Bm: biomass.

Ranges and averages of surface Coomassie stainable particles (CSP) concentrations were also similar for both coastal stations, but temporal dynamics were different, resulting in no significant correlation ( $p > 0.05$ ) (Table 3.4). In BBMO, surface CSP concentration varied between 4.7 and 24.8  $\mu\text{g BSA eq L}^{-1}$  (average  $11.9 \pm 6.1 \mu\text{g BSA eq L}^{-1}$ ) (Fig. 3.2), while in EOS it varied between 4.5 and 22.4  $\mu\text{g BSA eq L}^{-1}$  (average  $13.0 \pm 5.9 \mu\text{g BSA eq L}^{-1}$ ) (Fig. 3.3). At the surface, the coefficient of variation of CSP was 51 % in BBMO and 46 % in EOS. They did not follow recurrent seasonal patterns throughout the study (autocorrelation test,  $p > 0.05$ ), but they always presented highest concentrations between late winter and early summer (Fig. 3.3). There were also differences among seasons in CSP vertical distributions in EOS (Fig. S3.1). In the entire sampled water column, depth-integrated CSP values were the highest in spring (average  $15.2 \pm 5.4 \mu\text{g BSA eq L}^{-1}$ ) and summer (average  $10.6 \pm 6.5 \mu\text{g BSA eq L}^{-1}$ ), and the lowest in fall (average  $9.0 \pm 3.5 \mu\text{g BSA eq L}^{-1}$ ) and winter (average  $7.6 \pm 1.6 \mu\text{g BSA eq L}^{-1}$ ). In summer, CSP concentrations were always higher at 20 m, i. e., below the mixed layer depth. In spring, concentrations were higher within the mixed layer depth, although in April and May 2017, there was also a peak at 60 m. In fall, CSP concentrations were homogeneously distributed in 3 out of 4 samples, except in December 2015, where a peak at the surface occurred. In winter there was no clear pattern of CSP distribution in the vertical scale (Fig. S3.1). On average, CSP decreased with depth (Fig. 3.4). CSP size distribution followed an exponential shape towards higher abundances of the smaller particles in the four samples (Fig. S3.3).

Particulate organic carbon (POC) and nitrogen (PON) concentrations were also similar in both coastal stations. In BBMO, surface POC ranged from 5.82 to 33.16  $\mu\text{mol L}^{-1}$  (average  $12.1 \pm 6.0 \mu\text{mol L}^{-1}$ ) (Fig. 3.2); in EOS, it ranged from 4.33 to 18.02  $\mu\text{mol L}^{-1}$  (average  $9.9 \pm 4.1 \mu\text{mol L}^{-1}$ ) (Fig. 3.3). PON surface concentrations averaged  $1.8 \pm 1.0 \mu\text{mol L}^{-1}$  in BBMO and  $1.5 \pm 1.7 \mu\text{mol L}^{-1}$  in EOS. Surface POC and PON concentrations did not present clear seasonal cycling during the study. In BBMO and EOS, TEP and POC dynamics were significantly correlated ( $r = 0.40$ ,  $p < 0.05$ ,  $n = 29$  in BBMO and  $r = 0.50$ ,  $p < 0.05$ ,  $n = 19$ , Table 3.4) while CSP was coupled neither to TEP nor to POC ( $p > 0.05$ , Table 3.5). In EOS, CSP were correlated to PON ( $r = 0.57$ ,  $p < 0.05$ ,  $n = 16$ , Table 3.5).

**Table 3.4.** Spearman correlations between transparent exopolymer particle (TEP) concentration and other environmental and biological variables during the 2015-2017 period in surface BBMO and EOS. ns: no significant. CSP: Coomassie stainable particles. Chl *a*: chlorophyll *a*. B: biomass. POC: particulate organic carbon. PON: particulate organic nitrogen. PHA: prokaryotic heterotrophic abundance.

Variable		BBMO			EOS		
		r	p	n	r	p	n
TEP	Temperature (°C)		ns	30		ns	20
	Salinity	-0.46	< 0.05	29	-0.48	< 0.05	19
	Stratification Index (° C)		ns	29		-	
	Water transparency (m)		ns	30		-	
	Solar radiation dose (Wm <sup>-2</sup> )	0.36	0.06	29	0.58	< 0.05	16
	Nitrate (µmol L <sup>-1</sup> )		ns	30		ns	20
	Phosphate (µmol L <sup>-1</sup> )		ns	30		ns	20
	Silicate (µmol L <sup>-1</sup> )		ns	30	-0.47	< 0.05	20
	CSP (µg BSA eq L <sup>-1</sup> )		ns			ns	
	Chl <i>a</i> (µg L <sup>-1</sup> )		ns	30	-0.47	< 0.05	18
	<i>Prochlorococcus</i> (µg C L <sup>-1</sup> )	-0.51	<0.05	30	-0.61	< 0.01	18
	<i>Synechococcus</i> (µg C L <sup>-1</sup> )	-0.36	0.05	30		ns	18
	Picoeukaryotes (µg C L <sup>-1</sup> )		ns	30		ns	18
	Dinoflagellates (µg C L <sup>-1</sup> )	0.50	<0.05	30		ns	18
	Diatoms (µg C L <sup>-1</sup> )	0.44	<0.05	30		ns	18
	Coccolithophores (µg C L <sup>-1</sup> )		ns	30		ns	18
	“Other microalgae” (µg C L <sup>-1</sup> )	0.36	0.05	30	0.55	< 0.05	18
	Phytoplankton B (C) (µg C L <sup>-1</sup> )		ns	30	0.50	< 0.05	18
	POC (µmol L <sup>-1</sup> )	0.40	<0.05	29	0.50	< 0.05	19
	PON (µmol L <sup>-1</sup> )		ns	29		ns	19
PHA (x10 <sup>3</sup> cells mL <sup>-1</sup> )		ns	30		-		
TEP:Chl <i>a</i>	Solar radiation dose (Wm <sup>-2</sup> )	0.74	<0.001	30	0.96	<0.001	18
TEP:C	Solar radiation dose (Wm <sup>-2</sup> )		ns	30	0.76	< 0.05	18
Chl <i>a</i>	Solar radiation dose (Wm <sup>-2</sup> )	-0.72	<0.001	30	-0.80	<0.001	18
C:Chl <i>a</i>	Solar radiation dose (Wm <sup>-2</sup> )	0.72	<0.001	30	0.87	<0.001	18

r: Spearman's correlation coefficient; p: level of significance; n: sample size

**Table 3.5.** Spearman correlations between Coomassie stainable particles (CSP) concentration and other environmental and biological variables during the 2015-2017 period in surface BBMO and EOS. ns: no significant. Chl *a*: chlorophyll *a*. B: biomass. POC: particulate organic carbon. PON: particulate organic nitrogen. PHA: prokaryotic heterotrophic abundance. PHP: prokaryotic heterotrophic production.

Variable	BBMO			EOS			
	r	p	n	r	p	n	
CSP	Temperature (°C)	ns	24	ns	17		
	Salinity	ns	23	ns	16		
	Stratification Index (° C)	ns	23	-			
	Water transparency (m)	ns	24	-			
	Solar radiation dose (Wm <sup>-2</sup> )	ns	23	ns	13		
	Nitrate (µmol L <sup>-1</sup> )	ns	24	ns	17		
	Phosphate (µmol L <sup>-1</sup> )	ns	24	ns	17		
	Silicate (µmol L <sup>-1</sup> )	ns	24	ns	17		
	Chl <i>a</i> (µg L <sup>-1</sup> )	ns	24	ns	15		
	<i>Prochlorococcus</i> (µg C L <sup>-1</sup> )	ns	24	ns	15		
	<i>Synechococcus</i> (µg C L <sup>-1</sup> )	ns	24	ns	15		
	Picoeukaryotes (µg C L <sup>-1</sup> )	ns	24	ns	15		
	Dinoflagellates (µg C L <sup>-1</sup> )	0.40	0.06	24	ns	15	
	Diatoms (µg C L <sup>-1</sup> )		ns	24	ns	15	
	Coccolithophores (µg C L <sup>-1</sup> )		ns	24	ns	15	
	“Other microalgae” (µg C L <sup>-1</sup> )	0.59	<0.05	24	ns	15	
	Phytoplankton B (C) (µg C L <sup>-1</sup> )	0.46	<0.05	24	0.59	<0.05	15
	POC (µmol L <sup>-1</sup> )		ns	23	ns	16	
	PON (µmol L <sup>-1</sup> )		ns	23	0.57	<0.05	16
	PHA (x10 <sup>3</sup> cells mL <sup>-1</sup> )		ns	24	-		
PHP (µg C L <sup>-1</sup> d <sup>-1</sup> )		ns	24	-			

r: Spearman's correlation coefficient; p: level of significance; n: sample size

### 3.3.3 Variation of biological variables over the time series

Chlorophyll *a* (Chl *a*) concentrations were similar in both stations, varying between 0.13 and 1.52 µg L<sup>-1</sup> (average 0.49 ± 0.39 µg L<sup>-1</sup>) in the surface of BBMO (Fig. 3.2), between 0.13 and 0.75 µg L<sup>-1</sup> (average 0.31 ± 0.19 µg L<sup>-1</sup>) in the surface of EOS (Fig. 3.3) and between 0.05 and 0.84 µg L<sup>-1</sup> (average 0.34 ± 0.19 µg L<sup>-1</sup>) in the whole water column of EOS (Fig. S3.1). Maximum concentrations occurred in winter in both stations (Table 3.1). In the surface, the coefficient of variation of Chl *a* was 79 % in BBMO and 61 % in EOS. Total phytoplankton biomass was not correlated with Chl *a* in any of the two stations (p > 0.05), and was maximum in late winter in both cases. Prokaryotic heterotrophic abundance (PHA) at surface in BBMO ranged from 5 to 17.26 x 10<sup>5</sup> cell mL<sup>-1</sup> (Fig. 3.2) (data not available in EOS).

Regarding the variability of different phytoplankton groups, they were quite similar in both stations; *Prochlorococcus*, *Synechococcus*, picoeukaryotes, dinoflagellates and coccolithophores were all significantly and positively correlated between stations (Table 3.2).

The highest surface abundances of *Prochlorococcus* cells were found in fall, whereas maxima of *Synechococcus* occurred in spring. Picoeukaryote abundances were highest in the first four months of every year. Dinoflagellates were maxima in late spring. The biomass of coccolithophores and “other microalgae” did not present clear seasonal variations in any of the stations (Figs. 3.2 and 3.3). The highest diatom biomasses were found in late fall (when data available).

Regarding the entire sampled water column in EOS, *Prochlorococcus* biomass presented high values at 50 m in summer 2015 and 2017. *Synechococcus* showed maximum concentrations at 20 m and/or 40 m in spring and summer. Diatom biomass in November 2015 was very high in the upper 50 m (Fig. S3.1).

### **3.3.4 Variation of TEP:Chl *a*, CSP:Chl *a*, TEP: C, CSP: C, TEP:POC, CSP:POC, C:Chl *a* and POC: Chl *a*, and contribution of TEP to the POC pool**

Surface average TEP:Chl *a* ratio was highest in summer in both stations, and so was the ratio of TEP to phytoplankton carbon biomass (TEP:C) (Table 3.1, Fig. S3.2). Surface average CSP:Chl *a* ratio was higher in spring and summer, whereas CSP:C was higher in summer in BBMO and in spring in EOS (Table 3.1). The minimum values of TEP:Chl *a* and CSP:Chl *a* occurred in winter in both stations (Table 3.1). The ratio of carbon biomass to Chl *a* (C:Chl *a*) showed a clear seasonal cycle, with the lowest values in winter and fall (generally below 50), and the highest in spring and summer (generally above 50) (Table 3.1). Also the POC:Chl *a* ratios was highest in summer and lowest in winter in both stations (Table 3.1, Fig. S3.2). TEP:POC ratios peaked in summer, while CSP:POC peaked in spring (Table 3.1).

The estimated contribution of TEP-C to the POC pool in BBMO (surface) and EOS (depth-averaged) ranged between 4 and 34 % (average  $14 \pm 9$  %), and between 6 and 24 % (average  $12 \pm 4$  %), respectively. The highest shares were observed in summer in both stations; in this season TEP-C was the largest contributor to the POC pool, whereas phytoplankton was the largest POC carrier in spring (Fig. 3.5).

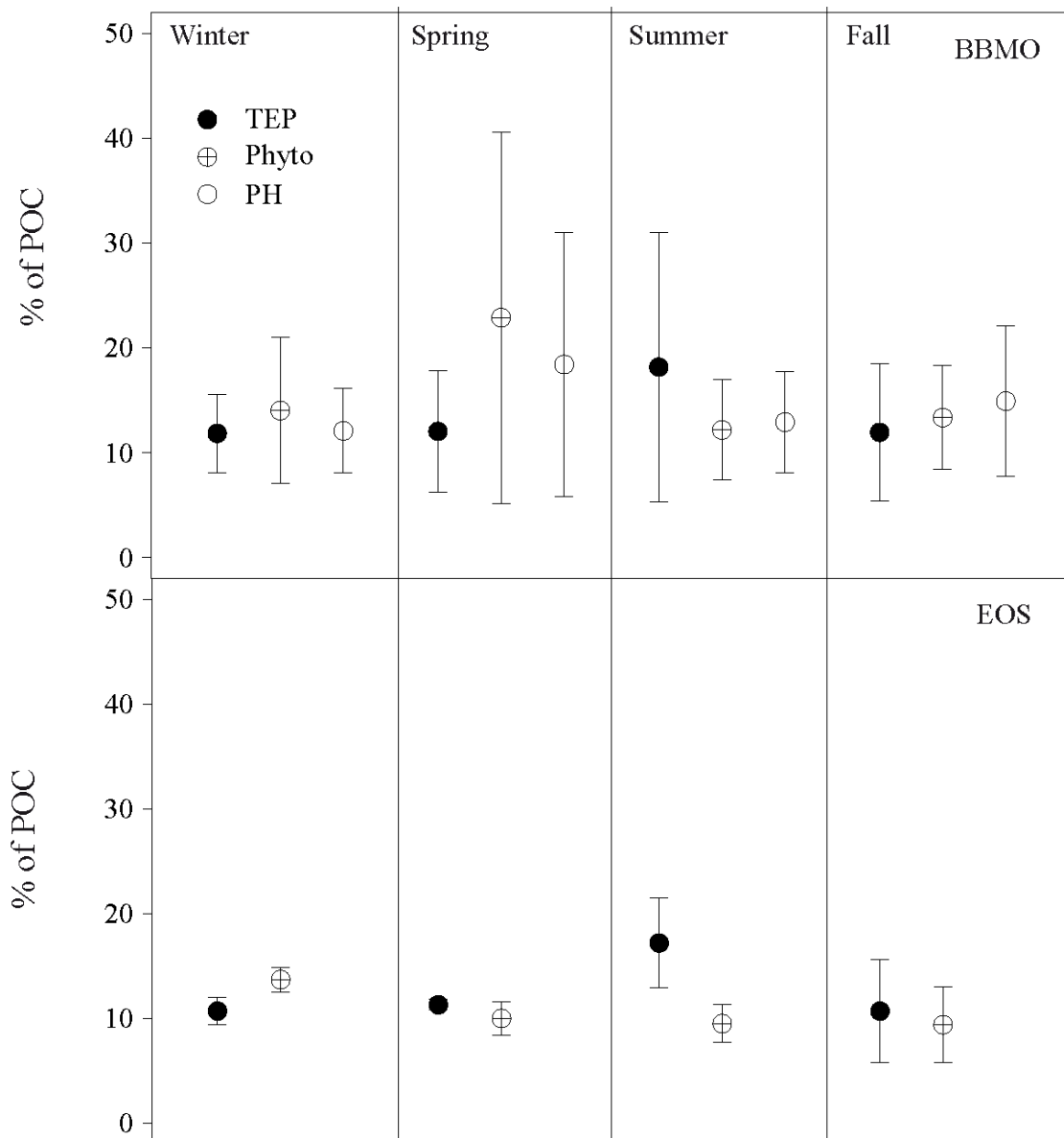


**Figure 3.5:** Averages and standard deviations of the contribution of TEP (estimated with the colorimetric method), phytoplankton and PH to the POC pool (%) in every season in BBMO at surface (0.5 m) (upper panel) and EOS (depth-integrated) (lower panel). The estimations of the contribution of TEP to the POC pool (%) in November 2016, April, August and October 2017 were all inside the range (standard deviation), whereas in October 2017 was slightly lower (3.6 %).

### 3.3.5 Environmental and biological variables as potential predictors of seasonal TEP and CSP dynamics

Regarding the correlations of TEP and CSP with other variables at surface in BBMO and EOS, differences were found between particle types and sampling stations. In BBMO, the variable that best correlated to TEP variability was dinoflagellate abundance ( $r=0.50$ ,  $p<0.05$ ,  $n=30$ ), followed by diatoms, “other microalgae” and solar radiation dose (Table 3.4). However, there was not a significant relationship with Chl *a* nor phytoplankton biomass, probably because cyanobacteria, which account for a remarkable share of phytoplankton biomass, showed a significant negative correlation to TEP (Table 3.5). CSP were best correlated to “other microalgae” ( $r=0.59$ ,  $p<0.05$ ,  $n=24$ ) and total phytoplankton biomass ( $r=0.46$ ,  $p<0.05$ ,  $n=24$ ) (Table 3.2).

In EOS, TEP were best positively correlated to the solar radiation dose ( $r=0.58$ ,  $p<0.05$ ,  $n=16$ ), “other microalgae” ( $r=0.55$ ,  $p<0.05$ ,  $n=18$ ), and total phytoplankton biomass ( $r=0.50$ ,  $p<0.05$ ,  $n=18$ ), and negatively correlated to Chl *a* ( $r=-0.47$ ,  $p<0.05$ ,  $n=18$ ). CSP positively correlated with total phytoplankton biomass ( $r=0.59$ ,  $p<0.05$ ,  $n=15$ ), but not with Chl *a*. Negative correlations occurred between TEP and *Prochlorococcus* in both study sites ( $r=-0.51$ ,  $p<0.05$ ,  $n=30$  in BBMO and  $r=0.61$ ,  $p<0.01$ ,  $n=18$  in EOS). Also in both study sites, TEP:Chl *a* ratio was positively correlated with solar radiation dose ( $r=-0.74$ ,  $p<0.001$ ,  $n=30$  in BBMO, and  $r=0.96$ ,  $p<0.001$ ,  $n=18$  in EOS). TEP:C was only correlated with solar radiation dose in EOS (Table 3.4).

At the vertical scale in EOS, TEP were best related to dinoflagellates ( $R^2=0.35$ ,  $p<0.001$ ,  $n=75$ ), silicate ( $R^2=0.32$ ), nitrate ( $R^2=0.23$ ), total phytoplankton biomass ( $R^2=0.22$ ) and “other microalgae” ( $R^2=0.20$ ) (Table 3.6). CSP were best related to total phytoplankton biomass ( $r=0.31$ ,  $p<0.001$ ,  $n=63$ ) and *Synechococcus* ( $r=0.29$ ,  $p<0.001$ ,  $n=63$ ) (Table 3.6).



**Table 3.6.** Regression equations and statistics describing the relationship between TEP (transparent exopolymer particles) or CSP (Coomassie stainable particles) and different variables in the vertical profiles of EOS (note all variables were  $\log_{10}$  transformed). ns: no significant. Chl *a*: chlorophyll *a*. PHA: prokaryotic heterotrophic abundance. B: biomass.

Var.	Ind. var	R <sup>2</sup>	p	Intercept	Slope	n
TEP	Temperature	0.21	<0.001	-0.83	1.79	83
	Salinity	0.29	<0.001	89.91	-56.03	79
	Nitrate	0.23	<0.001	1.25	-0.17	83
	Phosphate		ns			83
	Silicate	0.32	<0.001	1.32	-0.73	83
	Chl <i>a</i>	0.08	<0.05	1.12	-0.28	75
	PHA		ns			75
	<i>Prochlorococcus</i> B		ns			75
	<i>Synechococcus</i> B	0.11	<0.05	1.27	0.23	75
	Picoeukaryotes B		ns			75
	Diatoms B		ns			75
	Dinoflagellates B	0.35	<0.001	1.31	0.39	75
	Coccolithophores B		ns			75
	“Other microalgae” B	0.20	<0.001	1.22	0.34	75
	Phytoplankton B (C)	0.22	<0.001	0.82	0.52	75
CSP	Temperature		ns			68
	Salinity	0.17	<0.001	66.48	-41.44	64
	Nitrate		ns			68
	Phosphate		ns			68
	Silicate	0.06	<0.05	0.99	-0.37	68
	Chl <i>a</i>		ns			63
	PHA		ns			63
	<i>Prochlorococcus</i> B		ns			63
	<i>Synechococcus</i> B	0.29	<0.001	0.92	0.38	63
	Picoeukaryotes B		ns			63
	Diatoms B		ns			63
	Dinoflagellates B	0.23	<0.001	0.99	0.33	63
	Coccolithophores B		ns			63
	“Other microalgae” B	0.13	<0.05	0.90	0.27	63
	Phytoplankton B (C)	0.31	<0.001	0.40	0.61	63

R<sup>2</sup>: explained variance; p: level of significance; n: sample size

### 3.3.5 TEP and CSP distribution along the coast-to-open sea transect

Surface TEP concentrations (5 m) increased from the coast to the open ocean and ranged 21.5-36.5  $\mu\text{g XG eq L}^{-1}$  (average  $30.7 \pm 5.4 \mu\text{g XG eq L}^{-1}$ ). Surface CSP concentrations, which varied between 2.3 and 8.7  $\mu\text{g BSA eq L}^{-1}$  (average  $5.2 \pm 2.1 \mu\text{g BSA eq L}^{-1}$ ), decreased from the coast to the slope and beyond (Fig. 3.6), i.e., largely opposite to TEP. Surface CSP concentrations significantly and positively correlated with Chl *a* ( $r = 0.92$ ,  $p < 0.05$ ,  $n = 7$ ) and nanoeukaryotes ( $r = 0.86$ ,  $p < 0.05$ ,  $n = 7$ ). At the depth of the DCM, TEP and CSP concentrations were generally lower than surface concentrations (Fig. 3.6):  $11.4 \pm 3.6 \mu\text{g XG eq L}^{-1}$  for TEP and  $2.9 \pm 0.6 \mu\text{g BSA eq L}^{-1}$

for CSP. Unlike at surface, TEP concentrations at the DCM decreased from near coast to the slope, and so did CSP concentrations (Fig. 3.6).

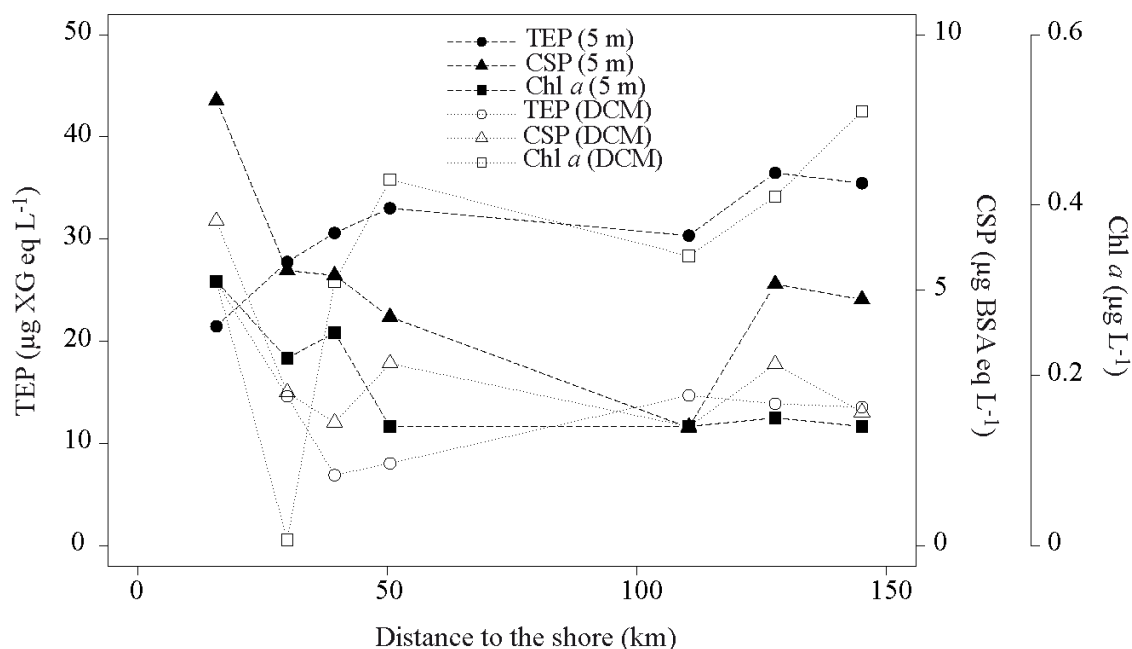


**Figure 3.6:** Transparent exopolymer particle (TEP) (circles) and Coomassie stainable particle (CSP) (triangles) and Chl *a* (squares) concentrations in the surface (5 m) (closed symbols) and deep chlorophyll maximum (DCM) (open symbols) in the transect, showing the distance to the shore. Note that in the M1 and M2, there was no DCM and the depth sampled was 25 and 200 m, respectively.

### 3.4 Discussion

#### 3.4.1 Dynamics of TEP and CSP over the seasonal cycle in the NW Mediterranean Sea

We present the first simultaneous distribution of TEP and CSP concentrations over two seasonal cycles in the Mediterranean Sea. The methods used to quantify these particles are based on the capability of a dye to stain acidic polysaccharides and proteins, respectively (Passow and Alldredge, 1995; Cisternas-Novoa et al., 2014). However, the actual composition of the particles is unknown and depends on the sources and degradation processes (Passow, 2012), and they are probably formed by a mixture of different organic and inorganic molecules and microbes. In the last years there has been an attempt to elucidate whether these stained particle types (TEP and CSP) are in fact the same particles or not (Cisternas-Novoa et al., 2015; Thornton et al., 2016; Thornton and Chen, 2017), and results suggest they mostly comprise different particulate

substances. Our results also support that TEP and CSP are different particles, since they presented uncorrelated temporal dynamics over seasonal cycles in two coastal sites (Figs. 3.2 and 3.3, Table 3.4 and 3.5), and also different vertical distributions (Fig. S3.1). This also suggests that they are produced by different organisms and/or subject to different aggregation and degradation processes, as suggested in previous studies (Cisternas-Novoa et al., 2015; Thornton et al., 2016; Thornton and Chen, 2017). It is worth mentioning, though, that the absence of parallel temporal patterns of TEP and CSP does not totally preclude that both particles are the same, at least in some cases. However, a previous study detected, through visual examination of the particles with the FlowCAM technique, that the Alcian Blue and CBB stains were frequently present in different particle types (Cisternas-Novoa et al., 2015), and therefore it is likely that at least some particles present Alcian-Blue stainable substances but not CBB stainable substances, and the opposite. On the other hand, Dreshchinskii and Engel (2017) observed that TEP and CSP dynamics were coupled during two seasonal cycles in the Baltic Sea, both in the SML and in subsurface water, which contrasts with our results.

TEP seasonality was similar in both coastal sites ( $r=0.58$ ; Table 3.2), probably indicating that the main drivers of TEP concentration were also similar in both stations (see next section). The maximum TEP concentrations found in early summer (Figs. 3.2 and 3.3) are in accordance with previous studies in the Mediterranean Sea (Beauvais et al., 2003; Ortega-Retuerta et al., 2018). It has been suggested that TEP maxima in summer could be due to the increase of TEP production under nutrient limitation, the presence of specific phytoplankton groups, and TEP accumulation due to positive buoyancy during water stratification (Ortega-Retuerta et al., 2018). This study expands the previous temporal study conducted in the BBMO (Ortega-Retuerta et al., 2018), incorporating information about phytoplankton biomass and solar radiation dose.

Our TEP ranges across the two stations ( $5.8-126.7 \mu\text{g XG eq L}^{-1}$ ) were similar to those found by Ortega-Retuerta et al. (2018) in BBMO during the three previous years ( $11.3-289.1 \mu\text{g XG eq L}^{-1}$ ), and by Iuculano et al. (2017b) in a rocky shore coastal site of the Balearic Sea ( $4.6-90.6 \mu\text{g XG eq L}^{-1}$ ), while they were lower than those found in a coastal site accumulating *Posidonia oceanica* leaf litter in the Balearic Sea ( $26.8-1878.4 \mu\text{g XG eq L}^{-1}$ ) (Iuculano et al., 2017b).

Temporal CSP patterns were different between coastal sites (Figs. 3.2 and 3.3), which may indicate differences in the main drivers of CSP concentration (see next section). Although no correlation was found among CSP and Chl *a* at any of the stations (Table 3.5), the highest CSP concentrations were found from late winter to early summer, coinciding with periods of relatively high Chl *a* values. A previous study showed stronger relationship with Chl *a* for CSP than for TEP (Cisternas-Novoa et al., 2015). Our surface CSP concentrations in both stations (0.5 and 5 m, respectively) ( $4.5\text{-}24.8 \mu\text{g BSA eq L}^{-1}$ ) were very similar to those found in the upper 100 m of the Sargasso Sea in several seasons of 2012 and 2013 ( $3.2 \pm 0.7 - 22.4 \pm 0.4 \mu\text{g BSA eq L}^{-1}$ ) (Cisternas-Novoa et al., 2015), probably because both the Mediterranean and Sargasso Sea are oligotrophic. By contrast, our CSP concentrations were lower than those found at 1 m in the Baltic Sea (Cisternas-Novoa et al., 2019) (Table 3.7), and our CSP microscopy-derived CSP abundance was lower than in the time series in the Baltic Sea (Dreshchinskii and Engel, 2017), probably due to the lower Chl *a* concentration in our study.

**Table 3.7.** Compilation of published Coomassie stainable particles (CSP) concentrations (mean  $\pm$  SE and ranges;  $\mu\text{g BSA eq L}^{-1}$ ), chlorophyll *a* (Chl *a*) concentrations (mean  $\pm$  SE and ranges;  $\mu\text{g L}^{-1}$ ) and CSP:Chl *a* ratios (mean  $\pm$  SE and ranges;  $\mu\text{g BSA eq } (\mu\text{g Chl } a)^{-1}$ ). bdl: below detection limit.

Location	Comments	CSP	Chl <i>a</i>	CSP:Chl <i>a</i>	Reference
Sargasso Sea	February, May, August, November 2012 and May 2013 0-100 m	$3.2 \pm 0.7 - 22.4 \pm 0.4$	$0.25\text{-}0.75^a$	-	Cisternas-Novoa et al. (2015)
Baltic Sea	3-19 June 2015 1 and 10 m	$15\text{-}56^a$	$1.2\text{-}1.7$	-	Cisternas-Novoa et al. (2019)
Mediterranean Sea	October 2015- October 2017 (time-series study) 0.5 m	$4.5\text{-}24.8$ ( $12.4 \pm 6.0$ )	$0.13\text{-}1.52$ ( $0.4 \pm 0.3$ )	$4.8\text{-}163.2$ ( $45.6 \pm 35.7$ )	This study

<sup>a</sup> Extracted from graphs

### 3.4.2 Main drivers of TEP and CSP dynamics

Chlorophyll *a* (Chl *a*), typically used as an indicator of phytoplankton biomass, was not positively correlated with TEP or CSP in any station, and in EOS it was negatively correlated with TEP ( $r = -0.45$ ,  $p < 0.05$ , Table 3.4). Ortega-Retuerta et al. (2018) also found negative correlation of TEP with Chl *a* ( $r = -0.45$ ,  $p = 0.007$ ) in BBMO. Previous time series studies reported covariation between TEP and Chl *a* (Beauvais et al., 2003; Scoullou et al., 2006; Engel et al., 2017; Parinos et al., 2017), while others did not (Bhaskar and Bhosle, 2006; Taylor et al., 2014), or only found it at certain periods of

the year (Dreshchinskii and Engel, 2017). However, it is worth mentioning that the C:Chl *a* ratio of phytoplankton changed throughout the year in both BBMO and EOS, in accordance with Gasol et al. (2016) and Gutiérrez-Rodríguez et al. (2010) for BBMO, being maximum in spring and summer (Table 3.1), which is explained by the high irradiance and low nutrients in these seasons (Geider et al., 1998). Consequently, Chl *a* cannot be considered a good indicator of phytoplankton biomass in these study sites.

CSP was correlated to total phytoplankton biomass in both stations (BBMO,  $r = 0.46$ ; EOS,  $r = 0.59$ ), while TEP only in EOS ( $r = 0.50$ ) (Table 3.4 and 3.5). This confirmed our hypothesis that CSP distribution and temporal dynamics, at least at sea surface, are more closely related to phytoplankton biomass than TEP, in agreement with Cisternas-Novoa et al. (2015). In addition, the highest CSP concentrations of the time series (from late winter to early summer), coincide with the period of maximum primary production (spring) recorded in a 12-year study (2003-2014) in the BBMO (Gasol et al., 2016), measured with the  $^{14}\text{C}$ -POC method, that is thought to estimate something near net primary production (Marra, 2002).

The same study observed that the Chl *a*-specific primary production (production per unit of Chl *a*) was highest in summer and lowest in winter, and that it correlated with the summer-enhanced variables (temperature, stratification and light). They suggested that the higher Chl *a*-specific primary production in summer could be due to higher efficiency of the phytoplankters that dominate the system in that season. It was reflected in their higher maximum Chl *a*-normalized photosynthetic rate ( $P_{\text{max}}^{\text{B}}$ ) values and higher light utilization in summer. Based on our observations, higher specific primary production in summer could be partially explained by the presence of TEP and CSP, with relatively high values also in summer, since these particles are partially retained in the filters used for PP measurements and thus included as they were phytoplankton biomass.

Our results suggest that TEP dynamics were more strongly affected by variables other than phytoplankton than CSP. In fact, CSP did not correlate with any other measured variables in any of the two stations (Table 3.5). Instead, TEP and TEP:Chl *a* correlated positively with solar radiation dose in both stations (and TEP: C only in EOS) (Table 3.4), which could be indicative of either the stimulation of TEP release by microbes by light stress, as suggested by Iuculano et al. (2017c), Agustí and Llabrés (2007) and

Zamanillo et al. (2019b), or the enhancement of abiotic self-assembly of dissolved exopolymers into TEP (Shammi et al., 2017). In EOS, TEP correlated negatively with salinity and silicate at surface (Table 3.4) and with nitrate across vertical profiles (Table 3.6). The negative relationship with nitrate could be due to the stimulation of phytoplankton TEP production under nutrient limitation in summer, as suggested by Ortega-Retuerta et al. (2018).

Gasol et al. (2016) found relatively high saturating irradiance or light saturation parameter ( $E_k$ ) values all year round in BBMO, which is typical of regions receiving relatively high light intensities.  $E_k$  was always within the values delimited by the surface irradiance and that at 5 m depth, indicating photoacclimation (physiological adjustments in response to changing light) of algal communities. In winter, the observed values of  $E_k$  are close to the surface irradiance at the time of sampling, whereas in summer they are close to the irradiance values observed at 5 m depth. This indicates that in summer, the phytoplankton living above 5 m receives irradiance in excess of their saturating irradiance, which may favour TEP production.

Along these same lines, Alonso-Sáez et al. (2008) found that DOC release accounted for up to 45 % of total primary production in BBMO, being lower in winter. Since DOC can self-assemble to form TEP, and possibly CSP, this release of primary production as DOC could have further contributed to increased TEP and CSP concentrations in spring and summer.

Neither TEP nor CSP were correlated with PHA, suggesting that heterotrophic prokaryotes played much less of a role than phytoplankton in driving the temporal variation of these two particle types.

Different phytoplankton groups appeared to be responsible for TEP and CSP distributions: TEP mainly correlated to dinoflagellates, diatoms and “other microalgae” over time (Table 3.4), whereas CSP correlated to dinoflagellates and “other microalgae” over time (Table 3.5), and also to *Synechococcus* in the vertical scale. While *Synechococcus* as a CSP source was already suggested by Cisternas-Novoa et al. (2015), this is the first study that suggests dinoflagellates and “other microalgae” to be also CSP producers. The lack of correlation of “other microalgae” between the two stations (Table 3.2) could be responsible for the differences in the temporal patterns of CSP.

A recent study has found enhanced production of TEP in a xenic culture of *Prochlorococcus* compared to an axenic one, suggesting that heterotrophic bacteria exude TEP or stimulate TEP production by *Prochlorococcus*. In this study, the negative correlation of TEP with *Prochlorococcus* in both study sites (Table 3.4) indicates that either *Prochlorococcus* were not major TEP producers, in agreement with Zamanillo et al. (2019c).

### 3.4.3 Contribution of TEP, phytoplankton and PH to the POC pool

The contribution of TEP to the POC pool in this study was in a similar range to that measured in the northeastern Atlantic Ocean (Harlay et al., 2009; Harlay et al., 2010), but lower than those reported across the Atlantic Ocean (Zamanillo et al., 2019c), eastern Mediterranean Sea (Bar-Zeev et al., 2011; Parinos et al., 2017) and the western Arctic (Yamada et al., 2015). Only two previous studies have compared the carbon content of TEP estimated with the colorimetric and microscopic methods. Berman and Viner-Mozzini (2001) did not find a good correlation, while Engel and Passow (2001) obtained similar results with both methods. In this study we have obtained a similar result, suggesting a good approximation to the reality.

Interestingly, only in summer in both stations, the TEP contribution to the POC pool at surface was larger than the contribution of phytoplankton and PH (Fig. 3.5). In addition, TEP:POC was also higher in summer (Table 3.1), indicating a higher TEP contribution to POC pool in this season. This may affect particle density: Particles with relatively higher TEP would be low dense (Engel and Schartau, 1999), and, consequently, these aggregates would present a lower sinking velocity, or could even ascend (Azetsu-Scott and Passow, 2004; Mari et al., 2007), with a tendency to accumulate at or near the surface. We hypothesize that the lower density of TEP-rich particles in summer would lead to their accumulation in the surface.

### 3.4.4 Distribution of TEP and CSP in the coast-to-offshore transect

The different dynamics of TEP and CSP along the coast-to-offshore transect (Fig. 3.6) indicate that the two particle types are also uncoupled at the spatial scale. The positive correlation of CSP with Chl *a* illustrates, as in the temporal scale, that CSP distribution is more strongly affected by phytoplankton biomass than TEP.

### 3.4.7 Conclusions

TEP and CSP seem to be independent particles since they followed uncoupled temporal dynamics at two coastal sites and at a coast-to-offshore transect in the NW Mediterranean Sea. Phytoplankton biomass was the main driver of TEP and CSP distribution, although not all phytoplankton groups contributed equally. Diatoms, dinoflagellates and “other microalgae” were the main drivers of TEP distribution, whereas dinoflagellates, “other microalgae” and *Synechococcus* were those of CSP. In addition, TEP distribution and temporal dynamics were also subjected to nutrient limitation, excretion of organics under saturating irradiance, and the proportion of TEP and solid particles in aggregates. The fact that two close coastal sites exhibit similar seasonal patterns of TEP concentrations indicates that opens up the possibility to define (and therefore predict) TEP seasonality in regions with similar biological, chemical and physical characteristics.

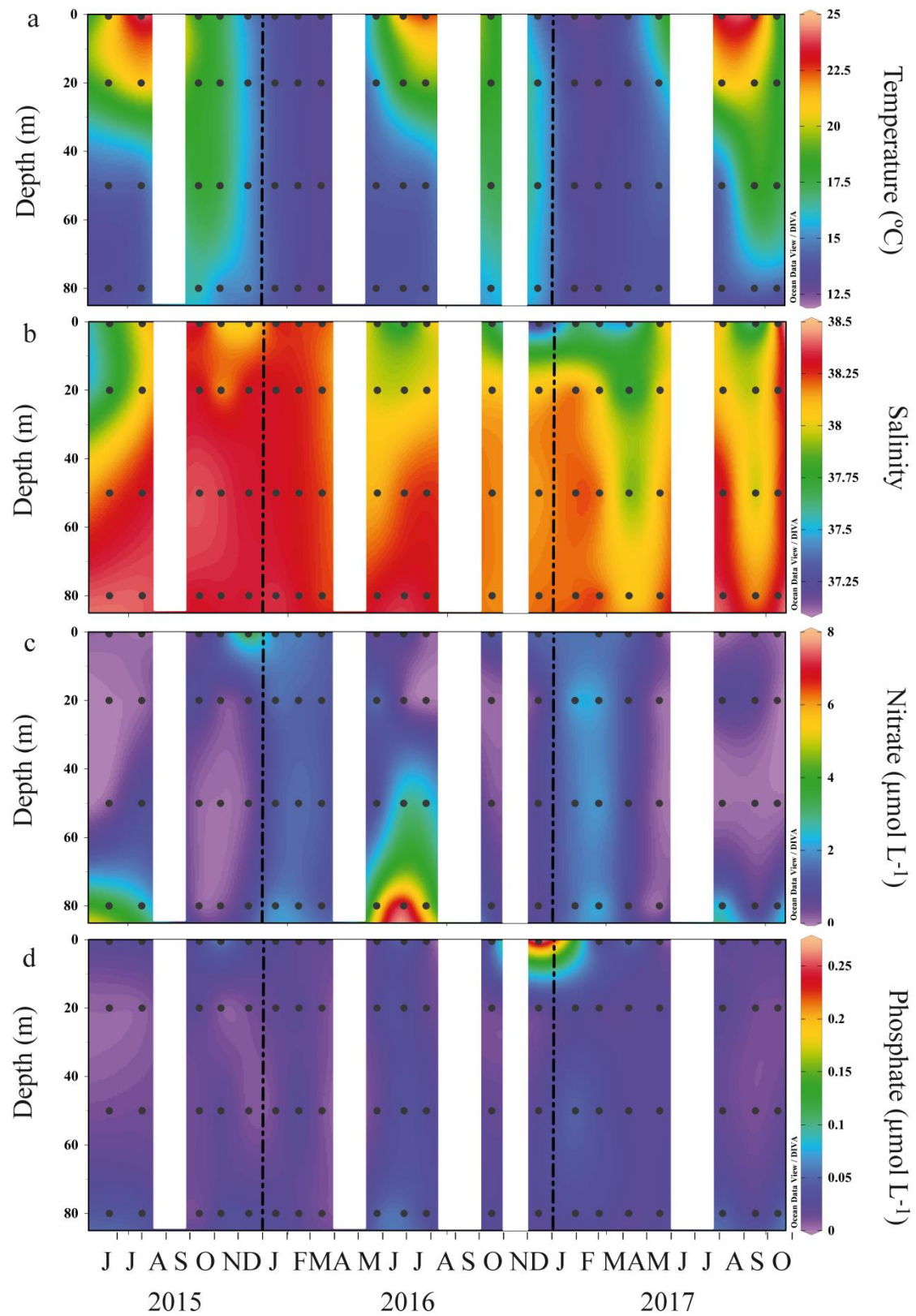
### 3.5 Acknowledgements

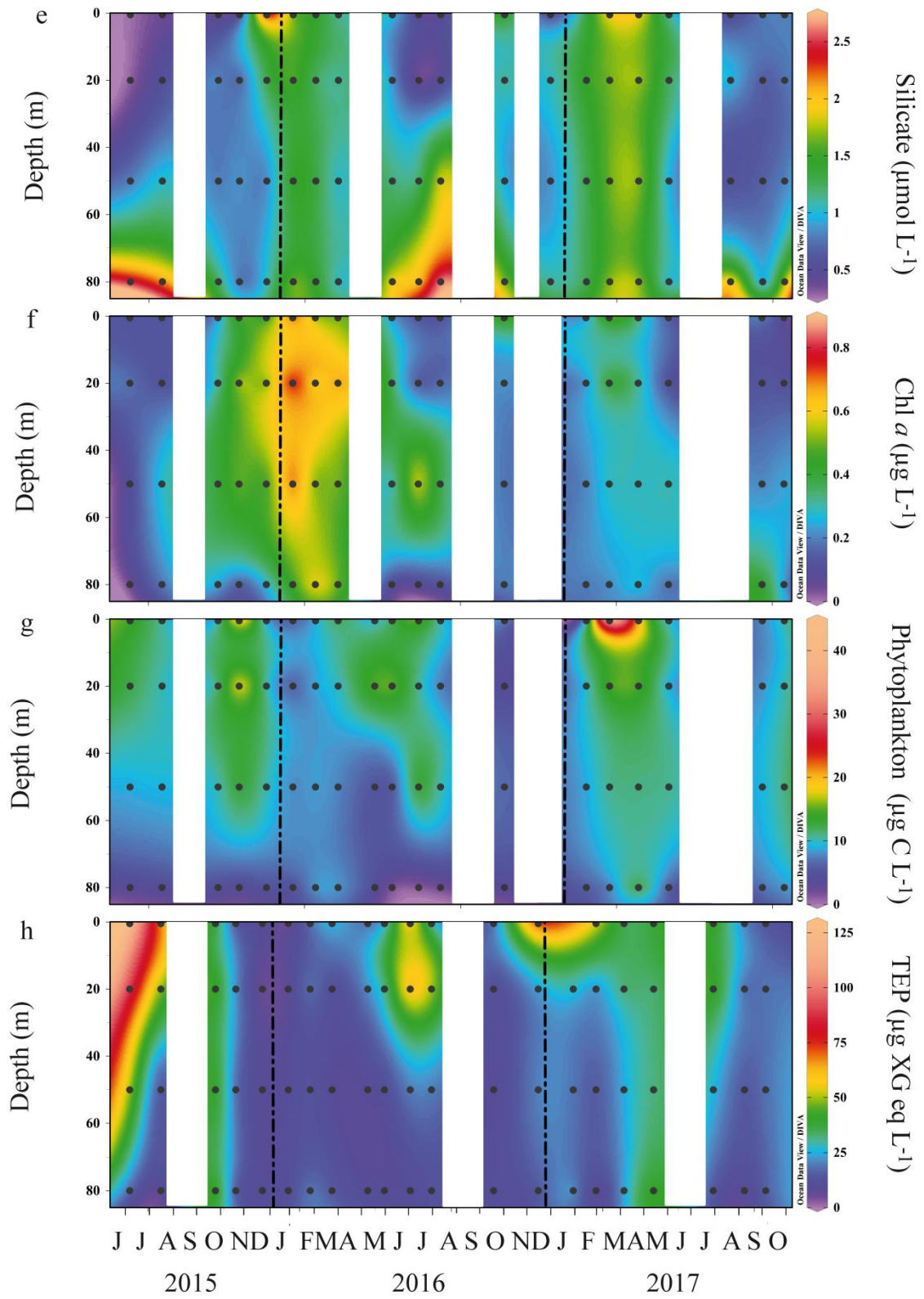
This research was funded by the Spanish Ministry of Economy and Competitiveness through projects PEGASO, BIOGAPS and MIFASOL II. M.Z. was supported by a FPU predoctoral fellowship (FPU13/04630) from the Spanish Ministry of Education and Culture. The EOS Monitoring Program is supported by the Institut de Ciències del Mar (ICM-CSIC) and the Parc Natural del Montgrí, les Illes Medes i el Baix Ter (Generalitat de Catalunya). We would like to thank all the Blanes and Medes team, especially Clara Cardelús, Vanessa Balagué, Ángel López, Irene Forn, Raquel Gutiérrez, Carolina Antequera, Mara Abad, Josep Pascual and Anselm, for their organization, sampling efforts and variable measurements. We also want to thank Maria Castellví and Idaira Santos for helping with TEP and CSP measurements and Jon Roa, Alexandra Loginova, Sonja Endres, Judith Piontek, Katja Lass, Ruth Flerus, Tania Klüver, Marie Massmig and Birthe Zancker for technical support. We also thank the scientists and technicians on board the RV “García del Cid” during the MIFASOL II cruise by providing data.

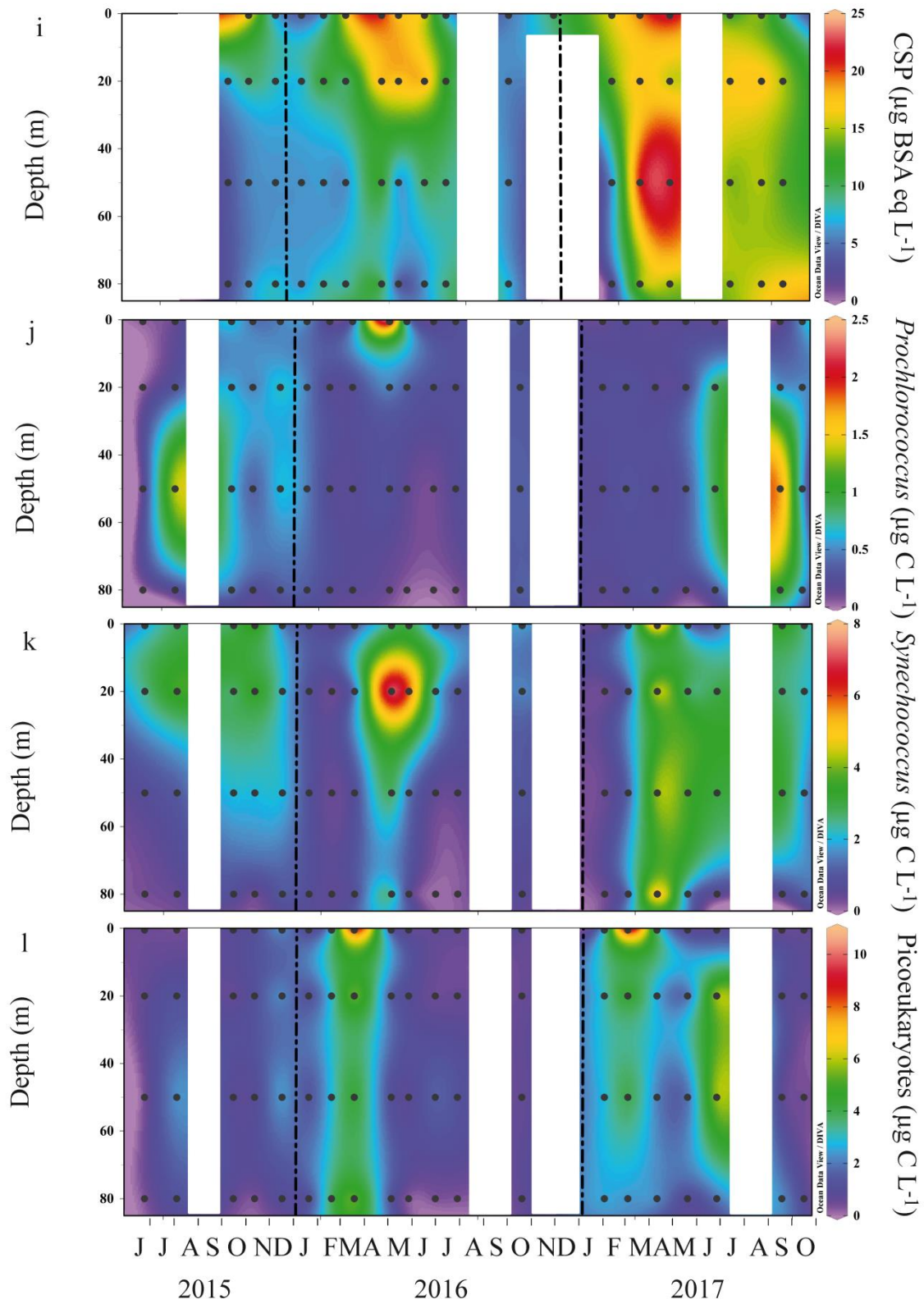


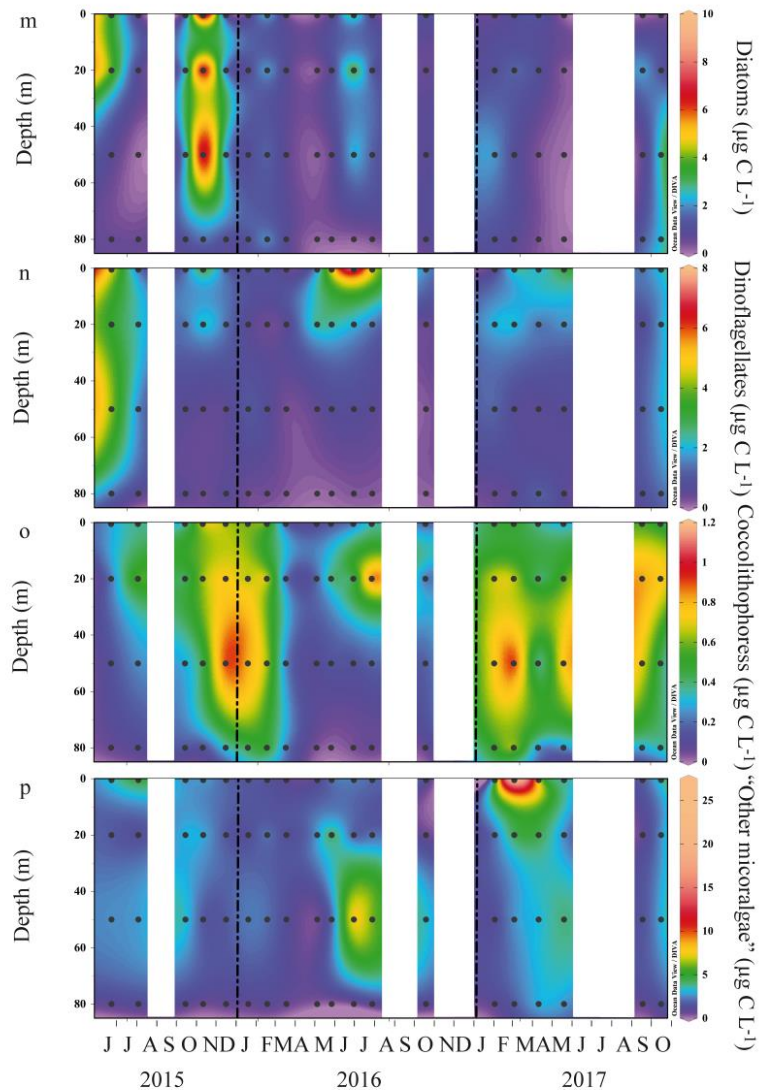
### 3.6 Supplementary material

#### 3.6.1 Supplementary Figures

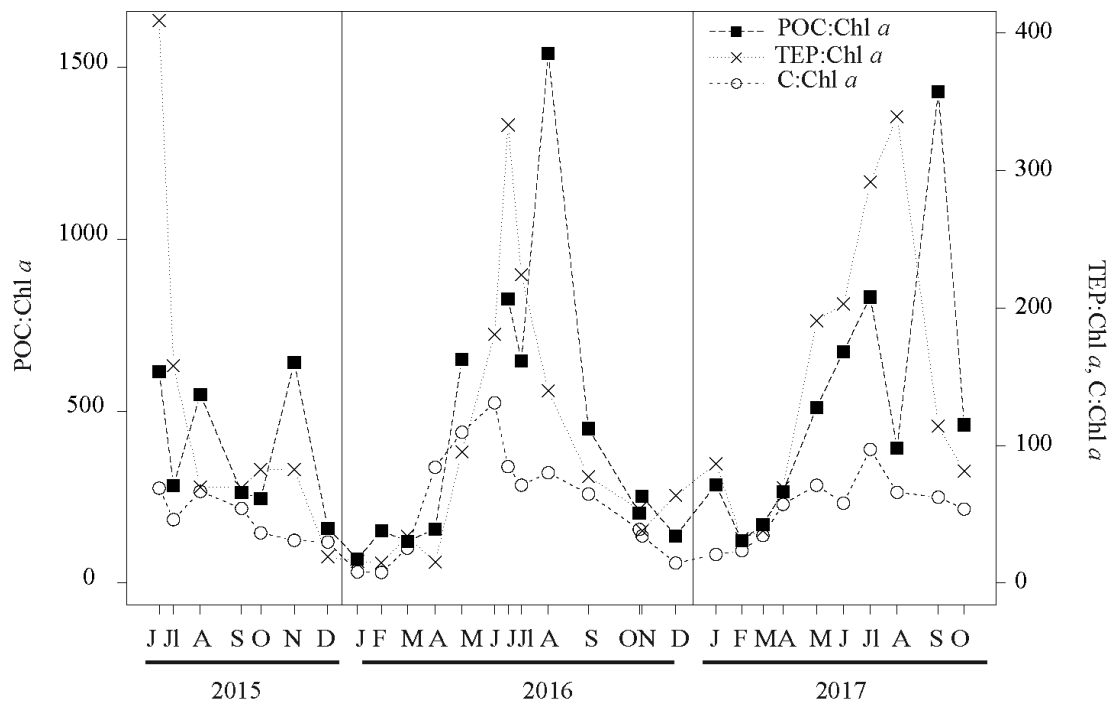




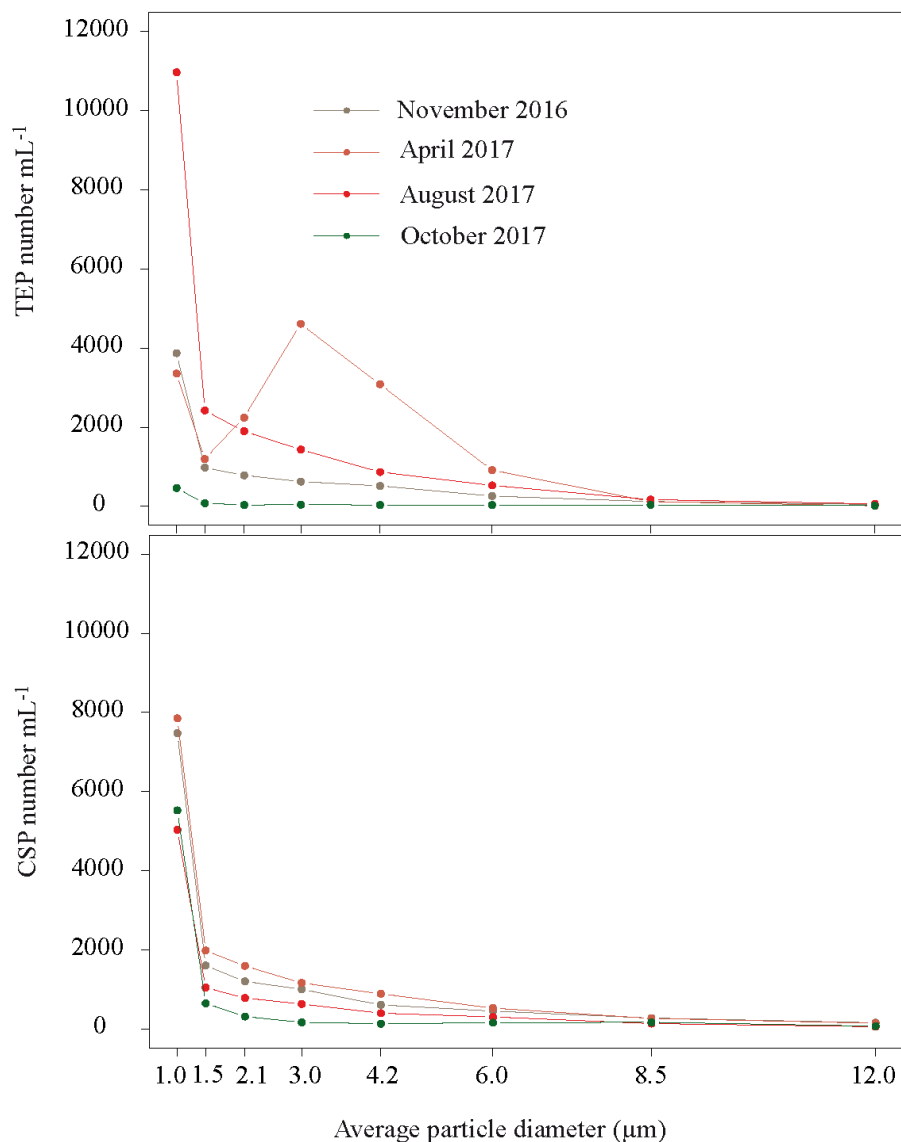




**Supplementary Figure S3.1:** Water column distribution of a) temperature, b) salinity, nitrate, phosphate, silicate, chlorophyll *a* (Chl *a*), phytoplankton biomass, transparent exopolymer particles (TEP), Coomassie stainable particles (CSP), *Prochlorococcus*, *Synechococcus* and picoeukaryotes, diatoms and dinoflagellates biomasses, coccolithophores and “other microalgae” biomasses, from June 2017 to October 2017. The black dots represent sampling points. Blank spaces represent periods when the weather conditions did not allow sampling. The plots were drawn using the software Ocean Data View Schlitzer 2017.



**Supplementary Figure S3.2:** Values of POC:Chl *a*, TEP:Chl *a* and C:Chl *a* over the study in BBMO. Time scale is in Julian days, starting on 1 June 2015. Every tick indicates the sampling month. See Figure 2 for abbreviations.



**Supplementary Figure S3.3:** Size distribution of TEP (upper panel) and CSP (lower panel) (number mL<sup>-1</sup>) obtained with the microscopic method for four samplings in BBMO. Numbers of particles are binned by their mean diameter: those ranging 0-1.3 μm are grouped as 1.0 μm, those ranging 1.3-1.8 μm as 1.5 μm, 1.8-2.5 μm as 2.1 μm, 2.5-3.5 μm as 3.0 μm, 3.5-5.0 μm as 4.2 μm, 5.0-7.0 μm as 6.0 μm, 7.0-10.0 μm as 8.5 μm, and 10.0-14.0 μm as 12.0 μm. In November 2016, total area of TEP and CSP averaged  $14 \pm 12$  and  $38 \pm 5$  mm<sup>2</sup> L<sup>-1</sup>, respectively. In April 2017 they averaged  $41 \pm 12$  and  $42 \pm 10$  mm<sup>2</sup> L<sup>-1</sup>, respectively. In August 2017, they averaged  $25 \pm 7$  and  $19 \pm 4$  mm<sup>2</sup> L<sup>-1</sup>, respectively. In October 2017, they averaged,  $6 \pm 3$  and  $16 \pm 1$  mm<sup>2</sup> L<sup>-1</sup>, respectively.

# Chapter 4



## **Distribution of transparent exopolymer particles (TEP) and Coomassie stainable particles (CSP) in the Southern Ocean around Antarctica**

*Marina Zamanillo, Eva Ortega-Retuerta, Charlotte Robinson, Pablo Rodríguez-Ros, Carolina Cisternas-Novoa, Anja Engel and Rafel Simó*







**Abstract**

Transparent exopolymer particles (TEP) and Coomassie stainable particles (CSP) are organic particles that play an important role in ocean biogeochemistry. Since the Southern Ocean stands out by its ability to sequester anthropogenic CO<sub>2</sub>, there is a need to understand the role that these particles play in this process and predict their distribution around the Southern Ocean. In addition, whether these particles are the same or not remains uncertain. Here we have measured, for the first time, TEP and CSP concentrations simultaneously over an entire season around Antarctica, from December 2016 to March 2017, in both the horizontal and vertical scale. In addition, prokaryotic heterotrophic abundance, Chl *a* and other pigments were measured in parallel to study the controlling variables of TEP and CSP distribution. TEP and CSP were weakly dependent ( $R^2 = 0.14$ ), suggesting to be different types of particles, and phytoplankton were the main biological driver of these particles. TEP concentrations in the entire transect ranged from below detection limit to 201.8  $\mu\text{g XG eq L}^{-1}$ , and averaged  $34.0 \pm 28.8 \mu\text{g XG eq L}^{-1}$ , and their production was spread among many phytoplankton groups. CSP concentrations ranged between 0.3 and 52.2  $\mu\text{g BSA eq L}^{-1}$ , and averaged  $21.9 \pm 10.7 \mu\text{g BSA eq L}^{-1}$ , being diatoms their main producers. Our study also suggests that phytoplankton mortality favoured the production of both types of particles.



## 4.1 Introduction

Transparent exopolymer particles (TEP) and Coomassie stainable particles (CSP) are gel-like exopolymer particles that have been increasingly studied in the last decades because of their role in ocean biogeochemistry. They comprise the fraction of the natural organic matter present in the ocean that is retained on 0.4  $\mu\text{m}$  polycarbonate filters and is stained with Alcian blue in the case of TEP, (Alldredge et al., 1993; Passow and Alldredge, 1995) and with Coomassie brilliant blue for CSP (Long and Azam, 1996). Their relevance lies in their special properties and characteristics. TEP increase the biological carbon pump efficiency via two mechanisms: they account for an important fraction of marine primary production, estimated to be 5-10 % (Mari et al., 2017), and they favour the aggregation of particles and their subsequent sinking into the deep ocean (Engel et al., 2004b; Burd and Jackson, 2009). In addition, both particle types have been found enriched in the sea surface microlayer. Organic matter accumulated in the surface microlayer can influence air-sea gas exchanges (Calleja et al., 2009; Jenkinson et al., 2018) and be released to the atmosphere as aerosols (Aller et al., 2005; Aller et al., 2017) that affect the Earth's radiative budget (Brooks and Thornton, 2018).

The Southern Ocean (SO) is thought to sequester a large fraction of the anthropogenic  $\text{CO}_2$  (Frölicher et al., 2015), especially due to the high solubility of this gas in cold waters, and to the relatively high export of particulate organic carbon in the high latitudes of this ocean (Boyd and Trull, 2007; Marinov et al., 2008). Understanding the role that TEP and CSP play in the Southern Ocean and the prediction of their distribution should improve our ability to predict the magnitude of the biological carbon pump and the future dynamics of atmospheric  $\text{CO}_2$ . However, previous studies of TEP in the Southern Ocean are limited to the Antarctic Peninsula (Passow et al., 1995b; Corzo et al., 2005; Ortega-Retuerta et al., 2009b; Zamanillo et al., 2019b), South Georgia (Zamanillo et al., 2019b) and the Ross Sea (Hong et al., 1997), and there are no previous studies of CSP. In the present study we provide the first simultaneous distribution of CSP and TEP, in both the horizontal and vertical scales, in the Southern Ocean, all around Antarctica. The aims of the study were: (a) to elucidate whether both particle types present similar trends across the horizontal and vertical scales, and (b) to identify the main planktonic drivers of TEP and CSP distributions.

## 4.2 Material and methods

### 4.2.1 Study site and sampling

Sampling was performed during the Antarctic Circumnavigation Expedition (ACE) across the Southern Ocean, on board the Russian RV *Akademik Threshnikov* throughout an entire austral summer, from 23<sup>rd</sup> December 2016 to 17<sup>th</sup> March 2017. A total of 182 sampling stations were conducted along a circular transit around Antarctica, divided in three legs: 1) from Cape Town (South Africa) to Hobart (Australia); 2) from Hobart to Punta Arenas (Chile); 3) From Punta Arenas to Cape Town (Fig. 1).

Seawater surface samples (5 m) were collected four times a day (00:00, 06:00, 12:00 and 18:00 local time (LT)) from the ship's underway pump. In addition, vertical profiles (6 depths, generally from 5 to 100-150 m) were sampled from 19 CTD casts using a SBE 911 Plus attached to a rosette of 24 12-L PVC Niskin bottles.

### 4.2.2 Chemical and biological analyses

#### 4.2.3.1 Particulate organic matter (TEP and CSP)

TEP concentration was determined by spectrophotometry following Passow and Alldredge (1995). Duplicate samples (150-300 mL) were filtered through 25 mm diameter 0.4  $\mu\text{m}$  pore size Polycarbonate filters (DHI) using a constant low filtration pressure ( $\sim 150$  mmHg). The samples were immediately stained with 500  $\mu\text{L}$  of Alcian blue solution (0.02 %, pH 2.5) for 5 s and rinsed with Milli-Q water. Duplicate blanks (empty stained filters) were prepared at every station. The filters were stored frozen until further processing in the laboratory (within 5-8 months). All sample and blank filters were soaked in 5 mL of 80 % sulfuric acid and shaken intermittently for 3 h. The samples were then measured spectrophotometrically at 787 nm (Varian Cary spectrophotometer). The Alcian blue dye solution calibration was done in January 2017 using a standard solution of Xanthan Gum (XG). The absorbance values of filter blanks did not change substantially between batches of samples, suggesting stability in the staining capacity of the Alcian blue solution throughout the cruise. The detection limit was 0.04 absorbance units and the mean range between duplicates was 15.7%.

CSP concentration was determined by spectrophotometry following (Cisternas-Novoa et al., 2014). Duplicate samples (150-300 mL) were filtered through 25 mm diameter

0.4  $\mu\text{m}$  pore size Polycarbonate filters (Whatman) using a constant low filtration pressure ( $\sim 150$  mmHg). The samples were immediately stained with 700  $\mu\text{L}$  of working Coomassie Brilliant Blue (CBB-G 250) solution (0.04 %, pH 7.4), which was prepared with 0.2- $\mu\text{m}$  filtered sample seawater (one working solution per day) for 30 s, and rinsed with Milli-Q water three times. The filters were stored frozen until further processing in the laboratory (within 1-4 months). Duplicate blanks (empty filters stained as stated earlier) were prepared at every station. Both the sample and blank filters were soaked in 4 mL of extraction solution (3 % SDS in 50 % isopropyl alcohol; Ball 1986) and the tube sonicated in a water bath (50-60 kHz) for 2 h at 37° C. The filters were shaken intermittently during this period. The samples were then measured spectrophotometrically at 615 nm (Shimadzu UV-Vis spectrophotometer UV120). The CBB dye solution calibrations were done in May 2017. A total of three calibrations were conducted, using three sea waters of different salinities (filtered by 0.2- $\mu\text{m}$ ) to prepare the working CBB solution. These waters were collected during the cruise (stations UW 78,143 and 162), whose salinities ranged 31.8-34.6. The f-values, calculated as 1/slope of the calibration regressions, ranged 93.3-97.1, so we decided to use the average f-value to all samples along the cruise. The detection limit was 0.045 absorbance units and the mean range between duplicates was 15.6 %.

#### **4.2.3.2 Chl *a***

Seawater (up to 2 L) was filtered through 25 mm diameter glass filters (Whatman GF/F) under low vacuum pressure and remained frozen ( $-80$  °C) until further processing on-board the ship. Pigment extraction was done at 4 °C in the dark for 24 h with 90 % acetone. Fluorescence of extracts was measured with a calibrated AU-10 Turner Designs fluorometer (Yentsch and Menzel, 1963).

#### **4.2.3.3 Prokaryotic heterotrophic abundance (PHA)**

Prokaryotic heterotrophic abundance (PHA) was determined by flow cytometry. Samples were fixed with 1% paraformaldehyde plus 0.05 % glutaraldehyde (final concentrations), for 15 min at room temperature and stored frozen at  $-80$  °C. Samples were analyzed 12 months after the cruise end, using a Cube 8 flow cytometer equipped with a 50 mW argon-ion laser emitting at 488 nm. Before analyses, samples were unfrozen, stained with SYBRGreen I (Molecular Probes) (1:100 vol:vol) and left in the dark for about 15 min. Samples were run at a low flow rate (approx. 24  $\mu\text{L min}^{-1}$ ) for 2

min with Milli-Q water as a sheath fluid. Heterotrophic prokaryotes were detected by their signature in a plot of side scatter versus FL1 (green fluorescence) and they were expressed in cells mL<sup>-1</sup>.

#### **4.2.3.4 HPLC pigment analysis**

HPLC was used to determine pigment composition, following Van Heukelem and Thomas (2001) and Ras et al. (2007). Twenty-five pigments were identified between 450 and 770 nm. Pigments were also used as indicators of phytoplankton photoacclimation. Diadinoxanthin (Ddx) is the main light-protecting pigment in diatoms, dinoflagellates, haptophytes and pelagophytes. The Ddx:LHC ratio, between Ddx and the sum of the main light-harvesting carotenoids (LHC: fucoxanthin, 19'-butanoyloxyfucoxanthin, 19'-hexanoyloxyfucoxanthin and peridinin) was measured, since it varies with the exposure of phytoplankton to underwater solar radiation (Higgins et al., 2011; Nunes et al., 2019).

#### **4.2.4 Statistical analyses**

We performed pairwise Spearman correlation analyses to test for covariations between TEP and CSP concentrations with other environmental and biological variables. Bivariate analyses (ordinary least squares, OLS) between TEP and CSP concentrations with other biological and environmental were also conducted to explore the potential controlling variables of TEP and CSP distribution across the transect. We log transformed data to fulfil the requirements of parametric tests. Statistical tests, calculations and illustration were performed with Microsoft Office Excel 2010, Ocean Data View software (version 4) (Schlitzer and 2017) and R programming software (version 3.5.1) (RStudio Team, 2016).

### **4.3 Results**

#### **4.3.1 TEP and CSP distribution across the Southern Ocean**

TEP and CSP presented positively correlated distributions in surface waters (5 m) ( $r=0.39$ ,  $p<0.01$ ). Nonetheless, remarkable differences in these distributions (Table 4.2 and Figs. 4.1 and 4.2) suggested that they were governed by different sources and controlling processes in the different regions. Surface TEP concentrations ranged from

below detection limit (bdl) to 201.8  $\mu\text{g XG eq L}^{-1}$  (average  $34.0 \pm 28.8 \mu\text{g XG eq L}^{-1}$ ; Table 4.1), and the maximum concentrations were found in coastal Antarctica next to Mertz Glacier and Siple Island (Figs. 4.1 and 4.2). Surface CSP concentrations ranged from 0.3 to 52.2  $\mu\text{g BSA eq L}^{-1}$  (average  $21.9 \pm 10.7 \mu\text{g BSA eq L}^{-1}$ ; Table 4.1), and maximum concentrations were found next to Mertz Glacier and Siple Island, but also in the Drake Passage and South Georgia areas. The surface Chl *a* concentration varied widely, from 0.15 to 8.71  $\mu\text{g L}^{-1}$  ( $1.16 \pm 1.46 \mu\text{g L}^{-1}$ ; Table 4.1), with the highest values next to Mertz Glacier and Siple Island, in a region influenced by the Malvinas current and north of Heard and McDonald Islands (Fig. 4.1). CSP:Chl *a* ratios also varied widely, between 0.5 and 136.1  $\mu\text{g BSA eq } \mu\text{g}^{-1}$  ( $35.7 \pm 25.2 \mu\text{g BSA eq } \mu\text{g}^{-1}$ ; Table 4.1), with the highest values at the first half of the second leg, before Mertz glacier, and west Antarctic Peninsula (Figs. 4.2 and 4.3). The sea surface temperature during the cruise ranged between -0.5 and 13.9 °C ( $4.8 \pm 3.4 \text{ }^\circ\text{C}$ ; Table 4.1). Surface prokaryotic heterotrophic abundance ranged from  $1.08 \times 10^5$  to  $3.21 \times 10^6 \text{ cells mL}^{-1}$  ( $6.6 \pm 4.5 \times 10^5 \text{ cells mL}^{-1}$ ) (Table 4.1). TEP:Chl *a* ratios varied widely from 5.1 to 141.5  $\mu\text{g XG eq } \mu\text{g}^{-1}$  (average  $48.4 \pm 34.0 \mu\text{g XG eq } \mu\text{g}^{-1}$ ), with the highest values at the end of leg 1, south of the west Australian Current (Figs. 4.2 and 4.3). In the vertical scale, TEP and CSP broadly decreased with depth, but they were not generally coupled (Fig. 4.4). A peak of TEP was usually found above the deep chlorophyll maximum (DCM) (4 out of 6), whereas CSP were usually higher at the DCM or quite homogeneous around DCM .

**Table 4.1.** Average and standard deviation of temperature, transparent exopolymer particles (TEP), Coomassie stainable particles (CSP), chlorophyll *a* (Chl *a*) and prokaryotic heterotrophic abundance (PHA) in the surface (5 m) of ACE cruise.

	Average $\pm$ SD (ranges)	n
Temperature ( $^\circ\text{C}$ )	$4.8 \pm 3.4$ (-0.5 – 13.9)	121
TEP ( $\mu\text{g XG eq L}^{-1}$ )	$34.0 \pm 28.8$ (bdl – 201.8)	181
CSP ( $\mu\text{g BSA eq L}^{-1}$ )	$21.9 \pm 10.7$ (0.3 – 52.2)	181
Chl <i>a</i> ( $\mu\text{g L}^{-1}$ )	$1.16 \pm 1.46$ (0.15 – 8.71)	145
PHA ( $\text{cell mL}^{-1}$ )	$6.6 \pm 4.5 \times 10^5$	121
TEP:Chl <i>a</i> ( $\mu\text{g XG eq } \mu\text{g}^{-1}$ )	$48.4 \pm 34.0$ (5.1 – 141.5)	145
CSP:Chl <i>a</i> ( $\mu\text{g BSA eq } \mu\text{g}^{-1}$ )	$35.7 \pm 25.2$ (0.5 – 136.1)	145



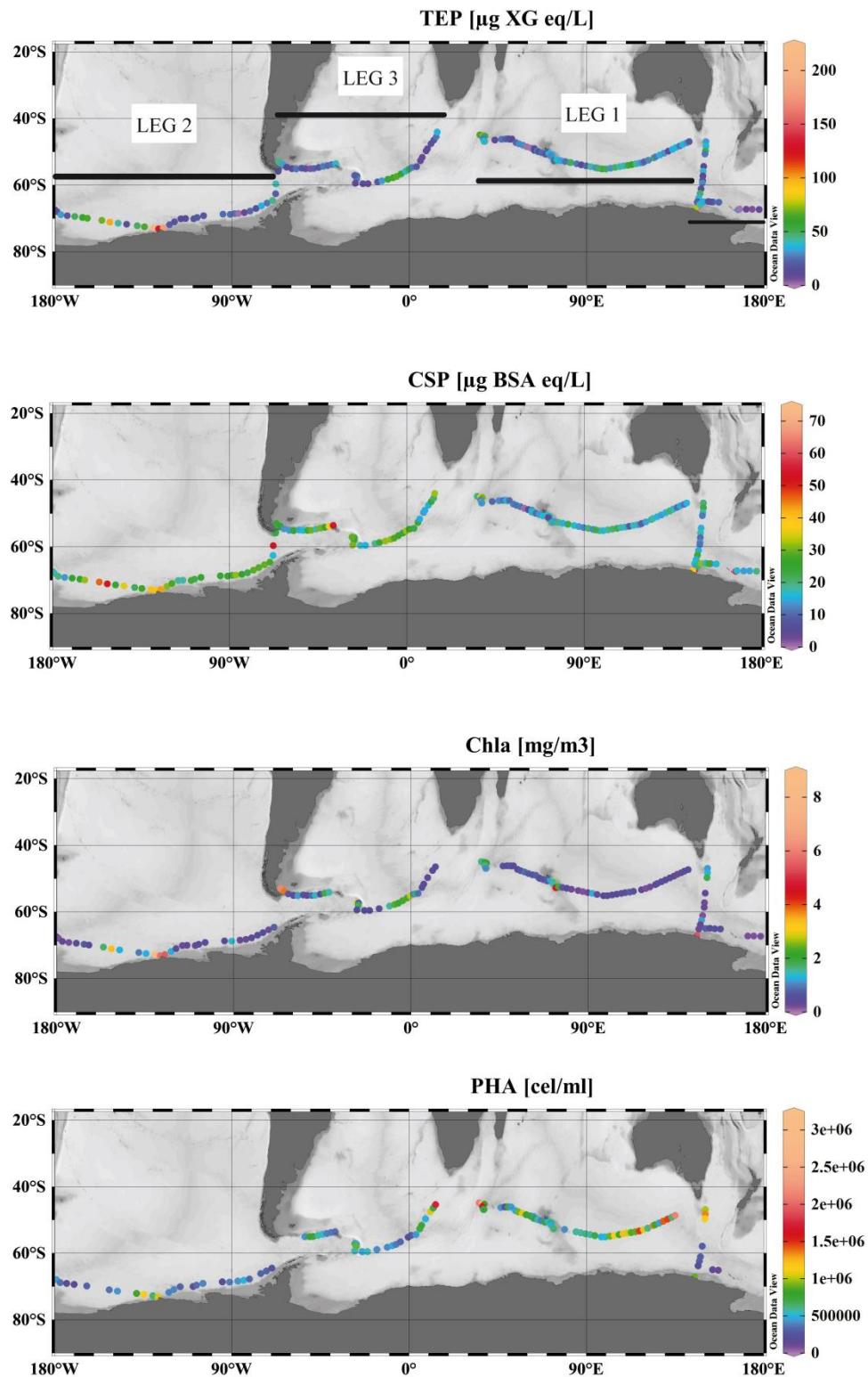


**Figure 4.1.** Concentration of transparent exopolymer particles (TEP) ( $\mu\text{g XG eq L}^{-1}$ ) (upper panel), Coomassie stainable particles (CSP) ( $\mu\text{g BSA eq L}^{-1}$ ) (middle panel) and Chl *a* ( $\text{mg m}^{-3}$ ) (lower panel) in surface waters (5 m) of the ACE cruise, sampled from 23<sup>rd</sup> December 2016 to 17<sup>th</sup> March 2017 in the Southern Ocean. Values below detection limit are set to 0.

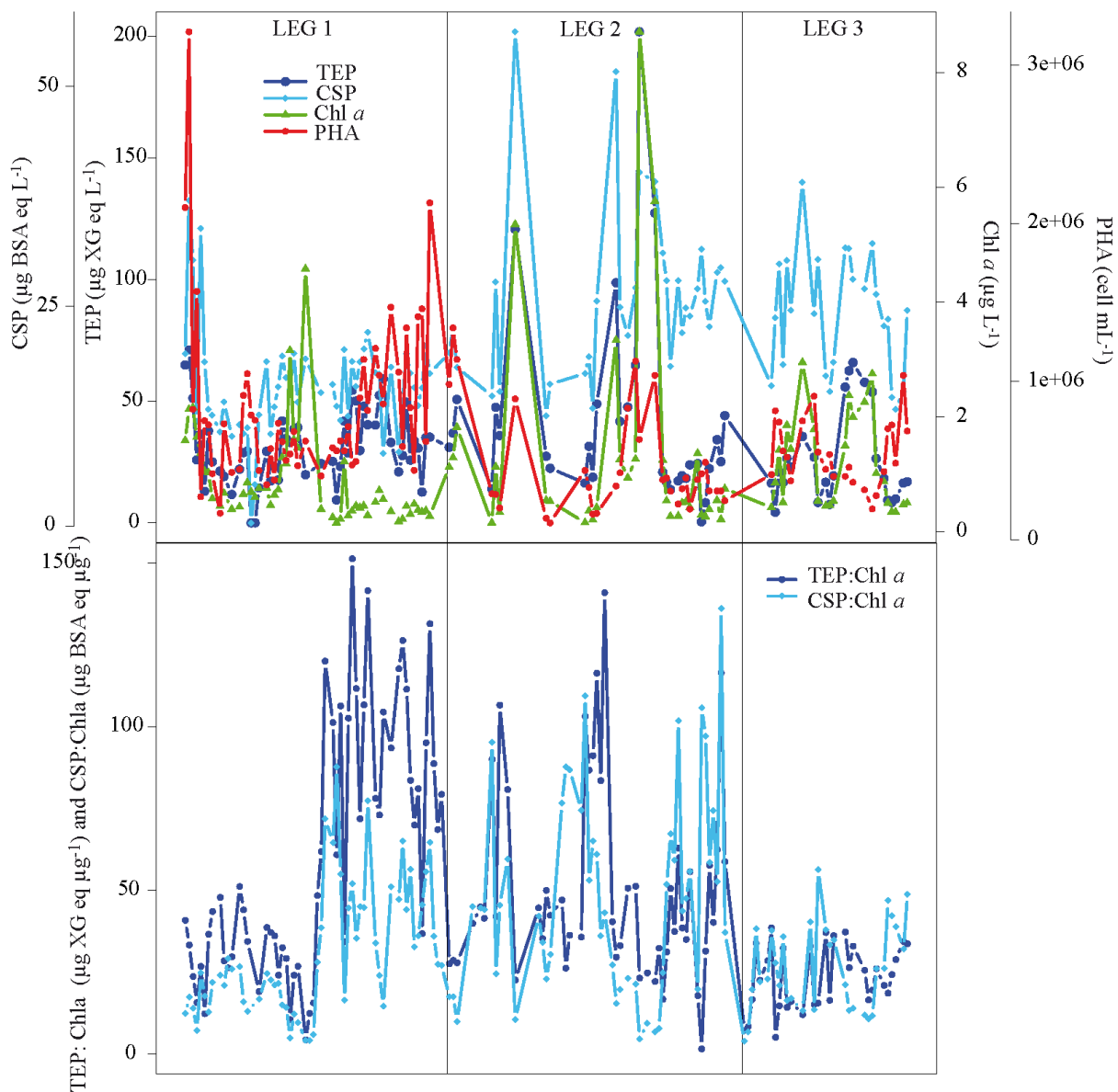


**Figure 4.2.** a) Variations of TEP ( $\mu\text{g XG eq L}^{-1}$ ), CSP ( $\mu\text{g BSA eq L}^{-1}$ ) and Chl *a* ( $\mu\text{g L}^{-1}$ ) throughout the ACE cruise. Values below detection limit are set to 0. Vertical lines separate legs. b) Variations of TEP:Chl *a* and CSP:Chl *a*.

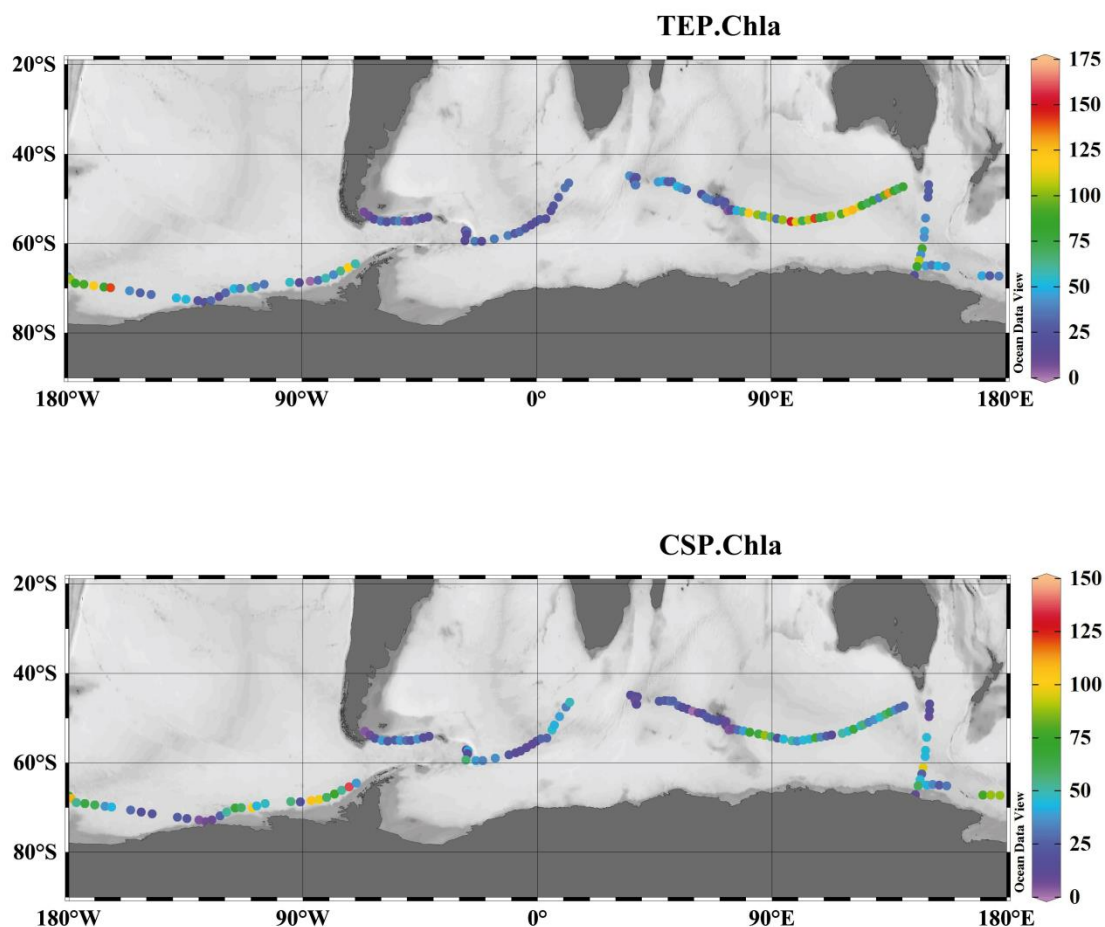


**Figure 4.3.** TEP:Chl *a* ( $\mu\text{g XG eq } \mu\text{g}^{-1}$ ) (upper panel) and CSP:Chl *a* ( $\mu\text{g BSA eq } \mu\text{g}^{-1}$ ) (lower panel) ratios and Chl *a* ( $\text{mg m}^{-3}$ ) (lower panel) in surface waters (5 m) of the ACE cruise, sampled from 23<sup>rd</sup> December 2016 to 17<sup>th</sup> March 2017 in the Southern Ocean. See Figure 4.1 for abbreviations.

#### 4.3.2 Relationship of TEP and CSP with other biological variables

TEP were significantly and positively correlated to Chl *a* ( $r= 0.58$ ,  $p<0.001$ ,  $n=145$ ; Table 4.2). The regression equation for log converted TEP vs Chl *a* was  $\log \text{ TEP}= 1.49 (\pm 0.02) + 0.50 (\pm 0.06) \times \log \text{ Chl } a$  ( $R^2= 0.36$ ,  $p<0.001$ ,  $n= 145$ ; Table 4.3). TEP were also correlated with Spearman coefficient higher than 0.40 to the following pigments; zeaxanthin, alloxanthin, fucoxanthin, peridinin, 19'-hexanoyloxyfucoxanthin, chlorophyllide *a* and phaeophorbid *a* (Table 4.2). CSP were also significant and positively correlated to Chl *a*, but less than TEP ( $r= 0.49$ ,  $p<0.001$ ,  $n= 145$ ; Table 4.2), and to the pigments fucoxanthin ( $r=0.38$ ,  $n= 93$ ), chlorophyllide *a* ( $r= 0.61$ ,  $n= 93$ ) and phaeophorbid *a* ( $r= 0.55$ ,  $n=93$ ) (Table 4.2).

**Table 4.2.** Spearman correlations between transparent exopolymer particles (TEP) or Coomassie stainable particle (CSP) concentrations and other biological variables at 5 m during ACE cruise. Values below detection limit are considered as missing values (NA).

Var.	r	p	n		
TEP	Temperature	ns	121		
	CSP	0.39	<0.001	181	
	Chl <i>a</i> ( $\mu\text{g L}^{-1}$ )	0.58	<0.001	145	
	PHA ( $\times 10^3$ cells $\text{mL}^{-1}$ )		ns	121	
	Violaxanthin	0.38	<0.05	93	
	Prasinolaxanthin		ns	93	
	Lutein		ns	93	
	Zeaxanthin	0.44	<0.01	93	
	Alloxanthin	0.50	<0.01	93	
	Fucoxanthin	0.43	<0.001	93	
	19'-butanoyloxyfucoxanthin	0.27	<0.05	93	
	Peridinin	0.49	<0.001	93	
	19'-hexanoyloxyfucoxanthin	0.41	<0.001	93	
	Chlorophyllide <i>a</i>	0.71	<0.001	93	
	Phaeophorbid <i>a</i>	0.46	<0.001	93	
	Ddx:LHC		ns	93	
	CSP	Temperature	-0.43	<0.001	121
		TEP	0.39	<0.001	181
		Chl <i>a</i> ( $\mu\text{g L}^{-1}$ )	0.49	<0.001	145
PHA ( $\times 10^3$ cells $\text{mL}^{-1}$ )		-0.20	<0.05	121	
Violaxanthin			ns	93	
Prasinolaxanthin			ns	93	
Lutein			ns	93	
Zeaxanthin			ns	93	
Alloxanthin			ns	93	
Fucoxanthin		0.38	<0.001	93	
19'-butanoyloxyfucoxanthin			ns	93	
Peridinin			ns	93	
19'-hexanoyloxyfucoxanthin			ns	93	
Chlorophyllide <i>a</i>		0.61	<0.001	93	
Phaeophorbid <i>a</i>		0.55	<0.001	93	
Ddx:LHC			ns	93	

r: Spearman's correlation coefficient; p: level of significance; n: sample size

## 4.4 Discussion

### 4.4.1 TEP and CSP concentrations in the Southern Ocean

This is the first study that reports CSP concentrations in the SO. In addition, it is also the first time that both TEP and CSP are measured across the SO around Antarctica in one same season. Previous TEP studies in the SO were limited to the Antarctic Peninsula (Passow et al., 1995b; Corzo et al., 2005; Ortega-Retuerta et al., 2009b; Zamanillo et al., 2019b), South Georgia (Zamanillo et al., 2019b), the Drake Passage (Corzo et al., 2005) and the Ross Sea (Hong et al., 1997) (see thesis chapter 2). Despite the fact that TEP and CSP were positively correlated along the cruise ( $r=0.39$ ; Table 4.2), their interdependence was weak and probably driven by the wide range in productivity in the visited regions, and one explained a small fraction of the variance of the other ( $R^2=0.14$ ; Table 4.3). These results indicate that TEP and CSP are different particle types that are produced by different organisms and influenced by different processes. In fact, previous studies already pointed in that direction (Cisternas-Novoa et al., 2015; Thornton et al., 2016; Thornton and Chen, 2017; Zamanillo et al., 2019a).

Our surface TEP concentrations are lower than those found by Zamanillo et al. (2019b) and Hong et al. (1997) in regions of the SO, probably due to lower Chl *a* concentrations, while they are similar to the other SO studies with similar Chl *a* concentrations (Table 4.4). Regarding CSP, the previous field studies have been conducted in the Arctic Ocean (Galgani et al., 2016; Busch et al., 2017), Baltic Sea (Dreshchinskii and Engel, 2017; Cisternas-Novoa et al., 2019), Pacific Ocean (Long and Azam, 1996; Engel and Galgani, 2016; Thornton et al., 2016), Sargasso Sea (Cisternas-Novoa et al., 2015), Arabian Sea (Long and Azam, 1996) and Mediterranean Sea (Zamanillo et al., 2019a), but only three used the spectrophotometric method (Cisternas-Novoa et al., 2015; Cisternas-Novoa et al., 2019; Zamanillo et al., 2019a). Our CSP concentrations were in the same range as in the Baltic Sea, with similar Chl *a* concentrations, whereas CSP concentrations in the Sargasso Sea and the Mediterranean Sea were in the lower range of our study, probably due to their lower Chl *a* concentrations (Table 4.5).

**Table 4.3.** Regression equations and statistics describing the relationship between transparent exopolymer particles (TEP) or Coomassie stainable particles (CSP), and several physical, chemical or biological variables in surface (5 m) of the ACE cruise. All variables were  $\log_{10}$  transformed.

Var.	Ind. var	R <sup>2</sup>	p	Intercept	Slope	n	
TEP	Temperature (K)		ns			121	
	CSP	0.14	<0.001	0.59	0.64	181	
	Chl <i>a</i>	0.36	<0.001	1.49	0.50	145	
	PHA		ns			121	
	Violaxanthin		ns			93	
	Prasincoxanthin		ns			93	
	Lutein		ns			93	
	Zeaxanthin	0.21	<0.01	2.10	0.27	93	
	Alloxanthin	0.22	<0.01	2.16	0.28	93	
	Fucoxanthin	0.17	<0.001	1.69	0.21	93	
	19'-	0.10	<0.01	1.77	1.17	93	
	butanoyloxyfucoxanthin						
	Peridinin	0.14	<0.001	2.11	0.30	93	
	19'-	0.22	<0.001	1.87	0.31	93	
	hexanoyloxyfucoxanthin						
	Chlorophyllide <i>a</i>	0.49	<0.001	2.11	0.35	93	
	Phaeophorbid <i>a</i>	0.16	<0.001	1.81	0.22	93	
	CSP	Temperature (K)	0.07	< 0.01	30.8	-12.10	121
		TEP	0.14	<0.001	0.99	0.22	181
		Chl <i>a</i>	0.17	<0.001	1.31	0.24	145
PHA			ns			121	
Violaxanthin			ns			93	
Prasincoxanthin			ns			93	
Lutein			ns			93	
Zeaxanthin			ns			93	
Alloxanthin			ns			93	
Fucoxanthin		0.08	<0.01	1.40	0.12	93	
19'-			ns			93	
butanoyloxyfucoxanthin							
Peridinin			ns			93	
19'-			ns			93	
hexanoyloxyfucoxanthin							
Chlorophyllide <i>a</i>	0.23	<0.001	1.78	0.28	93		
Phaeophorbid <i>a</i>	0.22	<0.001	1.62	0.21	93		

R<sup>2</sup>: explained variance; p: level of significance; n: sample size

**Table 4.4.** Compilation of published transparent exopolymer particle (TEP) concentrations (mean  $\pm$  SE and ranges;  $\mu\text{g XG eq L}^{-1}$ ), chlorophyll *a* (Chl *a*) concentrations (mean  $\pm$  SE and ranges;  $\mu\text{g L}^{-1}$ ) and TEP:Chl *a* ratios (mean  $\pm$  SE and ranges;  $\mu\text{g XG eq } (\mu\text{g Chl } a)^{-1}$ ) in the Southern Ocean. bdl: below detection limit.

Location	Comments	TEP	Chl <i>a</i>	TEP:Chl <i>a</i>	Reference
Anvers Island	Summer (November 1994-February 1995) 2- 6 m, coastal samples Two blooms observed (Cryptomonads and diatoms)	15 - >500	-	-	Passow et al. (1995)
Kita-no-seto Strait	Mid-January 1994 15 m	26-41 particles mL <sup>-1</sup>	-	-	Marchant et al. (1996)
Ross Sea	Summer (November, December 1994) 0-150 m, <i>Phaeocystis</i> and diatoms bloom	Surface 308 (0-2800)	3.61 (0.27-8.81) (surface)	89.1 (surface)	Hong et al. (1997)
Bransfield Strait	Summer (13 December 1990- 3	56.77 $\pm$ 54.50 (bdl-345.9)	0.98 $\pm$ 0.83 (0.05-4.81)	51.0	Corzo et al. (2005)
Gerlache Strait	January 2000)	38 (0-283)	1.16	32.7	
Drake Passage	0-100 m	35 (0-157)	1.17	29.9	
Antarctic Peninsula (all the study)	Summer (February 2005), 0-200 m	15.4 $\pm$ 10.0 (bdl-48.9)	0.01-5.36	40.9 $\pm$ 157.8 (bdl-1492)	Ortega-Retuerta et al. (2009b)
Bellingshausen Sea		14.3 $\pm$ 9.5 (bdl-33.8)		84.2 $\pm$ 257.5 (bdl-1492)	
Weddell Sea		16.3 $\pm$ 12.5 (bdl-48.9)		9.8 $\pm$ 7.4 (1.2-28.4)	
Bransfield and Gerlache Strait		15.8 $\pm$ 8.9 (bdl-35.8)		15.0 $\pm$ 20.4 (3.0-18.0)	
Southern Ocean (all transect)	Summer (7 January-3 February 2015) 4 m	102.3 $\pm$ 40.4 (39.2- 177.6)	2.36 $\pm$ 1.92 (0.28-8.95)	79.3 $\pm$ 54.9 (10.9-239.0)	Zamanillo et al. (2019b)
South Orkney Islands (NSO)		144.4 $\pm$ 21.7 (97.8-177.6)	1.87 $\pm$ 0.23 (1.58-2.21)	76.7 $\pm$ 10.6 (60.4-97.5)	
southeast of the South Orkney Islands (SSO)		48.1 $\pm$ 6.5 (39.2-63.8)	0.32 $\pm$ 0.06 (0.28-0.45)	153.4 $\pm$ 29.8 (102.5-211.6)	
northwest of South Georgia (NSG)		125.5 $\pm$ 21.1 (93.6-157.4)	4.59 $\pm$ 1.97 (1.92-8.95)	32.3 $\pm$ 15.0 (17.6-70.0)	
west of Anvers Island (WA)		111.6 $\pm$ 13.0 (90.5-125.0)	4.05 $\pm$ 0.48 (3.41-4.91)	28.2 $\pm$ 4.8 (18.4-34.9)	
Whole Southern Ocean	Summer (23 December 2016-17 March 2017)	34.0 $\pm$ 28.8 (bdl-201.8)	1.16 $\pm$ 1.46 (0.15-8.71)	48.4 $\pm$ 34.0 (5.1- 141.5)	This study

**Table 4.5.** Compilation of published Coomassie stainable particles (CSP) concentrations (mean  $\pm$  SE and ranges;  $\mu\text{g BSA eq L}^{-1}$ ), chlorophyll *a* (Chl *a*) concentrations (mean  $\pm$  SE and ranges;  $\mu\text{g L}^{-1}$ ) and CSP:Chl *a* ratios (mean  $\pm$  SE and ranges;  $\mu\text{g BSA eq } (\mu\text{g Chl } a)^{-1}$ ). bdl: below detection limit.

Location	Comments	CSP	Chl <i>a</i>	CSP:Chl <i>a</i>	Reference
Sargasso Sea	February, May, August, November 2012 and May 2013 0-100 m	$3.2 \pm 0.7 - 22.4 \pm 0.4$	0.25-0.75 <sup>a</sup>	-	Cisternas-Novoa et al. (2015)
Baltic Sea	3-19 June 2015 1 and 10 m	15-56 <sup>a</sup>	1.2-1.7	-	Cisternas-Novoa et al. (2019)
Mediterranean Sea	October 2015- October 2017 (time-series study) 0.5 m	$4.5-24.8 (12.4 \pm 6.0)$ <sup>b</sup>	$0.13-1.52 (0.4 \pm 0.3)$ <sup>b</sup>	$4.8-163.2 (45.6 \pm 35.7)$ <sup>b</sup>	Zamanillo et al. (2019); in progress
Southern Ocean	23 December 2016- 17 March 2017 4 m	$0.3 - 52.2 (21.9 \pm 10.7)$	$0.15 - 8.71 (1.16 \pm 1.46)$	$0.5 - 136.1 (35.7 \pm 25.2)$	This study

<sup>a</sup> Extracted from graphs; <sup>b</sup> personally communicated



Concerning the vertical distribution of TEP and CSP, the differences between the two particle types (Fig. 4.4) is in accordance with previous studies. In the Sargasso Sea, Cisternas-Novoa et al. (2015) found that TEP were more abundant in the upper 100 m and decreased with depth, with the highest concentrations in the shallowest sample, usually at 50 m. CSP were maximum between 70 and 100 m, coinciding with the Chl *a* fluorescence maximum. In the Baltic, Cisternas-Novoa et al. (2019) found vertical covariation of TEP and CSP in one sampling station, and differences in another. At both stations the highest concentrations occurred in the upper 10 m. Zamanillo et al. (2019a) did not find covariations between TEP and CSP in the vertical profiles during a time-series study in the Mediterranean Sea.

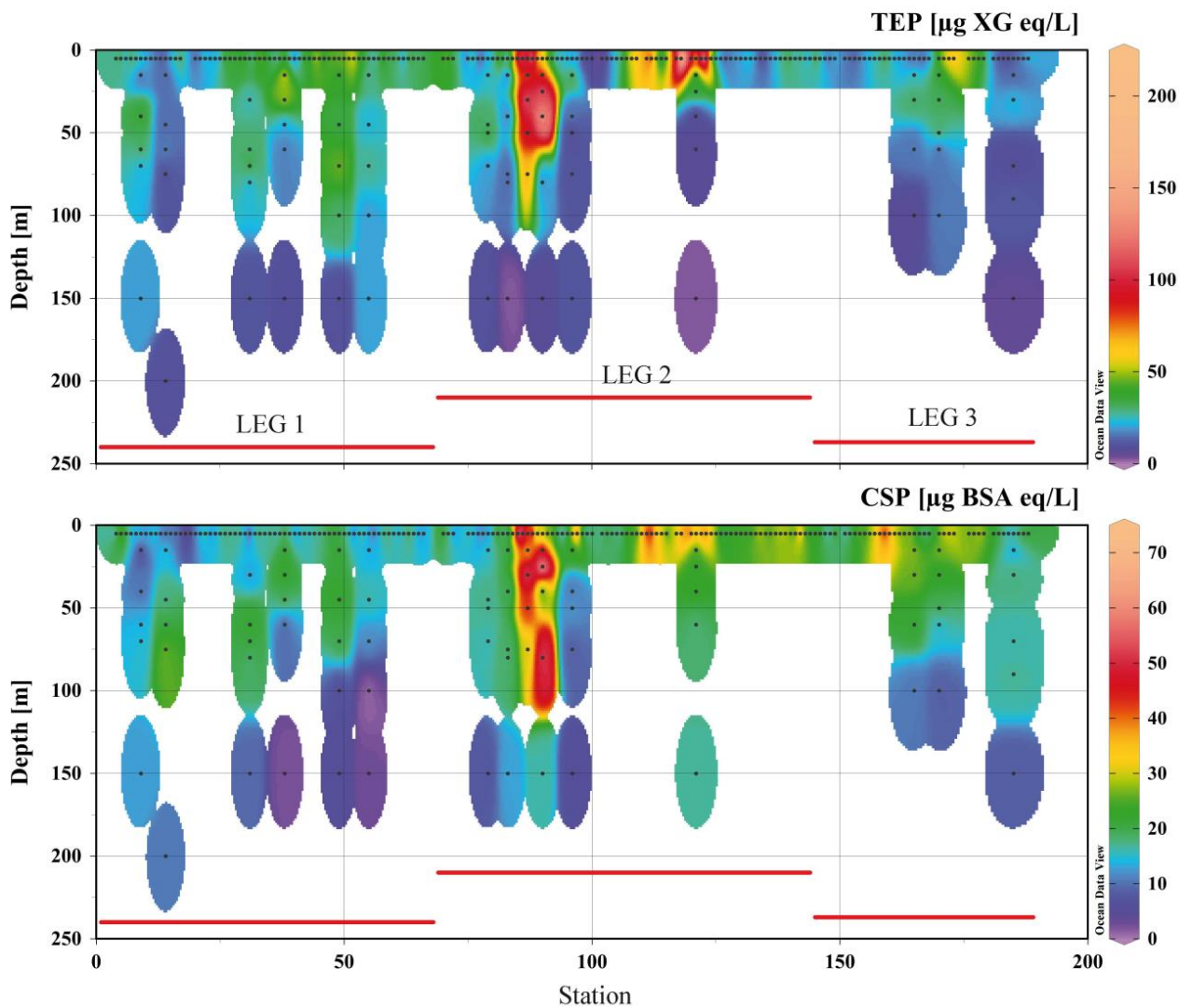


**Figure 4.4.** Water column distribution of transparent exopolymer particles (TEP) and Coomassie stainable particles (CSP). The black dots represent sampling points. The plots were drawn using the software Ocean Data View Schlitzer 2017.

#### 4.4.2 Main drivers of TEP and CSP distribution in the surface Southern Ocean

Of the two biological candidates to drive TEP and CSP concentration distributions, phytoplankton and bacterioplankton, the former seem to be the main driver, since a significant positive correlation was found with Chl *a* ( $r= 0.58$  for TEP and  $r= 0.49$  for CSP), and not with PHA (Table 4.2). The fact that TEP were more closely related to Chl *a* than CSP contrasts with previous studies where CSP presented a better relationship with Chl *a* or phytoplankton biomass (Cisternas-Novoa et al., 2015; Zamanillo et al., 2019a). The slope of the log-converted TEP:Chl *a* relationship for the entire study ( $\beta = 0.50 (\pm 0.06)$ ; Fig. 4.5) was lower than those found by Corzo et al. (2005) in the Gerlache Strait and Hong et al. (1997), and higher than those found by Zamanillo et al. (2019b), Ortega-Retuerta et al. (2009b) and Corzo et al. (2005) in the Antarctic Peninsula and South Georgia.

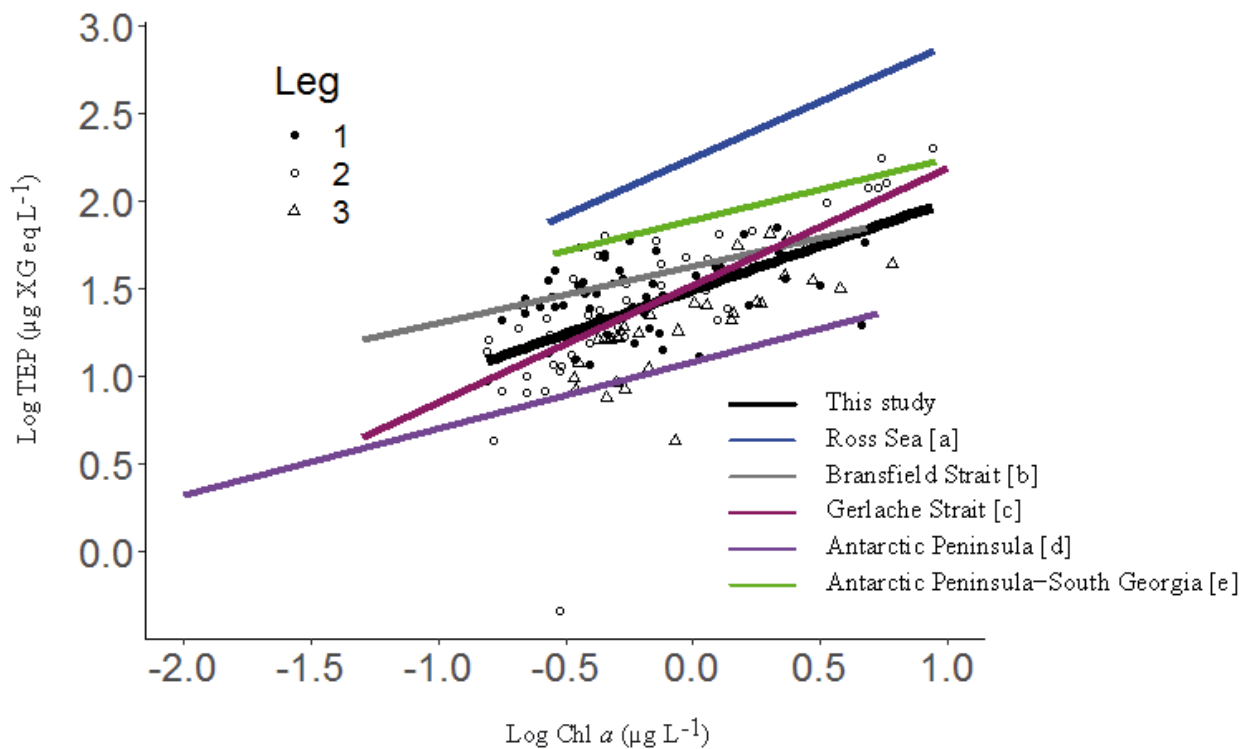


**Figure 4.5.** Log-log relationship between transparent exopolymer particle (TEP) and chlorophyll *a* (Chl *a*) concentrations from the ACE cruise, with the linear regression line (regression equation in the text). The three legs are distinguished by markers: Leg 1 (filled circles), Leg 2 (empty circles), Leg 3 (empty triangles). Regression lines from the literature in the Southern Ocean are also shown for comparison.  $\alpha$  and  $\beta$  indicate the intercept and the slope, respectively;  $\log \text{TEP} (\mu\text{g XG eq. L}^{-1}) = \alpha + \beta \times \log \text{Chl } a (\mu\text{g L}^{-1})$ ; [a]  $\alpha = 2.25$  and  $\beta = 0.65$ , (Hong et al., 1997); [b]  $\alpha = 1.63$  and  $\beta = 0.32$ , (Corzo et al., 2005); [c]  $\alpha = 1.52$  and  $\beta = 0.67$ , (Corzo et al., 2005); [d]  $\alpha = 1.08$  and  $\beta = 0.38$ , (Ortega-Retuerta et al., 2009b); [e]  $\alpha = 1.90$  and  $\beta = 0.35$ , (Zamanillo et al., 2019b).

According to their correlations and regressions to pigments, the phytoplankton taxa that are behind the distributions of TEP and CSP are different (Table 4.2). Pigments carry chemotaxonomic information of the phytoplankton community structure; for example, 19'-hexanoyloxyfucoxanthin generally indicates the presence of haptophytes, peridinin is a biomarker of dinoflagellates, alloxanthin of cryptophytes, and fucoxanthin is a pigment most commonly associated with diatoms, although other taxa such as pelagophytes and haptophytes also contain it (Mendes et al., 2015; Araujo et al., 2017). In the case of TEP, the positive correlation with most pigments suggests that there were no single phytoplankton group responsible for most of TEP production but it was spread amongst diatoms, dinoflagellates, haptophytes, cryptophytes, pelagophytes, prasinophytes and chlorophytes. In contrast, CSP were only correlated significantly correlated with fucoxanthin, thus suggesting that diatoms were the main responsible for CSP production. Indeed, previous studies have reported that diatoms are dominant in Antarctic waters (Bouman et al., 2003; Bouman et al., 2005; Mendes et al., 2015), where a large part of our study took place. Another large part of our cruise track was in Subantarctic waters, where nanoflagellates contribute large shares of phytoplankton biomass (Bouman et al., 2003; Bouman et al., 2005; Mendes et al., 2015). Previous studies have already found that diatoms can produce CSP (Bhaskar et al., 2005; Grossart et al., 2006; Galgani and Engel, 2013; Thornton, 2014; Thornton and Chen, 2017). In the future, it is planned to calculate the relative contribution of the main phytoplankton groups to total (T) Chl *a* from CHEMTAX analysis in this study to better relate phytoplankton community with TEP and CSP.

Regarding factors other than phytoplankton community composition driving TEP and CSP distribution, our results suggest that grazing pressure and senescence of phytoplankton cells also played an important role, since a remarkable positive correlation was found between the two particle types and the pigments chl *a* and pheophorbide *a* (Table 4.2). These pigments are products of Chl *a* and pheophytin *a* degradation, respectively, and therefore are used as proxies of phytoplankton mortality (Jeffrey, 1974). Physical disruption of the cells through mechanisms such as sloppy feeding by grazers (Møller et al., 2003; Møller, 2007) and viral lysis (Bratbak et al., 1993; Gobler et al., 1997; Mojica et al., 2016) are expected to play a significant role in TEP and CSP production. Previous studies have found that TEP production increases during the senescence phase in some cultured strains (Grossart and Simon, 1997;

Grossart et al., 1998; Cisternas-Novoa et al., 2015; Thornton and Chen, 2017), and as a consequence of viral infection (Brussaard et al., 2005; Vardi et al., 2012; Nissimov et al., 2018). Factors affecting CSP abundance have been scarcely investigated, but a previous study in an experimental mesocosms showed that CSP were maximum during the exponential growth phase of the phytoplankton, instead of the senescent phase (Cisternas-Novoa et al., 2015). Another study found that CSP dynamics did not correlate to indicators of cell death (Thornton and Chen, 2017). All in all, our results contrast with previous studies and suggest that phytoplankton mortality may also play an important role driving CSP distribution. More studies are needed to improve our knowledge on factors influencing TEP and CSP distribution in the ocean.

In conclusion, our results agree with previous studies in showing that TEP and CSP are different and independent particle types. Phytoplankton were the main drivers of their distribution in the SO, but the phytoplankton groups responsible for their production differed between the two types: while TEP correlate with diverse taxa, diatoms were the main CSP producer. Our data also suggests that phytoplankton mortality favours TEP and CSP production.

#### **4.5 Acknowledgements**

This research was supported by the Antarctic Circumnavigation Expedition (ACE), carried out under the auspices of the Swiss Polar Institute, and supported by funding from the ACE Foundation and Ferring Pharmaceuticals. MZ was supported by a FPU predoctoral fellowship (FPU13/04630) from the Spanish Ministry of Education and Culture. We thank all ACE members for their support, and particularly Maria Castellví, Pau Cortés and Miguel Cabrera, providing data and technical support. The authors also want to express their gratitude to Professor David Walton, chief scientist of ACE, who passed away on 12 February 2019.





Southern Ocean

## **General discussion and future perspectives**



Given the important roles that TEP and CSP play in the ocean carbon cycle (see introduction), there is a growing interest in finding the main drivers of these particles to predict their distribution in the ocean. In order to address this issue, we have gathered in situ measurements of these particle types in wide regions of the ocean, across the horizontal, vertical and temporal scales, and along with other biological, physical and chemical variables.

We showed that Chl *a* variations do not always mimic those of phytoplankton abundances due to changes in the C:Chl *a* ratios associated with processes such as photoacclimation. However, due to the simplicity and replicability of the measurement, Chl *a* is widely used as an estimator of phytoplankton biomass in the ocean, one that can also be estimated by remote sensing. Therefore, parallel measurements of Chl *a* and TEP and CSP across our study regions and seasons allow us to perform an intercomparison between this thesis' regions and other previously published (Fig. 1).

We observed a temporal disconnection between TEP, CSP and Chl *a* in the NW Mediterranean Sea, similar to various previous studies (Bhaskar and Bhosle, 2006; Taylor et al., 2014). We can conclude that Chl *a* is not a good predictor of TEP nor CSP at temporal scales, although it could work regionally at certain places, namely those with periods of high productivity such as the Arctic Ocean (Engel et al., 2017).



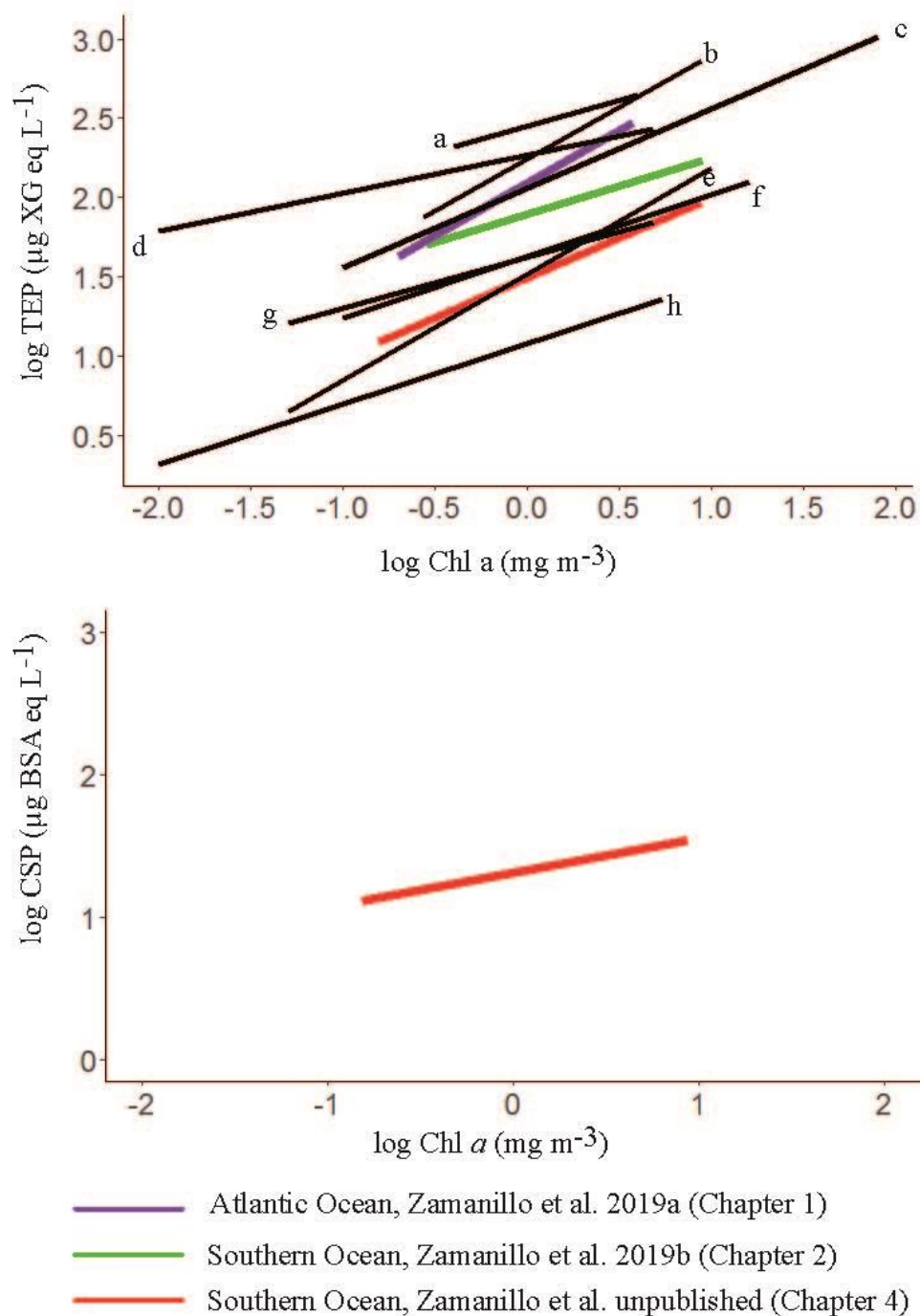


**Figure 1.** Relationship between TEP (upper panel) or CSP (lower panel) and Chl *a* concentration in this and other studies. Colour lines show the linear regressions of the present work (Chapters 1, 2, 4), while regressions from the literature are shown with black lines: (a) Baltic Sea (Engel, 1998 in Passow, 2002a); (b) Ross Sea (Hong et al., 1997); (c) Tokyo Bay (Ramaiah and Furuya, 2002); (d) Western Arctic (Yamada et al., 2015); (e) Gerlache Strait (Corzo et al., 2005); (f) Santa Barbara Channel (Passow and Alldredge, 1995); (g) Bransfield Strait (Corzo et al., 2005); (h) Antarctic Peninsula (Ortega-Retuerta et al., 2009b).

On the other hand, Chl *a* seems to be a good predictor of TEP and CSP concentrations across spatial scales (Fig. 1). However, the differences in the regression equations point to region-specific relationships between phytoplankton and TEP or CSP that are dependent on phytoplankton composition but also on environmental factors such as nutrient limitation and solar radiation. Therefore, TEP prediction from Chl *a* would work better on a regional scale. Indeed, if we take into account the TEP vs. Chl *a* relationship in the whole thesis dataset (temporal series excluded), the percentage of TEP variance explained by the linear model was lower ( $R^2 = 0.34$ ,  $p < 0.001$ ) than that found in every region separately: Atlantic Ocean ( $R^2 = 0.61$ ,  $p < 0.001$ , chapter 1), Southern Ocean ( $R^2 = 0.66$ ,  $p < 0.001$ , chapter 2;  $R^2 = 0.36$ ,  $p < 0.001$ , chapter 4).

**Table 1.** Review of the slope ( $\beta$ ) of the regression equations:  $\log \text{TEP } (\mu\text{g XG eq L}^{-1}) = \alpha + \beta \times \log \text{Chl } a$  ( $\text{mg m}^{-3}$ ), and Chl *a*.  $\alpha$ : y interception.

Geographic area	$\beta$	Chl <i>a</i> range (mean $\pm$ SE)	Study
Antarctic Peninsula	0.38	0.01-5.36	Ortega-Retuerta et al. (2009b)
Bransfield Strait	0.32	0.05-4.81 (0.98 $\pm$ 0.82)	Corzo et al. (2005)
Gerlache Strait	0.67	1.16 mean	Corzo et al. (2005)
Ross Sea	0.65	0.3-8.8 (3.6)	Hong et al. (1997)
<b>Antarctic Peninsula- South Georgia Southern Ocean</b>	<b>0.35</b>	<b>0.28 – 8.95 (2.36 <math>\pm</math> 1.92)</b>	<b>Zamanillo et al. (2019b)</b>
<b>Atlantic Ocean</b>	<b>0.50</b>	<b>0.15 – 8.71 (1.16 <math>\pm</math> 1.46)</b>	<b>Chapter 4</b>
<b>Open Atlantic Ocean</b>	<b>0.66</b>	<b>0.20-3.75</b>	<b>Zamanillo et al. (2019c)</b>
Western Arctic	1.13	0.20-0.57 (0.32 $\pm$ 0.10)	Zamanillo et al. (2019c)
Santa Barbara Channel	0.24	<0.1-4.8	Yamada et al. (2015)
Tokyo Bay	0.39	--	Passow and Alldredge (1995)
Baltic Sea	0.50	--	Ramaiah and Furuya (2002)
	0.33	--	Engel, 1998 in Passow, (2002a)

**Table 2.** Review of open-ocean surface TEP concentrations (mean and ranges;  $\mu\text{g XG eq. L}^{-1}$ ), Chl *a* (mean and ranges;  $\text{mg m}^{-3}$ ) and TEP:Chl *a* ratio (mean  $\pm$  SE and/or range) available in the literature. bdl: below detection limit.

Geographic area	Conditions	Sampling date	Depth (m)	TEP mean (range) ( $\mu\text{g XG eq. L}^{-1}$ )	Chl <i>a</i> mean (range) ( $\text{mg m}^{-3}$ )	TEP:Chl <i>a</i> mean (range)	Reference
Fram Strait (Arctic Ocean)	Bloom and non bloom	Summer 2009–2012 and 2014 (time series) and summer 2014 (transect)	5–150	$75 \pm 78$ (5–517)	0–4.2	$45 \pm 3$ – $107 \pm 10$	Engel et al. (2017)
Arctic Ocean	Sea ice covered	Autumn and Spring 2009–2010	Above mixed layer depth	125–1750 <sup>a</sup>	0.1–7.8 <sup>b</sup>	–	Wurl et al. (2011a)
Eastern tropical and Eastern subarctic, North Pacific Ocean	Eutrophic and oligotrophic	Summer 2009		78–970 <sup>a</sup>	0.3–1.7 <sup>b</sup>	–	
Western subarctic and North Pacific Ocean	Non bloom	Summer 2001	5	40–60	0.2–1.9	–	Ramaiah et al. (2005)
Northeast Atlantic Ocean	Different bloom stages	Summer 1996	0–70	10 <sup>c</sup> –124	0.1–1.1 <sup>c,d</sup>	49–104	Engel (2004)
Northeast Atlantic Ocean	Late stages bloom	Autumn 1996	0–50	$28.5 \pm 10.2$	0.07–0.6	61	
Northeast Atlantic Ocean	Late stages bloom	Spring 2005	0–10	20–420 <sup>c</sup>	0.1–3 <sup>c,e</sup>	–	Leblanc et al. (2009)
Western tropical North Pacific Ocean	Non bloom Oligotrophic	Spring 2013	Surface mixed layer (36 $\pm$ 12)	$43 \pm 7$ (18–67 <sup>c</sup> )	$0.05 \pm 0.01$	$832 \pm 314$	Kodama et al. (2014)
Western North Atlantic Ocean	Oligotrophic	Spring 2014	1	161–460	0.1–1 <sup>c</sup>	–	Jennings et al. (2017)
Western North Atlantic Ocean and Sargasso Sea	Eutrophic and oligotrophic	Spring 2014	2–5	100–200 <sup>c</sup>	0.1–2.2	–	Aller et al. (2017)
Sargasso Sea	Oligotrophic	Spring, summer, autumn 2012 and spring 2013	0–100	$21 \pm 2$ – $57 \pm 3$	0.05–1 <sup>c</sup>	–	Cisternas-Novoa et al. (2015)
Mediterranean Sea	Non bloom	Spring 2007	Upper mixed layer	29 (19–53)	bdl–1.8 <sup>f</sup>	484 (178–1293)	Ortega-Retuerta et al. (2010)
Western Mediterranean Sea	Oligotrophic	Spring 2012	0–200	16–25 <sup>c,g,h</sup>	0.1–0.7 <sup>c,h</sup>	–	Ortega-Retuerta et al. (2017)
<b>Western Mediterranean Sea</b>	<b>Oligotrophic</b>	<b>Autumn 2015</b>	<b>5</b>	<b><math>30.7 \pm 5.4</math> (21.4–36.5)</b>	<b><math>0.19 \pm 0.07</math> (0.14–0.31)</b>	<b><math>181 \pm 76</math> (69–253)</b>	<b>Chapter 3, transect</b>
Eastern Mediterranean Sea	Oligotrophic	Winter–Autumn 2008 Summer 2009	5	$345 \pm 143.2$ (116–420)	$0.04 \pm 0.01$ (0.04–0.07)	–	Bar-Zeev et al. (2011)

Gulf of Aqaba (Eilat, Israel)	Oligotrophic	Spring 2008	5	110–228 <sup>c</sup>	0.3–1.3 <sup>i</sup>	–	Bar-Zeev et al. (2009)
Tropical Atlantic Ocean	Oligotrophic	Spring–Summer 2011	3	8.18 ± 4.56	0.05–0.31	78.6 ± 9.3	Iuculano et al. (2017c)
Pacific Ocean	Oligotrophic	Spring–Summer 2011	3	24.45 ± 2.3		357 ± 127	
Global Subtropical Atlantic, Indian and Pacific Oceans	Non bloom	Winter 2010–Summer 2011	0–200	14.0 (0.4–173.6)	0–3 <sup>e</sup>	–	Mazuecos (2015)
North Indian Ocean -Arabian Sea -Bay of Bengal	Eutrophic	-August 1996 -September 1996	0–1000	-60 <sup>i,k</sup> (< 5–102 <sup>j</sup> ) -7–13 <sup>e,j</sup>	–	–	Kumar et al. (1998), Ramaiah et al. (2000)
Nearshore Cape Verde	Oligotrophic	September 2016	SML	94-187	0.29±0.1	–	Robinson et al. (2019b)
Baltic Sea	Oligo- eutrophic		SML and 1	123-1340	0.68- 1.56		
Norwegian Sea			SML and 1	50-424	0.29- 1.64 (SML)		
<b>Open Atlantic Ocean (OAO)</b> <b>OAO (CU excluded)</b> <b>CU (Canary Coastal Upwelling)</b> <b>SWAS (coast)</b>	<b>Oligotrophic</b>   <b>Eutrophic</b>	<b>Autumn 2014</b>	<b>4</b>	<b>72 ± 74 (18–446)</b> <b>60 ± 27(18–132)</b> <b>446</b> <b>256±130 (99–427)</b>	<b>0.4 ± 0.2 (0.2–0.6)</b> <b>0.3 ± 0.1 (0.2–0.6)</b> <b>0.2</b> <b>2.7±0.9 (1.1–3.7)</b>	<b>236 ± 293 (81–1760)</b> <b>183 ± 56 (81–360)</b> <b>1760</b> <b>97±42 (31–165)</b>	<b>Zamanillo et al. (2019c),Chapter 1</b>
<b>NSO, North of the South Orkney Islands</b> <b>SSO, South of the South Orkney Islands</b> <b>NSG, Northwest of South Georgia Island</b> <b>WA, West of Anvers Island</b>	<b>Oligotrophic-eutrophic</b>	<b>Austral summer 2015</b>	<b>4</b>	<b>144.4 ± 21.7 (98-168)</b> <b>48.1 ± 6.5 (39-64)</b> <b>125.5 ± 21.1 (94-157)</b> <b>111.6 ± 13.0 (90-125)</b>	<b>1.87 ± 0.23</b> <b>0.32 ± 0.06</b> <b>4.59 ± 1.97</b> <b>4.05 ± 0.48</b>	<b>76.7 ± 10.6</b> <b>153.4 ± 29.8</b> <b>32.3 ± 15.0</b> <b>28.2 ± 4.8</b>	<b>Zamanillo et al. (2019b), Chapter 2</b>
<b>Southern Ocean, circular transect around Antarctica</b>	<b>Oligotrophic-eutrophic</b>	<b>Austral summer 2017</b>	<b>5</b>	<b>34.0 ± 28.8 (bdl – 201.8)</b>	<b>1.16 ± 1.46 (0.15 – 8.71)</b>	<b>48.4 ± 34.0 (5.1 – 141.5)</b>	<b>Chapter 4</b>
Ross Sea	Bloom	Spring 1994	Surface	308 (0–2800)	3.6 (0.3–8.8)	85	Hong et al. (1997)

The slope of the TEP vs. Chl *a* regression equations varied widely among regions, ranging from 0.24 to 1.13 (Table 1). Although a more detailed analyses, including environmental and biological variables, would be needed, it seems that the highest slopes are characteristic of oligotrophic regions, whereas the lowest occur in eutrophic ones. That is, relative increases in phytoplankton abundance in oligotrophic waters would be accompanied by larger increases in TEP. Indeed, we found the highest slope reported so far in the oligotrophic open Atlantic Ocean ( $1.13 \pm 0.20$ ) (Table 1, Chapter 1).

The ratio TEP:Chl *a* also varied widely among regions. Grouping our samples by regions (Tropical Atlantic Ocean, Subtropical Atlantic Ocean, NW Mediterranean Sea and Southern Ocean), the TEP:Chl *a* ratio tends to decrease from the equator to the poles (Fig. 2), in parallel with a negative gradient in oligotrophy but also in irradiance. If we are to compare our TEP:Chl *a* values with other studies, we can observe a similar trend, with the highest values in the tropical ocean and the lowest in the poles (Table 2). In our study we have found that some variables other than phytoplankton are important drivers of TEP and CSP distributions (Fig. 3), and therefore could be responsible for the variations of TEP:Chl *a* and CSP:Chl *a* ratios, such as sea ice melting, nutrients, phytoplankton mortality and solar radiation. Although we found contrasting results regarding the role of solar radiation on TEP production (negative relationship in the open Atlantic Ocean and positive relationship in the Southern Ocean and Mediterranean Sea), the positive relationship ( $R^2 = 0.56$ ,  $p < 0.001$ ) between TEP:Chl *a* and solar radiation dose in the whole study (Mediterranean and Southern Ocean together) (Table 3) suggests that, at global scale, stimulation of TEP production by solar radiation would be more important than its degradation.

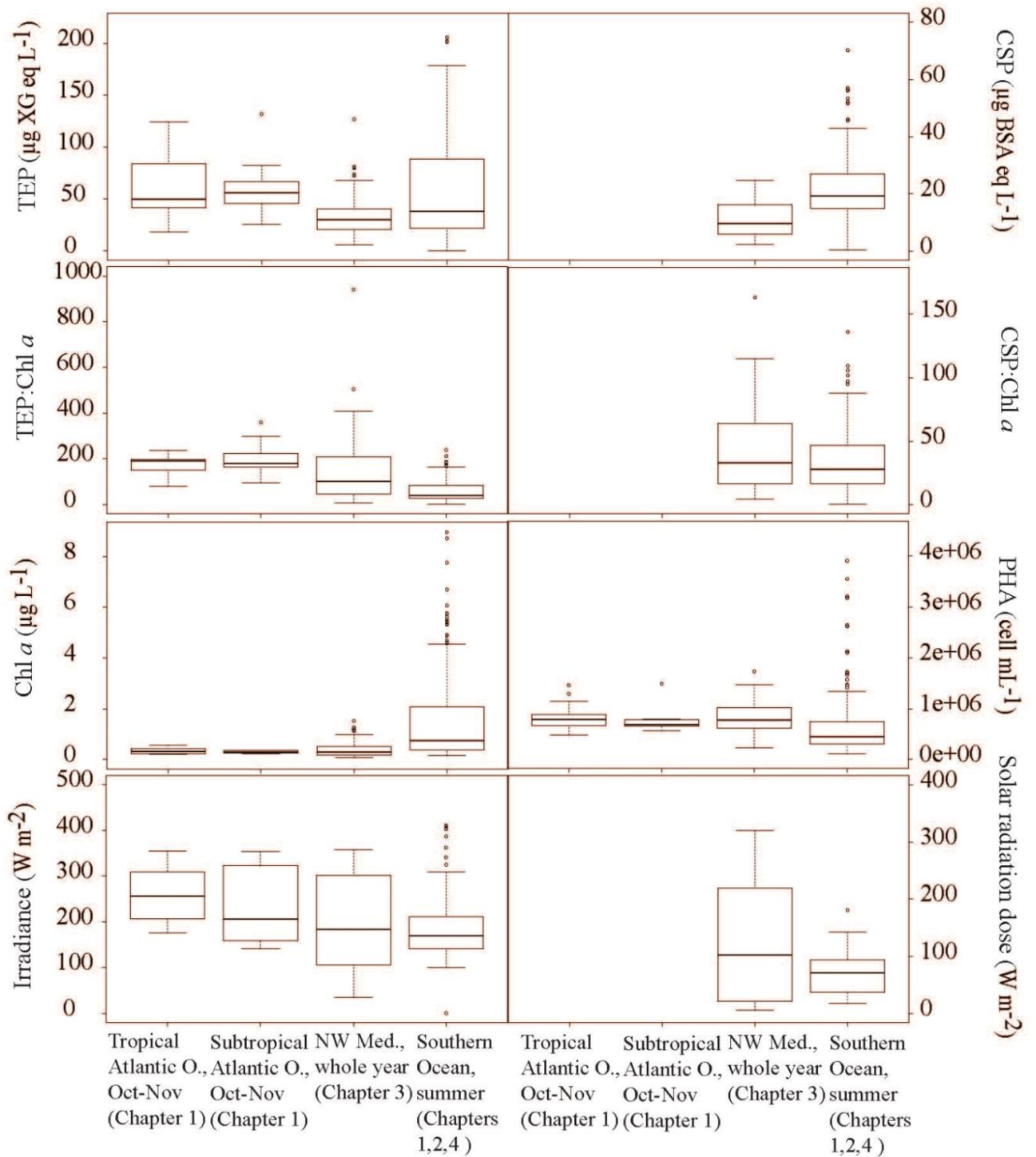


**Figure 2.** Boxplots of transparent exopolymer particles (TEP), Coomassie stainable particles (CSP), chlorophyll *a* (Chl *a*), TEP:Chl *a*, CSP:Chl *a*, prokaryotic heterotrophic abundance (PHA), averaged-24h surface irradiance, and averaged-24h solar radiation dose in the upper mixed layer, across regions visited for this work: tropical and subtropical Atlantic Ocean (4 m, chapter 1), NW Mediterranean Sea (BBMO (0.5 m), EOS (0.5 m) and transect (5 m), chapter 3) and Southern Ocean (4-5 m, chapters 2, 4). The horizontal lines of the boxes represent 25%, 50% (median) and 75% percentiles (from bottom to top). Whiskers represent minimum and maximum values.

**Table 3.** Regression equations and statistics describing the relationship between transparent exopolymer particles (TEP), Coomassie stainable particles (CSP), TEP:Chl *a*, CSP:Chl *a* and other physical and biological variables: temperature, chlorophyll *a* (Chl *a*), and prokaryotic heterotrophic abundance (PHA) in the surface of the ocean across all of the regions (Atlantic Ocean (4 m, chapter 1), NW Mediterranean Sea (BBMO (0.5 m), EOS (0.5 m) and transect (5 m), chapter 3) and Southern Ocean (4-5 m, chapters 2, 4). ns: not significant. All variables were log<sub>10</sub> transformed.

Var.	Ind. var	R <sup>2</sup>	p	Intercept	Slope	n
TEP	Temperature (K)		ns			279
	Chl <i>a</i>	0.29	<0.001	1.69 (± 0.02)	0.46 (± 0.04)	297
	PHA		ns			259
	Averaged-24h Irradiance (W/m <sup>2</sup> )	0.07	<0.001	0.74 (± 0.31)	0.46 (± 0.13)	154
	Averaged-24h Solar radiation dose		ns			92
TEP:Chl <i>a</i>	Averaged-24h Irradiance (W/m <sup>2</sup> )	0.23	<0.001	-0.06 (± 0.31)	0.88 (± 0.14)	154
	Averaged-24h Solar radiation dose	0.56	<0.001	0.58 (± 0.12)	0.71 (± 0.07)	92
CSP	Temperature (K)	0.25	<0.001	33.3 (± 4.2)	-13.1 (± 1.7)	168
	Chl <i>a</i>	0.21	<0.001	1.28 (± 0.02)	0.30 (± 0.04)	154
	PHA		ns			149
	Averaged-24h Irradiance (W/m <sup>2</sup> )	0.11	<0.05	0.50 (± 0.25)	0.24 (± 0.11)	48
	Averaged-24h Solar radiation dose	0.14	<0.05	0.75 (± 0.12)	0.15 (± 0.06)	37
CSP:Chl <i>a</i>	Averaged-24h Irradiance (W/m <sup>2</sup> )	0.45	<0.001	-0.53 (± 0.37)	0.92 (± 0.16)	46
	Averaged-24h Solar radiation dose	0.52	<0.001	0.47 (± 0.17)	0.54 (± 0.09)	35
Chl <i>a</i>	Averaged-24h Irradiance (W/m <sup>2</sup> )	0.03	<0.05	0.75 (± 0.45)	-0.40 (± 0.20)	154
	Averaged-24h Solar radiation dose	0.24	<0.001	0.93 (± 0.21)	.059 (± 0.11)	92

Phytoplankton has been found to be the main driver of TEP and CSP distributions in this thesis. In contrast, prokaryotic heterotrophs (PH) were only significantly related with TEP in the entire transect of the Atlantic Ocean (chapter 1). Considering the SWAS and OAO separately, only in the SWAS were TEP related to HNA, although in the OAO, multiple regression analyses showed that both PH and phytoplankton contributed to explain TEP concentration variance.

In the open Atlantic Ocean, *Synechococcus* and picoeukaryotes were best correlated to TEP (Chapter 1). In the Southern Ocean, diatoms and dinoflagellates were the best correlated (Chapters 2 and 4), and diatoms were the best correlated to CSP (Ch. 4). Finally, diatoms, dinoflagellates, and “other microalgae” were the groups explaining most of the variance of TEP throughout the time series in the NW Mediterranean Sea, whereas dinoflagellates and “other microalgae” were those of CSP at the same location. At the vertical scale in the NW Mediterranean Sea, the main apparent drivers of TEP

and CSP were dinoflagellates ( $R^2= 0.35$ ,  $p< 0.001$ ,  $n= 75$ ) and *Synechococcus* ( $r= 0.29$ ,  $p< 0.001$ ,  $n= 63$ ), respectively.

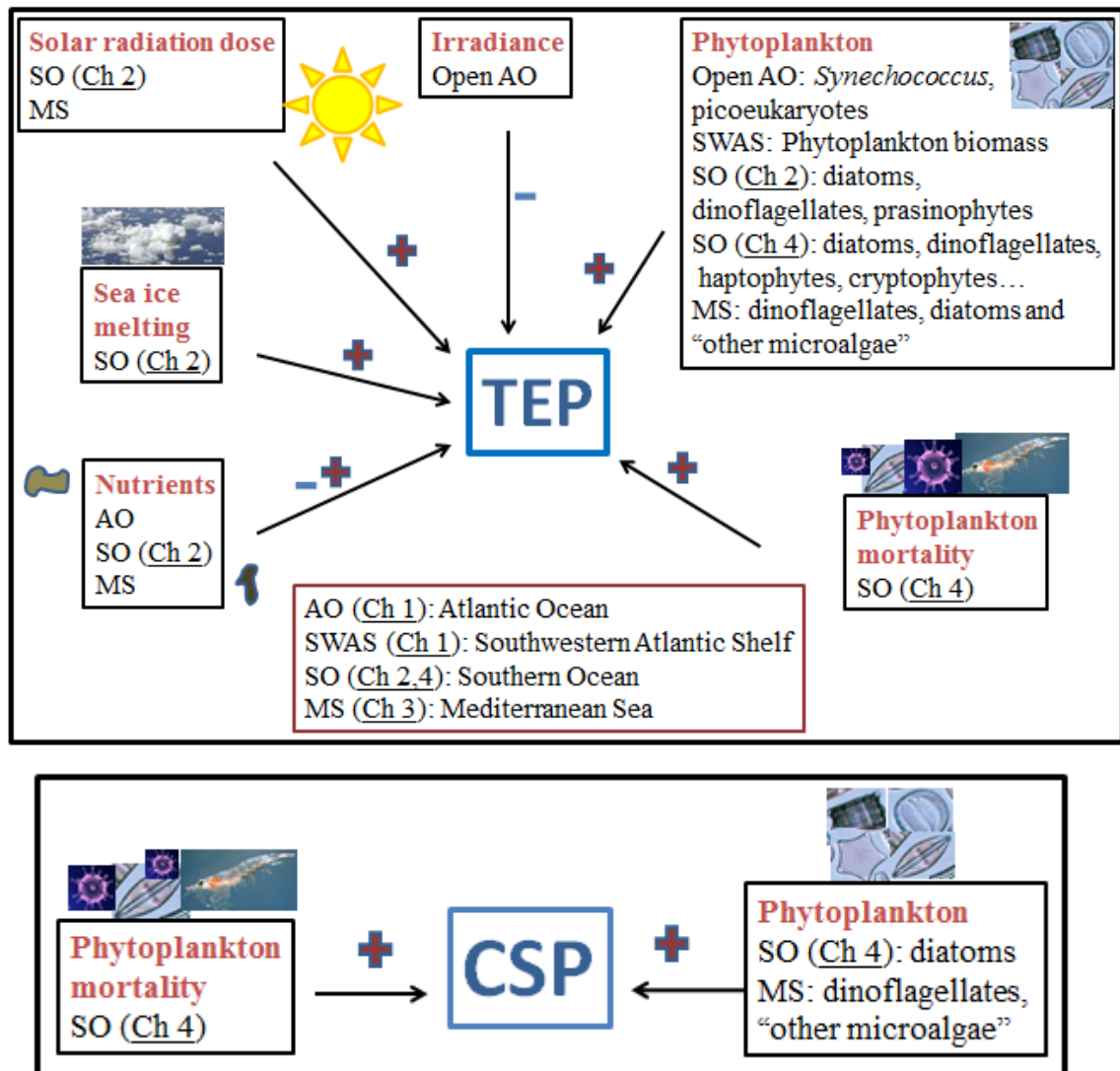


**Figure 3.** Main drivers of TEP and CSP distribution suggested from this thesis' results. +: positive relationship; -: negative relationship. Ch: chapter

Regarding the potential overlap of TEP and CSP, we observed that they followed distinct dynamics in both the Mediterranean Sea (Chapter 3) and the Southern Ocean (Chapter 4). This suggests they are different particles, produced by different organisms and/or subject to different aggregation and degradation processes, as suggested in previous studies (Cisternas-Novoa et al., 2015; Thornton et al., 2016; Thornton and Chen, 2017). However, the absence of parallel temporal patterns of TEP and CSP does not totally preclude that, on occasions, both particle types overlap by getting coloured by the two stains, and more research is needed.



All in all, in this thesis we have shed light on the possibility to predict TEP and CSP distribution in the surface ocean and the main drivers of their distribution. Out of the myriad of variables potentially involved in TEP and CSP production, accumulation and cycling in the surface ocean, we show that phytoplankton, Chl *a* or biomass are the only ones that hold predictive capability for the two particle types, even though they hardly explain more than one third of their variance. The fact that the TEP:Chl *a* and CSP:Chl *a* ratios are better correlated to the daily solar radiation dose in the upper mixed layer across the entire data set (with  $R^2 > 0.5$ , Table 3) opens the possibility to estimate surface ocean TEP and CSP distributions from remote sensing and climatological data.

However, if we are to predict the role of TEP and CSP in several biogeochemical processes, such as the ocean carbon cycle, the air-sea gas and particle exchanges and the formation of clouds, more studies are required to connect the distribution of these particle types with measurements of their specific impact on these processes, because it is anticipated that the biogeochemical impacts of TEP and CSP do not only depend on their concentration but also on many other process-driving variables. Before that, the role of CSP on processes like the biological carbon pump has not been yet demonstrated and needs to be further investigated.

Not all the work conducted during my PhD is reflected in this thesis. Some experiments did not go beyond the trial phase, and some measurements belong in side projects where they constitute a necessary yet not principal component. I have collaborated to explore the effects of TEP on aerosol composition and cloud formation, by carrying out sea-spray generation experiments. A tank was filled with seawater or melted sea ice from the Southern Ocean, aerosol was generated by bubble bursting caused by a recirculated jet stream, and the composition of both the bubbled sample and the generated aerosol were analysed. Results were compared with analyses of ambient ocean samples and aerosols. We showed that seawater or sea-ice TEP were not a good predictor of organic aerosol, and other components came into play (Dall'Osto et al., 2017).

I also tried to develop high-throughput methods to measure gel particles with different compositions and properties, using the dyes Nile Red (which stains lipidic material), DAPI (which stains DNA) and chlortetracycline (CHTC, which stains the calcium bridges that stabilize polymer gels). The idea was to quantify them by flow cytometry, which is a fast, repeatable and cost efficient technique. We started following Orellana et

al. (2011), who reported a method to quantify microgels by flow cytometry using CHTC. However, despite our efforts and the collaboration with Jordi Petriz (Institut de Recerca Contra la Leucèmia Josep Carreras), we did not obtain reliable results and we turned towards a more descriptive thesis using the state-of-the-art staining method.





Russian RV *Akademik Threshnikov* near Siple Island (Antarctica)

## Conclusions



1. Across the studied regions, TEP concentrations ranged from below detection limit to  $446 \mu\text{g XG eq L}^{-1}$ . Highest TEP concentrations were found in regions with high local productivity; such as upwellings (edge of the Canary Coastal Upwelling,  $446 \mu\text{g XG eq L}^{-1}$ ), or areas influenced by rivers (Southwestern Argentinian Shelf,  $256 \pm 130 \mu\text{g XG eq L}^{-1}$ ) or ice (Siple Island ( $202 \mu\text{g XG eq L}^{-1}$ ) and Mertz Glacier ( $160 \mu\text{g XG eq L}^{-1}$ )).
2. TEP:Chl *a* ratios ranged from 4 to 1760. The highest TEP:Chl *a* ratios were found in the tropical and subtropical Atlantic Ocean (81-1760) and in the Mediterranean Sea in summer ( $277.9 \pm 223.2$  (69.5-940.4)), whereas the lowest were found in winter in the Mediterranean Sea ( $41.7 \pm 30.8$ ), northwest of South Georgia ( $32.3 \pm 15.0$ ), west of Anvers Island ( $28.2 \pm 4.8$ ), and south of South Africa ( $29.2 \pm 11.7$ ).
3. CSP concentrations were measured for the first time in the Mediterranean Sea and in the Southern Ocean, where they ranged between 0.3 and  $52.2 \mu\text{g BSA eq L}^{-1}$ . The highest concentration was found in the Southern Ocean, specifically next to the Mertz Glacier. CSP:Chl *a* ratio varied widely in both the Mediterranean Sea (5-163) and the Southern Ocean (0.5-136.1).
4. The estimated contribution of TEP to the POC pool ranged between 28 and 110 % (average  $67 \pm 19$  %) in the Atlantic Ocean, 18 and 97 % (average  $39 \pm 12$  %) in the Southern Ocean, and 3-44 % (average  $15 \pm 9$  %) in the NW Mediterranean Sea. In the open Atlantic Ocean, TEP contributed the most to the POC pool, representing twice the contribution of phytoplankton. In the SWAS, conversely, the contribution of TEP was not significantly different from that of phytoplankton. In the Mediterranean Sea, only in summer the TEP contribution to the POC pool at surface was larger than the contribution of phytoplankton.
5. In the Southern Ocean, we found a general enrichment of TEP in the upper surface (10 cm), with respect to the underlying water (4 m). This TEP enrichment could be responsible for enhanced  $\beta$ -glucosidase, fucosidase and esterase activities in the upper surface. The positive relationship between TEP enrichment and wind speed, but not with Chl *a* and PHA, suggest that the

enrichment is mainly caused by wind, probably through bubble scavenging and rising.

6. TEP and CSP temporal patterns were uncoupled in two coastal stations in the NW Mediterranean Sea. Similarly, the two particle types showed uncoupled horizontal distributions around the Southern Ocean. These results support the idea that they are different particle types that are produced by different organisms and/or subject to different formation and degradation processes.
7. Regression analyses suggested that phytoplankton were found to be the main driver of TEP and CSP distribution in the ocean, although the taxonomic groups most contributing to the correlation varied among regions and were different for TEP and CSP. In the open Atlantic Ocean, *Synechococcus* and picoeukaryotes were the best correlated to TEP. In the Southern Ocean, diatoms and dinoflagellates were the best associated with TEP, and only diatoms with CSP. Over the time series in the NW Mediterranean Sea, diatoms, dinoflagellates, and “other microalgae” mainly drove TEP dynamics, whereas dinoflagellates and “other microalgae” were most coupled to CSP.
8. TEP distribution was also influenced by the daily solar radiation dose (in all studied regions), surface irradiance, sea ice melt (in Antarctic waters), nutrients (in the Southern Ocean and the Mediterranean Sea) and phytoplankton mortality (in the Southern Ocean). Only phytoplankton mortality provided additional explanation to CSP variance in the Southern Ocean.
9. The good statistical relationship found across the entire study between the TEP:Chl *a* and the CSP:Chl *a* ratios and the daily solar radiation dose opens the possibility to predict the surface ocean concentrations of the two particle types from satellite and climatological data.

## REFERENCES

Agawin, N. S. R., Duarte, C. M., and Agustí, S.: Nutrient and temperature control of the contribution of picoplankton to phytoplankton biomass and production, *Limnology and Oceanography*, 45, 591-600, 2000.

Agustí, S., and Llabrés, M.: Solar Radiation-induced Mortality of Marine Pico-phytoplankton in the Oligotrophic Ocean, *Photochemistry and Photobiology*, 83, 793-801, 2007.

Allredge, A. L., Cole, J. J., and Caron, D. A.: Production of heterotrophic Inc. bacteria inhabiting macroscopic organic aggregates (marine snow) from surface waters, *Limnology and Oceanography*, 31 68-78, 1986.

Allredge, A. L., and Silver, M. W.: Characteristics, Dynamics and Significance of Marine Snow, *Progress in Oceanography*, 20, 41-82, 1988.

Allredge, A. L., Passow, U., and Logan, B. E.: The abundance and significance of a class of large, transparent organic particles in the ocean, *Deep Sea Research Part I: Oceanographic Research Papers*, 40, 1131-1140, 1993.

Allredge, A. L., Passow, U., and Haddock, S. H. D.: The characteristics and transparent exopolymer particle (TEP) content of marine snow formed from thecate dinoflagellates, *Journal of Plankton Research*, 20, 393-406, 1998.

Aller, J. Y., Kuznetsova, M. R., Jahns, C. J., and Kemp, P. F.: The sea surface microlayer as a source of viral and bacterial enrichment in marine aerosols, *Journal of Aerosol Science*, 36, 801-812, 10.1016/j.jaerosci.2004.10.012, 2005.

Aller, J. Y., Radway, J. C., Kiltbau, W. P., Bothe, D. W., Wilson, T. W., Vaillancourt, R. D., Quinn, P. K., Coffman, D. J., Murray, B. J., and Knopf, D. A.: Size-resolved characterization of the polysaccharidic and proteinaceous components of sea spray aerosol, *Atmospheric Environment*, 154, 331-347, 10.1016/j.atmosenv.2017.01.053, 2017.

Alonso-Sáez, L., Vázquez-Domínguez, E., Cardelús, C., Pinhassi, J., Sala, M. M., Lekunberri, I., Balagué, V., Vila-Costa, M., Unrein, F., Massana, R., Simó, R., and Gasol, J. M.: Factors Controlling the Year-Round Variability in Carbon Flux Through Bacteria in a Coastal Marine System, *Ecosystems*, 11, 397-409, 10.1007/s10021-008-9129-0, 2008.

Aluwihare, L., Repeta, D. J., and Chen, R. F.: A major biopolymeric component to dissolved organic carbon in surface sea water, *Nature*, 387, 166-169, 1997.

Aluwihare, L., and Repeta, D. J.: A comparison of the chemical characteristics of oceanic DOM and extracellular DOM produced by marine algae, *Marine Ecology Progress Series*, 186, 105-117, 1999.

Aluwihare, L., Repeta, D., and Chen, R. F.: Chemical composition and cycling of dissolved organic matter in the Mid-Atlantic Bight, *Deep Sea Res II*, 49, 4421-4437, 2002.



- Andreae, M. O., and Rosenfeld, D.: Aerosol–cloud–precipitation interactions. Part 1. The nature and sources of cloud-active aerosols. , *Earth-Science Reviews*, 89(1-2), 13–41, 2008.
- Andreae, M. O.: Natural and anthropogenic aerosols and their effects on clouds, precipitation and climate, *Geochimica et Cosmochimica Acta*, 2009.
- Andreas, A. L., and Monahan, E. C.: The Role of Whitecap Bubbles in Air–Sea Heat and Moisture Exchange, *Journal of Physical Oceanography*, 30, 433-442, 2000.
- Araujo, M. L. V., Mendes, C. R. B., Tavano, V. M., Garcia, C. A. E., and Baringer, M. O. N.: Contrasting patterns of phytoplankton pigments and chemotaxonomic groups along 30°S in the subtropical South Atlantic Ocean, *Deep Sea Research Part I: Oceanographic Research Papers*, 120, 112-121, 10.1016/j.dsr.2016.12.004, 2017.
- Arnosti, C.: Microbial extracellular enzymes and the marine carbon cycle, *Ann Rev Mar Sci*, 3, 401-425, 10.1146/annurev-marine-120709-142731, 2011.
- Arrhenius, S.: On the influence of carbonic acid in the air upon the temperature of the ground, *The London, Edinburgh, and Dublin Philosophical Magazine and Journal of Science*, 41, 237-276, 10.1080/14786449608620846, 1896.
- Arruda Fatibello, S. H. S., Henriques Vieira, A. A., and Fatibello-Filho, O.: A rapid spectrophotometric method for the determination of transparent exopolymer particles (TEP) in freshwater, *Talanta*, 62, 81-85, 10.1016/s0039-9140(03)00417-x, 2004.
- Assmy, P., Ehn, J. K., Fernandez-Mendez, M., Hop, H., Katlein, C., Sundfjord, A., Bluhm, K., Daase, M., Engel, A., Fransson, A., Granskog, M. A., Hudson, S. R., Kristiansen, S., Nicolaus, M., Peeken, I., Renner, A. H., Spreen, G., Tatarek, A., and Wiktor, J.: Floating ice-algal aggregates below melting arctic sea ice, *PLoS One*, 8, e76599, 10.1371/journal.pone.0076599, 2013.
- Azam, F., and Malfatti, F.: Microbial structuring of marine ecosystems, *Nat Rev Microbiol*, 5, 782-791, 10.1038/nrmicro1747, 2007.
- Azetsu-Scott, K., and Passow, U.: Ascending marine particles: significance of transparent exopolymer particles (TEP) in the upper ocean, *Limnology and Oceanography*, 49 741-748, 2004.
- Azetsu-Scott, K., and Niven, S. E. H.: The role of transparent exopolymer particles (TEP) in the transport of <sup>234</sup>Th in coastal water during a spring bloom, *Continental Shelf Research*, 25, 1133-1141, 2005.
- Bach, L. T., Stange, P., Taucher, J., Achterberg, E. P., Algueró-Muñiz, M., Horn, H., Esposito, M., and Riebesell, U.: The influence of plankton community structure on sinking velocity and remineralization rate of marine aggregates, *Global Biogeochemical Cycles*, 10.1029/2019gb006256, 2019.
- Bar-Zeev, E., Berman-Frank, I., Stambler, N., Vázquez Domínguez, E., Zohary, T., Capuzzo, E., Meeder, E., Suggett, D. J., Iluz, D., Dishon, G., and Berman, T.: Transparent exopolymer particles (TEP) link phytoplankton and bacterial production in the Gulf of Aqaba, *Aquatic Microbial Ecology*, 56, 217-225, 10.3354/ame01322, 2009.

- Bar-Zeev, E., Berman, T., Rahav, E., Dishon, G., Herut, B., and Berman-Frank, I.: Transparent exopolymer particle (TEP) dynamics in the eastern Mediterranean Sea, *Marine Ecology Progress Series*, 431, 107-118, 10.3354/meps09110, 2011.
- Bar-Zeev, E., Berman-Frank, I., Girshevitz, O., and Berman, T.: Revised paradigm of aquatic biofilm formation facilitated by microgel transparent exopolymer particles, *Proc Natl Acad Sci U S A*, 109, 9119-9124, 10.1073/pnas.1203708109, 2012.
- Bar-Zeev, E., Passow, U., Castrillon, S. R., and Elimelech, M.: Transparent exopolymer particles: from aquatic environments and engineered systems to membrane biofouling, *Environ Sci Technol*, 49, 691-707, 10.1021/es5041738, 2015.
- Bar-Zeev, E., and Rahav, E.: Microbial metabolism of transparent exopolymer particles during the summer months along a eutrophic estuary system, *Front Microbiol*, 6, 403, 10.3389/fmicb.2015.00403, 2015.
- Barnett, T. P., Pierce, D. W., AchutaRao, K. M., Gleckler, P. J., Santer, B. D., Gregory, J. M., and Washington, W. M.: Penetration of Human-Induced Warming into the World's Oceans, *Science*, 309, 284-287, 2005.
- Bauer, J. E., and Bianchi, T. S.: Dissolved Organic Carbon Cycling and Transformation, in: *Treatise on Estuarine and Coastal Science*, 7-67, 2011.
- Beauvais, C., Pedrotti, M. L., Egge, J., Iversen, K., and Marrasé, C.: Effects of turbulence on TEP dynamics under contrasting nutrient conditions: implications for aggregation and sedimentation processes, *Marine Ecology Progress Series*, 323, 47-57, 2006.
- Beauvais, S., Pedrotti, M. L., Villa, E., and Lemée, R.: Transparent exopolymer particle (TEP) dynamics in relation to trophic and hydrological conditions in the NW Mediterranean Sea, *Marine Ecology Progress Series*, 262, 97-109, 2003.
- Behrenfeld, M.: Abandoning Sverdrup's Critical Depth Hypothesis on phytoplankton blooms, *Ecology*, 91, 977-989, 2010.
- Bélangier, S., Cizmeli, S. A., Ehn, J., Matsuoka, A., Doxaran, D., Hooker, S., and Babin, M.: Light absorption and partitioning in Arctic Ocean surface waters: impact of multiyear ice melting, *Biogeosciences*, 10, 6433-6452, 10.5194/bg-10-6433-2013, 2013.
- Bergmann, T., Richardson, T. L., Paerl, H. W., Pinckney, J. L., and Schofield, O.: Synergy of light and nutrients on the photosynthetic efficiency of phytoplankton populations from the Neuse River Estuary, North Carolina, *Journal of Plankton Research*, 24, 923-933, 2002.
- Berman-Frank, I., Rosenberg, G., Levitan, O., Haramaty, L., and Mari, X.: Coupling between autocatalytic cell death and transparent exopolymeric particle production in the marine cyanobacterium *Trichodesmium*, *Environ Microbiol*, 9, 1415-1422, 10.1111/j.1462-2920.2007.01257.x, 2007.
- Berman, T., and Viner-Mozzini, Y.: Abundance and characteristics of polysaccharide and proteinaceous particles in Lake Kinneret, *Aquatic Microbial Ecology*, 24, 255-264, 2001.

- Berman, T., and Holenberg, M.: Don't fall foul of biofilm through high TEP levels, *Filtration & Separation*, 42, 30-32, 10.1016/s0015-1882(05)70517-6, 2005.
- Berman, T., and Passow, U.: Transparent Exopolymer Particles (TEP): an overlooked factor in the process of biofilm formation in aquatic environments, *Nature Precedings*, 10.1038/npre.2007.1182.1, 2007.
- Berman, T., and Parparova, R.: Visualization of transparent exopolymer particles (TEP) in various source waters, *Desalination and Water Treatment*, 21, 382-389, 10.5004/dwt.2010.1860, 2010.
- Bhaskar, P. V., and Bhosle, N. B.: Microbial extracellular polymeric substances in marine biogeochemical processes, *Current Science*, 88, 45-53, 2005.
- Bhaskar, P. V., Grossart, H. P., Bhosle, N. B., and Simon, M.: Production of macroaggregates from dissolved exopolymeric substances (EPS) of bacterial and diatom origin, *Microb Ecol*, 53, 255-264, 10.1016/j.femsec.2004.12.013, 2005.
- Bhaskar, P. V., and Bhosle, N. B.: Dynamics of transparent exopolymeric particles (TEP) and particle-associated carbohydrates in the Dona Paula bay, west coast of India, *Journal of Earth System Science*, 115, 403-413, 10.1007/bf02702869, 2006.
- Bicke, M. J.: The role of metamorphic decarbonation reactions in returning strontium to the silicate sediment mass. , *Nature*, 367, 699-704, 1994.
- Biddanda, B., and Benner, R.: Carbon, nitrogen, and carbohydrate fluxes during the production of particulate and dissolved organic matter by marine phytoplankton, *Limnology and Oceanography*, 42 (3), 506-518, 1997.
- Biddanda, B. A.: Structure and function of marine microbial aggregates, *Oceanologica Acta*, 9, 209-211, 1986.
- Bigg, E. K., and Leck, C.: The composition of fragments of bubbles bursting at the ocean surface, *Journal of Geophysical Research*, 113, 10.1029/2007jd009078, 2008.
- Bittar, T. B., Passow, U., Hamaraty, L., Bidle, K. D., and Harvey, E. L.: An updated method for the calibration of transparent exopolymer particle measurements, *Limnology and Oceanography: Methods*, 16, 621-628, 10.1002/lom3.10268, 2018.
- Bohdansky, A. B., and Herndl, G. J.: Ecology of amorphous aggregations (marine snow) in the Northern Adriatic Sea. III. Zooplankton interactions with marine snow, *Marine Ecology Progress Series*, 87, 135-146, 10.3354/meps087135, 1992.
- Boden, T. A., Marland, G., and Andres, R. J.: Global, Regional, and National Fossil-Fuel CO<sub>2</sub> Emissions (1751 - 2014) (V. 2017) (Carbon Dioxide Information Analysis Center, Oak Ridge National Laboratory, Oak Ridge, TN). 1999.
- Borchard, C., and Engel, A.: Size-fractionated dissolved primary production and carbohydrate composition of the coccolithophore *Emiliana huxleyi*, *Biogeosciences*, 12, 1271-1284, 10.5194/bg-12-1271-2015, 2015.

- Bouman, H., T. P., Sathyendranath, S., Li, W. K. W., Stuart, V., Fuentes-Yaco, C., Maass, H., Horne, E. P. W., Ulloa, O., Lutz, V., and Kyewalyanga, M.: Temperature as indicator of optical properties and community structure of marine phytoplankton: implications for remote sensing, *Marine Ecology Progress Series*, 258, 19-30, 2003.
- Bouman, H., Platt, T., Sathyendranath, S., and Stuart, V.: Dependence of light-saturated photosynthesis on temperature and community structure, *Deep Sea Research Part I: Oceanographic Research Papers*, 52, 1284-1299, 10.1016/j.dsr.2005.01.008, 2005.
- Boyd, P. W., and Trull, T. W.: Understanding the export of biogenic particles in oceanic waters: Is there consensus?, *Progress in Oceanography*, 72, 276-312, 10.1016/j.pocean.2006.10.007, 2007.
- Boyd, P. W., Claustre, H., Levy, M., Siegel, D. A., and Weber, T.: Multi-faceted particle pumps drive carbon sequestration in the ocean, *Nature*, 568, 327-335, 10.1038/s41586-019-1098-2, 2019.
- Bradford, M.: A rapid and sensitive method for the quantification of microgram quantities of protein utilizing the principle of protein-dye binding, *Analytical Biochemistry*, 72, 248-254, 1976.
- Bratbak, G., Egge, J. K., and Heldal, M.: Viral mortality of the marine alga *Emiliania huxleyi* (Haptophyceae) and termination of algal blooms, *Marine Ecology Progress Series*, 93, 39-48, 1993.
- Broecker, W. S., and Peng, T.-H.: Interhemispheric transport of carbon dioxide by ocean circulation, *Science*, 356, 587-589, 1992.
- Brooks, S. D., and Thornton, D. C. O.: Marine Aerosols and Clouds, *Ann Rev Mar Sci*, 10, 289-313, 10.1146/annurev-marine-121916-063148, 2018.
- Brussaard, C. P. D.: Optimization of procedures for counting viruses by flow cytometry, *Applied and Environmental Microbiology*, 70, 1506-1513, 10.1128/aem.70.3.1506-1513.2004, 2004.
- Brussaard, C. P. D., Mari, X., Bleijswijk, J. D. L. V., and Veldhuis, M. J. W.: A mesocosm study of *Phaeocystis globosa* (Prymnesiophyceae) population dynamics, *Harmful Algae*, 4, 875-893, 10.1016/j.hal.2004.12.012, 2005.
- Brussaard, C. P. D., Payet, J. P., Winter, C., and Weinbauer, M. G.: Quantification of aquatic viruses by flow cytometry, in: *Manual of Aquatic Viral Ecology*, 102-109, 2010.
- Buchan, A., LeClerc, G. R., Gulvik, C. A., and Gonzalez, J. M.: Master recyclers: features and functions of bacteria associated with phytoplankton blooms, *Nat Rev Microbiol*, 12, 686-698, 10.1038/nrmicro3326, 2014.
- Buesseler, K. O.: *Ocean Biogeochemistry and the Global Carbon Cycle: An Introduction to the U.S. Joint Global Ocean Flux Study*, 2001.
- Burd, A. B., and Jackson, G. A.: Particle aggregation, *Ann Rev Mar Sci*, 1, 65-90, 10.1146/annurev.marine.010908.163904, 2009.

- Burns, W. G., Marchetti, A., and Ziervogel, K.: Enhanced formation of transparent exopolymer particles (TEP) under turbulence during phytoplankton growth *Journal of Plankton Research*, 2019.
- Busch, K., Endres, S., Iversen, M. H., Michels, J., Nöthig, E.-M., and Engel, A.: Bacterial Colonization and Vertical Distribution of Marine Gel Particles (TEP and CSP) in the Arctic Fram Strait, *Frontiers in Marine Science*, 4, 10.3389/fmars.2017.00166, 2017.
- Calleja, M. L., Duarte, C. M., Prairie, Y. T., Agustí, S., and Herndl, G. J.: Evidence for surface organic matter modulation of air-sea CO<sub>2</sub> gas exchange, *Biogeosciences Discussions*, 5, 4209-4233, 10.5194/bgd-5-4209-2008, 2008.
- Calleja, M. L., Duarte, C. M., Prairie, Y. T., Agustí, S., and Herndl, G. J.: Evidence for surface organic matter modulation of air-sea CO<sub>2</sub> gas exchange, *Biogeosciences*, 6, 1105-1114, 2009.
- Callieri, C., Sathicq, M. B., Cabello-Yeves, P. J., Eckert, E. M., and Hernández-Avilés, J. S.: TEP production under oxidative stress of the picocyanobacterium *Synechococcus*, *Journal of Limnology*, 10.4081/jlimnol.2019.1907, 2019.
- Calvo-Díaz, A., and Morán, X. A. G.: Seasonal dynamics of picoplankton in shelf waters of the southern Bay of Biscay, *Aquatic Microbial Ecology*, 42, 159-174, 10.3354/ame042159, 2006.
- Cao, X., Aiken, G. R., Butler, K. D., Mao, J., and Schmidt-Rohr, K.: Comparison of the Chemical Composition of Dissolved Organic Matter in Three Lakes in Minnesota, *Environ Sci Technol*, 52, 1747-1755, 10.1021/acs.est.7b04076, 2018.
- Carlson, C. A., Giovannoni, S. J., Hansell, D. A., Goldberg, S. J., Parsons, R., Otero, M. P., Vergin, K., and Wheeler, B. R.: Effect of nutrient amendments on bacterioplankton production, community structure, and DOC utilization in the northwestern Sargasso Sea, *Aquatic Microbial Ecology*, 30, 19-36, 2002.
- Carlson, C. A., and Hansell, D. A.: DOM Sources, Sinks, Reactivity, and Budgets, in: *Biogeochemistry of Marine Dissolved Organic Matter*, 65-126, 2015.
- Cassar, N., Wright, S. W., Thomson, P. G., Trull, T. W., Westwood, K. J., de Salas, M., Davidson, A., Pearce, I., Davies, D. M., and Matear, R. J.: The relation of mixed-layer net community production to phytoplankton community composition in the Southern Ocean, *Global Biogeochemical Cycles*, 29, 446-462, 10.1002/2014gb004936, 2015.
- Cefarelli, A. O., Vernet, M., and Ferrario, M. E.: Phytoplankton composition and abundance in relation to free-floating Antarctic icebergs, *Deep Sea Research Part II: Topical Studies in Oceanography*, 58, 1436-1450, 10.1016/j.dsr2.2010.11.023, 2011.
- Chen, J.: Transparent exopolymer particle production and aggregation by a marine planktonic diatom (*Thalassiosira weissflogii*) at different growth rates, 10.1111/jpy.12285-14-140,

- Cherrier, J., Bauer, J. E., and Druffel, E. R. M.: Utilization and turnover of labile dissolved organic matter by bacterial heterotrophs in eastern North Pacific surface waters, *Marine Ecology Progress Series*, 139, 267-279, 1996.
- Chin, W.-C., Orellana, M. V., and Verdugo, P.: Spontaneous assembly of marine dissolved organic matter into polymer gels, *Nature*, 391, 568-572, 1998.
- Cho, J.-C., Vergin, K. L., Morris, R. M., and Giovannoni, S. J.: *Lentisphaera araneosa* gen. nov., sp. nov, a transparent exopolymer producing marine bacterium, and the description of a novel bacterial phylum, *Lentisphaerae*, *Environmental Microbiology*, 6, 611-621, 2004.
- Cisternas-Novoa, C., Lee, C., and Engel, A.: A semi-quantitative spectrophotometric, dye-binding assay for determination of Coomassie Blue stainable particles, *Limnology and Oceanography: Methods*, 12, 604-616, 10.4319/lom.2014.12.604, 2014.
- Cisternas-Novoa, C.: *Effects of a Changing Ocean on Marine Gel Particles and Implications for Aggregation, Marine and Atmospheric Science*, Stony Brook University, 2015.
- Cisternas-Novoa, C., Lee, C., and Engel, A.: Transparent exopolymer particles (TEP) and Coomassie stainable particles (CSP): Differences between their origin and vertical distributions in the ocean, *Marine Chemistry*, 175, 56-71, 10.1016/j.marchem.2015.03.009, 2015.
- Cisternas-Novoa, C., Le Moigne, F. A. C., and Engel, A.: Composition and vertical flux of particulate organic matter to the oxygen minimum zone of the central Baltic Sea: impact of a sporadic North Sea inflow, *Biogeosciences*, 16, 927-947, 10.5194/bg-16-927-2019, 2019.
- Claquin, P., Probert, I., Lefebvre, S., and Veron, B.: Effects of temperature on photosynthetic parameters and TEP production in eight species of marine microalgae, *Aquatic Microbial Ecology*, 51, 1-11, 10.3354/ame01187, 2008.
- Corzo, A., Morillo, J. A., and Rodríguez, S.: Production of transparent exopolymer particles (TEP) in cultures of *Chaetoceros calcitrans* under nitrogen limitation, *Aquatic Microbial Ecology*, 23, 63-72, 10.3354/ame023063, 2000.
- Corzo, A., Rodríguez-Gálvez, S., Lubian, L., Sangrá, P., Martínez, A., and Morillo, J. A.: Spatial distribution of transparent exopolymer particles in the Bransfield Strait, Antarctica, *Journal of Plankton Research*, 27, 635-646, 10.1093/plankt/fbi038, 2005.
- Cruz, B. N., and Neuer, S.: Heterotrophic Bacteria Enhance the Aggregation of the Marine Picocyanobacteria *Prochlorococcus* and *Synechococcus*, *Frontiers in Microbiology*, 10, 10.3389/fmicb.2019.01864, 2019.
- Cunliffe, M., Salter, M., Mann, P. J., Whiteley, A. S., Upstill-Goddard, R. C., and Murrell, J. C.: Dissolved organic carbon and bacterial populations in the gelatinous surface microlayer of a Norwegian fjord mesocosm, *FEMS Microbiol Lett*, 299, 248-254, 10.1111/j.1574-6968.2009.01751.x, 2009.

- Cunliffe, M., Engel, A., Frka, S., Gašparović, B., Guitart, C., Murrell, J. C., Salter, M., Stolle, C., Upstill-Goddard, R., and Wurl, O.: Sea surface microlayers: A unified physicochemical and biological perspective of the air–ocean interface, *Progress in Oceanography*, 109, 104-116, 10.1016/j.pocean.2012.08.004, 2013.
- Cunliffe, M., and Wurl, O.: Guide to best practices to study the ocean's surface, Occasional Publications of the Marine Biological Association of the United Kingdom,, Plymouth, UK, 2014.
- Curry, R., and Mauritzen, C.: Dilution of the northern North Atlantic Ocean in recent decades, *Science*, 308, 1772-1774, 10.1126/science.1109477, 2005.
- Dall'Osto, M., Ovadnevaite, J., Paglione, M., Beddows, D. C. S., Ceburnis, D., Cree, C., Cortes, P., Zamanillo, M., Nunes, S. O., Perez, G. L., Ortega-Retuerta, E., Emelianov, M., Vaque, D., Marrase, C., Estrada, M., Sala, M. M., Vidal, M., Fitzsimons, M. F., Beale, R., Ains, R., Rinaldi, M., Decesari, S., Cristina Facchini, M., Harrison, R. M., O'Dowd, C., and Simo, R.: Antarctic sea ice region as a source of biogenic organic nitrogen in aerosols, *Sci Rep*, 7, 6047, 10.1038/s41598-017-06188-x, 2017.
- de Carvalho, C. C., and Fernandes, P.: Production of metabolites as bacterial responses to the marine environment, *Mar Drugs*, 8, 705-727, 10.3390/md8030705, 2010.
- De Jong, E., van Rens, L., Westbroek, P., and Bosch, L.: Biocalcification by the marine alga *Emiliania huxleyi* (Lohmann) Kamptner., *Eur. J. Biochem.*, 99, 559-567, 1979.
- De La Rocha, C. L., and Passow, U.: The biological pump, in: *Treatise on Geochemistry*, edited by: Turekian, K. K., and Holland, H. D., Elsevier, Oxford, 93-122, 2014.
- de Vicente, I., Ortega-Retuerta, E., Mazuecos, I. P., Pace, M. L., Cole, J. J., and Reche, I.: Variation in transparent exopolymer particles in relation to biological and chemical factors in two contrasting lake districts, *Aquatic Sciences*, 72, 443-453, 10.1007/s00027-010-0147-6, 2010.
- Deane, G. B., and Stokes, M. D.: Scale dependence of bubble creation mechanisms in breaking waves, *Nature*, 418, 839-844, 2002.
- Decho, A. W.: Microbial exopolymer secretions in ocean environments: their role (s) in food webs and marine processes, *Oceanography and Marine Biology*, 28, 73-153, 1990.
- Decho, A. W., and Moriarty, D. J. W.: Bacterial exopolymer utilization by a harpacticoid copepod: A methodology and results, *Limnology and Oceanography*, 35, 1039-1049, 1990.
- Decho, A. W., Visscher, P. T., and Reid, R. P.: Production and cycling of natural microbial EPS (EPS) within a marine stromatolite. , *Palaeogeography, Palaeoclimatology, Palaeoecology*, 219, 71-86, 2005.
- Decho, A. W., and Gutierrez, T.: Microbial Extracellular Polymeric Substances (EPSs) in Ocean Systems, *Front Microbiol*, 8, 922, 10.3389/fmicb.2017.00922, 2017.

- Deng, W., Monks, L., and Neuer, S.: Effects of clay minerals on the aggregation and subsequent settling of marine *Synechococcus*, *Limnology and Oceanography*, 60, 805-816, 10.1002/lno.10059, 2015.
- Deng, W., Cruz, B. N., and Neuer, S.: Effects of nutrient limitation on cell growth, TEP production and aggregate formation of marine *Synechococcus*, *Aquatic Microbial Ecology*, 78, 39-49, 10.3354/ame01803, 2016.
- Dilling, L., Wilson, J., Steinberg, D., and Alldredge, A. L.: Feeding by the euphasiid *Euphasia pacifica* and the copepod *Calanus pacificus* on marine snow, *Marine Ecology Progress Series*, 170, 189-201, 1998.
- Dilling, L., and Alldredge, A. L.: Fragmentation of marine snow by swimming macrozooplankton: A new process impacting carbon cycling in the sea, *Deep Sea Res I*, 47, 1227-1245, 2000.
- Ding, Y.-X., Chin, W.-C., Rodriguez, A., Hung, C.-C., Santschi, P. H., and Verdugo, P.: Amphiphilic exopolymers from *Sagittula stellata* induce DOM self-assembly and formation of marine microgels, *Marine Chemistry*, 112, 11-19, 10.1016/j.marchem.2008.05.003, 2008.
- Discart, V., Bilad, M. R., and Vankelecom, I. F. J.: Critical Evaluation of the Determination Methods for Transparent Exopolymer Particles, Agents of Membrane Fouling, *Critical Reviews in Environmental Science and Technology*, 45, 167-192, 10.1080/10643389.2013.829982, 2014.
- Doney, S. C., Fabry, V. J., Feely, R. A., and Kleypas, J. A.: Ocean acidification: the other CO<sub>2</sub> problem, *Ann Rev Mar Sci*, 1, 169-192, 10.1146/annurev.marine.010908.163834, 2009.
- Dreshchinskii, A., and Engel, A.: Seasonal variations of the sea surface microlayer at the Boknis Eck Times Series Station (Baltic Sea), *Journal of Plankton Research*, 39, 943-961, 10.1093/plankt/fbx055, 2017.
- Druffel, E. R. M., Williams, P. M., Bauer, J. E., and Ertel, J. R.: Cycling of dissolved and particulate organic matter in the open ocean, *Journal of Geophysical Research*, 97, 10.1029/92jc01511, 1992.
- Duarte, C. M., Agustí, S., and Vaqué, D.: Controls on planktonic metabolism in the Bay of Blanes, northwestern Mediterranean littoral, *Limnology and Oceanography*, 49(6), 2162-2170, 2004.
- Ducklow, H.: Bacterial production and biomass in the oceans, in: *Microbial Ecology of the Oceans*, edited by: Kirchman, D. L., and Gasol, J. M., Wiley, NJ, USA, 2000.
- Ducklow, H., Steinberg, D., and Buesseler, K. O.: Upper Ocean Carbon Export and the Biological Pump, *Oceanography*, 14, 50-58, 2001.
- Ducklow, H. W., and Doney, S. C.: What is the metabolic state of the oligotrophic ocean? A debate, *Ann Rev Mar Sci*, 5, 525-533, 10.1146/annurev-marine-121211-172331, 2013.



- Dunne, J. P., Sarmiento, J. L., and Gnanadesikan, A.: A synthesis of global particle export from the surface ocean and cycling through the ocean interior and on the seafloor, *Global Biogeochemical Cycles*, 21, n/a-n/a, 10.1029/2006gb002907, 2007.
- Endres, S., Unger, J., Wannicke, N., Nausch, M., Voss, M., and Engel, A.: Response of *Nodularia spumigena* to pCO<sub>2</sub> – Part 2: Exudation and extracellular enzyme activities, *Biogeosciences*, 10, 567-582, 10.5194/bg-10-567-2013, 2013.
- Engel, A., and Schartau, M.: Influence of transparent exopolymer particles (TEP) on sinking velocity of *Nitzschia closterium* aggregates, *Marine Ecology Progress Series*, 182, 69-76, 10.3354/meps182069, 1999.
- Engel, A.: The role of transparent exopolymer particles (TEP) in the increase in apparent particle stickiness ( $\alpha$ ) during the decline of a diatom bloom, *Journal of Plankton Research*, 22, 485-497, 2000.
- Engel, A., and Passow, U.: Carbon and nitrogen content of transparent exopolymer particles (TEP) in relation to their Alcian Blue adsorption, *Marine Ecology Progress Series*, 219, 1-10, 2001.
- Engel, A.: Direct relationship between CO<sub>2</sub> uptake and transparent exopolymer particles production in natural phytoplankton, *Journal of Plankton Research*, 24, 49-53, 2002.
- Engel, A., Goldthwait, S., Passow, U., and Alldredge, A. L.: Temporal decoupling of carbon and nitrogen dynamics in a mesocosm diatom bloom, *Limnology and Oceanography*, 47, 753-761, 2002a.
- Engel, A., Meyerhöfer, M., and von Bröckel, K.: Chemical and Biological Composition of Suspended Particles and Aggregates in the Baltic Sea in Summer (1999), *Estuarine, Coastal and Shelf Science*, 55, 729-741, 10.1006/ecss.2001.0927, 2002b.
- Engel, A.: Distribution of transparent exopolymer particles (TEP) in the northeast Atlantic Ocean and their potential significance for aggregation processes, *Deep Sea Research Part I: Oceanographic Research Papers*, 51, 83-92, 10.1016/j.dsr.2003.09.001, 2004.
- Engel, A., Delille, B., Jacquet, S., Riebesell, U., Rochelle-Newall, E., Terbrüggen, A., and Zondervan, I.: Transparent exopolymer particles and dissolved organic carbon production by *Emiliana huxleyi* exposed to different CO<sub>2</sub> concentrations: a mesocosm experiment, *Aquatic Microbial Ecology*, 34, 93-104, 2004a.
- Engel, A., Thoms, S., Riebesell, U., Rochelle-Newall, E., and Zondervan, I.: Polysaccharide aggregation as a potential sink of marine dissolved organic carbon, *Nature*, 428, 929-932, 2004b.
- Engel, A.: Determination of Marine Gel Particles, in: *Practical Guidelines for the Analysis of Seawater*, edited by: Wurl, O., CRC Press, Taylor & Francis Group, Boca Raton, Florida, 125-142, 2009.
- Engel, A., Borchard, C., Loginova, A., Meyer, J., Hauss, H., and Kiko, R.: Effects of varied nitrate and phosphate supply on polysaccharidic and proteinaceous gel particle

- production during tropical phytoplankton bloom experiments, *Biogeosciences*, 12, 5647-5665, 10.5194/bg-12-5647-2015, 2015.
- Engel, A., and Galgani, L.: The organic sea-surface microlayer in the upwelling region off the coast of Peru and potential implications for air–sea exchange processes, *Biogeosciences*, 13, 989-1007, 10.5194/bg-13-989-2016, 2016.
- Engel, A., Piontek, J., Metfies, K., Endres, S., Sprong, P., Peeken, I., Gabler-Schwarz, S., and Nothig, E. M.: Inter-annual variability of transparent exopolymer particles in the Arctic Ocean reveals high sensitivity to ecosystem changes, *Sci Rep*, 7, 4129, 10.1038/s41598-017-04106-9, 2017.
- Ewert, M., and Deming, J. W.: Sea ice microorganisms: environmental constraints and extracellular responses, *Biology (Basel)*, 2, 603-628, 10.3390/biology2020603, 2013.
- Falkowski, P. G., Scholes, R. J., Boyle, E. A., Canadell, J. G., Canfield, D., Elser, J., Gruber, N., Hibbard, K., Högberg, P., Linder, S., Mackenzie, F. T., Moore III, B., Pedersen, T., Rosenthal, Y., Seitzinger, S., Smetacek, V., and Steffen, W.: The Global Carbon Cycle: A Test of Our Knowledge of Earth as a System, *Science*, 290, 291-296, 2000.
- Fasham, M., Baliño, B. M., Bowles, M. C., and XXX: A New Vision of Ocean Biogeochemistry After a Decade of the Joint Global Ocean Flux Study (JGOFS), *AMBIO*, 10, 4-31, 2001.
- Field, C. B., Behrenfeld, M. J., Randerson, J. T., and Falkowski, P.: Primary Production of the Biosphere: Integrating Terrestrial and Oceanic Components, *Science*, 281, 237-240, 1998.
- Field, D., and Timothy R. Baumgartner, C. D. C., 1 Vicente Ferreira-Bartrina, 2 Mark D. Ohman<sup>1</sup>: Planktonic Foraminifera of the California Current Reflect 20th-Century Warming, *Science*, 311 (5757), 63-66, 10.1021/jp053848o, 2006.
- Filella, M.: Freshwaters: which NOM matters?, *Environmental Chemistry Letters*, 7, 21-35, 10.1007/s10311-008-0158-x, 2008.
- Flemming, H. C., and Wingender, J.: Relevance of microbial extracellular polymeric substances (EPSs) – Part I: Structural and ecological aspects, *Water Science and Technology*, 43, 1-8, 2001.
- Fowler, S. W., and Knauer, G.: Role of large particles in the transport of elements and organic compounds through the oceanic water column, *Progress in Oceanography*, 16, 147-194, 1986.
- Frölicher, T. L., Sarmiento, J. L., Paynter, D. J., Dunne, J. P., Krasting, J. P., and Winton, M.: Dominance of the Southern Ocean in Anthropogenic Carbon and Heat Uptake in CMIP5 Models, *Journal of Climate*, 28, 862-886, 10.1175/jcli-d-14-00117.1, 2015.
- Fukao, T., Kitahara, S., Karino, N., Yamatogi, T., Kimoto, K., and Kotani, Y.: Dynamics of transparent exopolymer particles in spring and autumn in Isahaya Bay, Japan, *Nippon Suisan Gakkaishi*, 77 1027 – 1033, 2011.

- Galgani, L., and Engel, A.: Accumulation of Gel Particles in the Sea-Surface Microlayer during an Experimental Study with the Diatom *Thalassiosira weissflogii*, *International Journal of Geosciences*, 04, 129-145, 10.4236/ijg.2013.41013, 2013.
- Galgani, L., Piontek, J., and Engel, A.: Biopolymers form a gelatinous microlayer at the air-sea interface when Arctic sea ice melts, *Sci Rep*, 6, 29465, 10.1038/srep29465, 2016.
- Gao, Q., Leck, C., Rauschenberg, C., and Matrai, P. A.: On the chemical dynamics of extracellular polysaccharides in the high Arctic surface microlayer, *Ocean Science*, 8, 401-418, 10.5194/os-8-401-2012, 2012.
- García, C. M., Prieto, L., Vargas, M., Echevarría, F., García-Lafuente, J., Ruiz, J., and Rubín, J. P.: Hydrodynamics and the spatial distribution of plankton and TEP in the Gulf of Cádiz (SW Iberian Peninsula), *Journal of Plankton Research*, 24, 817-833, 2002.
- Gärdes, A., Iversen, M. H., Grossart, H. P., Passow, U., and Ullrich, M. S.: Diatom-associated bacteria are required for aggregation of *Thalassiosira weissflogii*, *ISME J*, 5, 436-445, 10.1038/ismej.2010.145, 2011.
- Gärdes, A., Ramaye, Y., Grossart, H. P., Passow, U., and Ullrich, M. S.: Effects of *Marinobacter adhaerens* HP15 on polymer exudation by *Thalassiosira weissflogii* at different N:P ratios, *Marine Ecology Progress Series*, 461, 1-14, 10.3354/meps09894, 2012.
- Gasol, J. M., and Morán, X. A. G.: Effects of filtration on bacterial activity and picoplankton community structure as assessed by flow cytometry, *Aquatic Microbial Ecology*, 16, 251-264, 1999.
- Gasol, J. M., and del Giorgio, P. A.: Using flow cytometry for counting natural planktonic bacteria and understanding the structure of planktonic bacterial communities, *Scientia Marina*, 64, 197-224, 2000.
- Gasol, J. M., Massana, R., Simó, R., Marrasé, C., Acinas, S. G., Pedrós-Alió, C., Pelejero, C., Sala, M. M., Calvo, E., Vaqué, D., and Peters, F.: Blanes Bay, in: ICES Phytoplankton and Microbial Ecology Status Report 2010/2012, edited by: O'Brien, T. D., Li, W. K. W., and Morán, X. A. G., 138-141, 2012.
- Gasol, J. M., Cardelús, C., G. Morán, X. A., Balagué, V., Forn, I., Marrasé, C., Massana, R., Pedrós-Alió, C., Montserrat Sala, M., Simó, R., Vaqué, D., and Estrada, M.: Seasonal patterns in phytoplankton photosynthetic parameters and primary production at a coastal NW Mediterranean site, *Scientia Marina*, 80, 63-77, 10.3989/scimar.04480.06E, 2016.
- Geider, R. J., Macintyre, H. L., and Kana, T. M.: A dynamic regulatory model of phytoplankton acclimation to light, nutrients, and temperature, *Limnology and Oceanography*, 43, 679-694, 1998.
- Giering, S. L. C., and Humphreys, M. P.: Biological Pump, in: *Encyclopedia of Geochemistry*, *Encyclopedia of Earth Sciences Series*, 1-6, 2018.

- Gobler, C. J., Hutchins, D. A., Fisher, N. S., Cosper, E. M., and Safiudo-Wilhelmy, S. A.: Release and bioavailability Inc. of C, N, e Se, and Fe following viral lysis of a marine chrysophyte, *Limnology and Oceanography*, 42, 1492-1504, 1997.
- González-Fernández, C., Toullec, J., Lambert, C., Le Goïc, N., Seoane, M., Moriceau, B., Huvet, A., Berchel, M., Vincent, D., Courcot, L., Soudant, P., and Paul-Pont, I.: Do transparent exopolymeric particles (TEP) affect the toxicity of nanoplastics on *Chaetoceros neogracile*?, *Environmental Pollution*, 10.1016/j.envpol.2019.04.093, 2019.
- Gordon, A.: Brazil--Malvinas Confluence---1984, *Deep Sea Research*, 36, 359-384, 1989.
- Gordon, D. C.: A microscopic study of organic particles in the North Atlantic Ocean, *Deep Sea Res I*, 17, 175-185, 1970.
- Görs, S., Rentsch, D., Schiewer, U., Karsten, U., and Schumann, R.: Dissolved organic matter along the eutrophication gradient of the Darß-Zingst Bodden Chain, Southern Baltic Sea: I. Chemical characterisation and composition, *Marine Chemistry*, 104, 125-142, 10.1016/j.marchem.2006.10.009, 2007.
- Grossart, H.: Interactions between marine bacteria and axenic diatoms (*Cylindrotheca fusiformis*, *Nitzschia laevis*, and *Thalassiosira weissflogii*) incubated under various conditions in the lab, *Aquatic Microbial Ecology*, 19, 1-11, 1999.
- Grossart, H., Engel, A., Arnosti, C., De La Rocha, C. L., Murray, A. E., and Passow, U.: Microbial dynamics in autotrophic and heterotrophic seawater mesocosms. III. Organic matter fluxes, *Aquatic Microbial Ecology*, 49, 143-156, 10.3354/ame01140, 2007.
- Grossart, H. P., and Simon, M.: Formation of macroscopic organic aggregates (lake snow) in a large lake: The significance of transparent exopolymer particles, phytoplankton, and zooplankton, *Limnology and Oceanography*, 42 (8), 1651-1659, 1997.
- Grossart, H. P., Berman, T., Simon, M., and Pohlmann, K.: Occurrence and microbial dynamics of macroscopic organic aggregates (lake snow) in Lake Kinneret, Israel, in fall, *Aquatic Microbial Ecology*, 14, 59-67, 10.3354/ame014059, 1998.
- Grossart, H. P., Czub, G., and Simon, M.: Algae-bacteria interactions and their effects on aggregation and organic matter flux in the sea, *Environ Microbiol*, 8, 1074-1084, 10.1111/j.1462-2920.2006.00999.x, 2006.
- Gruber, N.: The oceanic sink for anthropogenic CO<sub>2</sub> from 1994 to 2007, *Science*, 2019.
- Guadayol, Ò., Marrasé, C., Peters, F., Berdalet, E., Roldán, C., and Sabata, A.: Responses of coastal osmotrophic planktonic communities to simulated events of turbulence and nutrient load throughout a year, *Journal of Plankton Research*, 31, 583-600, 10.1093/plankt/fbp019, 2009.
- Guerrini, F., Mazzotti, A., Boni, L., and Pistocchi, R.: Bacterial– algal interactions in polysaccharide production, *Aquatic Microbial Ecology*, 15, 247-253, 1998.

- Guo, L., Hung, C.-C., Santschi, P. H., and Walsh, I. D.: 234Th scavenging and its relationship to acid polysaccharide abundance in the Gulf of Mexico, *Marine Chemistry*, 78, 103-119, 2002.
- Gutiérrez-Rodríguez, A., Latasa, M., Estrada, M., Vidal, M., and Marrasé, C.: Carbon fluxes through major phytoplankton groups during the spring bloom and post-bloom in the Northwestern Mediterranean Sea, *Deep Sea Research Part I: Oceanographic Research Papers*, 57, 486-500, 10.1016/j.dsr.2009.12.013, 2010.
- Han, P. P., Sun, Y., Zhong, C., and L, T. Z.: Effects of light wavelengths on extracellular and capsular polysaccharide production by *Nostoc flagelliforme*, *Carbohydrate Polymers*, 105, 145-151, 2014.
- Hansell, D., Carlson, C., Repeta, D., and Schlitzer, R.: Dissolved Organic Matter in the Ocean: A Controversy Stimulates New Insights, *Oceanography*, 22, 202-211, 10.5670/oceanog.2009.109, 2009.
- Hansell, D. A., and Carlson, C. A.: Marine dissolved organic carbon and the Carbon Cycle, *Oceanography*, 14, 2001.
- Hansell, D. A., and Carlson, C. A.: *Biogeochemistry of Marine Dissolved Organic Matter*, 2002.
- Hansell, D. A.: Recalcitrant dissolved organic carbon fractions, *Ann Rev Mar Sci*, 5, 421-445, 10.1146/annurev-marine-120710-100757, 2013.
- Hansen, H. P., and Grasshoff, K.: Procedures for the automated determination of seawater constituents, in: *Methods of seawater analysis*, second, revised and extended edition ed., edited by: Grasshoff, K., Kremling, K., and Ehrhardt, M., Wiley, Weinheim, Germany, 1983.
- Harlay, J., De Bodt, C., Engel, A., Jansen, S., d'Hoop, Q., Piontek, J., Van Oostende, N., Groom, S., Sabbe, K., and Chou, L.: Abundance and size distribution of transparent exopolymer particles (TEP) in a coccolithophorid bloom in the northern Bay of Biscay, *Deep Sea Research Part I: Oceanographic Research Papers*, 56, 1251-1265, 10.1016/j.dsr.2009.01.014, 2009.
- Harlay, J., Borges, A. V., Van Der Zee, C., Delille, B., Godoi, R. H. M., Schiettecatte, L. S., Roevros, N., Aerts, K., Lapernat, P. E., Rebreaun, L., Groom, S., Daro, M. H., Van Grieken, R., and Chou, L.: Biogeochemical study of a coccolithophore bloom in the northern Bay of Biscay (NE Atlantic Ocean) in June 2004, *Progress in Oceanography*, 86, 317-336, 10.1016/j.pocan.2010.04.029, 2010.
- Hayat, M. A.: *Principles and techniques of electron microscopy: biological applications.*, *Annals of Botany*, 4, Cambridge University Press., 2000.
- Hedges, J. I., Eglinton, G., Hatcher, P. G., Kirchman, D. L., Arnosti, C., Derenne, S., Evershed, R. P., Kögel-Knabner, I., de Leeuw, J. W., Littke, R., Michaelis, W., and Rullkötter, J.: The molecularly-uncharacterized component of nonliving organic matter in natural environments, *Organic Geochemistry*, 31, 945-958, 2000.

- Hedges, J. I., Baldock, J. A., Gélina, Y., Lee, C., Peterson, M. L., and Wakeham, S. G.: The biochemical and elemental compositions of marine plankton: A NMR perspective, 2002.
- Heinonen, K. B., Ward, J. E., and Holohan, B. A.: Production of transparent exopolymer particles (TEP) by benthic suspension feeders in coastal systems, *Journal of Experimental Marine Biology and Ecology*, 341, 184-195, 10.1016/j.jembe.2006.09.019, 2007.
- Henson, S. A., Sanders, R., Madsen, E., Morris, P. J., Le Moigne, F., and Quartly, G. D.: A reduced estimate of the strength of the ocean's biological carbon pump, *Geophysical Research Letters*, 38, n/a-n/a, 10.1029/2011gl046735, 2011.
- Henson, S. A., Yool, A., and Sanders, R.: Variability in efficiency of particulate organic carbon export: A model study, *Global Biogeochemical Cycles*, 29, 33-45, 10.1002/2014gb004965, 2015.
- Hernández-León, S., Putzeys, S., Almeida, C., Bécognée, P., Marrero-Díaz, A., Arístegui, J., and Yebra, L.: Carbon export through zooplankton active flux in the Canary Current, *Journal of Marine Systems*, 189, 12-21, 10.1016/j.jmarsys.2018.09.002, 2019.
- Hewes, C. D., and Holm-Hansen, O.: A method for recovering nanoplankton from filters for identification with the microscope: The filter-transfer-freeze (FTF) technique, *Limnology and Oceanography*, 28, 389-394, 1983.
- Higgins, H. W., Wright, S. W., and Schlüter, L.: Quantitative interpretation of chemotaxonomic pigment data, *Phytoplankton Pigments*, in: *Characterization, Chemotaxonomy and Applications in Oceanography*, edited by: Roy, S., Llewellyn, C. A., Egeland, E. S., and Johnsen, G., Cambridge University Press, Cambridge, 257-313, 2011.
- Hoagland, K. D., Rosowski, J. R., Gretz, M. R., and Roemer, S. C.: Diatom extracellular polymeric substances: function, fine structure, chemistry, and physiology, *Journal of Phycology*, 29, 537-566, 1993.
- Hong, Y., Smith, W. O., and White, A.-M.: Studies of transparent exopolymer particles (TEP) produced in the Ross Sea (Antarctica) and by *Phaeocystis antarctica* (Prymnesiophyceae), *Journal of Phycology*, 33, 368 – 376, 1997.
- Honjo, S.: Material fluxes and modes of sedimentation in the mesopelagic and bathypelagic zones *J mar Res*, 38, 53-97, 1980.
- Honjo, S., Eglinton, T., Taylor, C., Ulmer, K., Sievert, S., Bracher, A., German, C., Edgcomb, V., Francois, R., Iglesias-Rodriguez, M. D., Van Mooy, B., and Rapeta, D.: Understanding the Role of the Biological Pump in the Global Carbon Cycle: An Imperative for Ocean Science, *Oceanography*, 27, 10-16, 10.5670/oceanog.2014.78, 2014.
- Hopkinson, C. S., and Vallino, J.: Efficient export of carbon to the deep ocean through dissolved organic matter, *Nature*, 433, 142-145, 2005.

- Hoppe, C. J. M., Klaas, C., Ossebaar, S., Soppa, M. A., Cheah, W., Laglera, L. M., Santos-Echeandia, J., Rost, B., Wolf-Gladrow, D. A., Bracher, A., Hoppema, M., Strass, V., and Trimborn, S.: Controls of primary production in two phytoplankton blooms in the Antarctic Circumpolar Current, *Deep Sea Res Part 2 Top Stud Oceanogr*, 138, 63-73, 10.1016/j.dsr2.2015.10.005, 2017.
- Horobin, R. W.: Understanding histochemistry: selection, evaluation and design of biological stains, in, Ellis Horwood Ltd, Chichester, 1988.
- Houghton, R. A., and Nassikas, A. A.: Global and regional fluxes of carbon from land use and land cover change 1850-2015, *Global Biogeochemical Cycles*, 31, 456-472, 10.1002/2016gb005546, 2017.
- Hu, S., and Smith Jr., W. O.: The effects of irradiance on nitrate uptake and dissolved organic nitrogen release by phytoplankton in the Ross Sea, *Continental Shelf Research*, 18, 971-990, 1998.
- Hugler, M., and Sievert, S. M.: Beyond the Calvin cycle: autotrophic carbon fixation in the ocean, *Ann Rev Mar Sci*, 3, 261-289, 10.1146/annurev-marine-120709-142712, 2011.
- Hung, C.-C., Guo, L., Santschi, P. H., Alvarado-Quiroz, N., and Haye, J. M.: Distributions of carbohydrate species in the Gulf of Mexico, *Marine Chemistry*, 81, 119-135, 10.1016/S0304-4203(03)00012-4, 2003a.
- Hung, C.-C., Guo, L., Schultz Jr, G. E., Pinckney, J. L., and Santschi, P. H.: Production and flux of carbohydrate species in the Gulf of Mexico, *Global Biogeochemical Cycles*, 17 (2), 10.1029/2002GB001988, 2003b.
- Hunt, D. E., Ortega-Retuerta, E., and Nelson, C. E.: Connections between bacteria and organic matter in aquatic ecosystems: Linking microscale ecology to global carbon cycling., *Eco-DAS VIII Symposium Proceedings*, 110-128, 10.4319/ecodas.2010.978-0-9845591-1-4.110, 2010.
- Iuculano, F., Duarte, C. M., Marbà, N., and Agustí, S.: Seagrass as major source of transparent exopolymer particles in the oligotrophic Mediterranean coast, *Biogeosciences*, 14, 5069-5075, 10.5194/bg-14-5069-2017, 2017a.
- Iuculano, F., Duarte, C. M., Marbà, N., and Agustí, S.: Seagrass as major source of transparent exopolymer particles in the oligotrophic Mediterranean coast, *Biogeosciences Discussions*, 1-12, 10.5194/bg-2016-558, 2017b.
- Iuculano, F., Mazuecos, I. P., Reche, I., and Agusti, S.: *Prochlorococcus* as a Possible Source for Transparent Exopolymer Particles (TEP), *Front Microbiol*, 8, 709, 10.3389/fmicb.2017.00709, 2017c.
- Jähmlich, S., Thomsen, L., and Graf, G.: Factors controlling aggregate formation in the benthic boundary layer of the Mecklenburg Bight (western Baltic Sea), *Journal of Sea Research*, 41, 245-254, 1998.
- Jeffrey, S. W.: Profiles of Photosynthetic Pigments in the Ocean Using Thin-Layer Chromatography, *Marine Biology*, 26, 101-110, 1974.

- Jenkinson, I. R., Seuront, L., Ding, H., and Elias, F.: Biological modification of mechanical properties of the sea surface microlayer, influencing waves, ripples, foam and air-sea fluxes, *Elem Sci Anth*, 6:26, 1-32, 10.1525/journal.elementa.283, 2018.
- Jennings, M. K., Passow, U., Wozniak, A. S., and Hansell, D. A.: Distribution of transparent exopolymer particles (TEP) across an organic carbon gradient in the western North Atlantic Ocean, *Marine Chemistry*, 190, 1-12, 10.1016/j.marchem.2017.01.002, 2017.
- Jiao, N., Herndl, G. J., Hansell, D. A., Benner, R., Kattner, G., Wilhelm, S. W., Kirchman, D. L., Weinbauer, M. G., Luo, T., Chen, F., and Azam, F.: Microbial production of recalcitrant dissolved organic matter: long-term carbon storage in the global ocean, *Nat Rev Microbiol*, 8, 593-599, 10.1038/nrmicro2386, 2010.
- Jurado, E., Dachs, J., Duarte, C. M., and Simó, R.: Atmospheric deposition of organic and black carbon to the global oceans, *Atmospheric Environment*, 42, 7931-7939, 10.1016/j.atmosenv.2008.07.029, 2008.
- Kahl, L. A., Vardi, A., and Schofield, O.: Effects of phytoplankton physiology on export flux, *Marine Ecology Progress Series*, 354, 3-19, 10.3354/meps07333, 2008.
- Kaiblinger, C., Greisberger, S., Teubner, K., and Dokulil, M. T.: Photosynthetic efficiency as a function of thermal stratification and phytoplankton size structure in an oligotrophic alpine lake, *Hydrobiologia*, 578, 29-36, 10.1007/s10750-006-0430-7, 2007.
- Karavoltos, S., Kalambokis, E., Sakellari, A., Plavsic, M., Dotsika, E., Karalis, P., Leondiadis, L., Dassenakis, M., and Scoullou, M.: Organic matter characterization and copper complexing capacity in the sea surface microlayer of coastal areas of the Eastern Mediterranean, *Marine Chemistry*, 173, 234-243, 2015.
- Kennedy, A. F. D., and Sutherland, I. W.: Analysis of bacterial exopolysaccharides, *Biotechnol. Appl. Biochem*, 9, 12-19, 1987.
- Kiefer, D. A., Olson, R. J., and Holm-Hansen, O.: Another look at the nitrite and chlorophyll maxima in the central North Pacific, *Deep Sea Research*, 23, 1199-1208, 1976.
- Kiorboe, T., Hansen, J. L. S., Alldredge, A. L., Jackson, G. A., Passow, U., Dam, H. G., Drapeau, D. T., Waite, A., and Garcia, C. M.: Sedimentation of phytoplankton during a diatom bloom: Rates and mechanisms, *Journal of Marine Science*, 54, 1123-1148, 1996.
- Kiorboe, T., and Thygesen, U. H.: Fluid motion and solute distribution around sinking aggregates. II. Implications for remote detection by colonizing zooplankters, 211, 15-25, 2001.
- Kirchman, D. L., K'Neas, E., and Hodson, R.: Leucine Incorporation and Its Potential as a Measure of Protein Synthesis by Bacteria in Natural Aquatic Systems, *Applied and Environmental Microbiology*, 49, 599-607, 1985.
- Kirk, J. T. P.: *Light and photosynthesis in aquatic ecosystems*, edited by: Ed., n., Cambridge University Press, 1994.



- Klein, C., Claquin, P., Pannard, A., Napoléon, C., Le Roy, B., and Véron, B.: Dynamics of soluble extracellular polymeric substances and transparent exopolymer particle pools in coastal ecosystems, *Marine Ecology Progress Series*, 427, 13-27, 10.3354/meps09049, 2011.
- Kodama, T., Kurogi, H., Okazaki, M., Jinbo, T., Chow, S., Tomoda, T., Ichikawa, T., and Watanabe, T.: Vertical distribution of transparent exopolymer particle (TEP) concentration in the oligotrophic western tropical North Pacific, *Marine Ecology Progress Series*, 513, 29-37, 10.3354/meps10954, 2014.
- Kozłowski, W., and Vernet, M.: Palmer LTER: Predominance of cryptomonads and diatoms in antarctic coastal waters, *Antarctic Journal of the United States*, 30, 267-268, 1995.
- Kozłowski, W. A., Deutschman, D., Garibotti, I., Trees, C., and Vernet, M.: An evaluation of the application of CHEMTAX to Antarctic coastal pigment data, *Deep Sea Research Part I: Oceanographic Research Papers*, 58, 350-364, 10.1016/j.dsr.2011.01.008, 2011.
- Kumar, M. D., Sarma, V. V. S. S., Ramaiah, N., Gauns, M., and de Sousa, S. N.: Biogeochemical significance of transport exopolymer particles in the Indian Ocean, *Geophysical Research Letters*, 25, 81-84, 10.1029/97gl03481, 1998.
- Kuznetsova, M., Lee, C., and Aller, J.: Characterization of the proteinaceous matter in marine aerosols, *Marine Chemistry*, 96, 359-377, 10.1016/j.marchem.2005.03.007, 2005.
- Kwon, E. Y., Primeau, F., and Sarmiento, J. L.: The impact of remineralization depth on the air-sea carbon balance, *Nature Geoscience*, 2, 630-635, 2009.
- Latasa, M.: A simple method to increase sensitivity for RP-HPLC phytoplankton pigment analysis, *Limnology and Oceanography: Methods*, 12, 46-53, 10.4319/lom.2014.12.46, 2014.
- Lebaron, P., Servais, P., Agogue, H., Courties, C., and Joux, F.: Does the high nucleic acid content of individual bacterial cells allow us to discriminate between active cells and inactive cells in aquatic systems?, *Appl Environ Microbiol*, 67, 1775-1782, 10.1128/AEM.67.4.1775-1782.2001, 2001.
- Leblanc, K., Hare, C. E., Feng, Y. y., Berg, G. M., DiTullio, G. R., Neeley, A., Benner, I., Sprengel, C., Beck, A., Sanudo-Wilhelmy, S. A., Passow, U., Klinck, K., Rowe, J. M., Wilhelm, S. W., Brown, C. W., and Hutchins, D. A.: Distribution of calcifying and silicifying phytoplankton in relation to environmental and biogeochemical parameters during the late stages of the 2005 North East Atlantic Spring Bloom, *Biogeosciences*, 6, 1-25, 2009.
- Leck, C., and Bigg, E. K.: Biogenic particles in the surface microlayer and overlying atmosphere in the central Arctic Ocean during summer, *X*, 57B, 305-316, 2005.
- Leck, C., Gao, Q., Mashayekhy Rad, F., and Nilsson, U.: Size-resolved atmospheric particulate polysaccharides in the high summer Arctic, *Atmospheric Chemistry and Physics*, 13, 12573-12588, 10.5194/acp-13-12573-2013, 2013.

- Legendre, L., and Le Fèvre, J.: Microbial food webs and the export of biogenic carbon in oceans \*, *Aquatic Microbial Ecology*, 9, 69-77, 1995.
- Lemarchand, C., Jardillier, L., Carrias, J. F., Richardot, M., Debroas, D., Sime-Ngando, T., and Amblard, C.: Community composition and activity of prokaryotes associated to detrital particles in two contrasting lake ecosystems, *FEMS Microbiol Ecol*, 57, 442-451, 10.1111/j.1574-6941.2006.00131.x, 2006.
- Ling, S., and Alldredge, A. L.: Does the marine copepod *Calanus pacificus* consume transparent exopolymer particles (TEP)?, *Journal of Plankton Research*, 25, 507-515, 2003.
- Logan, B. E., Grossart, H. P., and M., S.: Direct observation of phytoplankton, TEP and aggregates on polycarbonate filters using brightfield microscopy, 1994.
- Logan, B. E., Passow, U., Alldredge, A. L., Grossart, H. P., and Simon, M.: Rapid formation and sedimentation of large aggregates is predictable from coagulation rates (half-lives) of transparent exopolymer particles (TEP), *Deep Sea Research Part II: Topical Studies in Oceanography*, 42, 203-214, 1995.
- Lønborg, C., Middelboe, M., and Brussaard, C. P. D.: Viral lysis of *Micromonas pusilla*: impacts on dissolved organic matter production and composition, *Biogeochemistry*, 116, 231-240, 10.1007/s10533-013-9853-1, 2013.
- Long, M., Moriceau, B., Gallinari, M., Lambert, C., Huvet, A., Raffray, J., and Soudant, P.: Interactions between microplastics and phytoplankton aggregates: Impact on their respective fates, *Marine Chemistry*, 175, 39-46, 10.1016/j.marchem.2015.04.003, 2015.
- Long, R. A., and Azam, F.: Abundant protein-containing particles in the sea, *Aquatic Microbial Ecology*, 10, 213-221, 1996.
- Longhurst, A. R.: *Ecological Geography of the Sea*, Second Edition ed., Academic Press, San Diego, Academic Press, 402 pp., 1998.
- López-Sandoval, D. C., Fernández, A., and Marañón, E.: Dissolved and particulate primary production along a longitudinal gradient in the Mediterranean Sea, *Biogeosciences*, 8, 815-825, 10.5194/bg-8-815-2011, 2011.
- Louis, J., Pedrotti, M. L., Gazeau, F., and Guieu, C.: Experimental evidence of formation of transparent exopolymer particles (TEP) and POC export provoked by dust addition under current and high pCO<sub>2</sub> conditions, *PLoS One*, 12, e0171980, 10.1371/journal.pone.0171980, 2017.
- Lucea, A., Duarte, C. M., Agustí, S., and Kennedy, H.: Nutrient dynamics and ecosystem metabolism in the Bay of Blanes (NW Mediterranean), *Biogeochemistry*, 73, 303-323, 10.1007/s10533-004-0059-4, 2005.
- Mackey, M. D., Mackey, D. J., Higgings, H. W., and Wright, S. W.: CHEMTAX- a program for estimating class abundances from chemical markers: application to HPLC measurements of phytoplankton, *Marine Ecology Progress Series*, 144, 265-283, 1996.

- Majumdar, I., D'souza, F., and Bhosle, N. B.: Microbial exopolysaccharides: Effect on corrosion and partial chemical characterization, *J Indian Inst. Sci.*, 79, 539-550, 1999.
- Marchant, H. J., Watanabe, K., and Kawachi, M.: Marine snow in Antarctic coastal waters, *Polar Biology*, 9, 75-83, 1996.
- Mari, X., and Kiorboe, T.: Abundance, size distribution and bacterial colonization of transparent exopolymeric particles (TEP) during spring in the Kattegat, *Journal of Plankton Research*, 18, 969-986, 1996.
- Mari, X., and Burd, A.: Seasonal size spectra of transparent exopolymeric particles (TEP) in a coastal sea and comparison with those predicted using coagulation theory, 1998.
- Mari, X.: Carbon content and C:N ratio of transparent exopolymeric particles (TEP) produced by bubbling exudates of diatoms, *Marine Ecology Progress Series*, 183, 59-71, 1999.
- Mari, X., Beauvais, S., Lemée, R., and Pedrotti, M. L.: Non-Redfield C:N ratio of transparent exopolymeric particles in the northwestern Mediterranean Sea, *Limnology and Oceanography*, 46, 1831-1836, 2001.
- Mari, X., and Dam, H. G.: Production, concentration, and isolation of transparent exopolymeric particles using paramagnetic functionalized microspheres, *Limnology and Oceanography: Methods*, 2, 13-24, 2004.
- Mari, X., and Rassoulzadegan, F.: Role of TEP in the microbial food web structure. I. Grazing behavior of a bacterivorous pelagic ciliate, *Marine Ecology Progress Series*, 279, 13-22, 2004.
- Mari, X., Rassoulzadegan, F., Brussaard, C. P. D., and Wassmann, P.: Dynamics of transparent exopolymeric particles (TEP) production by *Phaeocystis globosa* under N- or P-limitation: a controlling factor of the retention/export balance, *Harmful Algae*, 4, 895-914, 10.1016/j.hal.2004.12.014, 2005.
- Mari, X., Rochelle-Newall, E., Torrétón, J.-P., Pringault, O., and Jouon, A.: Water residence time: A regulatory factor of the DOM to POM transfer efficiency, *Limnology and Oceanography*, 52(2), 808-819, 2007.
- Mari, X.: Does ocean acidification induce an upward flux of marine aggregates?, *Biogeosciences*, 5, 1023-1031, 2008.
- Mari, X., and Robert, M.: Metal induced variations of TEP sticking properties in the southwestern lagoon of New Caledonia, *Marine Chemistry*, 110, 98-108, 10.1016/j.marchem.2008.02.012, 2008.
- Mari, X., Torrétón, J.-P., Bich-Thuy Trinh, C., Bouvier, T., Van Thuoc, C., Lefebvre, J.-P., and Ouillon, S.: Aggregation dynamics along a salinity gradient in the Bach Dang estuary, North Vietnam, *Estuarine, Coastal and Shelf Science*, 96, 151-158, 10.1016/j.ecss.2011.10.028, 2012.

- Mari, X., Passow, U., Migon, C., Burd, A. B., and Legendre, L.: Transparent exopolymer particles: Effects on carbon cycling in the ocean, *Progress in Oceanography*, 151, 13-37, 10.1016/j.pocean.2016.11.002, 2017.
- Marinov, I., Gnanadesikan, A., Sarmiento, J. L., Toggweiler, J. R., Follows, M., and Mignone, B. K.: Impact of oceanic circulation on biological carbon storage in the ocean and atmospheric  $p\text{CO}_2$ , *Global Biogeochemical Cycles*, 22, 1-15, 10.1029/2007gb002958, 2008.
- Marra, J.: Approaches to the measurement of plankton production, in: *Phytoplankton Productivity: Carbon Assimilation in Marine and Freshwater Ecosystems*, edited by: Williams, P. J., Thomas, D. N., and Reynolds, C. S., Oxford, UK, 78-108, 2002.
- Mayol, E., Arrieta, J. M., Jimenez, M. A., Martinez-Asensio, A., Garcias-Bonet, N., Dachs, J., Gonzalez-Gaya, B., Royer, S. J., Benitez-Barrios, V. M., Fraile-Nuez, E., and Duarte, C. M.: Long-range transport of airborne microbes over the global tropical and subtropical ocean, *Nat Commun*, 8, 201, 10.1038/s41467-017-00110-9, 2017.
- Mazuecos, I. P.: Exopolymer particles in the ocean: in the ocean: Production by microorganisms, carbon export and by microorganisms, carbon export and ation mesopelagic respiration, Ph.D. thesis, University of Granada, Spain, 281 pp., 2015.
- Menden-Deuer, S., and Lessard, E. J.: Carbon to volume relationships for dinoflagellates, diatoms, and other protist plankton, *Limnology and Oceanography*, 45, 569-579, 2000.
- Mendes, C. R. B., Kerr, R., Tavano, V. M., Cavalheiro, F. A., Garcia, C. A. E., Dessai, D. R. G., and Anilkumar, N.: Cross-front phytoplankton pigments and chemotaxonomic groups in the Indian sector of the Southern Ocean, *Deep Sea Research Part II: Topical Studies in Oceanography*, 118, 221-232, 10.1016/j.dsr2.2015.01.003, 2015.
- Meng, S., Rzechowicz, M., Winters, H., Fane, A. G., and Liu, Y.: Transparent exopolymer particles (TEP) and their potential effect on membrane biofouling, *Appl Microbiol Biotechnol*, 97, 5705-5710, 10.1007/s00253-013-4979-6, 2013.
- Millero, F. J.: The Marine Inorganic Carbon Cycle, *Chem Rev*, 107, 308-341, 2007.
- Mishra, A., and Jha, B.: Isolation and characterization of extracellular polymeric substances from micro-algae *Dunaliellasalina* under salt stress, *Bioresour Technol*, 100, 3382-3386, 10.1016/j.biortech.2009.02.006, 2009.
- Mitchell, J. F. B., Johns, T. C., Gregory, J. M., and Tett, S. F. B.: Climate response to increasing levels of greenhouse gases and sulphate aerosols, *Nature*, 376, 501-504, 1995.
- Mohamed, M. N., Lawrence, J. R., and Robarts, R. D.: Phosphorus Limitation of Heterotrophic Biofilms from the Fraser River, British Columbia, and the Effect of Pulp Mill Effluent, *Microb Ecol*, 36, 121-130, 1998.
- Mojica, K. D., Huisman, J., Wilhelm, S. W., and Brussaard, C. P.: Latitudinal variation in virus-induced mortality of phytoplankton across the North Atlantic Ocean, *ISME J*, 10, 500-513, 10.1038/ismej.2015.130, 2016.

- Møller, E. F., Thor, P., and Nielsen, T. G.: Production of DOC by *Calanus finmarchicus*, *C. glacialis* and *C. hyperboreus* through sloppy feeding and leakage from fecal pellets, *Marine Ecology Progress Series*, 262, 185-191, 2003.
- Møller, E. F.: Production of dissolved organic carbon by sloppy feeding in the copepods *Acartia tonsa*, *Centropages typicus*, and *Temora longicornis*, *Limnology and Oceanography*, 52(1), 79-84, 2007.
- Monterey, G., and Levitus, S.: Seasonal variability of mixed layer depth for the world ocean, NOAA ATLAS, NESDIS, 14, 96 pp, 1997.
- Moore, C. M., Mills, M. M., Arrigo, K. R., Berman-Frank, I., Bopp, L., Boyd, P. W., Galbraith, E. D., Geider, R. J., Guieu, C., Jaccard, S. L., Jickells, T. D., La Roche, J., Lenton, T. M., Mahowald, N. M., Marañón, E., Marinov, I., Moore, J. K., Nakatsuka, T., Oschlies, A., Saito, M. A., Thingstad, T. F., Tsuda, A., and Ulloa, O.: Processes and patterns of oceanic nutrient limitation, *Nature Geoscience*, 6, 701-710, 10.1038/ngeo1765, 2013.
- Mopper, K., Schultz, C. A., Chevolut, L., Germain, C., Revuelta, R., and Dawson, R.: Determination of Sugars in Unconcentrated Seawater and Other Natural Waters by Liquid Chromatography and Pulsed Amperometric Detection, *Environ. Sci. Technol.*, 26, 133-138, 1991.
- Mopper, K., Zou, J., Ramana, K. S., Passow, U., Dam, H. G., and Drapeau, D. T.: The role of surface-active carbohydrates in the flocculation of a diatom bloom in a mesocosm, *Deep Sea Res Part 2 Top Stud Oceanogr*, 42, 47-73, 1995.
- Morris, P. J., and Sanders, R.: A carbon budget for a naturally iron fertilized bloom in the Southern Ocean, *Global Biogeochemical Cycles*, 25, n/a-n/a, 10.1029/2010gb003780, 2011.
- Mueller, J. L., Morel, A., Frouin, R., Davis, C. O., Arnone, R. A., Carder, K. L., Lee, Z., Steward, R. G., Hooker, S. B., Mobley, C. D., McLean, S., Holben, B. N., Miller, M., Pietras, C., Knobelspiesse, K. D., Fargion, G. S., Porter, J., and Voss, J. L.: Ocean optics protocols for satellite ocean color sensor validation, revision 4, volume III: radiometric measurements and data analysis protocols. , *Ocean Opt. Protoc. Satell. Ocean Color Sens*, 4 (III), 78, 2003.
- Myklesstad, S.: Production of carbohydrates by marine planktonic diatoms. , *J. exp. mar. Biol. Ecol.*, 29, 161-179, 1977.
- Myklesstad, S.: Release of extracellular products by phytoplankton with special emphasis on polysaccharides, 1995.
- Nagata, T.: Production mechanisms of dissolved organic matter., in: Kirchman, D.L. (Ed.) *Microbial Ecology of the Oceans*, Wiley-Liss Inc., New York, 121-152, 2000.
- Nicolaus, B., Panico, A., Lama, L., Romano, I., Manca, M. C., De Giulio, A., and Gambacorta, A.: Chemical composition and production of exopolysaccharides from representative members of heterocystous and non-heterocystous cyanobacteria, *Phytochemistry*, 52, 639-647, 1999.

- Nissimov, J. I., Vandzura, R., Johns, C. T., Natale, F., Haramaty, L., and Bidle, K. D.: Dynamics of transparent exopolymer particle production and aggregation during viral infection of the coccolithophore, *Emiliania huxleyi*, *Environ Microbiol*, 20, 2880-2897, 10.1111/1462-2920.14261, 2018.
- Norland, S.: The relationship between biomass and volume of bacteria, in: Handbook of methods in aquatic microbial ecology, edited by: Kemp PF, S. B., Sherr EB, Cole JJ (eds), Lewis Publishers, Boca Raton, 303-307, 1993.
- Norris, S. J., Brooks, I. M., de Leeuw, G., Sirevaag, A., Leck, C., Brooks, B. J., Birch, C. E., and Tjernström, M.: Measurements of bubble size spectra within leads in the Arctic summer pack ice, *Ocean Science*, 7, 129-139, 10.5194/os-7-129-2011, 2011.
- Nunes, S., Latasa, M., Delgado, M., Emelianov, M., Simó, R., and Estrada, M.: Phytoplankton community structure in contrasting ecosystems of the Southern Ocean: South Georgia, South Orkneys and western Antarctic Peninsula, *Deep Sea Research I*, in press, 10.1016/j.dsr.2019.06.005, 2019.
- O'Dowd, C., Ceburnis, D., Ovadnevaite, J., Bialek, J., Stengel, D. B., Zacharias, M., Nitschke, U., Connan, S., Rinaldi, M., Fuzzi, S., Decesari, S., Facchini, M. C., Marullo, S., Santoleri, R., Dell'Anno, A., Corinaldesi, C., Tangherlini, M., and Danovaro, R.: Connecting marine productivity to sea-spray via nanoscale biological processes: Phytoplankton Dance or Death Disco?, *Sci Rep*, 5, 14883, 10.1038/srep14883, 2015.
- O'Dowd, C. D., Lowe, J., Smith, M. H., and Kaye, A. D.: The relative importance of sea-salt and nss-sulphate aerosol to the marine CCN population: an improved multi-component aerosol droplet parameterisation, *Meteor. Soc*, 125, 1295-1313, 1999.
- Ogawa, H., and Tanoue, E.: Dissolved Organic Matter in Oceanic Waters, *Journal of Oceanography*, 59, 129-147, 2003.
- Olson, R. J., Zettler, E. R., and DuRand, M. D.: Phytoplankton analysis using flow cytometry, in: Handbook of Methods in Aquatic Microbial Ecology, Boca Raton ed., edited by: Kemp PF, S. B., Sherr EB, Cole JJ (eds), Lewis Publishers, Boca Raton, 1993.
- Orellana, M. V., and Verdugo, P.: Ultraviolet radiation blocks the organic carbon exchange between the dissolved phase and the gel phase in the ocean, *Limnology and Oceanography*, 48 (4), 1618-1623, 2003.
- Orellana, M. V., Matrai, P. A., Leck, C., Rauschenberg, C. D., Lee, A. M., and Coz, E.: Marine microgels as a source of cloud condensation nuclei in the high Arctic, *Proc Natl Acad Sci U S A*, 108, 13612-13617, 10.1073/pnas.1102457108, 2011.
- Orr, J. C., Fabry, V. J., Aumont, O., Bopp, L., Doney, S. C., Feely, R. A., Gnanadesikan, A., Gruber, N., Ishida, A., Joos, F., Key, R. M., Lindsay, K., Maier-Reimer, E., Matear, R., Monfray, P., Mouchet, A., Najjar, R. G., Plattner, G. K., Rodgers, K. B., Sabine, C. L., Sarmiento, J. L., Schlitzer, R., Slater, R. D., Totterdell, I. J., Weirig, M. F., Yamanaka, Y., and Yool, A.: Anthropogenic ocean acidification over the twenty-first century and its impact on calcifying organisms, *Nature*, 437, 681-686, 10.1038/nature04095, 2005.

- Ortega-Retuerta, E., Passow, U., Duarte, C. M., and Reche, I.: Effects of ultraviolet B radiation on (not so) transparent exopolymer particles, *Biogeosciences*, 6, 3071-3080, 10.5194/bg-6-3071-2009, 2009a.
- Ortega-Retuerta, E., Reche, I., Pulido-Villena, E., Agustí, S., and Duarte, C. M.: Uncoupled distributions of transparent exopolymer particles (TEP) and dissolved carbohydrates in the Southern Ocean, *Marine Chemistry*, 115, 59-65, 10.1016/j.marchem.2009.06.004, 2009b.
- Ortega-Retuerta, E., Duarte, C. M., and Reche, I.: Significance of bacterial activity for the distribution and dynamics of transparent exopolymer particles in the Mediterranean sea, *Microb Ecol*, 59, 808-818, 10.1007/s00248-010-9640-7, 2010.
- Ortega-Retuerta, E., Sala, M. M., Borrull, E., Mestre, M., Aparicio, F. L., Gallisai, R., Antequera, C., Marrase, C., Peters, F., Simo, R., and Gasol, J. M.: Horizontal and Vertical Distributions of Transparent Exopolymer Particles (TEP) in the NW Mediterranean Sea Are Linked to Chlorophyll *a* and O<sub>2</sub> Variability, *Front Microbiol*, 7, 2159, 10.3389/fmicb.2016.02159, 2017.
- Ortega-Retuerta, E., Marrase, C., Munoz-Fernandez, A., Sala, M. M., Simo, R., and Gasol, J. M.: Seasonal dynamics of transparent exopolymer particles (TEP) and their drivers in the coastal NW Mediterranean Sea, *Sci Total Environ*, 631-632, 180-190, 10.1016/j.scitotenv.2018.02.341, 2018.
- Ortega-Retuerta, E., Mazuecos, I. P., Reche, I., Gasol, J. M., Álvarez-Salgado, X. A., Álvarez, M., Montero, M. F., and Arístegui, J.: Transparent Exopolymer Particle (TEP) distribution and in situ prokaryotic generation across the deep Mediterranean Sea and nearby North East Atlantic Ocean, *Progress in Oceanography*, 10.1016/j.pocean.2019.03.002, 2019.
- Palma, E. D., Matano, R. P., and Piola, A. R.: A numerical study of the Southwestern Atlantic Shelf circulation: Stratified ocean response to local and offshore forcing, *Journal of Geophysical Research*, 113, 10.1029/2007jc004720, 2008.
- Pannard, A., Pédrone, J., Bormans, M., Briand, E., Claquin, P., and Lagadeuc, Y.: Production of exopolymers (EPS) by cyanobacteria: impact on the carbon-to-nutrient ratio of the particulate organic matter, *Aquatic Ecology*, 50, 29-44, 10.1007/s10452-015-9550-3, 2015.
- Parekh, P., Dutkiewicz, S., Follows, M. J., and Ito, T.: Atmospheric carbon dioxide in a less dusty world, *Geophysical Research Letters*, 33, 10.1029/2005gl025098, 2006.
- Parinos, C., Gogou, A., Krasakopoulou, E., Lagaria, A., Giannakourou, A., Karageorgis, A. P., and Psarra, S.: Transparent Exopolymer Particles (TEP) in the NE Aegean Sea frontal area: Seasonal dynamics under the influence of Black Sea water, *Continental Shelf Research*, 149, 112-123, 10.1016/j.csr.2017.03.012, 2017.
- Partensky, F., Hess, W. R., and Vaultot, D.: Prochlorococcus, a Marine Photosynthetic Prokaryote of Global Significance, *Microbiology and molecular biology reviews* 63, 106-137, 1999.

- Passow, U., and Alldredge, A. L.: Distribution, size and bacterial colonization of transparent exopolymer particles (TEP) in the ocean, *Marine Ecology Progress Series*, 113, 185-198, 1994.
- Passow, U., Alldredge, A. L., and Logan, B. E.: The role of particulate carbohydrate exudates in the flocculation of diatom blooms, *Deep-Sea Res. I Oceanogr. Res.*, 41, 335-357, 1994.
- Passow, U., and Alldredge, A. L.: A dye-binding assay for the spectrophotometric measurement of transparent exopolymer particles (TEP), *Limnology and Oceanography*, 40, 1326-1335, 1995.
- Passow, U., Kozłowski, W., and Vernet, M.: Distribution of Transparent Exopolymer Particles (TEP) during summer at a permanent station in Antarctica, *Antarctic Journal of the United States*, 30, 265-266, 1995a.
- Passow, U., Kozłowski, W., and Vernet, M.: Palmer LTER: Temporal variability of transparent exopolymer particles in Arthur Harbor during the 1994-1995 growth season, *Antarctic Journal-Review*, 265-266, 1995b.
- Passow, U., and Alldredge, A. L.: Do transparent exopolymer particles (TEP) inhibit grazing by the euphausiid *Euphausia pacifica*?, *Journal of Plankton Research*, 21, 2203-2217, 1999.
- Passow, U.: Formation of transparent exopolymer particles, TEP, from dissolved precursor material, *Marine Ecology Progress Series*, 192, 1-11, 2000.
- Passow, U., Shipe, R. F., Murray, A., Pak, D. K., Brzezinski, M. A., and Alldredge, A. L.: The origin of transparent exopolymer particles (TEP) and their role in the sedimentation of particulate matter, *Continental Shelf Research*, 21, 327-346, 2001.
- Passow, U.: Production of transparent exopolymer particles (TEP) by phyto- and bacterioplankton, *Marine Ecology Progress Series*, 236, 1-12, 2002a.
- Passow, U.: Transparent exopolymer particles (TEP) in aquatic environments, *Progress in Oceanography*, 55, 287-333, 2002b.
- Passow, U., and De La Rocha, C. L.: Accumulation of mineral ballast on organic aggregates, *Global Biogeochemical Cycles*, 20, n/a-n/a, 10.1029/2005gb002579, 2006.
- Passow, U.: The abiotic formation of TEP under different ocean acidification scenarios, *Marine Chemistry*, 128-129, 72-80, 10.1016/j.marchem.2011.10.004, 2012.
- Paul-Pont, I., Tallec, K., Gonzalez-Fernandez, C., Lambert, C., Vincent, D., Mazurais, D., Zambonino-Infante, J.-L., Brotons, G., Lagarde, F., Fabioux, C., Soudant, P., and Huvet, A.: Constraints and Priorities for Conducting Experimental Exposures of Marine Organisms to Microplastics, *Frontiers in Marine Science*, 5, 10.3389/fmars.2018.00252, 2018.
- Pedrotti, M. L., Peters, F., Beauvais, S., Vidal, M., Egge, J., Jacobsen, A., and Marrasé, C.: Effects of nutrients and turbulence on the production of transparent exopolymer



particles: a mesocosm study, *Marine Ecology Progress Series*, 419, 57-69, 10.3354/meps08840, 2010.

Pedrotti, M. L., Fiorini, S., Kerros, M. E., Middelburg, J. J., and Gattuso, J. P.: Variable production of transparent exopolymeric particles by haploid and diploid life stages of coccolithophores grown under different CO<sub>2</sub> concentrations, *Journal of Plankton Research*, 34, 388-398, 10.1093/plankt/fbs012, 2012.

Pentice, I. C., Farquhar, G. D., Fasham, M., Goulden, M., Heimann, M., Jaramillo, V., Khashgi, H., {Le Quere}, C., Schole, s. R., and Wallace, D.: The carbon cycle and atmospheric carbon dioxide, in: *Climate change 2001: The Scientific Basis. Contribution of Working Group I to the Third Assessment Report of the Intergovernmental Panel on Climate Change (IPCC)*, edited by: Houghton, J. T., Ding, Y., Griggs, D. J., Noguer, M., Van der Linden, P. J., Dai, X., Maskell, K., and Johnson, C. A., Cambridge University Press, 2001.

Peterson, R. G., and Stramma, L.: Upper-level circulation in the South Atlantic Ocean, *Progress in Oceanography*, 26, 1-73, 1991.

Piola, A. R., and Gordon, A. L.: Intermediate waters in the southwest South Atlantic, *Deep-Sea Research*, 36, 1-16, 1989.

Piola, A. R.: The influence of the Plata River discharge on the western South Atlantic shelf, *Geophysical Research Letters*, 32, 10.1029/2004gl021638, 2005.

Pollard, R. T., Salter, I., Sanders, R., Lucas, M., Moore, C., Mills, R., Statham, P., Allen, J., Baker, A., Bakker, D., Charette, M., Fielding, S., Fones, G., French, M., Hickman, A., Holland, R., Hughes, J., Jickells, T., Lampitt, R., Morris, P., Nédélec, F. H., Nielsdótti, r. M., Planquette, H., Popova, E. E., Poulton, A. J., Read, J. F., Seeyave, S., Smith, T., Stinchombe, M., Taylor, S., Thomalla, S., Venables, H. J., Williamson, R., and Zubkov, M. V.: Southern Ocean deep-water carbon export enhanced by natural iron fertilisation, *Nature*, 457, 577-580, 2009.

Pounds, J. A., Bustamante, M. R., Coloma, L. A., Consuegra, J. A., Fogden, M. P., Foster, P. N., La Marca, E., Masters, K. L., Merino-Viteri, A., Puschendorf, R., Ron, S. R., Sanchez-Azofeifa, G. A., Still, C. J., and Young, B. E.: Widespread amphibian extinctions from epidemic disease driven by global warming, *Nature*, 439, 161-167, 10.1038/nature04246, 2006.

Prieto, L., Sommer, F., Stibor, H., and Koeve, W.: Effects of planktonic copepods on transparent exopolymeric particles (TEP) abundance and size spectra, *Journal of Plankton Research*, 5, 515-525, 2001.

Prieto, L., Ruiz, J., Echevarría, F., García, C. M., Bartual, A., Gálvez, J. A., Corzo, A., and Macías, D.: Scales and processes in the aggregation of diatom blooms: high time resolution and wide size range records in a mesocosm study, *Deep Sea Res I*, 49, 1233-1253, 2002.

Prieto, L., Navarro, G., Cózar, A., Echevarría, F., and García, C. M.: Distribution of TEP in the euphotic and upper mesopelagic zones of the southern Iberian coasts, *Deep Sea Research Part II: Topical Studies in Oceanography*, 53, 1314-1328, 10.1016/j.dsr2.2006.03.009, 2006.

- Quigley, M. S., Santschi, P. H., Hung, C.-C., Guo, L., and Honeyman, B. D.: Importance of acid polysaccharides for <sup>234</sup>Th complexation to marine organic matter, *Limnology and Oceanography*, 47 (2), 367-377, 2002.
- Radic, T., Kraus, R., Fuks, D., Radic, J., and Pecar, O.: Transparent exopolymeric particles' distribution in the northern Adriatic and their relation to microphytoplankton biomass and composition, *Sci Total Environ*, 353, 151-161, 10.1016/j.scitotenv.2005.09.013, 2005.
- Radic, T., Ivancic, I., Fuks, D., and Radic, J.: Marine bacterioplankton production of polysaccharidic and proteinaceous particles under different nutrient regimes, *FEMS Microbiol Ecol*, 58, 333-342, 10.1111/j.1574-6941.2006.00176.x, 2006.
- Ramaiah, N., Sarma, V. V. S. S., Gauns, M., Kumar, M. D., and Madhupratap, M.: Abundance and relationship of bacteria with transparent exopolymer particles during the 1996 summer monsoon in the Arabian Sea, *Proceedings of the Indian Academy of Sciences - Earth and Planetary Sciences*, 109, 443-451, 2000.
- Ramaiah, N., Yoshikawa, T., and Furuya, K.: Temporal variations in transparent exopolymer particles (TEP) associated with a diatom spring bloom in a subarctic ria in Japan, *Marine Ecology Progress Series*, 212, 79-88, 10.3354/meps212079, 2001.
- Ramaiah, N., and Furuya, K.: Seasonal variations in phytoplankton composition and transparent exopolymer particles in a eutrophicated coastal environment, *Aquatic Microbial Ecology*, 30, 69-82, 2002.
- Ramaiah, N., Takeda, S., Furuya, K., Yoshimura, T., Nishioka, J., Aono, T., Nojiri, Y., Imai, K., Kudo, I., Saito, H., and Tsuda, A.: Effect of iron enrichment on the dynamics of transparent exopolymer particles in the western subarctic Pacific, *Progress in Oceanography*, 64, 253-261, 10.1016/j.pocean.2005.02.012, 2005.
- Ramus, J.: Alcian Blue: a quantitative aqueous assay for algal acid and sulfated polysaccharides, *Journal of Phycology*, 13, 345-348, 1977.
- Raposo, M. F., de Morais, R. M., and Bernardo de Morais, A. M.: Bioactivity and applications of sulphated polysaccharides from marine microalgae, *Mar Drugs*, 11, 233-252, 10.3390/md11010233, 2013.
- Ras, J., Claustre, H., and Uitz, J.: Spatial variability of phytoplankton pigment distributions in the Subtropical South Pacific Ocean: comparison between in situ and predicted data, *Biogeosciences Discussions*, 4, 3409-3451, 10.5194/bgd-4-3409-2007, 2007.
- Rastelli, E., Corinaldesi, C., Dell'Anno, A., Lo Martire, M., Greco, S., Cristina Facchini, M., Rinaldi, M., O'Dowd, C., Ceburnis, D., and Danovaro, R.: Transfer of labile organic matter and microbes from the ocean surface to the marine aerosol: an experimental approach, *Sci Rep*, 7, 11475, 10.1038/s41598-017-10563-z, 2017.
- Riebesell, U., Reigstad, M., Wassmann, P., Noji, T., and Passow, U.: On the trophic fate of *Phaeocystis pouchetii* (Hariot): VI. Significance of *Phaeocystis*-derived mucus for vertical flux., *Journal of Sea Research*, 33, 193 – 203, 1995.

- Robinson, T.-B., Giebel, H.-A., and Wurl, O.: Riding the Plumes: Characterizing Bubble Scavenging Conditions for the Enrichment of the Sea-Surface Microlayer by Transparent Exopolymer Particles, *Atmosphere*, 10, 10.3390/atmos10080454, 2019a.
- Robinson, T.-B., Stolle, C., and Wurl, O.: Depth is Relative: The Importance of Depth on TEP in the Near Surface Environment, *Ocean Science Discussions*, 1-20, 10.5194/os-2019-79, 2019b.
- Robinson, T. B., Wurl, O., Bahlmann, E., Jürgens, K., and Stolle, C.: Rising bubbles enhance the gelatinous nature of the air–sea interface, *Limnology and Oceanography*, 10.1002/lno.11188, 2019c.
- Rochelle-Newall, E. J., Mari, X., and Pringault, O.: Sticking properties of transparent exopolymeric particles (TEP) during aging and biodegradation, *Journal of Plankton Research*, 32, 1433-1442, 10.1093/plankt/fbq060, 2010.
- Ros, J., and Gili, J.-M.: Four decades of research on the Medes Islands, *Contributions to Science*, 11, 75-83, 10.2436/20.7010.01.215, 2015.
- Royer, S. J., Mahajan, A. S., Galí, M., Saltzman, E., and Simó, R.: Small-scale variability patterns of DMS and phytoplankton in surface waters of the tropical and subtropical Atlantic, Indian, and Pacific Oceans, *Geophysical Research Letters*, 42, 475-483, 10.1002/2014gl062543, 2015.
- Russell, L. M., Hawkins, L. N., Frossard, A. A., Quinn, P. K., and Bates, T. S.: Carbohydrate-like composition of submicron atmospheric particles and their production from ocean bubble bursting, *Proc Natl Acad Sci U S A*, 107, 6652-6657, 10.1073/pnas.0908905107, 2010.
- Sabine, C. L., and Tanhua, T.: Estimation of anthropogenic CO<sub>2</sub> inventories in the ocean, *Ann Rev Mar Sci*, 2, 175-198, 10.1146/annurev-marine-120308-080947, 2010.
- Sala, M., Peters, F., Gasol, J. M., Pedrós-Alió, C., Marrasé, C., and Vaqué, D.: Seasonal and spatial variations in the nutrient limitation of bacterioplankton growth in the northwestern Mediterranean, *Aquatic Microbial Ecology*, 27, 47-56, 2002.
- Sala, M. M., Aparicio, F. L., Balagué, V., Boras, J. A., Borrull, E., Cardelús, C., Cros, L., Gomes, A., López-Sanz, A., Malits, A., Martínez, R. A., Mestre, M., Movilla, J., Sarmiento, H., Vázquez-Domínguez, E., Vaqué, D., Pinhassi, J., Calbet, A., Calvo, E., Gasol, J. M., Pelejero, C., and Marrasé, C.: Contrasting effects of ocean acidification on the microbial food web under different trophic conditions, *ICES Journal of Marine Science: Journal du Conseil*, 73, 670-679, 10.1093/icesjms/fsv130, 2016.
- Santschi, P. H., Hung, C.-C., Schultz, G., and Alvarado-Quiroz, N.: Control of acid polysaccharide production and <sup>234</sup>Th and POC export fluxes by marine organisms, *Geophysical Research Letters*, 30 (2), 10.1029/2002GL016046, 2003.
- Santschi, P. H., Murray, J. W., Baskaran, M., Benitez-Nelson, C. R., Guo, L. D., Hung, C. C., Lamborg, C., Moran, S. B., Passow, U., and Roy-Barman, M.: Thorium speciation in seawater, *Marine Chemistry*, 100, 250-268, 10.1016/j.marchem.2005.10.024, 2006.

- Sarmiento, J. L., and Bender, M.: Carbon biogeochemistry and climate change, *Photosynth Res*, 39, 209-234, 1994.
- Sarmiento, J. L., Gruber, N., Brzezinski, M. A., and Dunne, J. P.: High-latitude controls of thermocline nutrients and low latitude biological productivity, *Nature*, 427, 56-60, 2004.
- Schartau, M., Engel, A., Schröter, J., Thoms, S., Völker, C., and Wolf-Gladrow, D.: Modelling carbon overconsumption and the formation of extracellular particulate organic carbon, *Biogeosciences*, 4, 433-454, 2007.
- Schlesinger, W. H.: Evidence from chronosequence studies for a low carbon-storage potential of soils., *Nature*, 348, 232- 234, 1990.
- Schlitzer, R., and 2017: Ocean Data View, <http://odv.awi.de>,
- Schuster, S., and Herndl, G. J.: Formation and significance of transparent exopolymeric particles in the northern Adriatic Sea, 1995.
- Scoullou, M., Plavšić, M., Karavoltsos, S., and Sakellari, A.: Partitioning and distribution of dissolved copper, cadmium and organic matter in Mediterranean marine coastal areas: The case of a mucilage event, *Estuarine, Coastal and Shelf Science*, 67, 484-490, 10.1016/j.ecss.2005.12.007, 2006.
- Servais, P., Courties, C., Lebaron, P., and Troussellier, M.: Coupling Bacterial Activity Measurements with Cell Sorting by Flow Cytometry, *Microbial Ecology*, 38, 180-189, 10.1007/s002489900160, 1999.
- Shackelford, R., and Cowen, J. P.: Transparent exopolymer particles (TEP) as a component of hydrothermal plume particle dynamics, *Deep Sea Res*, 10, 1677–1694, 2006.
- Shammi, M., Pan, X., Mostofa, K. M. G., Zhang, D., and Liu, C. Q.: Photo-flocculation of microbial mat extracellular polymeric substances and their transformation into transparent exopolymer particles: Chemical and spectroscopic evidences, *Sci Rep*, 7, 9074, 10.1038/s41598-017-09066-8, 2017.
- Shibata, A., Kogure, K., Koike, I., and Ohwada, K.: Formation of submicron colloidal particles from marine bacteria by viral infection., *Marine Ecology Progress Series*, 155, 303-307, 1997.
- Shimada, A., Hitoshi, N., and Isei, N.: Exopolysaccharide produced by *Enterobacter* sp., *Journal of Fermentation and Bioengineering*, 2, 113-118, 1997.
- Shimeta, J.: Diffusional encounter of submicrometer particles and small cells by suspension feeders, *Limnology and Oceanography*, 38, 456-465, 1993.
- Shimotori, K., Satou, T., Imai, A., Kawasaki, N., Komatsu, K., Kohzu, A., Tomioka, N., Shinohara, R., and Miura, S.: Quantification and characterization of coastal dissolved organic matter by high-performance size exclusion chromatography with ultraviolet absorption, fluorescence, and total organic carbon analyses, *Limnology and Oceanography: Methods*, 14, 637-648, 10.1002/lom3.10118, 2016.

- Siegel, D. A., Buesseler, K. O., Behrenfeld, M. J., Benitez-Nelson, C. R., Boss, E., Brzezinski, M. A., Burd, A., Carlson, C. A., D'Asaro, E. A., Doney, S. C., Perry, M. J., Stanley, R. H. R., and Steinberg, D. K.: Prediction of the Export and Fate of Global Ocean Net Primary Production: The EXPORTS Science Plan, *Frontiers in Marine Science*, 3, 10.3389/fmars.2016.00022, 2016.
- Simó, R., Vila-Costa, M., Alonso-Sáez, L., Cardelús, C., Guadayol, Ò., Vázquez-Domínguez, E., and Gasol, J. M.: Annual DMSP contribution to S and C fluxes through phytoplankton and bacterioplankton in a NW Mediterranean coastal site, *Aquatic Microbial Ecology*, 57, 43-55, 10.3354/ame01325, 2009.
- Simó, R.: The role of marine microbiota in short-term climate regulation, in: *The Role of Marine Biota in the Functioning of the Biosphere*, edited by: Duarte, C. e. a., Fundación BBVA and Rubes Editorial, Bilbao, 107-130, 2011.
- Simon, M., Grossart, H. P., Schweitzer, B., and Ploug, H.: Microbial ecology of organic aggregates in aquatic ecosystems, *Aquatic Microbial Ecology*, 28, 175-211, 10.3354/ame028175, 2002.
- Slingo, A.: Sensitivity of the Earth's radiation budget to changes in low clouds, *Nature*, 343, 49-51, 1990.
- Smetacek, V., and Cloern, J. E.: Oceans. On phytoplankton trends, *Science*, 319, 1346-1348, 10.1126/science.1151330, 2008.
- Smith, D. C., and Azam, F.: A simple, economical method for measuring bacterial protein synthesis rates in seawater using  $^3\text{H}$ -leucine *Marine Microbial Food Web*, 6 (2), 107-114, 1992.
- Staats, N., Stal, L. J., and Mur, L. R.: Exopolysaccharide production by the epipelagic diatom *Cylindrotheca closterium*: effects of nutrient conditions, *Journal of Experimental Marine Biology and Ecology*, 249, 13-27, 2000.
- Steeman-Nielsen, E.: The Use of Radio-active Carbon ( $\text{C}^{14}$ ) for Measuring Organic Production in the Sea, *ICES Journal of Marine Science*, 18, 117-140, 1952.
- Steinberg, D., Van Mooy, B. A., Buesseler, K. O., Boyd, P. W., Kobari, T., and Karl, D.: Bacterial vs. zooplankton control of sinking particle flux in the ocean's twilight zone, *Limnology and Oceanography*, 53, 1327-1338, 2008.
- Steinberg, D. K., and Landry, M. R.: Zooplankton and the Ocean Carbon Cycle, *Ann Rev Mar Sci*, 9, 413-444, 10.1146/annurev-marine-010814-015924, 2017.
- Stocker, T. F.: The seesaw effect, *Science*, 282, 61-62, 1998.
- Stoderegger, K., and Herndl, G. J.: Production and release of bacterial capsular material and its subsequent utilization by marine bacterioplankton, *Limnology and Oceanography*, 43, 877-884, 1998.
- Stoderegger, K., and Herndl, G. J.: Production of exopolymer particles by marine bacterioplankton under contrasting turbulence conditions, *Marine Ecology Progress Series*, 189, 9-16, 1999.

- Stone, R.: The Invisible Hand Behind A Vast Carbon Reservoir, *Science*, 328, 1476-1477, 2010.
- Stukel, M. R., Kahru, M., Benitez-Nelson, C. R., Décima, M., Goericke, R., Landry, M. R., and Ohman, M. D.: Using Lagrangian-based process studies to test satellite algorithms of vertical carbon flux in the eastern North Pacific Ocean, *Journal of Geophysical Research: Oceans*, 120, 7208-7222, 10.1002/2015jc011264, 2015.
- Stukel, M. R., Song, H., Goericke, R., and Miller, A. J.: The role of subduction and gravitational sinking in particle export, carbon sequestration, and the remineralization length scale in the California Current Ecosystem, *Limnology and Oceanography*, 63, 363-383, 10.1002/lno.10636, 2018.
- Sugimoto, K., Fukuda, H., Baki, M. A., and Koike, I.: Bacterial contributions to formation of transparent exopolymer particles (TEP) and seasonal trends in coastal waters of Sagami Bay, Japan, *Aquatic Microbial Ecology*, 46, 31-41, 10.3354/ame046031, 2007.
- Sun, C.-C., Wang, Y.-S., Li, Q. P., Yue, W.-Z., Wang, Y.-T., Sun, F.-L., and Peng, Y.-L.: Distribution characteristics of transparent exopolymer particles in the Pearl River estuary, China, *Journal of Geophysical Research: Biogeosciences*, 117, 1-12, 10.1029/2012jg001951, 2012.
- Sun, C.-C., Sperling, M., and Engel, A.: Effect of wind speed on the size distribution of biogenic gel particles in the sea surface microlayer: Insights from a wind wave channel experiment, *Biogeosciences*, 15, 3577-3589, 10.5194/bg-2017-419, 2018.
- Suratman, S., Weston, K., Jickells, T., Chance, R., and Bell, T.: Dissolved organic matter release by an axenic culture of *Emiliana huxleyi*, *Journal of the Marine Biological Association of the United Kingdom*, 88, 10.1017/s0025315408002026, 2008.
- Takahashi, K. T., and Be, A.: Planktonic foraminifera: factors controlling sinking speeds, *Deep Sea Res*, 31, 1477-1500, 1984.
- Tanaka, T., Annaka, M., Ilmain, F., Ishii, K., Kokufuta, E., Suzuki, A., and Tokita, M.: Phase Transitions of Gels, *Mechanics of Swelling*, 64, 1992.
- Tang, K. W., Hutalle, K. M. L., and Grossart, H. P.: Microbial abundance, composition and enzymatic activity during decomposition of copepod carcasses, *Aquatic Microbial Ecology*, 45, 219-227, 10.3354/ame045219, 2006.
- Taylor, J. D., Cottingham, S. D., Billinge, J., and Cunliffe, M.: Seasonal microbial community dynamics correlate with phytoplankton-derived polysaccharides in surface coastal waters, *ISME J*, 8, 245-248, 10.1038/ismej.2013.178, 2014.
- Taylor, J. D., and Cunliffe, M.: Coastal bacterioplankton community response to diatom-derived polysaccharide microgels, *Environ Microbiol Rep*, 9, 151-157, 10.1111/1758-2229.12513, 2017.
- Taylor, J. R., and Ferrari, R.: Shutdown of turbulent convection as a new criterion for the onset of spring phytoplankton blooms, *Limnology and Oceanography*, 56, 2293-2307, 10.4319/lo.2011.56.6.2293, 2011.

- Thavasi, R., and Banat, I.: Biosurfactants and Bioemulsifiers from Marine Sources, in: *Biosurfactants: Research Trends and Applications*, edited by: Mulligan, C. N., Sharma, S. K., and Hardback, M. A., CRC Press, Boca Raton, 125-146, 2014.
- Thornton, D. C. O.: Formation of transparent exopolymeric particles (TEP) from macroalgal detritus, *Marine Ecology Progress Series*, 282, 1-12, 2004.
- Thornton, D. C. O.: Dissolved organic matter (DOM) release by phytoplankton in the contemporary and future ocean, *European Journal of Phycology*, 49, 20-46, 10.1080/09670262.2013.875596, 2014.
- Thornton, D. C. O., Brooks, S. D., and Chen, J.: Protein and Carbohydrate Exopolymer Particles in the Sea Surface Microlayer (SML), *Frontiers in Marine Science*, 3, 10.3389/fmars.2016.00135, 2016.
- Thornton, D. C. O., and Chen, J.: Exopolymer production as a function of cell permeability and death in a diatom (*Thalassiosira weissflogii*) and a cyanobacterium (*Synechococcus elongatus*), *J Phycol*, 53, 245-260, 10.1111/jpy.12470, 2017.
- Thornton, D. C. O.: Coomassie Stainable Particles (CSP): Protein Containing Exopolymer Particles in the Ocean, *Frontiers in Marine Science*, 5, 10.3389/fmars.2018.00206, 2018.
- Thuy, N. T., Lin, J. C., Juang, Y., and Huang, C.: Temporal variation and interaction of full size spectrum Alcian blue stainable materials and water quality parameters in a reservoir, *Chemosphere*, 131, 139-148, 10.1016/j.chemosphere.2015.03.023, 2015.
- Trabelsi, L., Ben Ouada, H., Bacha, H., and Ghoul, M.: Combined effect of temperature and light intensity on growth and extracellular polymeric substance production by the cyanobacterium *Arthrospira platensis*, *Journal of Applied Phycology*, 21, 405-412, 10.1007/s10811-008-9383-8, 2008.
- Tranvik, L. J., Sherr, E. B., and Sherr, B. F.: Uptake and utilization of colloidal DOM by heterotrophic flagellates in seawater, *Marine Ecology Progress Series*, 92, 301-309, 1993.
- Turner, A., and Millward, G. E.: Suspended Particles: Their Role in Estuarine Biogeochemical Cycles, *Estuarine, Coastal and Shelf Science*, 55, 857-883, 10.1006/ecss.2002.1033, 2002.
- Underwood, G. J. C., Boulcott, M., Raines, C. A., and Waldron, K.: Environmental Effects on Exopolymer Production by Marine Benthic Diatoms: Dynamics, Changes in Composition, and Pathways of Production<sup>1</sup>, *Journal of Phycology*, 40, 293-304, 10.1111/j.1529-8817.2004.03076.x, 2004.
- Utermöhl, H.: Zur Vervollkommnung der quantitativen Phytoplankton-Methodik, *Mitteilungen der International Vereinigung für heorestische und Angewandte Limnologie*, 9, 1-38, 1958.
- Van Heukelem, L., and Thomas, C. S.: Computer-assisted high-performance liquid chromatography method development with applications to the isolation and analysis of

- phytoplankton pigments, *Journal of Chromatography A*, 910, 31-49, 10.1016/s0378-4347(00)00603-4, 2001.
- van Loosdrecht, M. C. M., Lyklema, J., Norde, W., and Zehnder, A. J. B.: Bacterial adhesion: a physicochemical approach., 1989, 17, 1-15, 1989.
- Van Oostende, N., Harlay, J., Vanellander, B., Chou, L., Vyverman, W., and Sabbe, K.: Phytoplankton community dynamics during late spring coccolithophore blooms at the continental margin of the Celtic Sea (North East Atlantic, 2006–2008), *Progress in Oceanography*, 104, 1-16, 10.1016/j.pocean.2012.04.016, 2012.
- Van Oostende, N., Moerdijk-Poortvliet, T. C., Boschker, H. T., Vyverman, W., and Sabbe, K.: Release of dissolved carbohydrates by *Emiliana huxleyi* and formation of transparent exopolymer particles depend on algal life cycle and bacterial activity, *Environ Microbiol*, 15, 1514-1531, 10.1111/j.1462-2920.2012.02873.x, 2013.
- Vancoppenolle, M., Meiners, K. M., Michel, C., Bopp, L., Brabant, F., Carnat, G., Delille, B., Lannuzel, D., Madec, G., Moreau, S., Tison, J.-L., and van der Merwe, P.: Role of sea ice in global biogeochemical cycles: emerging views and challenges, *Quaternary Science Reviews*, 79, 207-230, 10.1016/j.quascirev.2013.04.011, 2013.
- Vardi, A., Haramaty, L., Van Mooy, B. A., Fredricks, H. F., Kimmance, S. A., Larsen, A., and Bidle, K. D.: Host-virus dynamics and subcellular controls of cell fate in a natural coccolithophore population, *Proc Natl Acad Sci U S A*, 109, 19327-19332, 10.1073/pnas.1208895109, 2012.
- Verdugo, P.: Polymer gel phase transition in condensation-decondensation of secretory products, *Adv. Polymer Sci.*, 110, 145–156, 1994.
- Verdugo, P., Alldredge, A. L., Azam, F., Kirchman, D. L., Passow, U., and Santschi, P. H.: The oceanic gel phase: a bridge in the DOM–POM continuum, *Marine Chemistry*, 92, 67-85, 10.1016/j.marchem.2004.06.017, 2004.
- Verdugo, P.: Marine microgels, *Ann Rev Mar Sci*, 4, 375-400, 10.1146/annurev-marine-120709-142759, 2012.
- Villacorte, L. O., Kennedy, M. D., Amy, G. L., and Schippers, J. C.: Measuring transparent exopolymer particles (TEP) as indicator of the (bio)fouling potential of RO feed water, *Desalination and Water Treatment*, 5, 207-212, 10.5004/dwt.2009.587, 2009a.
- Villacorte, L. O., Kennedy, M. D., Amy, G. L., and Schippers, J. C.: The fate of Transparent Exopolymer Particles (TEP) in integrated membrane systems: removal through pre-treatment processes and deposition on reverse osmosis membranes, *Water Res*, 43, 5039-5052, 10.1016/j.watres.2009.08.030, 2009b.
- Volk, T., and Hoffert, M. I.: Ocean carbon pumps: Analysis of relative strengths and efficiencies in ocean-driven atmospheric CO<sub>2</sub> changes, in: *The Carbon Cycle and Atmospheric CO<sub>2</sub>: Natural Variations Archean to Present*, edited by: Sundquist, E. T., and Broecker, W. S., *Geophysica*, Washington D. C., 99-110, 1985.



- Weiss, M., Abele, U., Weckesser, J., Welte, W., Schiltz, E., and Schulz, G.: Molecular architecture and electrostatic properties of a bacterial porin, *Science*, 254, 1627-1630, 10.1126/science.1721242, 1991.
- Welch, S. A., Barker, W. W., and Banfield, J. F.: Microbial extracellular polysaccharides and plagioclase dissolution, *Geochimica et Cosmochimica Acta*, 63, 1405-1419, 1999.
- Wild, C.: Effekte von “marine snow”—Sedimentation auf Steinkorallen (Hexacorallia, Scleractinia) des Great Barrier Reef, Australien, Department of Biology and Chemistry, University of Bremen, 110 pp., 2000.
- Williams, P. M., and Druffel, E. R. M.: Radiocarbon in dissolved organic matter in the central North Pacific Ocean, *Nature*, 330, 246-248, 10.1038/330246a0, 1987.
- Wilson, T. W., Ladino, L. A., Alpert, P. A., Breckels, M. N., Brooks, I. M., Browse, J., Burrows, S. M., Carslaw, K. S., Huffman, J. A., Judd, C., Kiltthau, W. P., Mason, R. H., McFiggans, G., Miller, L. A., Najera, J. J., Polishchuk, E., Rae, S., Schiller, C. L., Si, M., Temprado, J. V., Whale, T. F., Wong, J. P., Wurl, O., Yakobi-Hancock, J. D., Abbatt, J. P., Aller, J. Y., Bertram, A. K., Knopf, D. A., and Murray, B. J.: A marine biogenic source of atmospheric ice-nucleating particles, *Nature*, 525, 234-238, 10.1038/nature14986, 2015.
- Worm, J., and Søndergaard, M.: Alcian Blue-stained particles in a eutrophic lake, *Journal of Plankton Research*, 20, 179-186, 10.1093/plankt/20.2.179, 1998.
- Wotton, R. S.: The essential role of exopolymers (EPS) in aquatic systems, in: *Oceanography and Marine Biology: An Annual Review*, edited by: Gibson, R. N., Atkinson, R. J. A., and Gordon, J. D. M., CRC Press, Boca Raton, 57-94, 2004.
- Wurl, O., and Holmes, M.: The gelatinous nature of the sea-surface microlayer, *Marine Chemistry*, 110, 89-97, 10.1016/j.marchem.2008.02.009, 2008.
- Wurl, O., Miller, L., Röttgers, R., and Vagle, S.: The distribution and fate of surface-active substances in the sea-surface microlayer and water column, *Marine Chemistry*, 115, 1-9, 10.1016/j.marchem.2009.04.007, 2009.
- Wurl, O., Miller, L., and Vagle, S.: Production and fate of transparent exopolymer particles in the ocean, *Journal of Geophysical Research*, 116, 10.1029/2011jc007342, 2011a.
- Wurl, O., Wurl, E., Miller, L., Johnson, K., and Vagle, S.: Formation and global distribution of sea-surface microlayers, *Biogeosciences*, 8, 121-135, 10.5194/bg-8-121-2011, 2011b.
- Wurl, O., Stolle, C., Van Thuoc, C., The Thu, P., and Mari, X.: Biofilm-like properties of the sea surface and predicted effects on air-sea CO<sub>2</sub> exchange, *Progress in Oceanography*, 144, 15-24, 10.1016/j.pocean.2016.03.002, 2016.
- Wurl, O., Ekau, W., Landing, W. M., and Zappa, C. J.: Sea surface microlayer in a changing ocean – A perspective, *Elem Sci Anth*, 5, 10.1525/elementa.228, 2017.

- Yamada, Y., Fukuda, H., Uchimiya, M., Motegi, C., Nishino, S., Kikuchi, T., and Nagata, T.: Localized accumulation and a shelf-basin gradient of particles in the Chukchi Sea and Canada Basin, western Arctic, *Journal of Geophysical Research: Oceans*, 120, 4638-4653, 10.1002/2015jc010794, 2015.
- Yentsch, C. S., and Menzel, D. W.: A method for the determination of phytoplankton chlorophyll and phaeophytin by fluorescence, *Deep Sea Res I*, 10, 221-231, 1963.
- Zamanillo, M., Ortega-Retuerta, E., Cisternas-Novoa, C., Marrasé, C., Pelejero, C., Gasol, J. M., Estrada, M., Engel, A., and Simó, R.: Seasonal variability of transparent exopolymer particles (TEP) and coomassie stainable particles (CSP) in the coastal NW Mediterranean Sea in prep., 2019a.
- Zamanillo, M., Ortega-Retuerta, E., Nunes, S., Estrada, M., Sala, M. M., Royer, S.-J., López-Sandoval, D. C., Emelianov, M., Vaqué, D., Marrasé, C., and Simó, R.: Distribution of transparent exopolymer particles (TEP) in distinct regions of the Southern Ocean, *Science of The Total Environment*, 691, 736-748, 10.1016/j.scitotenv.2019.06.524, 2019b.
- Zamanillo, M., Ortega-Retuerta, E., Nunes, S., Rodríguez-Ros, P., Dall'Osto, M., Estrada, M., Sala, M. M., and Simó, R.: Main drivers of transparent exopolymer particle distribution across the surface Atlantic Ocean, *Biogeosciences*, 16, 733-749, 10.5194/bg-16-733-2019, 2019c.
- Zancker, B., Bracher, A., Rottgers, R., and Engel, A.: Variations of the Organic Matter Composition in the Sea Surface Microlayer: A Comparison between Open Ocean, Coastal, and Upwelling Sites Off the Peruvian Coast, *Front Microbiol*, 8, 2369, 10.3389/fmicb.2017.02369, 2017.
- Zäncker, B., Engel, A., and Cunliffe, M.: Bacterial communities associated with individual transparent exopolymer particles (TEP) *Journal of Plankton Research*, 0, 1-5, 2019.
- Zhao, S., Danley, M., Ward, J. E., Li, D., and Mincer, T. J.: An approach for extraction, characterization and quantitation of microplastic in natural marine snow using Raman microscopy, *Analytical Methods*, 9, 1470-1478, 10.1039/c6ay02302a, 2017.
- Zhou, J., Mopper, K., and Passow, U.: The role of surface-active carbohydrates in the formation of transparent exopolymer particles by bubble adsorption of seawater, *Limnology and Oceanography*, 43, 1860-1871, 1998.
- Zubkov, M. V., Sleight, M. A., Tarran, G. A., Burkill, P. H., Raymond, J. A., and Leakey, R. J. G.: Picoplanktonic community structure on an Atlantic transect from 50°N to 50°S, *Deep Sea Research Part I: Oceanographic Research Papers*, 45, 1339-1355, 1998.



## Acknowledgments/Agradecimientos

Esta tesis doctoral es el resultado de varios años de trabajo, pero que sin la ayuda inestimable de muchas personas no hubiera sido posible. En primer lugar, quiero agradecer inmensamente a Rafel S. y Eva O. toda la ayuda prestada. Habéis sido unos directores de tesis ejemplares. Muchas gracias por todas las ideas, comentarios, correcciones que me habéis proporcionado a lo largo de la tesis, así como vuestro apoyo, entusiasmo y cercanía. Agradezco enormemente vuestra dedicación, siempre dispuestos a echarme una mano, fueran Navidades, vacaciones de verano o fines de semana (sorry!). También agradecer a Manuel E. el apoyo prestado, siempre disponible para ayudar sobre cualquier asunto.

Como no, agradecer a todos los compañeros/as (y excompañeros/as) del ICM los buenos momentos que me han brindado. Hemos compartido congresos, campañas oceanográficas, los cafés de los jueves, comidas debajo de las palmeras, conferencias, excursiones por la montaña, charlas de despacho, largas horas de laboratorio, cursos,...y de todos ellos me llevo un buen recuerdo. Además, también habéis participado en múltiples estudios de esta tesis, resuelto dudas de todo tipo y ayudado con mis muestreos. Por todo ello, os lo agradezco: Denisse S., Isabel M., Lucía Q., Sarah-Jeanne R. Pablo R., Ariadna M., Daffne L., Mireia M., Maria C., Isabel S., Estitxu T., Pau C., Elena G., Yaiza C., Idaira S., Carolina A., Fran A., Fran C., Ángel L., Isabel F., Caterina R., Carolina M., Laura G., Sdena N., Eva F., Mariona C., Miguel C., Vanessa B., Irene F., Clara C., Manuel D., Ana A., Dorleta O., Marta M., Estela R., Ramiro L., Xavier L., Dolors V., Montse S., Celia M., Pep G., Marta E., Elisa B., Marta S., Clara R., Eva C., Carles P., Adrià A., Encarna B., Marta R, Alberto H., Gustavo A., Quim R. También quiero dar las gracias a Jordi P. (Josep Carreras Leukaemia Research Institute) por abrirme las puertas de su centro y poder colaborar juntos, aunque finalmente los análisis no llegaran a buen puerto.

También doy las gracias a todos los compañeros/as de las campañas oceanográficas donde he participado (HOTMIX, TransPEGASO, PEGASO, ACE), que contribuyeron a convertirlas en experiencias inolvidables y maravillosas (científicos, tripulación, UTMeros...).

Agradecer también a Conchita B., Miriam E., Eva L., Núria A., Jordi E., Rafa H., Genoveva C. (UPC) y Rosa O. (UPC) la gran ayuda prestada con los temas burocráticos...Con vuestro buen humor ha sido mucho más llevadero gestionar el papeleo.

I would also like to thank all the people I met in GEOMAR Helmholtz Centre for Ocean Research Kiel during my short stays, who contributed to improve this thesis considerably and to make the stays unforgettable: Anja E., Carolina C., Marie M., Birthe Z., Judith P., Sonja E., Alexandra L., Ruth F., Katja L., Jon R., Frédéric M. Thank you all for your help and the moments we shared!

A parte de trabajar, durante la tesis también he vivido momentos geniales con amigos/as ajenos a esta “secta”, con los que he podido desconectar y pasarlo en grande: Happy U., Miquel G., Nieves T., Marta S., Irene J., Carmen M., Anna E., Sabrina K., Martin K., Javi M., Brad M., Jose M., Yairon C., Fernando H., Irene M., Ainara G., Xisco C., Rafa C., Jonathan D., Mian N., Reyniel H., Loreidis C., Toni R., David A., Oscar G., Doaa Y., Sara S., Alex F., Didac Z., Andrés G., Daniel, Natalie D., Josiah S., Giri, Melly, Goratz, Jose A. Por todos esos momentos juntos, muchas gracias! Y que sigan por muchos años más.

Finalmente, quiero dar las gracias a toda mi familia, simplemente por ser como es. Vuestra compañía es el mejor regalo que podía tener en esta vida. Me habéis enseñado a valorar las pequeñas cosas de la vida y a disfrutar al máximo del tiempo presente. Agradezco especialmente a mis padres, Tomi y Carlos, y mi hermana Rocío, todo el apoyo que he recibido durante la tesis y fuera de ella (entre muchas otras cosas). Sin vosotros, nada de esto hubiera sido posible. Sois lo más valioso que tengo, y desde luego, una familia ejemplar.

Para terminar, una confesión: puedo afirmar que, a pesar del esfuerzo que conlleva realizar una tesis doctoral, estos años han sido los mejores de mi vida, gracias a todos vosotros y a la ciencia! ¡Que no decaiga!





UNIVERSITAT POLITÈCNICA  
DE CATALUNYA  
BARCELONATECH



Institut  
de Ciències  
del Mar



**CSIC**

CONSEJO SUPERIOR DE INVESTIGACIONES CIENTÍFICAS

*T. Garcia*